MULTIFUNCTIONAL ROLES OF APL-1 IN *C. ELEGANS*

by

COLLIN Y. EWALD

A dissertation submitted to the Graduate Faculty in Biology in partial fulfillment of the requirements for the degree of Doctor of Philosophy, The City University of New York

2011

This manuscript has been read and accepted for the
Graduate Faculty in Biology in satisfaction of the
dissertation requirement for the degree of Doctor of Philosophy.

Dr. Christine Li
Chair of Examining Committee

Dr. Laurel A. Eckhardt
Executive Officer

Dr. Tadmiri Venkatesh
Dr. Alicia Meléndez
Dr. Cathy Savage-Dunn
Dr. Monica Driscoll
Supervisory Committee

THE CITY UNIVERSITY OF NEW YORK

Abstract

MULTIFUNCTIONAL ROLES OF APL-1 IN *C. ELEGANS*

by

Collin Y. Ewald

Advisor: Professor Dr. Christine Li

Alzheimer's disease is an age-dependent disorder and the most common type of dementia. The most prevalent mutations associated with familial Alzheimer's Disease are found in the gene encoding the amyloid precursor protein (APP) or in the presenilin genes, which encode proteases that cleave APP. In mice, knockout of the APP gene family leads to lethality and type II lissencephaly, while overexpression of APP causes a shortening in lifespan and learning defects. However, the cellular function of APP and the pathways in which APP acts are unknown.

Here we investigate the role of APL-1, the *Caenorhabditis elegans* orthologue of APP. Specifically, we expressed APL-1 with different promoters to determine the effect of APL-1 overexpression on several parameters: lifespan, development, and learning. Overexpression of APL-1 driven by its endogenous promoter accelerated aging and thereby shortened lifespan. By contrast, overexpression of APL-1 driven by the *snb-1* promoter slowed aging and thereby prolonged lifespan. This extended lifespan was dependent on signals from the gonad and activity of the transcription factor DAF-16/FOXO and the nuclear hormone receptor DAF-12/NHR. Several other APL-1 overexpression phenotypes, including slowed developmental progression, were also

dependent on *daf-16*/FOXO and *daf-12*/NHR activity. Lastly, pan-neuronal expression of APL-1 caused impairments in olfactory and gustatory avoidance behaviors as well as impairments in touch habituation. These defects were rescued by decreased activity of *daf-16*/FOXO and *daf-12*/NHR. Our results suggest that signaling of neuronally expressed APL-1 perturbs learning via the insulin/IGF-1 and the TGF-β pathways. Hence, APL-1 is a multifunctional protein that signals in multiple pathways to affect lifespan, development, and learning.

In light of our results, we suggest that the shortened lifespan and learning defects in mice with APP overexpression might be mediated via the insulin/IGF-1 pathway. Interestingly, AD is strongly associated with type 2 diabetes and some AD patients show brain specific diabetes.

Acknowledgements

I owe my deepest gratitude to my mentor Dr. Christine Li for been a wonderful advisor, for her guidance, for allowing me to develop and test my own ideas and endless support. I truly enjoyed our long discussions. I am also grateful for her support outside of the lab.

I would like to thank my committee members, Dr. Tadmiri Venkatesh, Dr. Alicia Meléndez, Dr. Cathy Savage-Dunn and Dr. Monica Driscoll for their suggestions, strains and other help. I also wish to thank all lab members: individual persons are thanked in subsequent chapters.

I want to thank my wife for giving up everything and leaving Switzerland with me to follow my dream. And I thank my parents for their support.

Table of Contents

List of Tables

List of Figures

List of Abbreviations

aa	amino acid
Aβ	β-amyloid peptide
$A\beta_{42}$	42 amino acid form of Aβ
AD	Alzheimer's disease
AICD	cytoplasmic fragment of APP
ANOVA	analysis of variance
APL-1	Amyloid Precursor Protein-like 1 (*C. elegans*)
APL-1ΔE1	deletion of E1 domain of APL-1
APL-1ΔE2	deletion of E2 domain of APL-1
APL-1ΔE1-E2	deletion of E1 through E2 domains of APL-1
$APL\text{-}1\Delta G_o$	deletion of G_o-binding sequence of APL-1
APL-1EXT	extracellular domain of APL-1 (*C. elegans*)
APLP1	Amyloid Precursor-like Protein 1 (mammalian)
APLP2	Amyloid Precursor-like Protein 2 (mammalian)
APP	Amyloid Precursor Protein (mammalian)
APPL	β-amyloid precursor protein-like (*Drosophila*)
bp	base pairs
bz	benzaldehyde
cDNA	complementary DNA
CGC	*Caenorhabditis* Genetics Center
Δ	deletion

DNA	deoxyribonucleic acid
dsRNA	double-stranded RNA
E1	cysteine-rich region within the extracellular domain of APP and related proteins
E2	acidic amino acid-rich region within the extracellular domain of APP and related proteins
EMS	methanesulfonic acid ethyl ester
F1	first generation
F2	second generation
FAD	familial Alzheimer's disease
FOXO	Forkhead box protein O
GFP	green fluorescent protein
h	hour
HRP	Horseradish peroxidase
Hz	Hertz
IGF-1	Insulin-like growth factor 1
IPTG	βD-isothiogalactopyranoside
kDa	kilodaltons
L1-L4	larval developmental stages
LB	Luria-Bertani medium
LG	linkage group (chromosome)
M9	physiological buffer (*C. elegans*)
ml	milliliter

mM	millimolar
min	minutes
RFP	red fluorescent protein
mRNA	messanger RNA
miRNA	micro RNA
MYOB	modified Youngren's only bacto-peptone medium
µg	microgram
µl	microliter
µm	micrometer
N	number
N2	wild type *C. elegans*
NaN_3	sodium azide
NaCl	sodium chloride
NaAc	sodium acetate
NGM	nematode growth medium
NHR	nuclear hormone receptor
NIH	National Institutes of Health
nm	nanometer
No.	number
P_o	parental generation
pers. comm.	personal communication
polyQ	polyglutamine
PSEN1	presenilin 1 (mammalian)

PSEN2	presenilin 2 (mammalian)
RCMI	Research Centers in Minority Institutions
RNA	ribonucleic acid
RNAi	RNA interference
rpm	revolutions per minute
sa	sodium acetate
sAPL-1	secreted APL-1
sAPPα	secreted APP after α secretase cleavage
SDS	sodium dodecyl sulfate
SEM	standard error of the mean
T	trial
TAE	Tris-acetate buffer
US	United States
UTR	untranslated region
Z1-Z4	gonadal precursor cells

Chapter I: Introduction

I.1. Alzheimer's disease is an age-dependent disease

Alzheimer's Disease (AD) is a neurodegenerative disorder affecting 5.3 million Americans and over 26 million people worldwide (Hebert *et al*. 2003; Goedert & Spillantini 2006; Alzheimer's Association 2010). In the US, AD is the seventh leading cause of all deaths (Alzheimer's Association 2010). The prevalence of AD is above 50% for people 85 year old (Hebert *et al*. 2003). More than 99% of Alzheimer's disease (AD) cases are sporadic and occur late in life starting at the age of 65 years old (Alzheimer's Association 2010). Age and genetic preposition are the major risk factors for developing AD (Alzheimer's Association 2010). The onset of inherited AD or familial AD (FAD), the remaining 1% of AD cases, occurs much earlier at the age of 40-50 years old (Alzheimer's Association 2010). A major question in the AD field is how different aging parameters affect the development of AD.

I.2. Prolonging life must also overcome age-dependent diseases

During aging, damages accumulate in the genome and protein homeostasis declines. For a long time, aging was thought to be a passive process and driven simply by entropy, similar to that of wearing out a machine. In 1889, August Weismann noticed that individuals post-reproduction could be harmful to the species, since they compete with younger individuals for resources (Weismann 1889). Hence, he argued that aging might be programmed and that genes actively promote aging (Weismann 1889). Besides Weismann's theory of genetically programmed aging, there are about 300 other proposed

theories of aging (Medvedev 1990). Noteworthy aging theories are the accumulation of mutation theory from Peter Medawar (1952) and the antagonistic pleiotropy theory from George Williams (1957). Mutations in genes that act post-reproduction accumulate in populations, since they escape the natural selection process that acts before reproduction (Medawar 1952). Similarly, genes that might be beneficial to allow the highest reproductive outcome might be harmful later in life post reproduction (Williams 1957). Such pleiotropic genes might evolve, since natural selection pressure is highest before reproduction and lowest post-reproduction.

The discovery that mutations in genes could prolong lifespan suggested that animals are capable of living longer and that specific genes actively regulate aging (reviewed in (Kenyon 2010)). Interestingly, most of these mutations also increased cellular stress resistance and cellular maintenance (reviewed in (Kenyon 2010)), which presumably provided protection to the organism from many age-dependent diseases, such as cancer or Alzheimer's disease. However, because of age-dependent diseases, simply restoring age-declining factors is not sufficient to prolong longevity. For instance, telomeres shorten with age. Overexpression of telomerase reverse transcriptase, which slows telomeres shortening with age in mice, can prolong lifespan, but only in mice resistant to cancer (Tomas-Loba *et al*. 2008). Hence, mutations that slow aging must at the same time also delay age-dependent diseases to successfully prolong life.

I.3. Longevity genes

In recent years, several genes and pathways that increase lifespan have been determined in yeast, worms and flies; these pathways include the insulin/IGF-1 pathway (Kenyon

2005), the nutrient-sensing TOR pathway (Jia *et al*. 2004), the heat-shock-inducible transcription factor HSF-1 (Hsu *et al*. 2003), the kinase JNK (Oh *et al*. 2005; Wang *et al*. 2005), the AMP kinase AAK-2 (Apfeld *et al*. 2004), and the histone deacetylase SIR2 (Tissenbaum & Guarente 2001), which are all conserved in mammals (reviewed in (Kenyon 2005; Kenyon 2010)). However, thus far, only the insulin/IGF-1 pathway and the nutrient-sensing TOR pathway have been shown experimentally to promote longevity in mammals (reviewed in (Kenyon 2010)). Interestingly, with the exception of the TOR signalling pathway, all the other examples described above directly influence the activity of the transcription factor DAF-16/FOXO by either phosphorylation of deacetylation (Kenyon 2010). Furthermore, longevity in humans (e.g., centenarians from all over the world) has been associated with the insulin/IGF-1 signalling pathway, particularly with variations in FOXO3A (Suh *et al*. 2008; Willcox *et al*. 2008; Anselmi *et al*. 2009; Flachsbart *et al*. 2009; Li *et al*. 2009; Pawlikowska *et al*. 2009).

I.4. Insulin/IGF-1 pathway regulates aging and dauer formation in *C. elegans*

In 1988, *age-1,* which encodes a phosphatidylinositol-3-OH kinase (Morris *et al*. 1996), was the first mutation identified to prolonged lifespan by more than 60% compared to wild type (Friedman & Johnson 1988). Subsequently, a reduction-of-function mutations in the *daf-2* gene, which encodes an insulin/IGF-1 receptor (Kimura *et al*. 1997), was found to double the worm lifespan (Kenyon *et al*. 1993), although a null mutation in this same gene can lead to embryonic lethality (Gems *et al*. 1998). Both *age-1* and *daf-2* act in the same pathway to extend lifespan, since double mutant *age-1;daf-2* live not longer than either of the single mutants (Dorman *et al*. 1995). Further, the extended lifespan

phenotype of *daf-2* or *age-1* mutants is abolished by loss of *daf-16* (Kenyon *et al*. 1993; Dorman *et al*. 1995), which encodes a FOXO transcription factor (Lin *et al*. 1997; Ogg *et al*. 1997). Hence, DAF-2 insulin/IGF-1 receptor inhibits the longevity-promoting activity of DAF-16 FOXO. Although reducing DAF-2 activity during adulthood promotes longevity (Dillin *et al*. 2002), reducing DAF-2 activity during development forces the animals either in L1 arrest or in an alternative developmental state called dauer (Riddle & Albert 1997).

C. elegans eggs hatch and develop through four larval stages (L1-L4), each of which is punctuated by a molt, before becoming fertile adults (Sulston & Horvitz 1977). After hatching, *C. elegans* L1 larva halt development, a stage referred to as L1 arrest, unless food is present, whereupon they proceed with reproductive growth (Baugh & Sternberg 2006). The presence of food is sensed by the amphid chemosensory neurons. Laser ablations of the amphid neurons lead to transient dauer formation (Bargmann & Horvitz 1991). Amphid neurons release insulin-like peptides that regulate the *daf-2* insulin/IGF-1 receptor (Pierce et al. 2001; Li et al. 2003). Activated DAF-2 elicits a downstream kinase cascade, which phosphorylates DAF-16/FOXO (reviewed in (Kenyon 2005)). Mutations in the insulin/IGF-1 receptor *daf-2* that reduce DAF-2 activity keep the newly hatched eggs in L1 arrest, even when food is present (Gems *et al*. 1998; Baugh & Sternberg 2006). L1 arrest by starvation or *daf-2* mutation requires *daf-16*/FOXO (Baugh & Sternberg 2006). However, if eggs hatch in the presence of food, L1 development proceeds. If food becomes limited during the L1/L2 developmental period, L2 worms enter an alternate L3 stage, called dauer (Cassada & Russell 1975). Dauer animals can survive in a harsh environment for more than 3 months and are resistant to

heat and various noxious chemicals (Cassada & Russell 1975; Klass & Hirsh 1976; Larsen 1993; Lithgow *et al*. 1995). When environmental conditions improve, dauer animals resume development as fourth larval stage (L4) animals and subsequently become fertile adults (Riddle & Albert 1997). Low *daf-2* insulin/IGF-1 receptor activity forces L2 animals into the dauer pathway, even in the presence of food; *daf-16* null mutations completely suppress the *daf-2*-induced dauer formation (Lin et al. 1997; Ogg et al. 1997).

The DAF-2 receptor signals through a conserved PI3 kinase, AGE-1 (Morris *et al*. 1996) that antagonizes DAF-16 activity via kinases AKT-1, AKT-2 and SGK-1 by phosphorylating DAF-16 and thereby preventing DAF-16 from entering the nucleus (Paradis & Ruvkun 1998; Henderson & Johnson 2001; Lee *et al*. 2001; Lin *et al*. 2001; Hertweck *et al*. 2004). Hence, lowering DAF-2 or AGE-1 activity leads to lower DAF-16 phosphorylation and thereby more DAF-16 can enter can the nucleus to induce transcription of target genes. Microarray analysis of downstream targets of activated DAF-16 under low insulin signalling conditions revealed induction of several damage repair and stress resistant genes, such as *ctl-2*/peroxisomal catalase, *sod-3*/manganese superoxide dismutase, *hsp-16.2*/heat-shock protein, and *lys-7*/lysosyme (Murphy *et al*. 2003). However, DAF-16 nuclear localization is not sufficient to recapitulate dauer formation or longevity (Lin *et al*. 2001).

I.5. *daf-2* functions non-cell autonomously from neurons or intestine to promote longevity

Besides the stress resistant genes that are activated by low DAF-2 activity, mutants in the insulin/IGF-1 pathway that promote longevity also express genes specific to the germline (=stem cell) in the somatic cells (Curran *et al*. 2009). The germline by definition is immortal and most cells are post-mitotic in *C. elegans*. Presumably activating those genes in the somatic tissue could give somatic cells the renewal properties of stem cells. Whether this is the case and the mechanisms underlying this activation remain to be determined.

DAF-2 and AGE-1 are expressed in neurons and intestine (McKay *et al*. 2003; Hunt-Newbury *et al*. 2007) and function non-cell autonomously (Apfeld & Kenyon 1998; Wolkow *et al*. 2000). The long-lived phenotypes of *daf-2(e1370)* or *age-1(mg44)* was lost by the reintroduction of wild-type DAF-2 or AGE-1, respectively, in neurons, but not or only partially in intestine (Wolkow *et al*. 2000). By contrast, re-introducing DAF-16, which is expressed ubiquitously, into a short-lived *daf-16(mu86); daf-2(e1370)* mutant background, partially rescued the lifespan to 20% of the *daf-2(e1370)* mutants when expressed in neurons or to 60% when expressed in intestinal cells (Libina *et al*. 2003). Hence, these results demonstrate that longevity can be initiated by signaling from either neurons or intestinal cells. Moreover, these results suggest that spreading of a "longevity transforming signal" from cell to cell must be independent of *daf-16*, since introducing DAF-16 into the intestine of *daf-16(mu86); daf-2(e1370)*, which lack DAF-16 in all other cells, is sufficient to increase lifespan of the whole animal. What this signal might be

remains to be determined. However, unknown signals from the reproductive system have been shown to regulate aging.

The germline also sends signals to affect lifespan. Laser ablation of the germline precursor cells (Z2 and Z3) during the L1 stage increase lifespan by 60% (Hsin & Kenyon 1999). This germline-less induced longevity requires *daf*-16/FOXO and might act in parallel to the decreased *daf-2*-induced longevity pathway, since ablating the germline precursor cells (Z2 and Z3) in *daf-2(e1370)* mutants live longer than germline-less animals or *daf-2(e1370)* animals (Hsin & Kenyon 1999). This convergence of those two parallel pathways might synchronize the aging of somatic tissue to the reproductive system and vice versa. Hence, under stressful reproductive conditions, the aging of the reproductive system might be delayed together with the aging of the whole organism until better conditions occur. Interestingly, transplanting ovaries from young mice into old ones extended their lifespan (Cargill *et al*. 2003; Mason *et al*. 2009).

I.6. Lower Insulin/IGF-1 signaling might protect against age-dependent disease

Reducing *daf-2* insulin/IGF-1 receptor activity not only dramatically increases lifespan, but also makes worms much healthier and youthful (Kenyon et al. 1993). Although *C. elegans* does not suffer from age-dependent diseases such as Huntington or Alzheimer' s disease, introducing protein fragments from genes implicated in these diseases causes toxicity in *C. elegans*. For instance, introducing polyglutamine (polyQ) repeats implicated in Huntington's disease in muscles of *C. elegans* leads to formation of aggregates of these polyQ proteins and a dramatic decrease in motility with age (Morley *et al*. 2002; Hsu *et al*. 2003). Long-lived *daf-2* or *age-1* mutants showed less polyQ

aggregates and stayed mobile longer, whereas *daf-16* RNAi suppressed these improvements (Morley *et al*. 2002; Hsu *et al*. 2003). Hence, reducing insulin/IGF-1 signaling delayed the onset of this toxicity. Further, introducing human $A\beta_{42}$, which is implicated in Alzheimer's disease, into muscle cells of *C. elegans* resulted in a progressive, irreversible paralysis of those worms (Link 1995). Knockdown of *daf-2* by RNAi in worms expressing human $A\beta_{42}$ in muscles, not only decreases paralysis, but also dramatically increases their lifespan (Cohen *et al*. 2006). These effects are dependent on DAF-16 and HSF-1 (Cohen *et al*. 2006). A possible future approach to Alzheimer's disease could be a pharmacological treatment via the insulin signaling pathway. Although lowering insulin/IGF-1 signaling might delay $A\beta_{42}$ accumulation in *C. elegans*, some patients with AD have altered insulin signaling, which manifests in a brain-specific diabetes (Steen *et al*. 2005). Interestingly, nasal application of insulin not only improves cognition in healthy men, but also in AD patients (Benedict *et al*. 2010).

I.7. References

Alzheimer's Association KM (2010). 2010 Alzheimer's disease facts and figures. *Alzheimer's and Dementia*. **6**, 158-194.

Anselmi CV, Malovini A, Roncarati R, Novelli V, Villa F, Condorelli G, Bellazzi R , Puca AA (2009). Association of the FOXO3A locus with extreme longevity in a southern Italian centenarian study. *Rejuvenation Res*. **12**, 95-104.

Apfeld J , Kenyon C (1998). Cell nonautonomy of *C. elegans daf-2* function in the regulation of diapause and life span. *Cell*. **95**, 199-210.

Apfeld J, O'Connor G, McDonagh T, DiStefano PS , Curtis R (2004). The AMP-activated protein kinase AAK-2 links energy levels and insulin-like signals to lifespan in *C. elegans*. *Genes Dev*. **18**, 3004-3009.

Bargmann CI , Horvitz HR (1991). Control of larval development by chemosensory neurons in *Caenorhabditis elegans*. *Science*. **251**, 1243-1246.

Baugh LR , Sternberg PW (2006). DAF-16/FOXO regulates transcription of *cki-1*/Cip/Kip and repression of *lin-4* during *C. elegans* L1 arrest. *Curr Biol*. **16**, 780-785.

Benedict C, Frey WH, 2nd, Schioth HB, Schultes B, Born J , Hallschmid M (2010). Intranasal insulin as a therapeutic option in the treatment of cognitive impairments. *Experimental gerontology*. [Epub ahead of print].

Cargill SL, Carey JR, Muller HG , Anderson G (2003). Age of ovary determines remaining life expectancy in old ovariectomized mice. *Aging Cell*. **2**, 185-190.

Cassada RC , Russell RL (1975). The dauerlarva, a post-embryonic developmental variant of the nematode *Caenorhabditis elegans*. *Dev Bio*. **46**, 326-342.

Cohen E, Bieschke J, Perciavalle RM, Kelly JW , Dillin A (2006). Opposing activities protect against age-onset proteotoxicity. *Science*. **313**, 1604-1610.

Curran SP, Wu X, Riedel CG , Ruvkun G (2009). A soma-to-germline transformation in long-lived *Caenorhabditis elegans* mutants. *Nature*. **459**, 1079-1084.

Dillin A, Crawford DK , Kenyon C (2002). Timing requirements for insulin/IGF-1 signaling in *C. elegans*. *Science*. **298**, 830-834.

Dorman JB, Albinder B, Shroyer T , Kenyon C (1995). The *age-1* and *daf-2* genes function in a common pathway to control the lifespan of *Caenorhabditis elegans*. *Genetics*. **141**, 1399-1406.

Flachsbart F, Caliebe A, Kleindorp R, Blanche H, von Eller-Eberstein H, Nikolaus S, Schreiber S , Nebel A (2009). Association of FOXO3A variation with human longevity confirmed in German centenarians. *Proc Natl Acad Sci USA*. **106**, 2700-2705.

Florez-McClure ML, Hohsfield LA, Fonte G, Bealor MT , Link CD (2007). Decreased insulin-receptor signaling promotes the autophagic degradation of beta-amyloid peptide in *C. elegans*. *Autophagy*. **3**, 569-580.

Friedman DB , Johnson TE (1988). A mutation in the *age-1* gene in *Caenorhabditis elegans* lengthens life and reduces hermaphrodite fertility. *Genetics*. **118**, 75-86.

Gems D, Sutton AJ, Sundermeyer ML, Albert PS, King KV, Edgley ML, Larsen PL , Riddle DL (1998). Two pleiotropic classes of *daf-2* mutation affect larval arrest, adult behavior, reproduction and longevity in *Caenorhabditis elegans*. *Genetics*. **150**, 129-155.

Goedert M , Spillantini MG (2006). A century of Alzheimer's disease. *Science*. **314**, 777-781.

Hebert LE, Scherr PA, Bienias JL, Bennett DA , Evans DA (2003). Alzheimer disease in the US population: prevalence estimates using the 2000 census. *Archives of neurology*. **60**, 1119-1122.

Henderson ST , Johnson TE (2001). *daf-16* integrates developmental and environmental inputs to mediate aging in the nematode *Caenorhabditis elegans*. *Curr Biol*. **11**, 1975-1980.

Hertweck M, Gobel C , Baumeister R (2004). *C. elegans* SGK-1 is the critical component in the Akt/PKB kinase complex to control stress response and life span. *Dev Cell*. **6**, 577-588.

Hsin H , Kenyon C (1999). Signals from the reproductive system regulate the lifespan of *C. elegans*. *Nature*. **399**, 362-366.

Hsu A-L, Murphy CT , Kenyon C (2003). Regulation of Aging and Age-Related Disease by DAF-16 and Heat-Shock Factor. *Science*. **300**, 1142-1145.

Hunt-Newbury R, Viveiros R, Johnsen R, Mah A, Anastas D, Fang L, Halfnight E, Lee D, Lin J, Lorch A, McKay S, Okada HM, Pan J, Schulz AK, Tu D, Wong K, Zhao Z, Alexeyenko A, Burglin T, Sonnhammer E, Schnabel R, Jones SJ, Marra MA, Baillie DL , Moerman DG (2007). High-throughput in vivo analysis of gene expression in *Caenorhabditis elegans*. *PLoS Biol*. **5**, e237.

Jia K, Chen D , Riddle DL (2004). The TOR pathway interacts with the insulin signaling pathway to regulate *C. elegans* larval development, metabolism and life span. *Development*. **131**, 3897-3906.

Kenyon C (2005). The plasticity of aging: insights from long-lived mutants. *Cell*. **120**, 449-460.

Kenyon C, Chang J, Gensch E, Rudner A , Tabtiang R (1993). A *C. elegans* mutant that lives twice as long as wild type. *Nature*. **366**, 461-464.

Kenyon CJ (2010). The genetics of ageing. *Nature*. **464**, 504-512.

Kimura KD, Tissenbaum HA, Liu Y , Ruvkun G (1997). *daf-2*, an insulin receptor-like gene that regulates longevity and diapause in *Caenorhabditis elegans*. *Science*. **277**, 942-946.

Klass M , Hirsh D (1976). Non-ageing developmental variant of *Caenorhabditis elegans*. *Nature*. **260**, 523-525.

Larsen PL (1993). Aging and resistance to oxidative damage in *Caenorhabditis elegans*. *Proc Natl Acad Sci USA*. **90**, 8905-8909.

Lee RY, Hench J , Ruvkun G (2001). Regulation of *C. elegans* DAF-16 and its human ortholog FKHRL1 by the *daf-2* insulin-like signaling pathway. *Curr Biol*. **11**, 1950-1957.

Li W, Kennedy SG , Ruvkun G (2003). *daf-28* encodes a *C. elegans* insulin superfamily member that is regulated by environmental cues and acts in the DAF-2 signaling pathway. *Genes Dev*. **17**, 844-858.

Li Y, Wang WJ, Cao H, Lu J, Wu C, Hu FY, Guo J, Zhao L, Yang F, Zhang YX, Li W, Zheng GY, Cui H, Chen X, Zhu Z, He H, Dong B, Mo X, Zeng Y , Tian XL (2009). Genetic association of FOXO1A and FOXO3A with longevity trait in Han Chinese populations. *Hum Mol Genet*. **18**, 4897-4904.

Libina N, Berman JR , Kenyon C (2003). Tissue-specific activities of *C. elegans* DAF-16 in the regulation of lifespan. *Cell*. **115**, 489-502.

Lin K, Dorman JB, Rodan A , Kenyon C (1997). *daf-16*: An HNF-3/forkhead family member that can function to double the life-span of *Caenorhabditis elegans*. *Science*. **278**, 1319-1322.

Lin K, Hsin H, Libina N , Kenyon C (2001). Regulation of the *Caenorhabditis elegans* longevity protein DAF-16 by insulin/IGF-1 and germline signaling. *Nature genetics*. **28**, 139-145.

Link CD (1995). Expression of human beta-amyloid peptide in transgenic *Caenorhabditis elegans*. *Proc Natl Acad Sci USA*. **92**, 9368-9372.

Lithgow GJ, White TM, Melov S , Johnson TE (1995). Thermotolerance and extended life-span conferred by single-gene mutations and induced by thermal stress. *Proc Natl Acad Sci USA*. **92**, 7540-7544.

Mason JB, Cargill SL, Anderson GB , Carey JR (2009). Transplantation of young ovaries to old mice increased life span in transplant recipients. *J Gerontol A Biol Sci Med Sci*. **64**, 1207-1211.

McKay SJ, Johnsen R, Khattra J, Asano J, Baillie DL, Chan S, Dube N, Fang L, Goszczynski B, Ha E, Halfnight E, Hollebakken R, Huang P, Hung K, Jensen V, Jones SJ, Kai H, Li D, Mah A, Marra M, McGhee J, Newbury R, Pouzyrev A, Riddle DL, Sonnhammer E, Tian H, Tu D, Tyson JR, Vatcher G, Warner A, Wong K, Zhao Z , Moerman DG (2003). Gene expression profiling of cells, tissues, and developmental stages of the nematode *C. elegans*. *Cold Spring Harb Symp Quant Biol*. **68**, 159-169.

Medawar PB (1952). *An Unsolved Problem of Biology* London: Lewis.

Medvedev ZA (1990). An attempt at a rational classification of theories of ageing. *Biol Rev Camb Philos Soc*. **65**, 375-398.

Morley JF, Brignull HR, Weyers JJ , Morimoto RI (2002). The threshold for polyglutamine-expansion protein aggregation and cellular toxicity is dynamic and influenced by aging in *Caenorhabditis elegans*. *Proc Natl Acad Sci USA*. **99**, 10417-10422.

Morris JZ, Tissenbaum HA , Ruvkun G (1996). A phosphatidylinositol-3-OH kinase family member regulating longevity and diapause in *Caenorhabditis elegans*. *Nature*. **382**, 536-539.

Murphy CT, McCarroll SA, Bargmann CI, Fraser A, Kamath RS, Ahringer J, Li H , Kenyon C (2003). Genes that act downstream of DAF-16 to influence the lifespan of *Caenorhabditis elegans*. *Nature*. **424**, 277-283.

Ogg S, Paradis S, Gottlieb S, Patterson GI, Lee L, Tissenbaum HA , Ruvkun G (1997). The Fork head transcription factor DAF-16 transduces insulin-like metabolic and longevity signals in *C. elegans*. *Nature*. **389**, 994-999.

Oh SW, Mukhopadhyay A, Svrzikapa N, Jiang F, Davis RJ , Tissenbaum HA (2005). JNK regulates lifespan in *Caenorhabditis elegans* by modulating nuclear translocation of forkhead transcription factor/DAF-16. *Proc Natl Acad Sci USA*. **102**, 4494-4499.

Paradis S , Ruvkun G (1998). *Caenorhabditis elegans* Akt/PKB transduces insulin receptor-like signals from AGE-1 PI3 kinase to the DAF-16 transcription factor. *Genes Dev*. **12**, 2488-2498.

Pawlikowska L, Hu D, Huntsman S, Sung A, Chu C, Chen J, Joyner AH, Schork NJ, Hsueh WC, Reiner AP, Psaty BM, Atzmon G, Barzilai N, Cummings SR, Browner WS, Kwok PY , Ziv E (2009). Association of common genetic variation in the insulin/IGF1 signaling pathway with human longevity. *Aging Cell*. **8**, 460-472.

Pierce SB, Costa M, Wisotzkey R, Devadhar S, Homburger SA, Buchman AR, Ferguson KC, Heller J, Platt DM, Pasquinelli AA, Liu LX, Doberstein SK , Ruvkun G (2001). Regulation of DAF-2 receptor signaling by human insulin and ins-1, a member of the unusually large and diverse *C. elegans* insulin gene family. *Genes Dev*. **15**, 672-686.

Riddle DL , Albert PS (1997). Genetic and Environmental Regulation of Dauer Larva Development. In *C. elegans II*. (DL Riddle, T Blumenthal, BJ Meyer , JR Priess, eds). New York: Cold Spring Harbor Laboratory Press, pp. 739–768.

Steen E, Terry BM, Rivera EJ, Cannon JL, Neely TR, Tavares R, Xu XJ, Wands JR , de la Monte SM (2005). Impaired insulin and insulin-like growth factor expression and signaling mechanisms in Alzheimer's disease--is this type 3 diabetes? *J Alzheimers Dis*. **7**, 63-80.

Suh Y, Atzmon G, Cho MO, Hwang D, Liu B, Leahy DJ, Barzilai N , Cohen P (2008). Functionally significant insulin-like growth factor I receptor mutations in centenarians. *Proc Natl Acad Sci USA*. **105**, 3438-3442.

Sulston JE , Horvitz HR (1977). Post-embryonic cell lineages of the nematode, *Caenorhabditis elegans*. *Dev Bio*. **56,** 110-156.

Tissenbaum HA , Guarente L (2001). Increased dosage of a *sir-2* gene extends lifespan in *Caenorhabditis elegans*. *Nature*. **410**, 227-230.

Tomas-Loba A, Flores I, Fernandez-Marcos PJ, Cayuela ML, Maraver A, Tejera A, Borras C, Matheu A, Klatt P, Flores JM, Vina J, Serrano M , Blasco MA (2008). Telomerase reverse transcriptase delays aging in cancer-resistant mice. *Cell*. **135**, 609-622.

Wang MC, Bohmann D , Jasper H (2005). JNK extends life span and limits growth by antagonizing cellular and organism-wide responses to insulin signaling. *Cell*. **121**, 115-125.

Weismann A (1889). *Essays upon Heredity and Kindred Biological Problems*. Oxford: Oxford: Clarendon Press.

Willcox BJ, Donlon TA, He Q, Chen R, Grove JS, Yano K, Masaki KH, Willcox DC, Rodriguez B , Curb JD (2008). FOXO3A genotype is strongly associated with human longevity. *Proc Natl Acad Sci USA*. **105**, 13987-13992.

Williams GC (1957). Pleiotropy, Natural Selection, and the Evolution of Senescence. *Sci. Aging Knowl. Environ*. **2001**, cp13.

Wolkow CA, Kimura KD, Lee MS , Ruvkun G (2000). Regulation of *C. elegans* life-span by insulinlike signaling in the nervous system. *Science*. **290**, 147-150.

Chapter II: Background: Genetics of Alzheimer's Disease

II.1-II.10 has been published in: Collin Y. Ewald and Chris Li, **Understanding the molecular basis of Alzheimer's disease using a *Caenorhabditis elegans* model system**. Brain Struct Funct (2010) 214:263–283 DOI 10.1007/s00429-009-0235-3

II.1. Introduction

Alzheimer's disease (AD) is a progressive neurodegenerative disorder affecting over 5 million Americans and over 26 million people worldwide (Brookmeyer *et al*. 2007; Association 2008). As the US population lives longer, the prevalence of AD will increase and become more of a health concern and financial burden (Hebert *et al*. 2003; Association 2008). Thus far, AD is incurable and its etiology is unknown.

II.2. Inheritance of AD

One of the major risk factors for AD is family history and genetic predisposition (Association 2008). No mutation has been linked to sporadic AD, which is late in onset (>65 years) and accounts for most AD cases. In contrast, several mutations have been linked to familial AD (FAD), which has an early onset (<40 years) (Chartier-Harlin *et al*. 1991; Murrell *et al*. 1991; Campion *et al*. 1999) and can be seen in patients as young as 25 (Miklossy *et al*. 2003). The brains of AD patients are characterized by the accumulation of dense plaques and neurofibrillary tangles (Kidd 1964; Luse & Smith 1964; Terry *et al*. 1964; Krigman *et al*. 1965). The major components of the dense plaques is the β-amyloid peptide (Aβ; (Glenner & Wong 1984; Masters *et al*. 1985),

which is a cleavage product of the amyloid precursor protein (APP; (Kang *et al*. 1987); the major component of the neurofibrillary tangles is hyper-phosphorylated tau, a microtubule-associated protein (MAP; (Goedert *et al*. 1989). Mutations in the genes encoding APP (Chartier-Harlin *et al*. 1991; Goate *et al*. 1991; Murrell *et al*. 1991; Hardy 2009a) and presenilins (PSEN1 and PSEN2; (Levy-Lahad *et al*. 1995a; Levy-Lahad *et al*. 1995b; Rogaev *et al*. 1995; Sherrington *et al*. 1995; Hardy 2009b; Hardy 2009c), which are proteases that are part of the γ-secretase complex responsible for cleaving APP (Li *et al*. 2000; Kimberly *et al*. 2003), have been correlated to FAD. Moreover, a duplication of the APP locus can lead to FAD (Cabrejo *et al*. 2006; Rovelet-Lecrux *et al*. 2006; Sleegers *et al*. 2006). These data suggest that disruption of APP metabolism is one of the causative factors in the disease.

The APP gene is alternatively spliced to give rise to a single-pass transmembrane domain protein (Kang *et al*. 1987; Ponte *et al*. 1988; Tanzi *et al*. 1988; Yoshikai *et al*. 1990). APP is cleaved through two major proteolytic pathways: the α-or β-secretase pathways (Fig. 1; for reviews, see (Gralle and Ferreira 2007; Nunan and Small 2000; Selkoe 1999). Initial cleavage by the α- or β-secretase releases an extracellular fragment sAPPα or sAPPβ, respectively. Subsequent cleavage in the β-secretase pathway by γ-secretase leads to the production of Aβ and release of a cytoplasmic fragment (AICD). In contrast, because α-secretase cleaves within the Aβ sequence, the subsequent γ-secretase cleavage releases the cytoplasmic AICD fragment, but does not produce Aβ. Hence, the β/γ-secretase pathway is likely favored in the pathogenesis of AD (for reviews, see (Selkoe 1999; Nunan & Small 2000). Presenilin 1 (PSEN1) and 2 (PSEN2) are part of the γ-secretase complex that releases Aβ (Li *et al*. 2000; Kimberly *et al*. 2003). The

specificity of the secretase cleavage sites can vary. Normally, 90% of the derived Aβ consists of 40 amino acids (=$A\beta_{40}$) and the other 10% consists of 42 and 43 amino acids (=$A\beta_{42}$ and $A\beta_{43}$, respectively; (Haass & Selkoe 1993). $A\beta_{42}$ and $A\beta_{43}$ are highly fibrillogenic and readily aggregate (Haass & Selkoe 1993). Deposition of Aβ, and particularly $A\beta_{42}$, is presumed to be neurotoxic (Yankner *et al*. 1990; Pike *et al*. 1993).

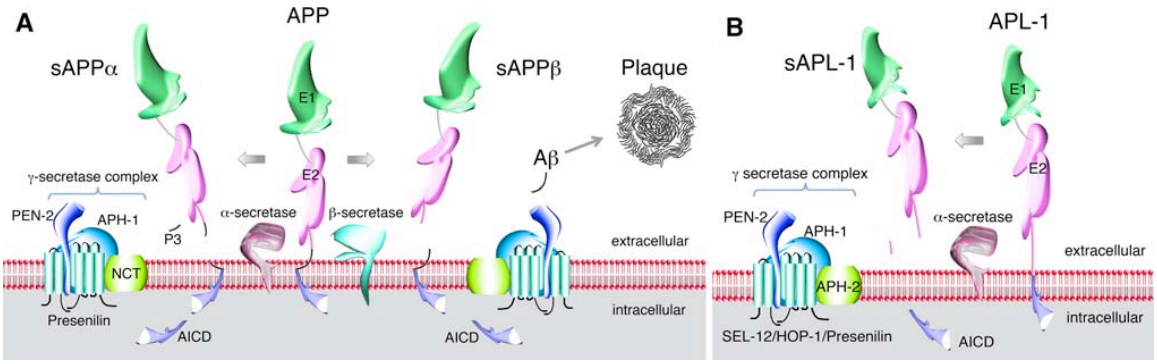

Fig. 1 Schematic of the processing pathways of human amyloid precursor protein (APP; **a**) and its *C. elegans* ortholog APL-1 (**b**). **a)** APP undergoes two processing pathways, α/γ-secretase or β/γ-secretase, to produce sAPPα/AICD or sAPPβ/AICD, respectively. Only the β/γ-secretase pathway produces the amyloid peptide (Aβ). α-Secretase corresponds to ADAM17/TACE, β-secretase to BACE. **b)** In *C. elegans*, APL-1 undergoes at least one processing pathway to produce sAPL-1 and presumably AICD. α-Secretase may correspond to SUP-17, ADAM10, or ADM-4 ADAM17/TACE. No β-secretase activity has been described in *C. elegans*. NCT/APH-2 nicastrin; conserved domains: cysteine-rich E1 and acidic residue-rich E2 domain, AICD APP or APL-1 intracellular cytoplasmic domain.

II.3. Understanding the role of APP: use of a mouse model system

A powerful approach to elucidate the in vivo function of a protein is to inactivate the gene and observe the defects caused in the organism. Inactivation of APP in Mus musculus revealed several deficits, such as reduced brain and body weight, a malformation of forebrain commissures, a deficit in grip strength, an alteration in circadian locomotor activity, a hypersensitivity to seizures, and impairments in spatial learning and long-term potentiation (Zheng *et al*. 1995; Li *et al*. 1996; Perez *et al*. 1997; Steinbach *et al*. 1998; Tremml *et al*. 1998; Magara *et al*. 1999). Overexpression of APP in mice also resulted in several phenotypes, which varied in severity, presumably because of varying levels of APP expression. These phenotypes include lethality, neophobia, impaired spatial alteration, reactive gliosis, and an increase in the number of synaptophysin and GAP-43 immunoreactive presynaptic terminals (Mucke *et al*. 1994; Hsiao *et al*. 1995).

APP is the canonical member of the APP family of proteins that includes APLP1 and APLP2, which share high sequence similarity to APP within the extracellular and cytoplasmic domains, but do not contain Aβ (Wasco *et al*. 1992; Sprecher *et al*. 1993; Wasco *et al*. 1993a; Wasco *et al*. 1993b; Slunt *et al*. 1994). The different members of the APP family probably originated from one ancestral gene, which was duplicated and translocated. Over time, the duplicated genes evolved to have slightly different, but still overlapping functions. Mice in which APLP1 is inactivated show a postnatal growth defect (Heber *et al*. 2000), whereas mice in which APLP2 is inactivated appear wild type (von Koch *et al*. 1997). However, APLP1-APLP2 and APLP2-APP, but not APLP1-APP, double knockouts show early postnatal lethality (Heber *et al*. 2000). Furthermore, in

addition to postnatal lethality, the triple APP-APLP1-APLP2 knockout mice also show a smoothened brain resembling human lissencephaly type II and neuronal ectopias (Herms *et al*. 2004). These experiments highlight an essential role for the APP family proteins in development and viability.

II.4. Understanding the role of APP: use of the *C. elegans* model system

The nematode *Caenorhabditis elegans* contains only one APP-related gene, *apl-1* (Daigle & Li 1993). Because genetic manipulations are easier and faster in *C. elegans* than in a mammalian system, *C. elegans* presents an attractive alternative model to examine APP function and its mechanisms of action. APL-1 is also a single-pass transmembrane domain protein and shares many conserved domains with the mammalian APP family members; however, like APLP1 and APLP2, APL-1 does not show any sequence similarity in the Aβ peptide region (Fig. 1). Nevertheless, a lack of sequence similarity does not exclude the possibility of APL-1 having an ‘‘Aβ peptide equivalent.’’ The *Drosophila* APP-related protein (Appl) also lacks sequence similarity to the mammalian Aβ peptide region (Rosen *et al*. 1989), but contains an Aβ peptide equivalent that upon cleavage can form neurotoxic plaques (Carmine-Simmen *et al*. 2009). Animals carrying mutations in *Drosophila appl* are viable (Luo *et al*. 1992), but unhealthy (D. Kretzschmar, personal communication).

Similar to the APP gene family, *apl-1* has an essential function. Knockout of *apl-1* causes 100% lethality during early larval development (Table 1; (Hornsten *et al*. 2007). The onset of *apl-1* lethality in *C. elegans* is comparable developmentally to the postnatal lethality seen in the APP family mouse knockouts. In wild-type *C. elegans*, each larval stage is punctuated by a molt, when the old cuticle is sloughed off and replaced by a new

cuticle. *apl-1* mutants synthesize a new cuticle, but have difficulty shedding their old cuticle; hence, *apl-1* mutants die during the transition from the first to second larval stage (L1–L2). Several other phenotypes were seen, some at low penetrance, including arrest as L1 larvae and/or severe morphogenetic defects, and some at high penetrance, such as the presence of large vacuoles in hypodermal cells. All phenotypes were rescued by germline transformation with a genomic fragment containing the *apl-1* region as well as an APL-1 translational fusion with green fluorescent protein (GFP) at the 3'end (APL-1::GFP; Table 1). The lethality was not rescued with a genomic fragment containing a premature stop codon in the coding region. Hence, APL-1 is an essential protein for postembryonic development. The goal of examining *apl-1* in *C. elegans* is to gain insight into the functional domains and pathways of APL-1 and translate these findings to mammals.

II.5. Functional domains within APL-1

In mammals, Fe65 binds to the APP cytoplasmic tail (Sabo *et al*. 2001). FEH-1, the *C. elegans* ortholog of Fe65, also binds directly to the cytoplasmic tail of APL-1 (Zambrano *et al*. 2002). Knockdown of *apl-1* or *feh-1* by RNAi causes hyperactive pharyngeal pumping (Zambrano *et al*. 2002); knockdown of *feh-1* also causes an incompletely penetrant embryonic lethality or L1 arrest (Zambrano *et al*. 2002). These findings suggest that APL-1 acts as a receptor, which transduces a signal through FEH-1 during postembryonic development. However, germline transformation of the transmembrane and cytoplasmic domains of APL-1 did not rescue the *apl-1* loss-of-function lethality, although this finding does not preclude that APL-1 signals through the cytoplasmic domain for other functions. In contrast, the extracellular domain of APL-1 was able to

rescue the loss-of-function *apl-1* lethality (Hornsten *et al*. 2007). Furthermore, *apl-1(yn5)* is a viable deletion allele that produces only the extracellular domain of APL-1 (APL-1EXT), indicating that only the extracellular part of APL-1 is necessary and sufficient for viability (Hornsten *et al*. 2007). APL-1EXT corresponds to the entire APL-1 extracellular domain and is not further cleaved by α-secretase (Hornsten *et al*. 2007). These findings lead to a new model whereby APL-1 is a multifunctional protein, and in one of its functions, APL-1 is cleaved and the extracellular fragment (sAPL-1) acts as a ligand. Similarly, a knockin of only the extracellular domain of mammalian APP (sAPPα) was able to rescue the phenotypes of an APP knockout mouse (Ring *et al*. 2007) and the lethality of APP-APLP2 double knockout mice (U. Muller, personal communication). Knockdown of *apl-1* by RNAi in wild-type animals shortened body size (Niwa *et al*. 2008), which is consistent with the reduced body size seen in APP knockout mice (Tremml *et al*. 1998). Hence, these results highlight how findings in the *C. elegans* model can be translated back to mammals.

To identify functional domains within sAPL-1, different domains were tested for their ability to rescue the *apl-1* loss-of-function lethality. The extracellular domain of the APP family contains two conserved domains, a cysteine-rich E1 domain and an E2 domain rich in acidic residues (Wang & Ha 2004; Zheng & Koo 2006); the E1 and E2 domains do not appear to share any structural similarities. Surprisingly, the presence of either the E1 or E2 domain was sufficient to rescue the *apl-1* loss-of-function lethality (Hornsten *et al*. 2007). The apparent functional redundancy between the two domains is unexpected, but suggests that the extracellular APL-1 fragment interacts through multiple domains.

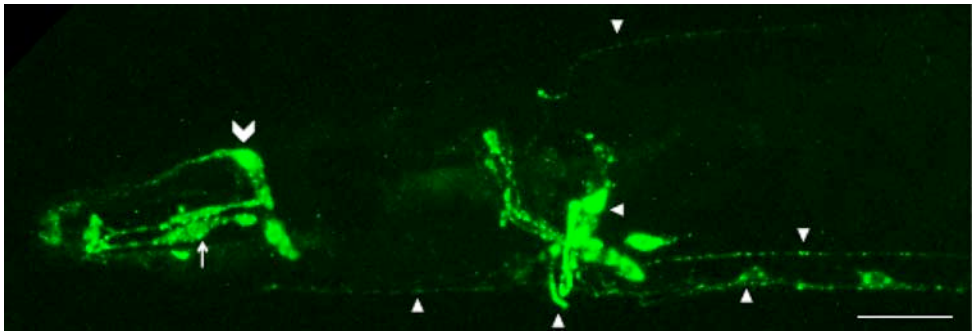

Fig. 2 Expression of an APL-1::GFP translational fusion in *C. elegans*. APL-1::GFP is seen in multiple cell types, including neurons and processes (arrowheads), glial sheath cells (arrow), and muscle cells (chevron). Anterior head region shown, ventral side is down. Scale bar = 10 μm

II.6. Functional localization of APL-1

Similar to the ubiquitously expressed human APP (Ponte *et al*. 1988; Tanzi *et al*. 1988), *apl-1* is expressed during all developmental stages and in many cell types, such as muscles, glial cells, hypodermal cells, and neurons (Fig. 2; (Hornsten *et al*. 2007). To determine in which cell-types *apl-1* expression is sufficient for viability, APL-1 expression was driven by different cell-type specific promoters. Because the *apl-1* loss-of-function lethality is due to a molting defect, APL-1 expression in hypodermis cells, which produce the cuticle during molting, was expected to rescue the lethality; however, no rescue was detected. In contrast, pan-neuronal APL-1 expression was able to rescue the *apl-1* loss-of-function lethality. Furthermore, pan-neuronal expression of only the extracellular domain of APL-1 was also sufficient to rescue lethality, suggesting that after APL-1 is cleaved, sAPL-1 is released from neurons to promote molting (Hornsten *et al*. 2007). These results raise several questions, including the fate of the extracellular sAPL-1

fragment, the identity of its binding partners, and whether sAPL-1 can be released from a subset of neurons for rescue.

II.7. The secretases in *C. elegans*

Although APL-1 has not been directly tested for cleavage by different secretases, *C. elegans* has several orthologues to the mammalian secretases. The secretases will be discussed briefly here, although in the reverse order in which they act. As mentioned above, APP undergoes two cleavages to release Aβ. The second cleavage is mediated by the γ-secretase complex, which consists of at least four proteins: presenilins (PSEN1 and PSEN2), APH-1, Nicastrin/ APH-2, and PEN-2 (Kimberly *et al*. 2003). Mutations in the presenilins were first correlated to FAD in 1995, but their cellular functions were initially unclear (Levy-Lahad *et al*. 1995a; Rogaev *et al*. 1995; Sherrington *et al*. 1995). A few months after these initial reports, the *C. elegans* ortholog SEL-12 PSEN was identified as a suppressor of LIN-12 Notch signaling (Levitan & Greenwald 1995). This work was significant to the AD field in two ways. First, it provided the first insights into the function of presenilins: presenilins were mediators of Notch signaling, which was well characterized for its critical role in cell-fate decisions during development (reviewed in (Greenwald 2005)). Second, it raised the possibility that presenilins mediated the activity of multiple proteins in addition to APP and Notch; hence, therapeutic strategies to disrupt presenilins would disrupt not only APP and Notch, but other proteins as well.

Some clues as to how SEL-12 PSEN was acting were made from analysis of *sel-12* PSEN suppression of different *lin-12* Notch alleles. Gain-of-function mutations in *lin-12* Notch cause production of ectopic pseudovulvae (Greenwald *et al*. 1983), whose

formation can be suppressed by decreased *sel-12* PSEN activity (Levitan & Greenwald 1995); however, when LIN-12 Notch was constitutively activated by removal of its extracellular domain, decreased sel-12 PSEN activity no longer suppressed formation of pseudovulvae, suggesting that sel-12 PSEN acts either directly on the LIN-12 Notch receptor or upstream in the Notch pathway (Levitan & Greenwald 1998). Loss of *sel-12* PSEN caused defects in vulval morphogenesis, leading to an egg-laying defect (Levitan & Greenwald 1995) and deficits in thermal memory (Wittenburg *et al*. 2000). Germline transformation of *sel-12* PSEN mutants with human presenilins restored the egg-laying defect to wild type, indicating that the human and *C. elegans* genes are functionally homologous (Levitan *et al*. 1996). Subsequent screening in *C. elegans* revealed that, like the mammalian systems, *C. elegans* has multiple presenilins: SEL-12, HOP-1 (Li & Greenwald 1997; Westlund *et al*. 1999), and SPE-4 (L'Hernault & Arduengo 1992). SPE-4 is required only for spermatogenesis (Arduengo *et al*. 1998) and loss of *sel-12* PSEN cannot be rescued by *spe-4* (Eimer 2003). In contrast, loss of *sel-12* PSEN can be rescued by *hop-1* and knockout of *sel-12* and *hop-1* in a double mutant caused a synthetic lethality, indicating that the two genes are not only functionally homologous, but have functional overlap (Li & Greenwald 1997; Westlund *et al*. 1999).

By cleverly tagging each transmembrane domain with a lacZ reporter tag, the Greenwald group demonstrated that SEL-12 PSEN undergoes an obligatory endoproteolysis after the sixth transmembrane domain (Li & Greenwald 1996), similar to the obligatory endoproteolysis of mammalian presenilins (Thinakaran *et al*. 1996). Mutations in *sel-12* PSEN or human presenilins that lead to its own miscleavage increased the levels of Aβ42 in human cell cultures (Okochi *et al*. 2000). Four years after

the initial identification of the presenilins, several groups, including a *C. elegans* and *Drosophila* group, proposed that the presenilins were the proteases within the γ-secretase complex (De Strooper *et al*. 1999; Struhl & Greenwald 1999; Wolfe *et al*. 1999; Ye *et al*. 1999).

Multiple lines of evidence, however, indicated that γ-secretase was a complex of proteins; mammalian PSEN1, for instance, co-fractionated in a high molecular weight complex (Li *et al*. 2000). Further immunoextraction of proteins tightly associated with PSEN1 yielded nicastrin, a glycosylated transmembrane protein that binds PSEN1/2 and APP, suggesting that nicastrin's role was to target a substrate to the γ-secretase complex (Yu *et al*. 2000). Loss of a*ph-2*/nicastrin in *C. elegans* resulted in maternal effect embryonic lethality, similar to the phenotype seen in *glp-1* Notch mutants (Goutte *et al*. 2000; Levitan *et al*. 2001). Given the high molecular weight complex that co-fractionated with PSEN1, other components in addition to nicastrin had to be present. The power of the genetic approaches available in *C. elegans* again contributed to the identification of these other components. Genetic screens for enhancers of sel-12 PSEN phenotypes in *C. elegans* pulled out APH-1 and PEN-2 (Goutte *et al*. 2000; Francis *et al*. 2002), whose mammalian orthologues were the major missing components within the γ-secretase complex. Loss of *aph-1* or *pen-2* conferred maternal effect embryonic lethality, similar to the phenotypes seen in *glp-1* Notch and *aph-2*/nicastrin mutants (Goutte *et al*. 2000; Francis *et al*. 2002). APH-1, a seven transmembrane domain protein, and PEN-2, a two transmembrane domain protein, bind PSENs and nicastrin to facilitate assembly and maturation of the γ-secretase complex (Goutte *et al*. 2000; Levitan *et al*. 2001; Francis *et al*. 2002; Goutte *et al*. 2002; Gu *et al*. 2003). An additional gene identified in a genetic

screen for suppression of *sel-12* PSEN activity was *sel-10*, which encodes a protein of the CDC4/CUL-1 E2-E3 ubiquitin ligase family (Hubbard *et al*. 1997). SEL-10 physically interacts with SEL-12 PSEN, presumably to target it for degradation (Wu *et al*. 1998). Similarly, the human homolog SEL-10 physically interacts with and facilitates ubiquitination of human PSEN1 and affects Ab42 production in mammalian cells (Li *et al*. 2002).

Two α-secretases, *sup-17* ADAM10 and *adm-4* ADAM17/TACE, have been identified in *C. elegans* (Tax *et al*. 1997; Jarriault & Greenwald 2005). These two proteases act redundantly to process LIN-12 Notch (Jarriault & Greenwald 2005) and presumably APL-1. Loss of *sup-17* ADAM10 results in lethality, which can be rescued by germline transformation with either *sup-17* ADAM10 or *adm-4* ADAM17/TACE (Tax *et al*. 1997; Wen *et al*. 1997; Jarriault & Greenwald 2005). Thus far, no β-secretase activity that can cleave human APP has been identified in *C. elegans* (Link 2006).

Table 1. Knockouts of *C. elegans* orthologues of human genes implicated in AD

Human		***Caenorhabditis elegans***			
Role	**Gene**	**Gene**	**Knockout (null) alleles**	**Phenotypes of null alleles**	**References**
Amyloid Precursor Protein Family					
APP	*APP/ APLP1/ APLP2*	*apl-1*	*yn10, yn23, yn28, yn29, yn30, yn31, yn32*	larval lethal; molting defect; vacuoles; morphological defects	(Hornsten *et al*. 2007)
Processing Enzymes of APP					
α-secretase					
	ADAM10	*sup-17*	*n1306, n1315, n1316, n1318, n1319am, n1320*	lethal	(Tax *et al*. 1997)
	ADAM17/ TACE	*adm-4*	*ok265*	wild type; functional redundancy between SUP-17 and ADM-4	(Jarriault & Greenwald 2005)
β-secretase					
	BACE1			no endogenous b-secretase activity that cleaves human APP found in transgenic *C. elegans*	(Link 2006)
γ-secretase complex					
Presenilins	*PSEN1* or 2	*sel-12*	*ar171, ty11*	disrupted vulva morphogenesis; egg laying defective	(Levitan & Greenwald 1995; Cinar *et al*. 2001)
	PSEN1 or *2*	*hop-1*	*ar179*	functionally redundant with *sel-12*	(Li & Greenwald 1997; Wen *et al*. 2000)
APH-1	*APH-1*	*aph-1*	*ep140, ep169, ep170, ep216, ep411, ep413, zu123, or28*	no anterior pharynx; maternal effect embryonic lethal; hypodermis fails to enclose body; egg laying defective; APH-2 localized to cytoplasm rather than cell surface	(Francis *et al*. 2002; Goutte *et al*. 2002)
Nicastrin	*APH-2*	*aph-2*	*zu181*	no anterior pharynx; maternal effect embryonic lethal	(Goutte *et al*. 2000)
PEN-2	*PEN-2*	*pen-2*	*ep219, ep220 ep221, ep336, ep412, ep423*	no anterior pharynx; maternal effect embryonic lethal; hypodermis fails to enclose body; egg laying defective	(Francis *et al*. 2002)
Physical Interactors with APP					
Fe65	*FE65*	*feh-1*	*gb561*	embryonic/larval lethal and larval arrest	(Zambrano *et al*. 2002; Napolitano *et al*. 2008)
Mena	*MENA*	*unc-34*	*e951, gm104, gm114*	uncoordinated; axon guidance defect; reduced brood size	(Withee *et al*. 2004; Kraemer & Schellenberg 2007)
Tau and Suppressors of Tau Pathogenesis					
Tau	*TAU*	*ptl-1*	*ok621*	incompletely penetrant embryonic lethal; escapers have mechanosensory defect	(Gordon *et al*. 2008)
		sut-1	*bk79*	suppresses tau pathogenesis	(Kraemer & Schellenberg 2007)
MSUT-2	*MSUT-2*	*sut-2*	*bk741*	suppresses tau pathogenesis	(Guthrie *et al*. 2009)

Not included: *ADAM9* and APOE4, since no orthologues identified in *C. elegans*

II.8. Regulation of APL-1 in *C. elegans*

Regulation of APL-1 expression has only been explored for the time point of the L4 larval-to-adult transition. In wild-type animals, the seams cells, a specialized type of hypodermal cells, serve as stem cells to generate new hypodermal cells during the different molts; however, during the L4 larval-to-adult transition, the seam cells undergo terminal differentiation and join the hypodermal syncytium (Sulston & White 1980). The L4 larval-to-adult transition is regulated by the heterochronic genes *hbl-1*, *lin-41*, and *lin-42* (Fay *et al*. 1999; Jeon *et al*. 1999; Slack *et al*. 2000; Abrahante *et al*. 2003). Loss of these heterochronic genes caused adult fates to be executed precociously and an incompletely penetrant molting defect from L4 to adult (Jeon *et al*. 1999; Slack *et al*. 2000; Abrahante *et al*. 2003); in contrast, overexpression of these genes caused a reiteration of larval cell fates (Slack *et al*. 2000; Abrahante *et al*. 2003). Hence, expression of these heterochronic genes must be down-regulated for entry into the adult stage. This down-regulation occurs in part through negative regulation by *let-7*, a heterochronic microRNA that has been shown to suppress human cancers (Kumar *et al*. 2008). *hbl-1* negatively regulates *let-7*, such that expression of *let-7* does not occur before L3 (Roush & Slack 2009). *mir-48* and *mir-84*, heterochronic microRNAs of the *let-7* family, are responsible for controlling the L2–L3 larval transition partially by negatively regulating *hbl-1* (Abbott *et al*. 2005). Loss-of-function *let-7* mutations cause a supernumerary fifth molt during the L4 to adult transition, resulting in the production of extra seam cells, and an adult lethality due to vulval bursting, presumably due to the extra hypodermal cells (Reinhart *et al*. 2000).

During the L4 larval-to-adult transition, *apl-1* expression appears in seam cells (Niwa

et al. 2008). Knockdown of *apl-1* by RNAi reduced *apl-1* levels to 40% of wild type and suppressed the vulval bursting and additional seam cells in *let-7* mutants (Niwa *et al*. 2008). These data suggest that APL-1 is regulated by *let-7* at the L4 larval-to-adult transition to allow proper molting. If *apl-1* acts downstream of the *let-7* targets *hbl-1*, *lin-41*, and *lin-42*, then loss of *apl-1* should enhance the molting phenotype of *hbl-1, lin-41*, and *lin-42* mutants. Knockdown of *apl-1* by RNAi indeed enhanced the L4 to adult molting defects in the *hbl-1, lin-41*, and *lin-42* single mutants, suggesting that *apl-1* acts downstream and is a potential target of these heterochronic genes (Niwa *et al*. 2008). A cold-sensitive mutation of *mir-48* causes a low penetrance supernumerary molt at the young adult stage, presumably because *hbl-1* is not down-regulated (Reinhart *et al*. 2000). The penetrance of this phenotype is enhanced in a non-temperature dependent manner in a *mir-84* loss-of-function background and the *mir-48; mir-84* double mutant shows two cuticles (Abbott *et al*. 2005). Knockdown of *apl-1* in *mir-48; mir-84* double mutants is sufficient to suppress the supernumerary molt and formation of a double cuticle (Niwa *et al*. 2008). These results indicate that APL-1 expression is temporally regulated by heterochronic microRNAs and regulators during the L4 larval-to-adult transition.

II.9. Overexpression of APL-1 induces several phenotypes

A duplication of the APP locus is correlated with FAD (Cabrejo *et al*. 2006; Rovelet-Lecrux *et al*. 2006; Sleegers *et al*. 2006), suggesting that increased Aβ levels contributes to the FAD pathology. However, overexpression of the APP extracellular fragment, hyper-signaling through the APP cytoplasmic domain, or toxicity of the APP cytoplasmic

fragment may also contribute to the FAD pathology. For instance, the extracellular domain of human APP (sAPP) can bind to the non-canonical DR6 death receptor to induce cell and axonal degeneration in the absence of trophic factors (Nikolaev *et al*. 2009). In addition, transgenic mice overexpressing an FAD version of human APP with an additional mutation (D664A) in a caspase cleavage site to inhibit the release of the cytoplasmic peptide (APP-C31) show reduced behavioral defects, despite increased Aβ deposits compared to the FAD version alone (Galvan *et al*. 2008), implicating an important role for the cytoplasmic tail in FAD pathogenesis. Hence, the effects of APL-1 overexpression were examined in *C. elegans* through the use of transgenic animals (Table 1). When generating transgenic animals, microinjected or co-injected DNA appear as extrachromosomal arrays, which are inherited by progeny at a low frequency because the arrays can be lost during cell division. The arrays, which are generally multiple tandem copies of the single or co-injected DNA, can be integrated into the genome, which allow their Mendelian transmission (Mello & Fire 1995). To determine whether APL-1 overexpression causes any phenotypes, several transgenic lines in which different *apl-1* transgenes were present as arrays or integrated into the genome in an otherwise wild-type background were examined. By Western blot analysis, the transgenic lines expressed APL-1 or APL-1::GFP at levels from 15-to 180-fold higher than wild type (Hornsten *et al*. 2007).

The overexpression lines had defects in brood size, movement, and viability (Table 1); the severity of these defects was strongly correlated with the level of APL-1 overexpression (Hornsten *et al*. 2007). Wild-type animals generally lay between 250 and 300 eggs (Byerly *et al*. 1976). Animals overexpressing APL-1 laid significantly fewer

eggs than wild type (Hornsten *et al*. 2007). Because *apl-1(yn5)* APL-1EXT animals also showed a decreased number of progeny, brood size may be decreased by elevated levels of sAPL-1, perhaps because of interference with cell–cell interactions or adhesion defects that disrupt morphogenesis and/or gonadal development (Hornsten *et al*. 2007). All *apl-1* transgenic overexpression strains also showed significantly reduced swimming and crawling rates compared to wild type (Table 1). Increasing levels of APL-1, therefore, inhibit movement, perhaps by interfering with motor neuron functions.

The overexpression line that had the highest levels of APL-1 (~180-fold higher than wild type), *ynIs79* APL-1::GFP, exhibited the most severe phenotypes, including an incompletely penetrant (70%) larval lethality (Table 1; (Hornsten *et al*. 2007). One other overexpression line, *ynIs86* APL-1, also showed lethality, but at a much lower rate (5.5%). *ynIs79* APL-1::GFP overexpression animals appear morphologically wild type at hatching. At variable times during L1, *ynIs79* APL-1::GFP animals became translucent and large gaps became evident between organs. These phenotypes are consistent with disruptions in cell adhesion whereby elevated levels of APL-1 interfere with normal adhesion contacts between cells. Alternatively, APL-1 overexpression could cause defects in osmoregulation. Mutations in *clr-1*, which encodes a phosphatase involved in regulating osmotic pressure (Kokel *et al*. 1998), also cause a translucent phenotype (Hedgecock *et al*. 1990). Decreased *sel-12* PSEN activity partially suppressed the *apl-1* overexpression lethality, suggesting that the interactions between the presenilins and the APP family are conserved between worms and mammals (Hornsten *et al*. 2007).

II.10. Loss-and gain-of-function *apl-1* lethality are not mediated by caspases

Mammalian APP can regulate apoptosis (for review, see (Chen 2004)) as well as be cleaved by different caspases (Barnes *et al*. 1998; Gervais *et al*. 1999). The *apl-1* loss-of-function and overexpression-induced lethality were examined for activation of an apoptotic or necrotic cell death pathway. *ced-3* encodes a caspase that is essential for execution of apoptosis in *C. elegans* (Horvitz 1999) and *crt-1* encodes calreticulin, which is essential for execution of necrotic cell deaths (Xu *et al*. 2001) in *C. elegans*. Neither loss of *ced-3* caspase nor loss of *crt-1* calreticulin activity rescued the *apl-1* loss-of-function lethality, indicating that this lethality is not due to ectopic activation of either cell death pathway. Similarly, the APL-1 overexpression lethality of *ynIs79* APL-1::GFP is not due to activation of the *ced-3* apoptotic pathway (Hornsten *et al*. 2007). Whether the *apl-1* lethality is mediated by an autophagic pathway is unknown.

Table 2. Overexpression of *C. elegans* proteins implicated in AD

***C. elegans* protein**	***C. elegans* promoter**	**Expression in *C. elegans***	**Fold over-expression**	**Rescuing ability & phenotypes**	**Transgene name/ (plasmid)**	**References**
Endogenous expression of APL-1						
APL-1	*apl-1*	head and tail neurons, ventral cord, hypodermis and supporting cells, vulva muscles	125x	rescues *apl-1* null lethality; low level (5.5%) L1 lethality; reduced brood size; sluggish	*ynIs86*	(Hornsten *et al*. 2007)
APL-1::GFP			180x	rescues *apl-1* null lethality; high level (70%) L1 lethality and morphological defects; cell and organ detachment; reduced brood size; sluggish	*ynIs79*	(Hornsten *et al*. 2007)
APL-1 extracellular domain				rescues *apl-1* null lethality; slowed development; reduced brood size; sluggish	*ynIs71*, *ynEx106*, *ynIs106A*	(Hornsten *et al*. 2007)
APL-1ΔG$_o$[a]				rescues *apl-1* null lethality		(Hornsten *et al*. 2007)
APL-1ΔE1[b]				rescues *apl-1* null lethality		(Hornsten *et al*. 2007)
APL-1ΔE2[c]				rescues *apl-1* null lethality		(Hornsten *et al*. 2007)
APL-1ΔE1-E2[d]				no rescue of *apl-1* null lethality		(Hornsten *et al*. 2007)
Neuronal expression of APL-1						
APL-1	*snb-1*	constitutively in all neurons; pharynx; arcade cells; distal tip cell; vulval muscle; spermatheca; gonad sheath cells; body wall muscle; hypodermis; seam cells[e]	71x and 17x res-pectively	rescues *apl-1* null lethality; reduced brood size; sluggishness	*ynIs12*, *ynIs13*	(Hornsten *et al*. 2007)
APL-1 extracellular domain[f]				rescues *apl-1* null lethality	*ynEx166*	(Hornsten *et al*. 2007)
APL-1::GFP	*rab-3*	constitutively in all neurons		rescues *apl-1* null lethality		(Hornsten *et al*. 2007)
Expression of Proteins in the γ-secretase complex[g]						
SEL-12	*sel-12*	constitutively in most cell types, except intestine		rescues *sel-12* null phenotypes	*byIs100*, *byIs101*, SEL-12	(Levitan *et al*. 1996; Wittenburg *et al*. 2000)
SEL-12	*ttx-3*	only in AIY neuron		rescues *sel-12* null phenotypes	(pBY478)	(Wittenburg *et al*. 2000)
SEL-12	*egl-13*	Pi cell, neurons, bodywall muscles, intestine		partially rescues egg laying defect and Pi cell fate of *sel-12* null worms	(cHNC2)	(Cinar *et al*. 2001)

HOP-1	*sel-12*	constitutively in most cell types, except intestine		rescues *sel-12* null phenotypes	HOP-1	(Li & Greenwald 1997)
APH-1	*sel-12*	constitutively in most cell types, except intestine		rescues egg laying defect of *aph-1* null worms (Note: no rescue under *aph-1* endogenous promoter)	*Ce aph-1*	(Francis *et al*. 2002)
PEN-2	*pen-2*	neurons, muscles, intestine, vulva		rescues egg laying defect of *pen-2* null worms	*pen-2 genomic*	(Francis *et al*. 2002)
PEN-2	*sel-12*	constitutively in most cell types, except intestine		rescues egg laying defect of *pen-2* null worms	*Ce pen-2*	(Francis *et al*. 2002)
Endogenous expression of the α-secretase						
ADM-4	*adm-4*	pharynx, intestine, tail		rescues sterility of *sup-17; adm-4* double mutants	*arEx399, arEx400*	(Jarriault & Greenwald 2005)

[a] APL-1ΔG$_o$: deletion of G$_o$-binding sequence

[b] APL-1ΔE1: deletion of E1 domain

[c] APL-1ΔE2: deletion of E2 domain

[d] APL-1ΔE1-E2: deletion of E1 through E2 domains

[e] Expression pattern of P*snb-1*::GFP (BC11116; (Hunt-Newbury *et al*. 2007))

[f] APL-1EXT: the entire extracellular domain of APL-1. APL-1EXT is not further cleaved and is slightly larger than sAPL-1

[g] No rescue of maternal effect lethal phenotype for *aph-1, aph-2, pen-2*, probably due to co-suppression of their endogenous locus in the germline, a general germline effect described in (Dernburg *et al*. 2000)

II.11. References

Abbott AL, Alvarez-Saavedra E, Miska EA, Lau NC, Bartel DP, Horvitz HR , Ambros V (2005). The *let-7* MicroRNA family members *mir-48*, *mir-84*, and *mir-241* function together to regulate developmental timing in *Caenorhabditis elegans*. *Dev Cell*. **9**, 403-414.

Abrahante JE, Daul AL, Li M, Volk ML, Tennessen JM, Miller EA , Rougvie AE (2003). The *Caenorhabditis elegans* hunchback-like gene *lin-57/hbl-1* controls developmental time and is regulated by microRNAs. *Dev Cell*. **4**, 625-637.

Arduengo PM, Appleberry OK, Chuang P , L'Hernault SW (1998). The presenilin protein family member SPE-4 localizes to an ER/Golgi derived organelle and is required for proper cytoplasmic partitioning during *Caenorhabditis elegans* spermatogenesis. *J. Cell Science*. **111,** 3645-3654.

Association As (2008). 2008 Alzheimer's disease facts and figures. *Alzheimers Dement*. **4**, 110-133.

Barnes NY, Li L, Yoshikawa K, Schwartz LM, Oppenheim RW , Milligan CE (1998). Increased production of amyloid precursor protein provides a substrate for caspase-3 in dying motoneurons. *J Neurosci*. **18**, 5869-5880.

Brookmeyer R, Johnson E, Ziegler-Graham K , Arrighi HM (2007). Forecasting the Global Burden of Alzheimer's Disease. *Alzheimer's and Dementia*. **3**, 186-191.

Byerly L, Cassada RC , Russell RL (1976). The life cycle of the nematode *Caenorhabditis elegans*. I. Wild-type growth and reproduction. *Dev bio*. **51**, 23-33.

Cabrejo L, Guyant-Marechal L, Laquerriere A, Vercelletto M, De la Fourniere F, Thomas-Anterion C, Verny C, Letournel F, Pasquier F, Vital A, Checler F, Frebourg T, Campion D , Hannequin D (2006). Phenotype associated with APP duplication in five families. *Brain*. **129**, 2966-2976.

Campion D, Dumanchin C, Hannequin D, Dubois B, Belliard S, Puel M, Thomas-Anterion C, Michon A, Martin C, Charbonnier F, Raux G, Camuzat A, Penet C, Mesnage V, Martinez M, Clerget-Darpoux F, Brice A , Frebourg T (1999). Early-onset autosomal dominant Alzheimer disease: prevalence, genetic heterogeneity, and mutation spectrum. *Am J Hum Genet*. **65**, 664-670.

Carmine-Simmen K, Proctor T, Tschape J, Poeck B, Triphan T, Strauss R , Kretzschmar D (2009). Neurotoxic effects induced by the *Drosophila* amyloid-beta peptide suggest a conserved toxic function. *Neurobiol Dis*. **33**, 274-281.

Chartier-Harlin MC, Crawford F, Houlden H, Warren A, Hughes D, Fidani L, Goate A, Rossor M, Roques P, Hardy J , et al. (1991). Early-onset Alzheimer's disease caused by mutations at codon 717 of the beta-amyloid precursor protein gene. *Nature*. **353**, 844-846.

Chen YZ (2004). APP induces neuronal apoptosis through APP-BP1-mediated downregulation of beta-catenin. *Apoptosis*. **9**, 415-422.

Cinar HN, Sweet KL, Hosemann KE, Earley K , Newman AP (2001). The SEL-12 presenilin mediates induction of the *Caenorhabditis elegans* uterine pi cell fate. In *Dev Bio*. **237**, 173-182.

Daigle I , Li C (1993). *apl-1*, a *Caenorhabditis elegans* gene encoding a protein related to the human beta-amyloid protein precursor. *Proc Natl Acad Sci USA*. **90**, 12045-12049.

De Strooper B, Annaert W, Cupers P, Saftig P, Craessaerts K, Mumm JS, Schroeter EH, Schrijvers V, Wolfe MS, Ray WJ, Goate A , Kopan R (1999). A presenilin-1-dependent gamma-secretase-like protease mediates release of Notch intracellular domain. *Nature*. **398**, 518-522.

Dernburg AF, Zalevsky J, Colaiacovo MP , Villeneuve AM (2000). Transgene-mediated

cosuppression in the *C. elegans* germ line. *Genes Dev*. **14**, 1578-1583.
Eimer S (2003). Analysis and suppression of mutant presenilin *sel-12* in *Caenorhabditis elegans*. In *Chemie und Pharmazie*. Muenchen: Ludwig-Maximilians-Universitaet Muenchen, pp. 150.
Fay DS, Stanley HM, Han M , Wood WB (1999). A *Caenorhabditis elegans* homologue of hunchback is required for late stages of development but not early embryonic patterning. *Dev Bio*. **205**, 240-253.
Francis R, McGrath G, Zhang J, Ruddy DA, Sym M, Apfeld J, Nicoll M, Maxwell M, Hai B, Ellis MC, Parks AL, Xu W, Li J, Gurney M, Myers RL, Himes CS, Hiebsch R, Ruble C, Nye JS , Curtis D (2002). *aph-1* and *pen-2* are required for Notch pathway signaling, gamma-secretase cleavage of betaAPP, and presenilin protein accumulation. *Dev Cell*. **3**, 85-97.
Galvan V, Zhang J, Gorostiza OF, Banwait S, Huang W, Ataie M, Tang H , Bredesen DE (2008). Long-term prevention of Alzheimer's disease-like behavioral deficits in PDAPP mice carrying a mutation in Asp664. *Behav Brain Res*. **191**, 246-255.
Gervais FG, Xu D, Robertson GS, Vaillancourt JP, Zhu Y, Huang J, LeBlanc A, Smith D, Rigby M, Shearman MS, Clarke EE, Zheng H, Van Der Ploeg LH, Ruffolo SC, Thornberry NA, Xanthoudakis S, Zamboni RJ, Roy S , Nicholson DW (1999). Involvement of caspases in proteolytic cleavage of Alzheimer's amyloid-beta precursor protein and amyloidogenic A beta peptide formation. *Cell*. **97**, 395-406.
Glenner GG , Wong CW (1984). Alzheimer's disease and Down's syndrome: sharing of a unique cerebrovascular amyloid fibril protein. *Biochem Biophys Res Commun*. **122**, 1131-1135.
Goate A, Chartier-Harlin MC, Mullan M, Brown J, Crawford F, Fidani L, Giuffra L, Haynes A, Irving N, James L , et al. (1991). Segregation of a missense mutation in the amyloid precursor protein gene with familial Alzheimer's disease. *Nature*. **349**, 704-706.
Goedert M, Spillantini MG, Jakes R, Rutherford D , Crowther RA (1989). Multiple isoforms of human microtubule-associated protein tau: sequences and localization in neurofibrillary tangles of Alzheimer's disease. *Neuron*. **3**, 519-526.
Gordon P, Hingula L, Krasny ML, Swienckowski JL, Pokrywka NJ , Raley-Susman KM (2008). The invertebrate microtubule-associated protein PTL-1 functions in mechanosensation and development in *Caenorhabditis elegans*. *Development genes and evolution*. **218**, 541-551.
Goutte C, Hepler W, Mickey KM , Priess JR (2000). *aph-2* encodes a novel extracellular protein required for GLP-1-mediated signaling. *Development*. **127**, 2481-2492.
Goutte C, Tsunozaki M, Hale VA , Priess JR (2002). APH-1 is a multipass membrane protein essential for the Notch signaling pathway in Caenorhabditis elegans embryos. In *Proc Natl Acad Sci USA*. **99**, 775-779.
Greenwald I (2005). LIN-12/Notch signaling in *C. elegans*. In *WormBook : the online review of C elegans*. pp. 1-16.
Greenwald IS, Sternberg PW , Horvitz HR (1983). The *lin-12* locus specifies cell fates in *Caenorhabditis elegans*. *Cell*. **34**, 435-444.
Gu Y, Chen F, Sanjo N, Kawarai T, Hasegawa H, Duthie M, Li W, Ruan X, Luthra A, Mount HT, Tandon A, Fraser PE , St George-Hyslop P (2003). APH-1 interacts with mature and immature forms of presenilins and nicastrin and may play a role in maturation of presenilin.nicastrin complexes. In *J Biol Chem*. **278**, 7374-7380.
Guthrie CR, Schellenberg GD , Kraemer BC (2009). SUT-2 potentiates tau-induced neurotoxicity in *Caenorhabditis elegans*. *Hum Mol Genet*. **18**, 1825-1838.
Haass C , Selkoe DJ (1993). Cellular processing of beta-amyloid precursor protein and the genesis of amyloid beta-peptide. *Cell*. **75**, 1039-1042.
Hardy J (2009a). *APP* MUTATIONS TABLE; http://www.alzforum.org/res/com/mut/app/table1.asp).

Hardy J (2009b). PRESENILIN-1 MUTATIONS TABLE.
Hardy J (2009c). PRESENILIN-2 MUTATIONS TABLE.
Heber S, Herms J, Gajic V, Hainfellner J, Aguzzi A, Rulicke T, von Kretzschmar H, von Koch C, Sisodia S, Tremml P, Lipp HP, Wolfer DP , Muller U (2000). Mice with combined gene knock-outs reveal essential and partially redundant functions of amyloid precursor protein family members. *J Neurosci*. **20**, 7951-7963.
Hebert LE, Scherr PA, Bienias JL, Bennett DA , Evans DA (2003). Alzheimer disease in the US population: prevalence estimates using the 2000 census. *Archives of neurology*. **60**, 1119-1122.
Hedgecock EM, Culotti JG , Hall DH (1990). The *unc-5, unc-6*, and *unc-40* genes guide circumferential migrations of pioneer axons and mesodermal cells on the epidermis in *C. elegans*. *Neuron*. **4**, 61-85.
Herms J, Anliker B, Heber S, Ring S, Fuhrmann M, Kretzschmar H, Sisodia S , Muller U (2004). Cortical dysplasia resembling human type 2 lissencephaly in mice lacking all three APP family members. *Embo J*. **23**, 4106-4115.
Hornsten A, Lieberthal J, Fadia S, Malins R, Ha L, Xu X, Daigle I, Markowitz M, O'Connor G, Plasterk R , Li C (2007). APL-1, a *Caenorhabditis elegans* protein related to the human beta-amyloid precursor protein, is essential for viability. *Proc Natl Acad Sci USA*. **104**, 1971-1976.
Horvitz HR (1999). Genetic control of programmed cell death in the nematode *Caenorhabditis elegans*. *Cancer Res*. **59**, 1701s-1706s.
Hsiao KK, Borchelt DR, Olson K, Johannsdottir R, Kitt C, Yunis W, Xu S, Eckman C, Younkin S , Price D (1995). Age-related CNS disorder and early death in transgenic FVB/N mice overexpressing Alzheimer amyloid precursor proteins. *Neuron*. **15**, 1203-1218.
Hubbard EJ, Wu G, Kitajewski J , Greenwald I (1997). *sel-10*, a negative regulator of *lin-12* activity in *Caenorhabditis elegans*, encodes a member of the CDC4 family of proteins. *Genes Dev*. **11**, 3182-3193.
Hunt-Newbury R, Viveiros R, Johnsen R, Mah A, Anastas D, Fang L, Halfnight E, Lee D, Lin J, Lorch A, McKay S, Okada HM, Pan J, Schulz AK, Tu D, Wong K, Zhao Z, Alexeyenko A, Burglin T, Sonnhammer E, Schnabel R, Jones SJ, Marra MA, Baillie DL , Moerman DG (2007). High-throughput in vivo analysis of gene expression in *Caenorhabditis elegans*. *PLoS Biol*. **5**, e237.
Jarriault S , Greenwald I (2005). Evidence for functional redundancy between *C. elegans* ADAM proteins SUP-17/Kuzbanian and ADM-4/TACE. *Dev Bio*. **287**, 1-10.
Jeon M, Gardner HF, Miller EA, Deshler J , Rougvie AE (1999). Similarity of the *C. elegans* developmental timing protein LIN-42 to circadian rhythm proteins. *Science*. **286**, 1141-1146.
Kang J, Lemaire HG, Unterbeck A, Salbaum JM, Masters CL, Grzeschik KH, Multhaup G, Beyreuther K , Muller-Hill B (1987). The precursor of Alzheimer's disease amyloid A4 protein resembles a cell-surface receptor. *Nature*. **325**, 733-736.
Kidd M (1964). Alzheimer's Disease--an Electron Microscopical Study. *Brain*. **87**, 307-320.
Kimberly WT, LaVoie MJ, Ostaszewski BL, Ye W, Wolfe MS , Selkoe DJ (2003). Gamma-secretase is a membrane protein complex comprised of presenilin, nicastrin, Aph-1, and Pen-2. *Proc Natl Acad Sci USA*. **100**, 6382-6387.
Kokel M, Borland CZ, DeLong L, Horvitz HR , Stern MJ (1998). *clr-1* encodes a receptor tyrosine phosphatase that negatively regulates an FGF receptor signaling pathway in *Caenorhabditis elegans*. *Genes Dev*. **12**, 1425-1437.
Kraemer BC , Schellenberg GD (2007). SUT-1 enables tau-induced neurotoxicity in *C. elegans*. *Hum Mol Genet*. **16**, 1959-1971.
Krigman MR, Feldman RG , Bensch K (1965). Alzheimer's Presenile Dementia. A Histochemical and Electron Microscopic Study. *Lab Invest*. **14**, 381-396.
Kumar MS, Erkeland SJ, Pester RE, Chen CY, Ebert MS, Sharp PA , Jacks T (2008).

Suppression of non-small cell lung tumor development by the let-7 microRNA family. *Proc Natl Acad Sci USA*. **105**, 3903-3908.
L'Hernault SW , Arduengo PM (1992). Mutation of a putative sperm membrane protein in *Caenorhabditis elegans* prevents sperm differentiation but not its associated meiotic divisions. *J Cell Bio*. **119**, 55-68.
Levitan D, Doyle TG, Brousseau D, Lee MK, Thinakaran G, Slunt HH, Sisodia SS , Greenwald I (1996). Assessment of normal and mutant human presenilin function in *Caenorhabditis elegans*. *Proc Natl Acad Sci USA*. **93**, 14940-14944.
Levitan D , Greenwald I (1995). Facilitation of *lin-12*-mediated signalling by *sel-12*, a *Caenorhabditis elegans* S182 Alzheimer's disease gene. *Nature*. **377**, 351-354.
Levitan D , Greenwald I (1998). Effects of SEL-12 presenilin on LIN-12 localization and function in *Caenorhabditis elegans*. *Development*. **125**, 3599-3606.
Levitan D, Yu G, St George Hyslop P , Goutte C (2001). APH-2/nicastrin functions in LIN-12/Notch signaling in the *Caenorhabditis elegans* somatic gonad. *Dev Bio*. **240**, 654-661.
Levy-Lahad E, Wasco W, Poorkaj P, Romano DM, Oshima J, Pettingell WH, Yu CE, Jondro PD, Schmidt SD, Wang K , et al. (1995a). Candidate gene for the chromosome 1 familial Alzheimer's disease locus. *Science*. **269**, 973-977.
Levy-Lahad E, Wijsman EM, Nemens E, Anderson L, Goddard KA, Weber JL, Bird TD , Schellenberg GD (1995b). A familial Alzheimer's disease locus on chromosome 1. *Science*. **269**, 970-973.
Li J, Pauley AM, Myers RL, Shuang R, Brashler JR, Yan R, Buhl AE, Ruble C , Gurney ME (2002). SEL-10 interacts with presenilin 1, facilitates its ubiquitination, and alters A-beta peptide production. *Journal of neurochemistry*. **82**, 1540-1548.
Li X , Greenwald I (1996). Membrane topology of the *C. elegans* SEL-12 presenilin. *Neuron*. **17**, 1015-1021.
Li X , Greenwald I (1997). HOP-1, a *Caenorhabditis elegans* presenilin, appears to be functionally redundant with SEL-12 presenilin and to facilitate LIN-12 and GLP-1 signaling. *Proc Natl Acad Sci USA*. **94**, 12204-12209.
Li YM, Lai MT, Xu M, Huang Q, DiMuzio-Mower J, Sardana MK, Shi XP, Yin KC, Shafer JA , Gardell SJ (2000). Presenilin 1 is linked with gamma-secretase activity in the detergent solubilized state. *Proc Natl Acad Sci USA*. **97**, 6138-6143.
Li ZW, Stark G, Gotz J, Rulicke T, Gschwind M, Huber G, Muller U , Weissmann C (1996). Generation of mice with a 200-kb amyloid precursor protein gene deletion by Cre recombinase-mediated site-specific recombination in embryonic stem cells. *Proc Natl Acad Sci USA*. **93**, 6158-6162.
Link CD (2006). *C. elegans* models of age-associated neurodegenerative diseases: lessons from transgenic worm models of Alzheimer's disease. *Exp Gerontol*. **41**, 1007-1013.
Luo L, Tully T , White K (1992). Human amyloid precursor protein ameliorates behavioral deficit of flies deleted for Appl gene. *Neuron*. **9**, 595-605.
Luse SA , Smith KR, Jr. (1964). The ultrastructure of senile plaques. *Am J Pathol*. **44**, 553-563.
Magara F, Muller U, Li ZW, Lipp HP, Weissmann C, Stagljar M , Wolfer DP (1999). Genetic background changes the pattern of forebrain commissure defects in transgenic mice underexpressing the beta-amyloid-precursor protein. *Proc Natl Acad Sci USA*. **96**, 4656-4661.
Masters CL, Simms G, Weinman NA, Multhaup G, McDonald BL , Beyreuther K (1985). Amyloid plaque core protein in Alzheimer disease and Down syndrome. *Proc Natl Acad Sci USA*. **82**, 4245-4249.
Mello C , Fire A (1995). DNA transformation. *Methods Cell Biol*. **48**, 451-482.
Miklossy J, Taddei K, Suva D, Verdile G, Fonte J, Fisher C, Gnjec A, Ghika J, Suard F, Mehta PD, McLean CA, Masters CL, Brooks WS , Martins RN (2003). Two

novel presenilin-1 mutations (Y256S and Q222H) are associated with early-onset Alzheimer's disease. *Neurobiology of aging*. **24**, 655-662.

Mucke L, Masliah E, Johnson WB, Ruppe MD, Alford M, Rockenstein EM, Forss-Petter S, Pietropaolo M, Mallory M , Abraham CR (1994). Synaptotrophic effects of human amyloid beta protein precursors in the cortex of transgenic mice. *Brain Res*. **666**, 151-167.

Murrell J, Farlow M, Ghetti B , Benson MD (1991). A mutation in the amyloid precursor protein associated with hereditary Alzheimer's disease. *Science*. **254**, 97-99.

Napolitano F, D'Angelo F, Bimonte M, Perrina V, D'Ambrosio C, Scaloni A, Russo T , Zambrano N (2008). A differential proteomic approach reveals an evolutionary conserved regulation of Nme proteins by Fe65 in *C. elegans* and mouse. *Neurochem Res*. **33**, 2547-2555.

Nikolaev A, Mclaughlin T, O'Leary DD , Tessier-Lavigne M (2009). APP binds DR6 to trigger axon pruning and neuron death via distinct caspases. *Nature*. **457**, 981-989.

Niwa R, Zhou F, Li C , Slack FJ (2008). The expression of the Alzheimer's amyloid precursor protein-like gene is regulated by developmental timing microRNAs and their targets in *Caenorhabditis elegans*. *Dev Bio*. **315**, 418-425.

Nunan J , Small DH (2000). Regulation of APP cleavage by alpha-, beta- and gamma-secretases. *FEBS Lett*. **483**, 6-10.

Okochi M, Eimer S, Bottcher A, Baumeister R, Romig H, Walter J, Capell A, Steiner H , Haass C (2000). A loss of function mutant of the presenilin homologue SEL-12 undergoes aberrant endoproteolysis in *Caenorhabditis elegans* and increases abeta 42 generation in human cells. *The Journal of biological chemistry*. **275**, 40925-40932.

Perez RG, Zheng H, Van der Ploeg LH , Koo EH (1997). The beta-amyloid precursor protein of Alzheimer's disease enhances neuron viability and modulates neuronal polarity. *J Neurosci*. **17**, 9407-9414.

Pike CJ, Burdick D, Walencewicz AJ, Glabe CG , Cotman CW (1993). Neurodegeneration induced by beta-amyloid peptides in vitro: the role of peptide assembly state. *J Neurosci*. **13**, 1676-1687.

Ponte P, Gonzalez-DeWhitt P, Schilling J, Miller J, Hsu D, Greenberg B, Davis K, Wallace W, Lieberburg I , Fuller F (1988). A new A4 amyloid mRNA contains a domain homologous to serine proteinase inhibitors. *Nature*. **331**, 525-527.

Reinhart BJ, Slack FJ, Basson M, Pasquinelli AE, Bettinger JC, Rougvie AE, Horvitz HR , Ruvkun G (2000). The 21-nucleotide *let-7* RNA regulates developmental timing in *Caenorhabditis elegans*. *Nature*. **403**, 901-906.

Ring S, Weyer SW, Kilian SB, Waldron E, Pietrzik CU, Filippov MA, Herms J, Buchholz C, Eckman CB, Korte M, Wolfer DP , Muller UC (2007). The secreted beta-amyloid precursor protein ectodomain APPs alpha is sufficient to rescue the anatomical, behavioral, and electrophysiological abnormalities of APP-deficient mice. *J Neurosci*. **27**, 7817-7826.

Rogaev EI, Sherrington R, Rogaeva EA, Levesque G, Ikeda M, Liang Y, Chi H, Lin C, Holman K, Tsuda T , et al. (1995). Familial Alzheimer's disease in kindreds with missense mutations in a gene on chromosome 1 related to the Alzheimer's disease type 3 gene. *Nature*. **376**, 775-778.

Rosen DR, Martin-Morris L, Luo LQ , White K (1989). A *Drosophila* gene encoding a protein resembling the human beta-amyloid protein precursor. *Proc Natl Acad Sci USA*. **86**, 2478-2482.

Roush SF , Slack FJ (2009). Transcription of the *C. elegans let-7* microRNA is temporally regulated by one of its targets, *hbl-1*. *Dev Bio*.

Rovelet-Lecrux A, Hannequin D, Raux G, Le Meur N, Laquerriere A, Vital A, Dumanchin C, Feuillette S, Brice A, Vercelletto M, Dubas F, Frebourg T , Campion D (2006). APP locus duplication causes autosomal dominant early-onset

Alzheimer disease with cerebral amyloid angiopathy. *Nature genetics*. **38**, 24-26.
Sabo SL, Ikin AF, Buxbaum JD , Greengard P (2001). The Alzheimer amyloid precursor protein (APP) and FE65, an APP-binding protein, regulate cell movement. *The Journal of cell biology*. **153**, 1403-1414.
Selkoe DJ (1999). Translating cell biology into therapeutic advances in Alzheimer's disease. *Nature*. **399**, A23-31.
Sherrington R, Rogaev EI, Liang Y, Rogaeva EA, Levesque G, Ikeda M, Chi H, Lin C, Li G, Holman K , et al. (1995). Cloning of a gene bearing missense mutations in early-onset familial Alzheimer's disease. *Nature*. **375**, 754-760.
Slack FJ, Basson M, Liu Z, Ambros V, Horvitz HR , Ruvkun G (2000). The *lin-41* RBCC gene acts in the *C. elegans* heterochronic pathway between the *let-7* regulatory RNA and the LIN-29 transcription factor. *Mol Cell*. **5**, 659-669.
Sleegers K, Brouwers N, Gijselinck I, Theuns J, Goossens D, Wauters J, Del-Favero J, Cruts M, van Duijn CM , Van Broeckhoven C (2006). APP duplication is sufficient to cause early onset Alzheimer's dementia with cerebral amyloid angiopathy. *Brain*. **129**, 2977-2983.
Slunt HH, Thinakaran G, Von Koch C, Lo AC, Tanzi RE , Sisodia SS (1994). Expression of a ubiquitous, cross-reactive homologue of the mouse beta-amyloid precursor protein (APP). *The Journal of biological chemistry*. **269**, 2637-2644.
Sprecher CA, Grant FJ, Grimm G, O'Hara PJ, Norris F, Norris K , Foster DC (1993). Molecular cloning of the cDNA for a human amyloid precursor protein homolog: evidence for a multigene family. *Biochemistry*. **32**, 4481-4486.
Steinbach JP, Muller U, Leist M, Li ZW, Nicotera P , Aguzzi A (1998). Hypersensitivity to seizures in beta-amyloid precursor protein deficient mice. *Cell Death Differ*. **5**, 858-866.
Struhl G , Greenwald I (1999). Presenilin is required for activity and nuclear access of Notch in *Drosophila*. *Nature*. **398**, 522-525.
Sulston JE , White JG (1980). Regulation and cell autonomy during postembryonic development of *Caenorhabditis elegans*. *Dev Bio*. **78**, 577-597.
Tanzi RE, McClatchey AI, Lamperti ED, Villa-Komaroff L, Gusella JF , Neve RL (1988). Protease inhibitor domain encoded by an amyloid protein precursor mRNA associated with Alzheimer's disease. *Nature*. **331**, 528-530.
Tax FE, Thomas JH, Ferguson EL , Horvitz HR (1997). Identification and characterization of genes that interact with *lin-12* in *Caenorhabditis elegans*. *Genetics*. **147**, 1675-1695.
Terry RD, Gonatas NK , Weiss M (1964). Ultrastructural Studies in Alzheimer's Presenile Dementia. *Am J Pathol*. **44**, 269-297.
Thinakaran G, Borchelt DR, Lee MK, Slunt HH, Spitzer L, Kim G, Ratovitsky T, Davenport F, Nordstedt C, Seeger M, Hardy J, Levey AI, Gandy SE, Jenkins NA, Copeland NG, Price DL , Sisodia SS (1996). Endoproteolysis of presenilin 1 and accumulation of processed derivatives in vivo. *Neuron*. **17**, 181-190.
Tremml P, Lipp HP, Muller U, Ricceri L , Wolfer DP (1998). Neurobehavioral development, adult openfield exploration and swimming navigation learning in mice with a modified beta-amyloid precursor protein gene. *Behav Brain Res*. **95**, 65-76.
von Koch CS, Zheng H, Chen H, Trumbauer M, Thinakaran G, van der Ploeg LH, Price DL , Sisodia SS (1997). Generation of APLP2 KO mice and early postnatal lethality in APLP2/APP double KO mice. *Neurobiology of aging*. **18**, 661-669.
Wang Y , Ha Y (2004). The X-ray structure of an antiparallel dimer of the human amyloid precursor protein E2 domain. *Mol Cell*. **15**, 343-353.
Wasco W, Bupp K, Magendantz M, Gusella JF, Tanzi RE , Solomon F (1992). Identification of a mouse brain cDNA that encodes a protein related to the Alzheimer disease-associated amyloid beta protein precursor. *Proc Natl Acad Sci USA*. **89**, 10758-10762.

Wasco W, Gurubhagavatula S, Paradis MD, Romano DM, Sisodia SS, Hyman BT, Neve RL , Tanzi RE (1993a). Isolation and characterization of APLP2 encoding a homologue of the Alzheimer's associated amyloid beta protein precursor. *Nature genetics*. **5**, 95-100.

Wasco W, Peppercorn J , Tanzi RE (1993b). Search for the genes responsible for familial Alzheimer's disease. *Annals of the New York Academy of Sciences*. **695**, 203-208.

Wen C, Levitan D, Li X , Greenwald I (2000). *spr-2*, a suppressor of the egg-laying defect caused by loss of *sel-12* presenilin in *Caenorhabditis elegans*, is a member of the SET protein subfamily. *Proc Natl Acad Sci USA*. **97**, 14524-14529.

Wen C, Metzstein MM , Greenwald I (1997). SUP-17, a *Caenorhabditis elegans* ADAM protein related to *Drosophila* KUZBANIAN, and its role in LIN-12/NOTCH signalling. *Development*. **124**, 4759-4767.

Westlund B, Parry D, Clover R, Basson M , Johnson CD (1999). Reverse genetic analysis of *Caenorhabditis elegans* presenilins reveals redundant but unequal roles for *sel-12* and *hop-1* in Notch-pathway signaling. *Proc Natl Acad Sci USA*. **96**, 2497-2502.

Withee J, Galligan B, Hawkins N , Garriga G (2004). *Caenorhabditis elegans* WASP and Ena/VASP proteins play compensatory roles in morphogenesis and neuronal cell migration. *Genetics*. **167**, 1165-1176.

Wittenburg N, Eimer S, Lakowski B, Röhrig S, Rudolph C , Baumeister R (2000). Presenilin is required for proper morphology and function of neurons in *C. elegans*. *Nature*. **406**, 306-309.

Wolfe MS, Xia W, Ostaszewski BL, Diehl TS, Kimberly WT , Selkoe DJ (1999). Two transmembrane aspartates in presenilin-1 required for presenilin endoproteolysis and gamma-secretase activity. *Nature*. **398**, 513-517.

Wu G, Hubbard EJ, Kitajewski JK , Greenwald I (1998). Evidence for functional and physical association between *Caenorhabditis elegans* SEL-10, a Cdc4p-related protein, and SEL-12 presenilin. *Proc Natl Acad Sci USA*. **95**, 15787-15791.

Xu K, Tavernarakis N , Driscoll M (2001). Necrotic cell death in *C. elegans* requires the function of calreticulin and regulators of Ca(2+) release from the endoplasmic reticulum. *Neuron*. **31**, 957-971.

Yankner BA, Duffy LK , Kirschner DA (1990). Neurotrophic and neurotoxic effects of amyloid beta protein: reversal by tachykinin neuropeptides. *Science*. **250**, 279-282.

Ye Y, Lukinova N , Fortini ME (1999). Neurogenic phenotypes and altered Notch processing in *Drosophila* Presenilin mutants. *Nature*. **398**, 525-529.

Yoshikai S, Sasaki H, Doh-ura K, Furuya H , Sakaki Y (1990). Genomic organization of the human amyloid beta-protein precursor gene. *Gene*. **87**, 257-263.

Yu G, Nishimura M, Arawaka S, Levitan D, Zhang L, Tandon A, Song YQ, Rogaeva E, Chen F, Kawarai T, Supala A, Levesque L, Yu H, Yang DS, Holmes E, Milman P, Liang Y, Zhang DM, Xu DH, Sato C, Rogaev E, Smith M, Janus C, Zhang YJ, Aebersold R, Farrer LS, Sorbi S, Bruni A, Fraser P , St George-Hyslop P (2000). Nicastrin modulates presenilin-mediated notch/*glp-1* signal transduction and betaAPP processing. *Nature*. **407**, 48-54.

Zambrano N, Bimonte M, Arbucci S, Gianni D, Russo T , Bazzicalupo P (2002). *feh-1* and *apl-1*, the *Caenorhabditis elegans* orthologues of mammalian Fe65 and beta-amyloid precursor protein genes, are involved in the same pathway that controls nematode pharyngeal pumping. *J Cell Sci*. **115**, 1411-1422.

Zheng H, Jiang M, Trumbauer ME, Sirinathsinghji DJ, Hopkins R, Smith DW, Heavens RP, Dawson GR, Boyce S, Conner MW, Stevens KA, Slunt HH, Sisoda SS, Chen HY , Van der Ploeg LH (1995). beta-Amyloid precursor protein-deficient mice show reactive gliosis and decreased locomotor activity. *Cell*. **81**, 525-531.

Zheng H , Koo E (2006). The amyloid precursor protein: beyond amyloid. *Mol*

Neurodegeneration. **1**, 5.

Chapter III: APL-1, an APP-related protein, acts via DAF-16/FOXO and DAF-12 to affect lifespan in *C. elegans*

Collin Y. Ewald and Chris Li

III.1. Abstract

Alzheimer's disease is an age-related neurodegenerative disease. Mutations and duplications in the amyloid precursor protein (*APP*) gene are correlated with cases of familial Alzheimer's disease. Furthermore, Down Syndrome patients, who have a trisomy of chromosome 21, the chromosome on which APP is located, and families in whom regions of chromosome 21 containing APP are duplicated show a high incidence of early-onset Alzheimer's disease. Here, we investigate the effects of overexpression of an *APP*-related protein, APL-1, the *Caenorhabditis elegans* orthologue of mammalian *APP*. Transgenic animals driving APL-1 overexpression either with its endogenous promoter or with a pan-neuronal promoter displayed a shortened mean lifespan. Surprisingly, transgenic animals driving APL-1 overexpression with the *snb-1* promoter, which expresses in many tissue types including all neurons, showed an increased mean lifespan. The increased lifespan is dependent on signals from the gonad and activity of the DAF-16/ FOXO transcription factor and DAF-12 nuclear hormone receptor. APL-1 modulates the cellular localization of DAF-16/FOXO: endogenous APL-1 expression slowed, whereas APL-1 overexpression driven by the *snb-1* promoter accelerated DAF-16 nuclear localization. Lowering *daf-2* insulin/IGF-1 receptor activity suppresses the

negative lifespan effects of endogenous APL-1 overexpression. Our results demonstrate a molecular link between APL-1 and the insulin/IGF-1 signaling pathway on lifespan; such a link may also occur in mammals.

III.2. Introduction

Alzheimer's disease is a neurodegenerative disorder affecting over five million Americans (Alzheimer's Association 2010). The disease is characterized by the deposition of amyloid plaques in brain tissue; the major component of the plaques is the beta-amyloid peptide, a cleavage product of the amyloid precursor protein (APP) (Glenner & Wong 1984; Masters *et al*. 1985; Kang *et al*. 1987). Mutations in *APP*, which is located on chromosome 21, and in genes that produce the *presenilin 1* and *presenilin 2* enzymes that cleave APP are correlated with cases of familial Alzheimer's disease (Chartier-Harlin *et al*. 1991; Goate *et al*. 1991; Murrell *et al*. 1991; Levy-Lahad *et al*. 1995a; Levy-Lahad *et al*. 1995b; Rogaev *et al*. 1995; Sherrington *et al*. 1995; Li *et al*. 2000; Kimberly *et al*. 2003). In mammals, the functional analysis of APP is complicated by the presence of two APP-related proteins, APLP1 and APLP2 (von Koch *et al*. 1997; Heber *et al*. 2000; Herms *et al*. 2004). Whereas knockouts of individual *APP* family members are viable, double knockouts of *APP* and *APLP2* or *APLP1* and *APLP2* result in postnatal lethality (von Koch *et al*. 1997; Heber *et al*. 2000; Herms *et al*. 2004), indicating an essential role for the APP family and functional overlap among family members. Interestingly, duplication of the *APP* gene has also been associated with families that develop early-onset Alzheimer's disease (Cabrejo *et al*. 2006; Rovelet-Lecrux *et al*. 2006; Sleegers *et al*. 2006). More strikingly, Down Syndrome patients, who

have a trisomy of chromosome 21 (Glenner & Wong 1984), have a high incidence of early-onset Alzheimer's disease (Mann & Esiri 1989; Schupf *et al*. 1998; Korbel *et al*. 2009). These findings suggest that higher levels of APP, whether it be higher levels of the beta-amyloid peptide, the extracellular or cytoplasmic fragments, and/or full-length APP, is correlated with early-onset Alzheimer's disease. However, the cellular functions of APP and related proteins remain unclear. The functions of genes correlated with Alzheimer's disease, including the presenilin genes, were first identified in genetic screens of the model organism *Caenorhabditis elegans* (reviewed in (Ewald & Li 2010)). We have been examining the role of APL-1, the *C. elegans* orthologue of mammalian APP. Loss of *apl-1* results in a completely penetrant larval lethality that can be rescued by the reintroduction of either full-length APL-1 or only the extracellular domain of APL-1 (APL-1EXT; (Hornsten *et al*. 2007)). Overexpression of APL-1 also causes a larval lethality, but the lethality shows an incomplete penetrance that is correlated with levels of APL-1 (Hornsten *et al*. 2007). Similarly, overexpression of APP in mice causes early developmental lethality (Hsiao *et al*. 1995). In addition, mice that escape this lethality also display a shortened lifespan (Hsiao *et al*. 1995). Here, we examine the effects of overexpression of APL-1 on longevity. We find that the tissues in which APL-1 is overexpressed determine how APL-1 modulates lifespan. These lifespan effects are dependent on DAF-16/FOXO, a transcription factor that is a main regulator of lifespan and reproductive growth in *C. elegans*.

III.3. Results

III.3.1. Endogenous overexpression of APL-1 shortens lifespan

Transgenic lines *ynIs86* and *ynIs79* overexpress full-length APL-1 under its endogenous promoter (Hornsten *et al*. 2007); these lines showed a 16% and 18% shorter mean lifespan compared to wild-type animals, respectively (Figs. 1A and B and Table 1). Furthermore, the mean lifespans of animals overexpressing APL-1EXT, as in a mutant allele [*apl-1*(*yn5*)] or by a transgene (*ynIs71*), were 12% and 18% shorter compared to wild-type animals, respectively (Figs. 1C and D and Table 1). Animals that overexpressed a mutated, non-functional APL-1 protein (*ynIs100* or *ynIs107*) or a non-functional APL-1EXT (*ynIs106*) or carried only the transgenic markers exhibited a normal lifespan (Table 1). Hence, endogenously driven overexpression of APL-1 or APL-1EXT shortens lifespan.

III.3.2. Ectopic pan-neuronal expression of APL-1 shortens lifespan

Although *apl-1* is expressed in many cell types, including neurons (roughly 50 of the 302 neurons), head and vulval muscles, and hypodermal and seam cells, pan-neuronal expression of APL-1 with the *rab-3* promoter (P*rab-3*::APL-1) is sufficient to rescue the *apl-1* loss-of-function lethality (Hornsten *et al*. 2007; Niwa *et al*. 2008). To determine the effects of ectopic APL-1 expression in neurons, we examined how lifespan is affected in animals expressing the P*rab-3*::APL-1 transgene. Consistent with endogenous APL-1 overexpression, P*rab-3*::APL-1 animals showed a 9-23% decrease in mean lifespan (*ynIs91*, -15%; *ynIs104*, -23%; *ynEx193*, -9%) compared to wild type (Figs. 1E and Table 1). Hence, overexpression of APL-1 in neurons is sufficient to shorten lifespan.

III.3.3. Ectopic expression of APL-1 driven by the *snb-1* promoter increases lifespan

Driving APL-1 overexpression with the *snb-1* promoter also rescues the *apl-1* loss-of-function lethality (Hornsten *et al*. 2007). Surprisingly, however, animals with P*snb-1*::APL-1 or P*snb-1*::APL-1EXT expression showed a 13-25% increase in mean lifespan (P*snb-1*::APL-1: *ynIs13*, +21%; *ynIs12*, +24%; P*snb-1*::APL-1EXT: *ynIs105*, +25%; *ynEx165*, +13%) compared to wild-type animals (Figs. 1G and J and Table 1). Varying levels of APL-1 expression, however, do not appear to account for the differential lifespan effects (Fig. S1; (Hornsten *et al*. 2007)). As determined by western blot analysis, short-lived *ynIs104* [P*rab-3*::APL-1] and *ynIs86* [P*apl-1*::APL-1] animals showed a 3-5-fold and 125-fold higher APL-1 expression level, respectively, whereas long-lived *ynIs12* [P*snb*::APL-1] animals showed a 71-fold higher APL-1 expression level compared to wild type (Fig. S1; (Hornsten *et al*. 2007)). Hence, P*snb-1*::APL-1 animals have an increased lifespan independent of the level of APL-1 expression.

III.3.4. Ectopic expression of APL-1 driven by the *snb-1* promoter may activate a protective mechanism

Because endogenous and *snb-1* promoter driven APL-1 overexpression has opposing effects on lifespan, we generated animals carrying both transgenes to determine the effect on lifespan. The double transgenic animals (*ynIs12* [P*snb-1*::APL-1]; *ynIs86* [P*apl-1*::APL-1]) produced higher levels of APL-1 protein than in the single transgenic animals (Fig. S1) and showed the same enhanced lifespan as *ynIs12* [P*snb-1*::APL-1 animals] (P=0.4; Fig. S2, Table 1). Thus, P*snb-1*::APL-1 expression activates a pathway that

promotes longevity and protects against the negative effects of high levels of endogenous APL-1 overexpression.

The different lifespans seen in transgenic animals overexpressing APL-1 with the *snb-1* or endogenous *apl-1* promoters are presumably due to the different tissues in which APL-1 is overexpressed. Although there is considerable overlap in the expression patterns of the two promoters, highest levels of GFP-tagged APL-1 (APL-1::GFP) driven by the *snb-1* promoter was seen in neurons, supporting cells, and the somatic gonad (Fig. S3). Interestingly, signals from the somatic gonad as well as germline have been reported to affect lifespan in *C. elegans* (Hsin & Kenyon 1999; Arantes-Oliveira *et al*. 2002; Berman & Kenyon 2006; Yamawaki *et al*. 2008).

III.3.5. Increased lifespan in P*snb-1*::APL-1 animals depends on signals from the gonad

As with other organisms, lifespan is dependent on environmental and genetic factors in *C. elegans*. For instance, the gonad generates two opposing signals to modulate lifespan: the somatic gonad releases a signal that promotes lifespan, whereas the germline precursors produce a signal that inhibits lifespan (Hsin & Kenyon 1999; Lin *et al*. 2001; Arantes-Oliveira *et al*. 2002; Berman & Kenyon 2006; Yamawaki *et al*. 2008). Hence, ablation of germline precursors extends lifespan, while loss of the somatic gonad decreases lifespan (Hsin & Kenyon 1999; Arantes-Oliveira *et al*. 2002; Berman & Kenyon 2006; Yamawaki *et al*. 2008). To determine the contribution of gonadal signals on lifespan extension, we ablated the gonadal precursor cells Z1-Z4 in P*snb-1*::APL-1 animals; the ablated transgenic animals no longer showed an increased lifespan (Fig. 3

and Table 1). By contrast, using a *glp-1* mutation to delete the germline precursor cells (Arantes-Oliveira *et al*. 2002), we found an enhancement of the extended lifespan in P*snb-1*::APL-1EXT animals compared to *glp-1* mutants alone (Fig. 3 and Table 1). Hence, the lifespan extension of P*snb-1*::APL-1 animals requires the gonad and the APL-1 effects are synergistic to signals that promote longevity.

III.3.6. P*snb-1*::APL-1 animals age slower than wild-type animals

To determine whether different APL-1 overexpression lines express aging biomarkers at different rates, we measured two age-specific phenotypes: pharyngeal pumping as an indicator for organ function (Johnston *et al*. 2008) and lipofuscin autofluorescence as a marker for accumulation of waste products (Gerstbrein *et al*. 2005). Transgenic adult animals that overexpress APL-1 (*ynIs86* and *ynIs79*) or APL-1EXT (*ynIs71*) under its endogenous promoter showed a strong decline in pharyngeal pumping at day 8, whereas animals with P*snb-1*::APL-1 expression (*ynIs12* and *ynIs13*) showed the same or slightly higher pumping rates compared to wild-type worms at day 8 and even up to day 15 (Figs. 2 and S2). Similarly, the levels of autofluorescent lipofuscin in the intestine of animals with P*snb-1*::APL-1 expression were much lower than wild-type levels at days 8 and 11 of adulthood (Fig. 2 and Table S1). As judged by these aging markers, transgenic animals with P*snb-1*::APL-1 expression appear to age slower than wild-type animals, whereas P*apl-1*::APL-1 animals appear to have accelerated aging.

III.3.7. Lifespan extension in P*snb-1*::APL-1 animals requires DAF-12 nuclear hormone receptor and DAF-16 FOXO transcription factor activity

Activity of DAF-12, a putative steroid hormone receptor (NHR) homologous to the human vitamin D receptor, and DAF-16, a FOXO transcription factor, is required to promote lifespan extension in germline-ablated animals (Hsin & Kenyon 1999). To determine whether DAF-12 and DAF-16 activity are also required for lifespan extension in P*snb-1*::APL-1 animals, we examined P*snb-1*::APL-1 animals in *daf-16* null or *daf-12* mutant backgrounds. The lifespan extension of transgenic animals with P*snb-1*::APL-1 or P*snb-1*::APL-1EXT expression were abolished in the absence of *daf-16* (*daf-16(0); ynIs12* [P*snb-1*::APL-1], *daf-16(0); ynIs13* [P*snb-1*::APL-1], *daf-16(0);ynIs105* [P*snb-1*::APL-1EXT]) or decreased *daf-12* (*ynIs12* [P*snb-1*::APL-1]*; daf-12(m20)* and *ynIs105* [P*snb-1*::APL-1EXT]*; daf-12(m20)*) activity. The increased longevity in the P*snb-1*::APL-1 transgenic animals, therefore, requires DAF-16 and DAF-12 activity (Figs. 1H, 1I, 1K, and S2 and Table 1). The simplest model would be that APL-1 expression in the somatic gonad enhances longevity, presumably through DAF-16 and DAF-12 activity; these APL-1 effects in the somatic gonad are inhibited by signals from the germline.

III.3.8. Decreased signaling from the insulin/IGF-1 pathway is protective against the effects of endogenous APL-1 overexpression

DAF-16/FOXO acts in multiple pathways to execute its function as a major regulator of lifespan and reproductive growth. Loss of *daf-16*, such as in *daf-16(mu86)* mutants, causes a decreased lifespan (Apfeld & Kenyon 1999). The shortened lifespan of *daf-16(mu86)* mutants was further enhanced by either endogenous [-7 to -17%; *daf-16(0);*

ynIs86, daf-16(0); ynIs79, and *daf-16(0); apl-1(yn5)*] or pan-neuronal [-27%; *daf-16(0); ynIs104* P*rab-3*::APL-1] APL-1 expression, suggesting that the lack of DAF-16 activity accelerates the detrimental effects of endogenous or pan-neuronal APL-1 overexpression on lifespan (Fig. 1F and Table 1).

Under favorable environmental conditions, the DAF-2/insulin/IGF-1 receptor is activated to initiate a signaling cascade that results in the phosphorylation of DAF-16/FOXO. Phosphorylated DAF-16/FOXO is retained in the cytoplasm, whereas non-phosphorylated DAF-16/FOXO enters the nucleus to initiate transcription of genes that can promote longevity (reviewed in (Kenyon 2005)). Hence, reducing DAF-2 activity, whether by mutation [e.g., *daf-2(e1370)*] and/or by RNAi, promotes longevity and an extended lifespan, presumably by increasing DAF-16 activity (Kenyon *et al*. 1993; Hsin & Kenyon 1999; Lin *et al*. 2001; Arantes-Oliveira *et al*. 2003; Libina *et al*. 2003; Yamawaki *et al*. 2008); conversely, lack of DAF-16 activity, such as with the *daf-16(mu86)* null allele, abolishes the extended lifespan of *daf-2(e1370)* mutants (Kenyon *et al*. 1993; Hsin & Kenyon 1999; Lin *et al*. 2001; Libina *et al*. 2003). Similar to loss of *daf-16*, loss of *daf-12* NHR decreases lifespan, suggesting that *daf-12* activity promotes longevity (Larsen *et al*. 1995). In a *daf-2(e1370); daf-12(m20)* double mutant, the extended lifespan of *daf-2(e1370)* mutants is enhanced, but this enhancement and extended lifespan are abolished in a *daf-16* null background (Larsen *et al*. 1995), suggesting that *daf-16* acts downstream of *daf-2* and *daf-12* to promote longevity.

How does DAF-2 activity affect mean lifespans in animals that overexpress APL-1? *daf-2(e1370)* mutants that overexpress APL-1 or APL-1EXT under its endogenous promoter (*daf-2(e1370); ynIs79* [APL-1::GFP] or *daf-2(e1370); apl-1(yn5)* APL-1EXT)

showed a similar mean lifespan compared to *daf-2(e1370)* mutants alone, suggesting that decreased *daf-2* insulin/IGF-1 receptor activity protects against the negative lifespan effects due to endogenous APL-1 overexpression (Fig. 1L and Table 1). Although their maximal lifespans were similar, *daf-2(e1370)* mutants with pan-neuronal APL-1 expression (*daf-2(e1370); ynIs104* P*rab-3*::APL-1]) showed a shorter mean lifespan (-31%) than *daf-2(e1370)* animals alone (Fig. 1L and Table 1), suggesting that reduced *daf-2* activity is not sufficient to negate the effects of pan-neuronal APL-1 expression. By contrast, *daf-2(e1370)* mutants with P*snb-1*::APL-1 expression (*daf-2(e1370); ynIs12* [P*snb-1*::APL-1]) showed a 14% enhancement of the extended lifespan in *daf-2(e1370)* mutants, suggesting that P*snb-1*::APL-1 expression either further reduces DAF-2 activity or activates a parallel pathway that synergizes with the activated longevity pathway in *daf-2(e1370)* mutants (Fig. 1L and Table 1).

Collectively, these results suggest that APL-1 activity can modulate lifespan: decreased insulin/IGF-1 signaling suppresses the decreased lifespan due to endogenous APL-1 overexpression, while P*snb-1*::APL-1 signaling is dependent on gonadal signals and DAF-16/FOXO and DAF-12 NHR activity to enhance longevity.

III.3.9. APL-1 modulates DAF-16 nuclear localization

Because *daf-16*/FOXO is required for the increased longevity in P*snb-1*::APL-1 animals, we examined whether APL-1 overexpression affects DAF-16 activity on a molecular level. Animals carrying a GFP-tagged DAF-16 transgene (DAF-16::GFP) showed an ~16% increased lifespan (Henderson & Johnson 2001). We monitored whether APL-1 overexpression modulated the translocation of DAF-16::GFP in response to a heat stress.

In wild-type animals, a heat stress of 35ºC causes all DAF-16::GFP to translocate from the cytoplasm into the nucleus within 3 hours (Henderson & Johnson 2001). Transgenic animals that overexpress APL-1 under its endogenous promoter delayed translocation of DAF-16::GFP into the nucleus by 30 minutes [DAF-16::GFP; *ynIs79*]; by contrast, animals expressing P*snb-1*::APL-1 accelerated translocation of DAF-16::GFP into the nucleus by 30 minutes (Figs. 4A and S4 and Table S2). These results suggest that endogenous APL-1 overexpression slows, whereas P*snb-1*::APL-1 expression accelerates DAF-16 nuclear translocation. Furthermore, these results indicate that APL-1 acts upstream of DAF-16 and, depending on the tissue in which APL-1 is expressed, differentially regulates DAF-16 localization.

III.3.10. DAF-16::GFP nuclear localization correlates with development progression

While performing these assays, we noticed that double transgenic P*apl-1*::APL-1; DAF-16::GFP animals developed very slowly. *ynIs79* [P*apl-1*::APL-1] animals developed at the same rate as wild-type animals at 20ºC (23; not shown). Animals that overexpress DAF-16 (e.g., DAF-16::GFP animals), however, had a slowed developmental progression through the four larval stages (L1 to L4; (Henderson & Johnson 2001); Fig. 4B). The delayed development of DAF-16::GFP animals was further retarded by endogenous overexpression of APL-1 [DAF-16::GFP; *ynIs79*] (Fig. 4B), suggesting that APL-1 modulates the activity of DAF-16.

Like P*apl-1*::APL-1 animals, P*snb-1*::APL-1 animals developed at a similar rate as wild type at 20ºC (Hornsten *et al*. 2007). In contrast to P*apl-1*::APL-1 expression,

P*snb-1*::APL-1 expression suppressed the delayed development of animals with increased DAF-16 activity, such that the developmental progression was similar to wild type; however, 20% of the DAF-16::GFP; *ynIs12* animals remained in L1 arrest (Figure 4B). Hence, when DAF-16 activity is increased, endogenous APL-1 overexpression slows, whereas P*snb-1*::APL-1 expression accelerates developmental progression, perhaps by modulating the nuclear translocation rate of DAF-16::GFP.

III.4. Discussion

Longevity is the result of a combination of environmental effects and genetic factors. *C. elegans* is constantly monitoring its surroundings and integrating this information to regulate its metabolic and reproductive processes, which ultimately determine the animal's lifespan. Several tissues, such as neurons, intestine and gonad, have been implicated in regulating lifespan in *C. elegans* (Kenyon 2005). For instance, ablation of certain amphidial neurons, which sense the environment, can either lead to an increased or a decreased lifespan mediated at least partly via DAF-16/FOXO activity (Alcedo & Kenyon 2004). Similarly, ablation of germline precursor cells (Z2 and Z3), which give rise of the germline, leads to an increase of lifespan mediated via *daf-12*/nuclear hormone receptor and *daf-16*/FOXO, whereas ablating the whole gonad (Z1-Z4) leads to a decreased lifespan (Hsin & Kenyon 1999).

The effects of APL-1 overexpression on lifespan were far more complex than anticipated. Endogenous overexpression of APL-1 accelerated aging and decreased lifespan. These effects were suppressed by decreasing *daf-2* insulin/IGF-1 receptor activity, presumably resulting in increased *daf-16*/FOXO activity. *daf-2* mutant animals

live twice as long as wild type and are much healthier than wild-type animals (Kenyon *et al*. 1993). Hence, lowering *daf-2* activity when APL-1 is overexpressed appears to delay aging, thereby counteracting the negative effects of APL-1. Similarly, lowering *daf-2* activity is proteoprotective during aging against the paralysis caused by overexpression of the human Aβ peptide in *C. elegans* (Cohen *et al*. 2006).

By contrast, APL-1 overexpression with the *snb-1* promoter delayed aging and increased lifespan. Because the extended lifespan of P*snb-1*::APL-1 animals is dependent on the presence of the gonad, the simplest model is that increased APL-1 expression in the gonad activates DAF-16/FOXO and DAF-12 NHR to extend lifespan. The site of DAF-16/FOXO and DAF-12 NHR activation is unclear. APL-1 activity in the somatic gonad could decrease the inhibitory signal from the reproductive system that modulates *daf-16* and *daf-12* activity (Figure 5). Because the increased lifespan of *daf-2* insulin/IGF-1 receptor mutants is further enhanced in P*snb-1*::APL-1 animals, APL-1 is likely to act in a parallel pathway as DAF-2 or further lowers DAF-2 insulin/IGF-1 receptor activity, thereby increasing DAF-16 activity.

Pan-neuronal APL-1 expression also decreased lifespan. However, these effects were independent of *daf-2* and *daf-16* activity. Because the animals carrying the P*rab-3*::APL-1 transgene were unhealthy and lines were difficult to isolate, we hypothesize that increasing APL-1 levels in neurons has a toxic effect on the cells. Although the P*snb-1*::APL-1 transgene also expresses in all neurons, the beneficial effects of APL-1 expression in other cell types appears to suppress the toxic effects of APL-1 expression in neurons. Collectively, our results indicate that cell-specific APL-1 expression activates different cellular and metabolic pathways, which cause a range of effects on lifespan.

Although the predominant cause of neurodegeneration in Alzheimer's disease patients appears to be the neurotoxic effects of beta-amyloid peptide deposition, overexpression of the different APP fragments may also cause have negative effects on the viability of neurons and/or metabolism of the organism.

III.5. Materials and methods

III.5.1. Strains

Caenorhabtitis elegans strains were grown and maintained on MYOB plates (Church *et al*. 1995) containing OP50 Escherichia coli bacteria at 20ºC using methods as described (Brenner 1974), unless noted. All mutations used are described in Wormbase (www.wormbase.org) and include: LGI: *daf-16(mu86)* (Lin *et al*. 1997); LGIII: *daf-2(e1370)* (Kimura *et al*. 1997), *glp-1(e2141)* (Priess *et al*. 1987); LGX: *daf-12(m20)* (Larsen *et al*. 1995), *lon-2(e678), apl-1(yn5* and *yn10)* (Hornsten *et al*. 2007), and *dpy-8(e130)*. Construction of the APL-1 transgenes and the resulting transgenic lines are described (Hornsten *et al*. 2007). Non-integrated transgenic lines used were: *ynEx30* (P*apl-1*::APL-1, *sur-5*::GFP), *ynEx65* (P*snb-1*::APL-1(*yn5*)(cDNA), *sur-5*::GFP), *ynEx93* (P*rab-3*::APL-1(cDNA)::GFP, pRF4 *rol-6(su1006gf)*), and *ynEx109* (P*snb-1*::APL-1(cDNA)::GFP). Integrated transgenic lines used were: *ynIs106* (P*apl-1*::APL-1(*yn32 yn5*) P*myo-2*::GFP); LGI: *ynIs109* (P*snb-1*::APL-1(cDNA)::GFP); LGII: *ynIs105* (P*snb-1*::APL-1(*yn5*)(cDNA), *sur-5*::GFP); LGIII: *ynIs12* (P*snb-1*::APL-1(cDNA), *lin-15B*(+)); LGIV: *vsIs13* (*lin-11*::*pes-10*::GFP, *lin-15*(+))(Bany *et al*. 2003), *ynIs104* (P*rab-3*::APL-1(cDNA)::GFP, P*myo-2*::GFP), *zIs356* (P*daf-16*::DAF-16::GFP, pRF4 *rol-6(su1006gf)*) (Henderson & Johnson 2001); LGV: *ynIs13* (P*snb-1*::APL-1(cDNA), *lin-*

15B(+)), *ynIs71* (P*apl-1*::APL-1(*yn5*)), *ynIs79* (P*apl-1*::APL-1::GFP), *ynIs100* (P*apl-1*::APL-1(*yn32*)::GFP, pRF4 *rol-6(su1006gf)*); and LGX: *ynIs86* (P*apl-1*::APL-1, *sur-5*::GFP), *ynIs91* (P*rab-3*::APL-1, pRF4 *rol-6(su1006gf)*), and *ynIs107* (P*apl-1*::APL-1(*yn32* E71K/D342C/S362C)::GFP, P*myo-2*::GFP) (Hoopes *et al*. 2010).

III.5.2. Adult lifespan assays

All strains were grown for at least two generations at 20ºC, except for *daf-2(e1370)* and *glp-1(e2141)* animals, which were raised at 15ºC. All adult lifespans [except *glp-1(e2141)*] were measured starting from the L4 stage at 20ºC and assayed as described (Kenyon *et al*. 1993; Larsen *et al*. 1995). Animals carrying the temperature sensitive *glp-1(e2141)* allele and appropriate control animals were shifted from 15ºC to 25ºC at the L1 stage and lifespan assays were performed at 25ºC as described (Arantes-Oliveira *et al*. 2002). Note that the wild-type N2 var. Bristol strain has been maintained for many generations in different labs and can have mean lifespans ranging from 12 to 17 days at 20ºC (Gems & Riddle 2000). In addition, for all experiments MYOB plates were used instead of NGM plates; N2 animals grown on MYOB plates have a slightly shorter lifespan (14 days) (Keightley & Caballero 1997) than N2 animals grown on NGM plates (~16 days). N2 animals from another lab (kindly provided by Cathy Savage-Dunn) showed a similar lifespan as our N2 stock on MYOB plates in 4 independent trials (N=198/398). To determine whether the laboratory N2 animals had a longer lifespan on NGM plates, N2 animals were grown on MYOB until the L4 stage and then transferred onto NGM plates for lifespan analysis; these animals showed a mean lifespan of 18.62±0.47days (60/111 animals). These results indicate that the N2 mean lifespan of 14

days reported here is due to the different composition of the MYOB plates compared to NGM plates.

III.5.3. Ablation of gonadal precursor cells (Z1-4) and lifespan assays

ynIs12 [P*snb-1*::APL-1] animals at the L1 stage were mounted onto agar pads containing 20 mM sodium azide. The gonadal precursor cells (Z1-4) were ablated by using a laser microbeam at 10-15 Hz (laser was set to the minimum intensity required to crack the cover slip). Wild type (N2) and *ynIs12* [P*snb-1*::APL-1] animals were also were mounted onto agar pads containing 20 mM sodium azide and dismounted without laser ablation as control animals (sham animals).

III.5.4. Pharyngeal pumping assays

The pharyngeal pumping rate was determined by the number of pumps per 20 seconds; measurements were only taken when worms were on bacteria and pumped at a constant rate without any pauses.

III.5.5. Autofluorescense assays

L4 animals were picked and scored at appropriate times. Animals were placed on an agar pad containing a drop of 10 mM NaN_3. Pictures were taken with a Hamamatsu ORCA-ER digital camera on a Zeiss Axioplan microscope. The area directly behind the last bulb of the pharynx was photographed using Openlab 3.1.3 software (Improvision) with the same settings for all animals and conditions. The autofluorescence intensities were derived by selecting a defined area of the worm in the pictures and computing the "mean gray value" by ImageJ software (NIH).

III.5.6. Developmental timing assays

To synchronize worm populations ~15 gravid adult worms were placed into a NaOCl solution to release the eggs. Hatched worms were raised at 20ºC. Four days later [or five days for slower developing strains such as *zIs356* (DAF-16::GFP)], 10 synchronized adults were placed onto a fresh plate and allowed to lay eggs for 1-1.5 hours at room temperature (22-24ºC). Eggs were counted, F1 progeny were placed at 20ºC to allow development. After 70-72 hours, the developmental stages of the animals at 20ºC were scored.

III.5.7. DAF-16::GFP nuclear translocation assays

L4 animals were placed onto new plates and grown at 20ºC. One day later, animals were placed at 35ºC and scored at different times (T=0, 30, 60, 90, 120, 150, 180, 210 and 240 minutes) by mounting the animals onto 2% agar pads containing a drop of M9 physiological buffer (M9 is defined (Brenner 1974)) and viewing the worms at 100x magnification on a Zeiss Axioplan microscope. To ensure exact timing, the individual strains were placed at 35ºC in five minutes intervals. Upon 35ºC heat stress, DAF-16::GFP translocates from the cytoplasm into the nucleus (Henderson & Johnson 2001). The rate of DAF-16::GFP nuclear translocation was scored as described (Curran & Ruvkun 2007): category 0: all DAF-16::GFP showing diffuse localization in the cytoplasm; category 1: more DAF-16::GFP localized in cytoplasm than in nucleus; category 2: more DAF-16::GFP localized in nucleus than in cytoplasm; category 3: almost all DAF-16::GFP localized in nucleus.

III.5.8. Western blot analysis

Preparations of animal lysates and western blots were performed as described (Hornsten *et al*. 2007). Protein levels were normalized to levels of actin (~40 kDa) for each strain, so that similar amounts of total protein were loaded for each strain. For each blot, the blot was first probed with an actin monoclonal antibody (JLA20 at 1:2000; Developmental Studies Hybridoma Bank; secondary antibody anti-mouse-goat-HRP at 1:1000), washed three times with TAE, and then re-probed with an anti-APL-1 antiserum against the extracellular domain of APL-1 (Hornsten *et al*. 2007). Relative protein levels were determined by relative intensity to wild type (N2) using NIH Image J Gel analyzer.

III.6. Acknowledgments

We wish to thank the labs of Iva Greenwald and Oliver Hobert for use of their lasers, Jane Hubbard's group for kindly providing *glp-1* mutants, Cathy Savage-Dunn's group for kindly providing their N2, Mahmoud Salem and Lana Tolen for confirming lifespan experiments, lab members for helpful discussions, Sarah Tichelli help with statistical analysis, Roy and Gab Ewald, Wolfgang Maier, Cathy Savage-Dunn, and Piali Sengupta for comments on the manuscript, and CGC, which is supported by the NIH National Center for Research Resources, for providing *daf-16,* DAF-16::GFP, and *daf-12* worms. This work was supported by grants from the Alzheimer's Association, National Institutes Health (R21AG0339 and R01AG32042), and National Science Foundation (IOS08207) (CL) and a National Institutes of Health RCMI grant (G12-RR03060-25) to City College.

III.7. References

Alcedo J , Kenyon C (2004). Regulation of *C. elegans* longevity by specific gustatory and olfactory neurons. *Neuron*. **41**, 45-55.

Alzheimer's Association KM (2010). 2010 Alzheimer's disease facts and figures. *Alzheimer's and Dementia*. **6**, 158-194.

Apfeld J , Kenyon C (1999). Regulation of lifespan by sensory perception in *Caenorhabditis elegans*. *Nature*. **402**, 804-809.

Arantes-Oliveira N, Apfeld J, Dillin A , Kenyon C (2002). Regulation of life-span by germ-line stem cells in *Caenorhabditis elegans*. *Science* **295**, 502-505.

Arantes-Oliveira N, Berman JR , Kenyon C (2003). Healthy animals with extreme longevity. *Science* **302**, 611.

Bany IA, Dong MQ , Koelle MR (2003). Genetic and cellular basis for acetylcholine inhibition of *Caenorhabditis elegans* egg-laying behavior. *J Neurosci*. **23**, 8060-8069.

Berman JR , Kenyon C (2006). Germ-cell loss extends *C. elegans* life span through regulation of DAF-16 by *kri-1* and lipophilic-hormone signaling. *Cell*. **124**, 1055-1068.

Brenner S (1974). The Genetics of *Caenorhabditis elegans*. *Genetics*. **77**, 71-94.

Cabrejo L, Guyant-Marechal L, Laquerriere A, Vercelletto M, De la Fourniere F, Thomas-Anterion C, Verny C, Letournel F, Pasquier F, Vital A, Checler F, Frebourg T, Campion D , Hannequin D (2006). Phenotype associated with APP duplication in five families. *Brain*. **129**, 2966-2976.

Chartier-Harlin MC, Crawford F, Houlden H, Warren A, Hughes D, Fidani L, Goate A, Rossor M, Roques P, Hardy J , et al. (1991). Early-onset Alzheimer's disease caused by mutations at codon 717 of the beta-amyloid precursor protein gene. *Nature*. **353**, 844-846.

Church DL, Guan KL , Lambie EJ (1995). Three genes of the MAP kinase cascade, *mek-2*, *mpk-1/sur-1* and *let-60 ras*, are required for meiotic cell cycle progression in *Caenorhabditis elegans*. *Development*. **121**, 2525-2535.

Cohen E, Bieschke J, Perciavalle RM, Kelly JW , Dillin A (2006). Opposing activities protect against age-onset proteotoxicity. *Science*. **313**, 1604-1610.

Curran SP , Ruvkun G (2007). Lifespan regulation by evolutionarily conserved genes essential for viability. *PLoS Genet*. **3**, e56.

Ewald CY , Li C (2010). Understanding the molecular basis of Alzheimer's disease using a *Caenorhabditis elegans* model system. *Brain Struct Funct*. **214**, 263-283.

Gems D , Riddle DL (2000). Defining wild-type life span in *Caenorhabditis elegans*. *J Gerontol A Biol Sci Med Sci*. **55**, B215-219.

Gerstbrein B, Stamatas G, Kollias N , Driscoll M (2005). In vivo spectrofluorimetry reveals endogenous biomarkers that report healthspan and dietary restriction in *Caenorhabditis elegans*. *Aging Cell*. **4**, 127-137.

Glenner GG , Wong CW (1984). Alzheimer's disease and Down's syndrome: sharing of a unique cerebrovascular amyloid fibril protein. *Biochem Biophys Res Commun*. **122**, 1131-1135.

Goate A, Chartier-Harlin MC, Mullan M, Brown J, Crawford F, Fidani L, Giuffra L, Haynes A, Irving N, James L , et al. (1991). Segregation of a missense mutation in the amyloid precursor protein gene with familial Alzheimer's disease. *Nature*. **349**, 704-706.

Heber S, Herms J, Gajic V, Hainfellner J, Aguzzi A, Rulicke T, von Kretzschmar H, von Koch C, Sisodia S, Tremml P, Lipp HP, Wolfer DP , Muller U (2000). Mice with combined gene knock-outs reveal essential and partially redundant functions of amyloid precursor protein family members. *J Neurosci*. **20**, 7951-7963.

Henderson ST , Johnson TE (2001). *daf-16* integrates developmental and environmental inputs to mediate aging in the nematode *Caenorhabditis elegans*. *Curr Biol*. **11**, 1975-1980.

Herms J, Anliker B, Heber S, Ring S, Fuhrmann M, Kretzschmar H, Sisodia S , Muller U (2004). Cortical dysplasia resembling human type 2 lissencephaly in mice lacking all three APP family members. *Embo J*. **23**, 4106-4115.

Hoopes JT, Liu X, Xu X, Demeler B, Folta-Stogniew E, Li C , Ha Y (2010). Structural characterization of the E2 domain of APL-1, a *Caenorhabditis elegans* homolog of human amyloid precursor protein, and its heparin binding site. *The Journal of biological chemistry*. **285**, 2165-2173.

Hornsten A, Lieberthal J, Fadia S, Malins R, Ha L, Xu X, Daigle I, Markowitz M, O'Connor G, Plasterk R , Li C (2007). APL-1, a *Caenorhabditis elegans* protein related to the human beta-amyloid precursor protein, is essential for viability. *Proc Natl Acad Sci USA*. **104**, 1971-1976.

Hsiao KK, Borchelt DR, Olson K, Johannsdottir R, Kitt C, Yunis W, Xu S, Eckman C, Younkin S , Price D (1995). Age-related CNS disorder and early death in transgenic FVB/N mice overexpressing Alzheimer amyloid precursor proteins. *Neuron*. **15**, 1203-1218.

Hsin H , Kenyon C (1999). Signals from the reproductive system regulate the lifespan of *C. elegans*. *Nature*. **399**, 362-366.

Johnston J, Iser WB, Chow DK, Goldberg IG , Wolkow CA (2008). Quantitative image analysis reveals distinct structural transitions during aging in *Caenorhabditis elegans* tissues. *PLoS One*. **3**, e2821.

Kang J, Lemaire HG, Unterbeck A, Salbaum JM, Masters CL, Grzeschik KH, Multhaup G, Beyreuther K , Muller-Hill B (1987). The precursor of Alzheimer's disease amyloid A4 protein resembles a cell-surface receptor. *Nature*. **325**, 733-736.

Keightley PD , Caballero A (1997). Genomic mutation rates for lifetime reproductive output and lifespan in *Caenorhabditis elegans*. *Proc Natl Acad Sci USA*. **94**, 3823-3827.

Kenyon C (2005). The plasticity of aging: insights from long-lived mutants. *Cell*. **120**, 449-460.

Kenyon C, Chang J, Gensch E, Rudner A , Tabtiang R (1993). A *C. elegans* mutant that lives twice as long as wild type. *Nature*. **366**, 461-464.

Kimberly WT, LaVoie MJ, Ostaszewski BL, Ye W, Wolfe MS , Selkoe DJ (2003). Gamma-secretase is a membrane protein complex comprised of presenilin, nicastrin, Aph-1, and Pen-2. *Proc Natl Acad Sci USA*. **100**, 6382-6387.

Kimura KD, Tissenbaum HA, Liu Y , Ruvkun G (1997). *daf-2*, an insulin receptor-like gene that regulates longevity and diapause in *Caenorhabditis elegans*. *Science* **277**, 942-946.

Korbel JO, Tirosh-Wagner T, Urban AE, Chen XN, Kasowski M, Dai L, Grubert F, Erdman C, Gao MC, Lange K, Sobel EM, Barlow GM, Aylsworth AS, Carpenter NJ, Clark RD, Cohen MY, Doran E, Falik-Zaccai T, Lewin SO, Lott IT, McGillivray BC, Moeschler JB, Pettenati MJ, Pueschel SM, Rao KW, Shaffer LG, Shohat M, Van Riper AJ, Warburton D, Weissman S, Gerstein MB, Snyder M , Korenberg JR (2009). The genetic architecture of Down syndrome phenotypes revealed by high-resolution analysis of human segmental trisomies. *Proc Natl Acad Sci USA*. **106**, 12031-12036.

Larsen PL, Albert PS , Riddle DL (1995). Genes that regulate both development and longevity in *Caenorhabditis elegans*. *Genetics*. **139**, 1567-1583.

Levy-Lahad E, Wasco W, Poorkaj P, Romano DM, Oshima J, Pettingell WH, Yu CE, Jondro PD, Schmidt SD, Wang K , et al. (1995a). Candidate gene for the chromosome 1 familial Alzheimer's disease locus. *Science* **269**, 973-977.

Levy-Lahad E, Wijsman EM, Nemens E, Anderson L, Goddard KA, Weber JL, Bird TD , Schellenberg GD (1995b). A familial Alzheimer's disease locus on chromosome 1. *Science* **269**, 970-973.

Li YM, Lai MT, Xu M, Huang Q, DiMuzio-Mower J, Sardana MK, Shi XP, Yin KC, Shafer JA , Gardell SJ (2000). Presenilin 1 is linked with gamma-secretase activity in the detergent solubilized state. *Proc Natl Acad Sci USA*. **97**, 6138-6143.

Libina N, Berman JR , Kenyon C (2003). Tissue-specific activities of *C. elegans* DAF-16 in the regulation of lifespan. *Cell*. **115**, 489-502.

Lin K, Dorman JB, Rodan A , Kenyon C (1997). *daf-16*: An HNF-3/forkhead family member that can function to double the life-span of *Caenorhabditis elegans*. *Science* **278**, 1319-1322.

Lin K, Hsin H, Libina N , Kenyon C (2001). Regulation of the *Caenorhabditis elegans* longevity protein DAF-16 by insulin/IGF-1 and germline signaling. *Nature genetics*. **28**, 139-145.

Mann DM , Esiri MM (1989). The pattern of acquisition of plaques and tangles in the brains of patients under 50 years of age with Down's syndrome. *J Neurol Sci*. **89**, 169-179.

Masters CL, Simms G, Weinman NA, Multhaup G, McDonald BL , Beyreuther K (1985). Amyloid plaque core protein in Alzheimer disease and Down syndrome. *Proc Natl Acad Sci USA*. **82**, 4245-4249.

Murrell J, Farlow M, Ghetti B , Benson MD (1991). A mutation in the amyloid precursor protein associated with hereditary Alzheimer's disease. *Science* **254**, 97-99.

Niwa R, Zhou F, Li C , Slack FJ (2008). The expression of the Alzheimer's amyloid precursor protein-like gene is regulated by developmental timing microRNAs and their targets in *Caenorhabditis elegans*. *Dev Bio*. **315**, 418-425.

Priess JR, Schnabel H , Schnabel R (1987). The *glp-1* locus and cellular interactions in early *C. elegans* embryos. *Cell*. **51**, 601-611.

Rogaev EI, Sherrington R, Rogaeva EA, Levesque G, Ikeda M, Liang Y, Chi H, Lin C, Holman K, Tsuda T , et al. (1995). Familial Alzheimer's disease in kindreds with

missense mutations in a gene on chromosome 1 related to the Alzheimer's disease type 3 gene. *Nature*. **376**, 775-778.

Rovelet-Lecrux A, Hannequin D, Raux G, Le Meur N, Laquerriere A, Vital A, Dumanchin C, Feuillette S, Brice A, Vercelletto M, Dubas F, Frebourg T , Campion D (2006). APP locus duplication causes autosomal dominant early-onset Alzheimer disease with cerebral amyloid angiopathy. *Nature genetics*. **38**, 24-26.

Schupf N, Kapell D, Nightingale B, Rodriguez A, Tycko B , Mayeux R (1998). Earlier onset of Alzheimer's disease in men with Down syndrome. *Neurology*. **50**, 991-995.

Sherrington R, Rogaev EI, Liang Y, Rogaeva EA, Levesque G, Ikeda M, Chi H, Lin C, Li G, Holman K , et al. (1995). Cloning of a gene bearing missense mutations in early-onset familial Alzheimer's disease. *Nature*. **375**, 754-760.

Sleegers K, Brouwers N, Gijselinck I, Theuns J, Goossens D, Wauters J, Del-Favero J, Cruts M, van Duijn CM , Van Broeckhoven C (2006). APP duplication is sufficient to cause early onset Alzheimer's dementia with cerebral amyloid angiopathy. *Brain*. **129**, 2977-2983.

von Koch CS, Zheng H, Chen H, Trumbauer M, Thinakaran G, van der Ploeg LH, Price DL , Sisodia SS (1997). Generation of APLP2 KO mice and early postnatal lethality in APLP2/APP double KO mice. *Neurobiology of aging*. **18**, 661-669.

Yamawaki TM, Arantes-Oliveira N, Berman JR, Zhang P , Kenyon C (2008). Distinct activities of the germline and somatic reproductive tissues in the regulation of *Caenorhabditis elegans*' longevity. *Genetics*. **178**, 513-526.

III.8. Figures and Tables

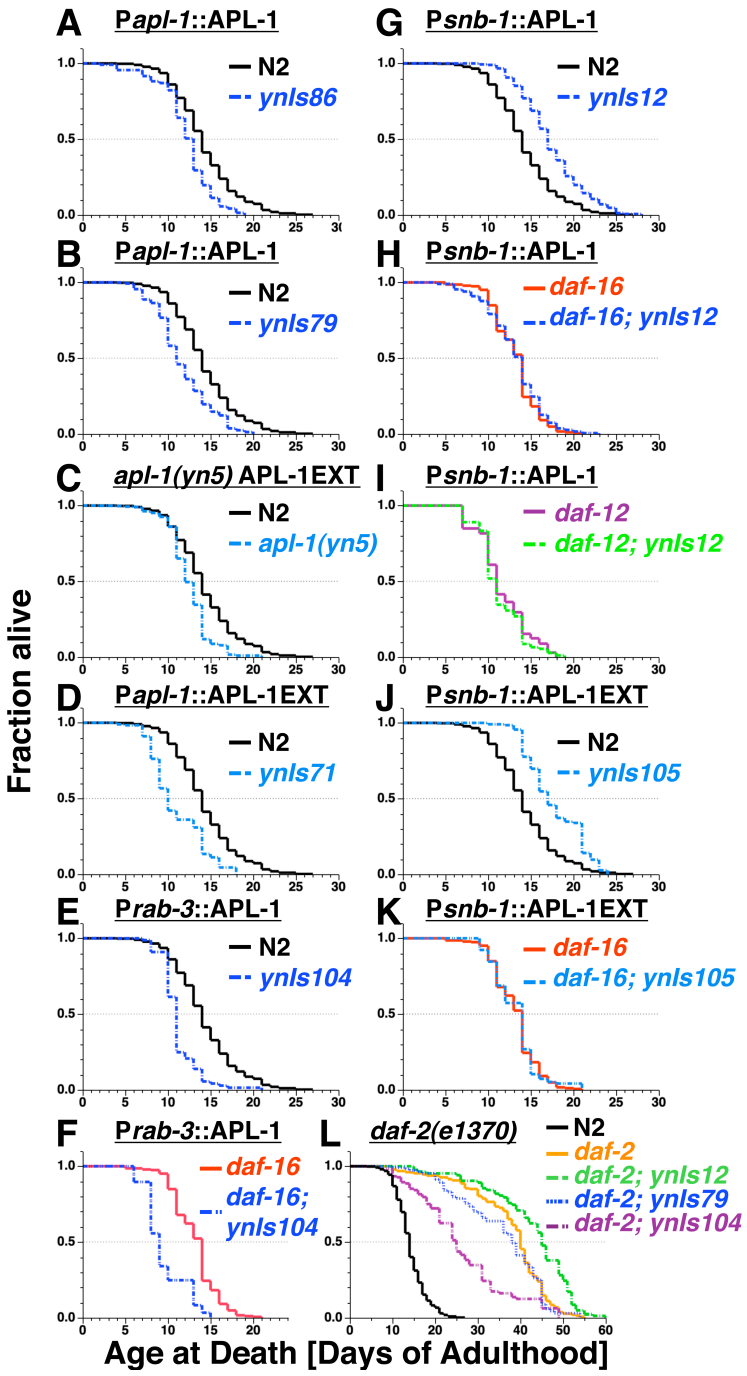

Figure 1. Lifespan modulation by APL-1 overexpression is dependent on *daf-16*/FOXO and *daf-12* nuclear hormone receptor activity. Endogenous overexpression of full-length APL-1 (A,B) or the extracellular domain of APL-1 (APL-1EXT; C,D)

causes a shortened lifespan. Pan-neuronal expression of APL-1 with the *rab-3* promoter (P*rab-3*::APL-1) shortened lifespan in a wild-type (E), *daf-16* null (F), and *daf-2(e1370)* (L) background. By contrast, ectopic overexpression of APL-1 or APL-1EXT with the *snb-1* promoter (P*snb-1*::APL-1 or P*snb-1*::APL-1EXT) increased lifespan in a wild-type (G,J) and a *daf-2(e1370)* (L) background. However, the longevity caused by P*snb-1*::APL-1 or P*snb-1*::APL-1EXT expression was completely abolished in a *daf-16* null (H,K) background. Furthermore, the increase in lifespan with the P*snb-1*::APL-1-transgene was completely abolished in a *daf-12(m20)* mutant background (I). Statistical analyses are shown in Table 1.

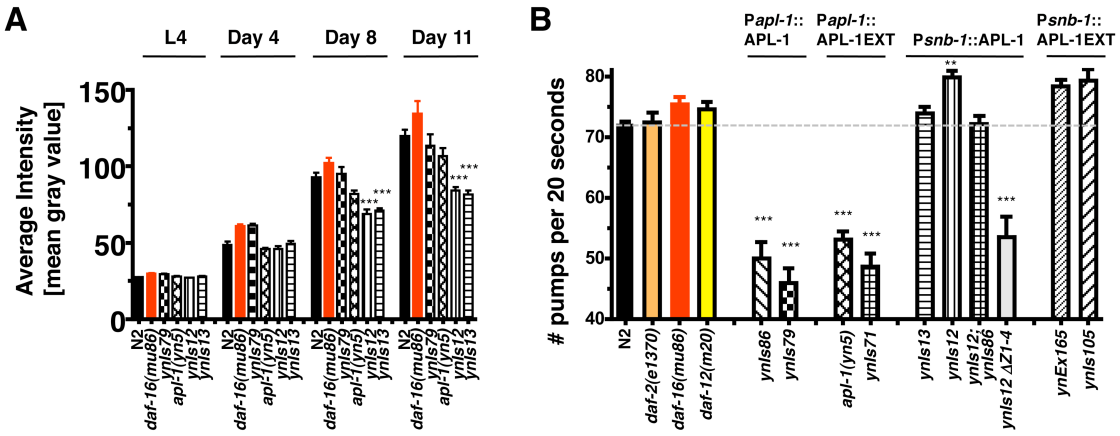

Figure 2. APL-1 signals through DAF-16 and DAF-12 to modulate aging. P*snb-1*::APL-1 animals age slower as determined by autofluorescence of lipofucin (A) as a marker for waste product accumulation and by pharyngeal pumping (B) as a marker for organ fitness in day 8 adults. See Table S1 for detailed statistical analysis. ***=P<0.001 determined by one-way ANOVA with Tukey post-test.

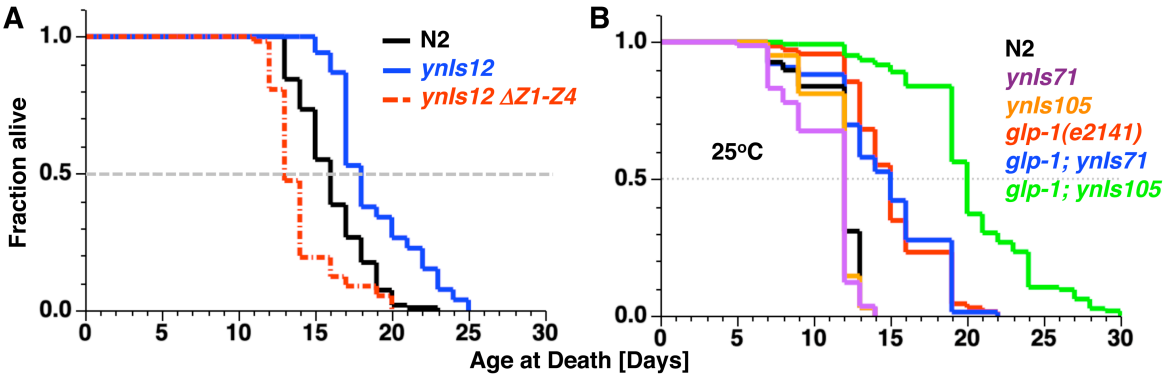

Figure 3. The gonad affects longevity in APL-1 overexpression animals. A. Ablation of the gonadal precursor cells Z1-Z4 in *ynIs12* (*ΔZ1-Z4*, P*snb-1*::APL-1) worms at the first larval stage (L1) shortened their mean lifespans compared to wild-type (N2) or *ynIs12* (P*snb-1*::APL-1) sham-operated animals. Lifespan measurements from L1 instead of L4 stage. B. All animals were shifted to 25ºC at the L1 stage to assay their lifespan. Animals carrying the *glp-1(e2141)* allele arrest in germ-line proliferation at 25ºC (Arantes-Oliveira *et al*. 2002). Transgenic animals *ynIs71* (P*apl-1*::APL-1EXT) and *ynIs105* (P*snb-1*::APL-1EXT) showed a similar lifespan as wild-type (N2) animals. Similarly, *glp-1; ynIs71* mutant transgenic animals showed a similar lifespan as *glp-1*(*e2141*) animals. However, *glp-1; ynIs105* mutant transgenic animals lived much longer (35%) than long-lived *glp-1(e2141)* mutants. Statistical analyses are shown in Table 1.

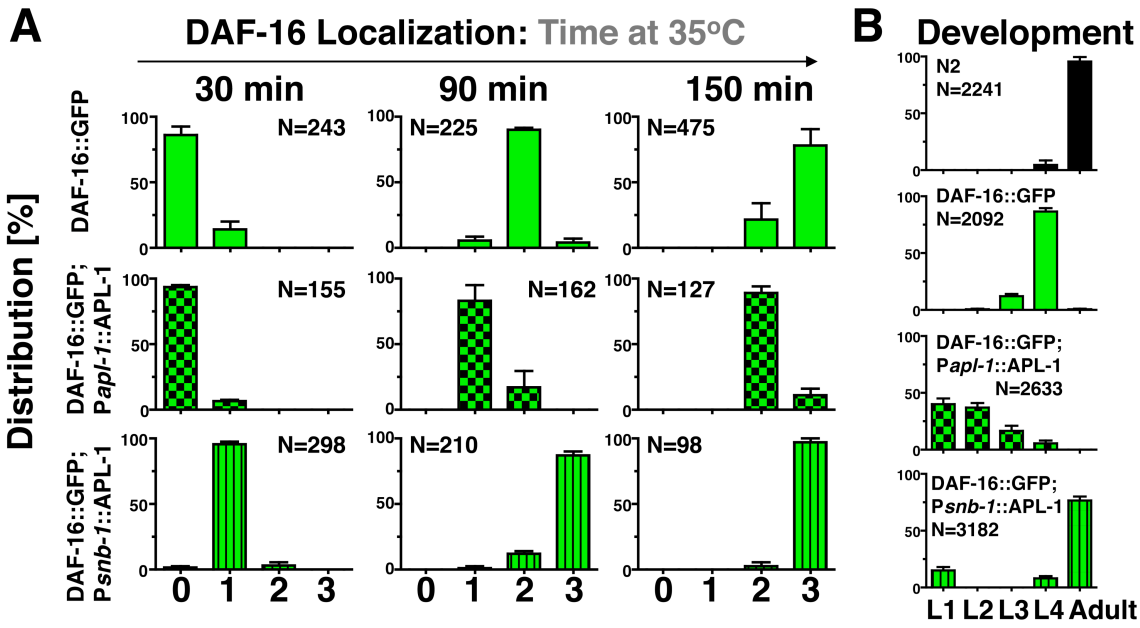

Figure 4. APL-1 influences nuclear translocation of DAF-16 and developmental progression. A. Overexpression of APL-1 delayed DAF-16 nuclear translocation in response to a 35ºC heat stress, whereas P*snb-1*::APL-1 expression accelerated DAF-16 nuclear translocation. Categories: 0, all cytoplasm; 1, more cytoplasm than nucleus; 2, more nucleus than cytoplasm, 3, all nucleus (as described in (Curran & Ruvkun 2007); Fig. S4 and Table S2). B. Overexpression of APL-1 further delayed the development of DAF-16::GFP animals, whereas P*snb-1*::APL-1 expression accelerated the development of DAF-16::GFP animals. Eggs were allowed to develop at 20ºC and scored after 72 hours. L1-L4 indicates different larval stages.

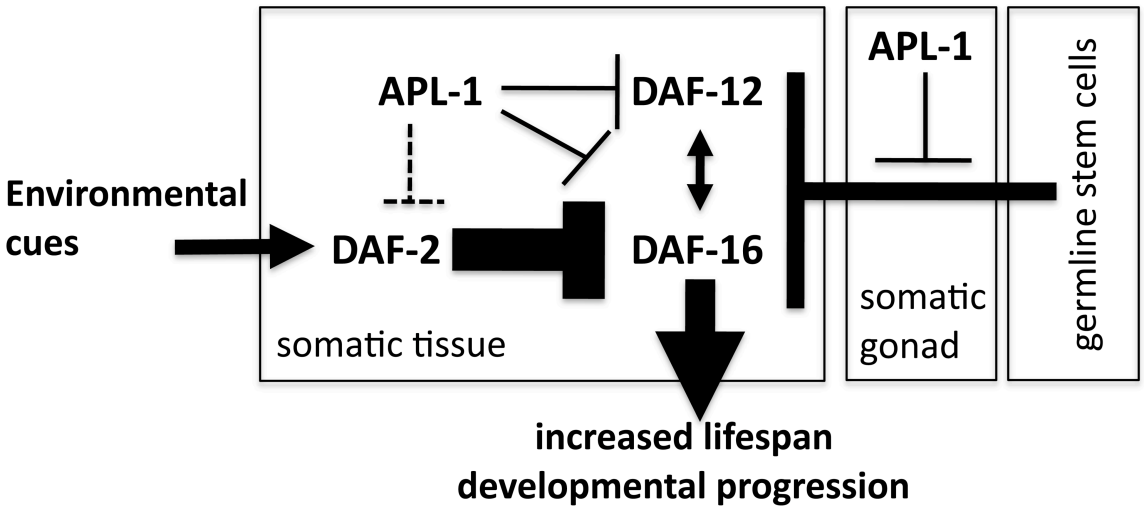

Figure 5. Model depicting multiple pathways in which APL-1 activity affects lifespan. Aging is regulated in part by cross talk between somatic cells and reproductive tissue. Environmental conditions (e.g., food) activate the DAF-2 insulin/IGF-1 receptor, whose signaling inhibits DAF-16 from entering the nucleus to activate "longevity or developmental" target genes (Kenyon 2005). Germline precursor cells activate pathways that inhibit longevity, presumably by decreasing *daf-12* and *daf-16*/FOXO activity (Arantes-Oliveira *et al*. 2002). APL-1 expression in somatic tissues can inhibit DAF-16 activity via *daf-12*, *daf-2* (dashed line), or other to-be-identified genes. APL-1 expressed in the somatic gonad may block the inhibitory signal from the germline from decreasing *daf-12* and *daf-16*/FOXO activity, thereby slowing aging.

Table 1. Adult Lifespan at 20°C

Strain (Genotype)	Mean lifespan ± S.E.M. [Days]*	75th percentile [Days]**	N died from senescence/ Initial N***, (T)	% Control(s) (†; ◊; ^; 0; #,@,Σ,∂,$,")	P-Value against Control(s) (†; ◊; ^; 0; #,@,Σ,∂,$,")
Controls					
N2 (wild type)	14.2 ± 0.1	16	1275/2537(31)		
lon-2(e678) apl-1(yn10)/ dpy-8(e130)	14.5 ± 0.3	17	67/107 (1)	+2%†	0.0729†
ynIs107 [P*apl-1*::APL-1(mut)::GFP]	14.3 ± 0.3	16	105/203 (2)	+1%†	0.4766†
ynIs100 [P*apl-1*::APL-1(mut)::GFP] 0.5x§	14.5 ± 0.3	15	100/153 (1)	+2%†	0.2481†
ynIs106 [P*apl-1*::APL-1EXT(mut)]	14.1 ± 0.2	15	115/144 (1)	-1%†	0.2481†
vsIs13 [*lin-15*(+)]	14.2± 0.2	15	232/345 (3)	0%†	0.2477†
Endogenous Overexpression of full-length APL-1					
ynIs86 [P*apl-1*::APL-1] 125x§	11.9 ± 0.2	13	151/240 (3)	-16%†	<0.0001†
ynIs79 [P*apl-1*::APL-1::GFP] 182x§	11.7 ± 0.3	14	145/203 (3)	-18%†	<0.0001†
apl-1(yn10) {P*apl-1*::APL-1}	11.9 ± 0.3	14	31/54 (1)	-16%†	<0.0001†
{P*apl-1*::APL-1}	13.4 ± 0.7	13	17/50 (1)	-6%†	0.2225†
Endogenous Overexpression of the Extracellular Domain of APL-1 (APL-1EXT)					
apl-1(yn5) 16x§	12.5 ± 0.1	14	341/563 (6)	-12%†	<0.0001†
ynIs71 [P*apl-1*::APL-1EXT]	11.7 ± 0.3	14	139/254 (3)	-18%†	<0.0001†
Pan-neural expression of APL-1 driven by* rab-3 *promoter					
ynEx93 {P*rab-3*::APL-1}	12.9 ± 0.5	14	29/119 (1)	-9%†	0.0352†
ynIs104 [P*rab-3*::APL-1] 8x§	10.9 ± 0.2	11	142/312 (3)	-23%†	<0.0001†
ynIs91 [P*rab-3*::APL-1]	12.1 ± 0.2	14	202/276 (3)	-15%†	<0.0001†
ynIs91 [P*rab-3*::APL-1]; *vsIs13* [*lin-15*(+)]	12.2 ± 0.3	14	71/152 (1)	-14%†	<0.0001†
Overexpression of APL-1 driven by* snb-1 *promoter					
ynIs12 [P*snb-1*::APL-1] 71x§	17.6 ± 0.2	20	309/746 (8)	+24%†	<0.0001†
ynIs13 [P*snb-1*::APL-1] 17x§	17.2 ± 0.2	20	257/529 (5)	+21%†	<0.0001†
ynIs12; ynIs86 205x§	17.7 ± 0.3	20	124/296 (3)	+25%†	<0.0001†
Overexpression of the Extracellular Domain of APL-1 driven by* snb-1 *promoter					
ynEx65 {P*snb-1*::APL-1EXT}	16.0 ± 0.3	17	59/120 (1)	+13%†	<0.0001†
ynIs105 [P*snb-1*::APL-1EXT]	17.7 ± 0.3	21	138/319 (3)	+25%†	<0.0001†
Overexpression of APL-1 in a* daf-16(mu38) *null background					
daf-16(mu86)	13.1 ± 0.1	14	264/408 (5)	-8%†	<0.0001†
daf-16(mu86); ynIs86	10.9 ± 0.2	12	91/120 (1)	-17%◊; -23%†	<0.0001◊
daf-16(mu86); ynIs79	12.2 ± 0.3	15	66/103 (1)	-7%◊; -14%†	0.0217◊
daf-16(mu86); apl-1(yn5)	10.9 ± 0.3	13	86/186 (2)	-17%◊; -23%†	<0.0001◊
daf-16(mu86); apl-1(yn10) {P*apl-1*::APL-1}	11.4 ± 0.3	13	96/122 (1)	-12%◊; -20%†; -4%0	<0.0001◊ 0.3398 0
daf-16(mu86); ynIs104	9.5 ± 0.3	10	80/125 (2)	-27%◊; -33%†	<0.0001◊
daf-16(mu86); ynIs12	13.2 ± 0.2	15	222/319 (3)	-1%◊; -7%†	0.9848◊
daf-16(mu86); ynIs13	13.1 ± 0.2	16	190/265 (3)	0%◊; -8%†	0.9852◊
daf-16(mu86); ynIs105	13.2 ± 0.2	15	109/191 (3)	-1%◊; -7%†	0.8374◊
Overexpression of APL-1 in a* daf-2(e1370) *reduction-of-function background					
daf-2(e1370)	37.8 ± 0.6	44	224/327 (3)	+166%†	<0.0001†
daf-2(e1370) {P*apl-1*::APL-1}	38.3 ± 1.3	46	70/111 (1)	+1%^; +169%†	0.1038^
daf-2(e1370); ynIs79	35.7 ± 1.0	44	85/124 (1)	-6%^; +151%†	0.0801^
daf-2(e1370); apl-1(yn10) {P*apl-1*::APL-1}	24.4 ± 0.6	31	148/253 (2)	-35%^; +72%†	<0.0001^
daf-2(e1370); apl-1(yn5)	35.8 ± 1.8	45	30/61 (1)	-6%^; +151%†	0.2482^
daf-2(e1370); ynIs12	43.0 ± 1.1	50	82/101 (1)	+14%^; +203%†	<0.0001^
daf-2(e1370); ynIs104	26.2 ± 1.0	31	97/176 (1)	-31%^; +85%†	<0.0001^
Overexpression of APL-1 and DAF-16					
zIs356 [DAF-16::GFP]	17.9 ± 0.2	19	173/242 (2)	+26%†	<0.0001†
zIs356; *ynIs79*	17.8 ± 0.5	24	156/204 (2)	-1%#; +25%†	0.7151#
zIs356; *apl-1(yn5)*	13.8 ± 0.2	16	157/288 (2)	-23%#; -3%†	<0.0001#; 0.6867†
zIs356; *ynIs104*	15.8 ± 0.2	18	106/153 (1)	-12%#; +11%†	<0.0001#
zIs356; *ynIs12*	20.2 ± 0.3	21	155/376 (2)	+13%#; +42%†	<0.0001#
Overexpression of APL-1 in a* daf-12(m20) *mutant background					
daf-12(m20)	11.6 ± 0.2	14	298/487 (4)	-18%†	<0.0001†

daf-12(m20); *ynIs12*	11.3 ± 0.2	14	241/402 (3)	-3%[@]; -20%[†]	0.5240[@]; <0.0001[†]
daf-12(m20); *ynIs105*	10.8 ± 0.3	11	60/102 (1)	-7%[@]; -24%[†]	0.0565[@]; <0.0001[†]
Laser ablation of gonadal precursor cells (Z1-Z4) of L1 animals that overexpress APL-1 driven by* snb-1 *promoter					
N2 (sham)	16.1 ± 0.2	18	109/190(3)		
ynIs12 (sham)	18.8 ± 0.5	21	151/178 (3)	+17%	<0.0001[Σ]
ynIs12 ΔZ1-Z4	14.0 ± 0.3	14	57/64 (3)	-13%	<0.0001[Σ;∂]
Lifespan at 25°C starting as L1 for APL-1 overexpression in a* glp-1(e2141ts) *mutant background					
N2	11.7 ± 0.2	13	68/87 (1)		
ynIs71 [P*apl-1*::APL-1EXT]	10.8 ± 0.3	12	58/76 (1)	-8%	0.0037"
ynIs105 [P*snb-1*::APL-1EXT]	11.5 ± 0.3	12	35/49 (1)	-2%	0.2213"
glp-1(e2141)	15.0 ± 0.4	16	69/69 (1)	+28%	<0.0001"
glp-1(e2141); ynIs71	14.6 ± 0.4	19	76/76 (1)	+25%	0.4962[$]
glp-1(e2141); ynIs105	20.3 ± 0.4	23	116/127 (1)	+74%	<0.0001[$]

All lifespans are shown in cumulative form, since individual trials do not differ significantly from cumulative and since experimental animals were always assayed with their proper control and wild-type animals. *Is,* **[]** = integrated transgene; *Ex*, **{}** = non integrated transgene; **(N)** = number of animals observed; **(T)** = number of independent trials the experiment was performed; ***** Measured from L4 stage. ****** 75_{th} percentile is the age when a quarter of the population is still alive; ******* Total number of initial animals includes animals that died from senescence and censored animals that crawled off the plates, buried into the agar, bagged or exploded; **†** = N2 (wild type); ◊ = *apl-1(yn10)* {P*apl-1*::APL-1}; ◊ = *daf-16(mu86)*, all APL-1 overexpression animals in a *daf-16(mu86)* null background are significantly different than wild type by P<0.0001; **^** = *daf-2(e1370)*, all APL-1 overexpression animals in a *daf-2(e1370)* background are significantly different than wild type by P<0.0001; **@** = *daf-12(m20)*, P-values for lifespans were determined by Log-Rank test. *lon-2(e678)* and *dpy-8(e130)* are flanking genetic markers of *apl-1*. [§] = fold overexpression of APL-1 determined by western blot analysis. For *ynIs12* and *ynIs13* P*snb-1*::APL-1 was co-injected *lin-15*(+) into *lin-15*(-) animals. When transgenes were integrated the *lin-15*(-) mutation was outcrossed. Note: All lifespan assays were performed on MYOB plates.

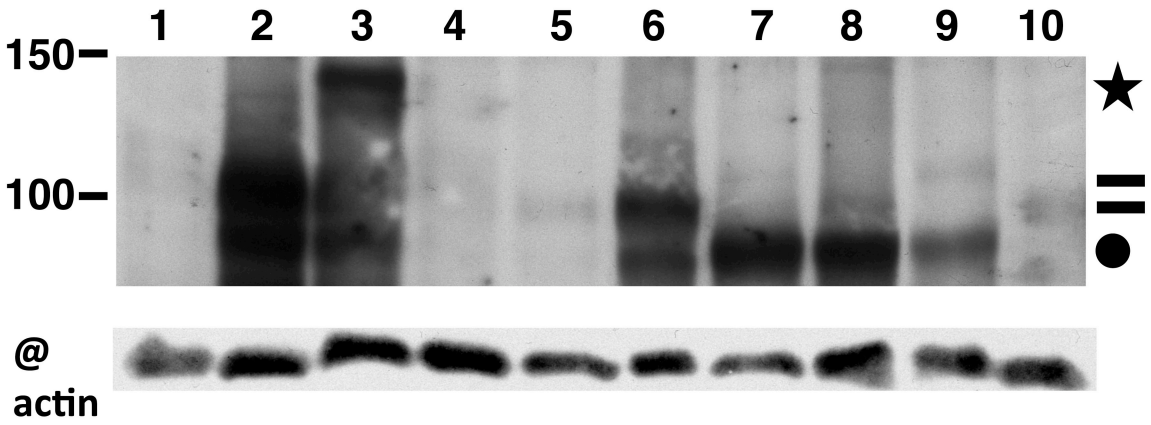

Lane	Strain	Fold APL-1 to N2
1	wild type (N2)	
2	*ynIs12; ynIs86*	205 ± 32 (N= 4)
3	APL-1::GFP (*ynIs79*)	180 ± 33 (N= 4)
4	P*rab-3*::APL-1 (*ynIs104*)	7.5 ± 3.4 (N= 4)
5	*apl-1(yn10); ynIs104*	5.9 ± 3.1 (N= 4)
6	*apl-1(yn10)* [APL-1]	25.2 ± 8.2 (N= 4)
7	APL-1EXT (*ynIs105*)	24.9 ± 15.9 (N= 4)
8	APL-1EXT (*ynIs71*)	25.4 ± 14.8 (N= 4)
9	*apl-1(yn5)*	16.3 ± 7.1 (N= 3)
10	DAF-16::GFP	1.6 ± 1.2 (N= 4)

Supporting Figure S1. APL-1 levels of different transgenic lines determined by western blot analysis. Blots were first probed with an anti-actin antibody (lower blot) and then re-probed with an antibody against the extracellular domain of APL-1 (upper blot; (Hornsten *et al*. 2007)). Full-length APL-1 protein (glycosylated and unglycosylated; bars; 105-110kDa), cleaved extracellular (sAPL-1) and an extracellular fragment from the *yn5* allele (APL-1EXT) (dot; ~90kDa), and the APL-1::GFP (star; ~135kDa) are shown. Standards in kDa. Protein levels were normalized to levels of actin (~40 kDa) for each strain, so that similar amounts of total protein were loaded for each strain. Loading scheme and approximate APL-1 fold overexpression compared to

wild type (N2) shown in table below. Values were determined by relative intensity to wild type (N2) with NIH Image J Gel analyzer. Value ± SEM (N = number of western blots).

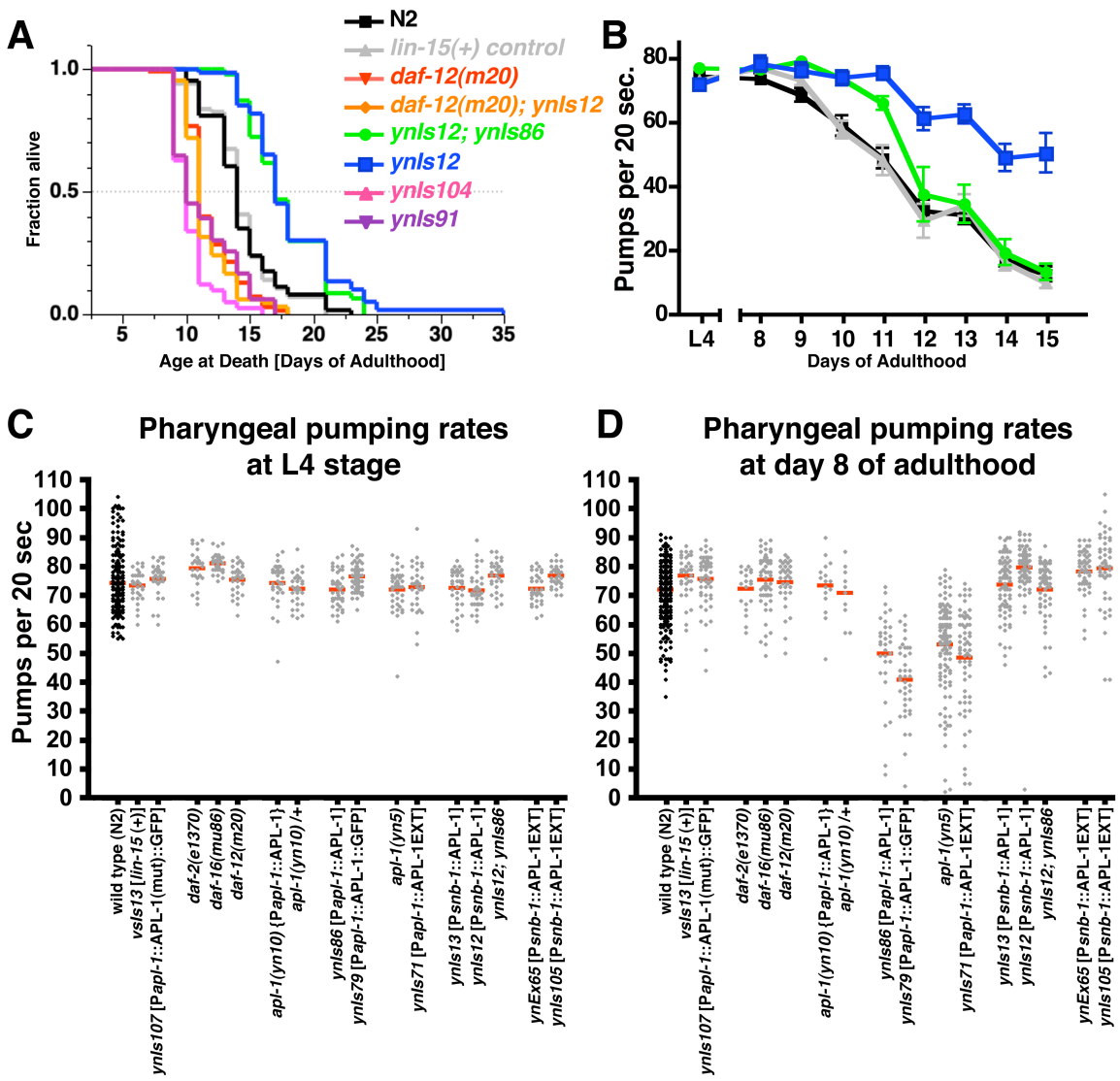

Supporting Figure S2. Pharyngeal pumping rates decline with age. One trial of lifespan assay (A) with parallel pharyngeal pumping measurements (B) is shown. Animals carrying only the co-injection marker (*lin-15*(+); grey) carried by *ynIs12* transgenic animals showed the same lifespan and pharyngeal pumping rate as wild type (black). Animals overexpressing APL-1 driven by the *rab-3* promoter [(*ynIs104* (pink), *ynIs91* (purple)] showed a decreased lifespan compared to wild-type animals. Animals that overexpress APL-1 with the *snb-1* promoter [*ynIs12* (blue)] showed an increased

lifespan and pharyngeal pumping rate compared to wild-type animals. The increased longevity in P*snb-1*::APL-1 animals is not further enhanced by increased APL-1 overexpression [*ynIs12; ynIs86* (green)]. Data from this trial is incorporated in cumulative statistics since no difference was found between cumulative and one trial statistics. C. All APL-1 overexpression lines showed similar pharyngeal pumping rates during the L4 stage. By contrast, overexpression of APL-1 or APL-1EXT driven by its endogenous promoter showed lower pumping rates compared to wild type (N2), P*snb-1*::APL-1, and P*snb- 1*::APL-1EXT day 8 adults (D). Neither loss of DAF-16 activity [*daf-16(mu86)*] or reduced DAF-2 activity [*daf-2(e1370)*] suppressed the decreased pumping rates of APL-1 endogenous overexpression at day 8 (D). For statistical significance, please see Table 1. Wild-type data include data from the N2 strain from our laboratory and the laboratory of Cathy Savage-Dunn; both laboratory strains showed the same pumping rates. *Is*, [], integrated transgene, *Ex*, {}, non-integrated transgene.

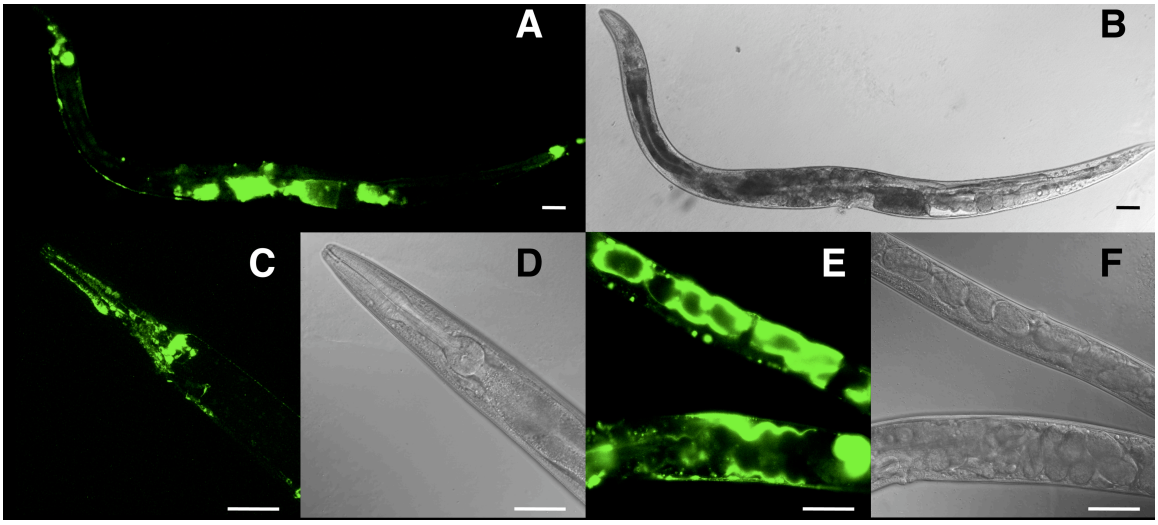

Supporting Figure S3. The *snb-1* promoter drives APL-1::GFP expression strongly in neurons and the somatic gonad. Non-integrated transgene P*snb-1*::APL-1::GFP rescues the lethality of *apl-1(yn10)* animals (Hornsten *et al*. 2007). A. P*snb-1*::APL-1::GFP expression in an adult (anterior left, ventral side down) and corresponding brightfield image (B; 100x). P*snb-1*::APL-1::GFP is expressed in neurons (A, C) and somatic gonad (A, E). C, D, head region. E, F, mid body region. Scale bar = 50 μm.

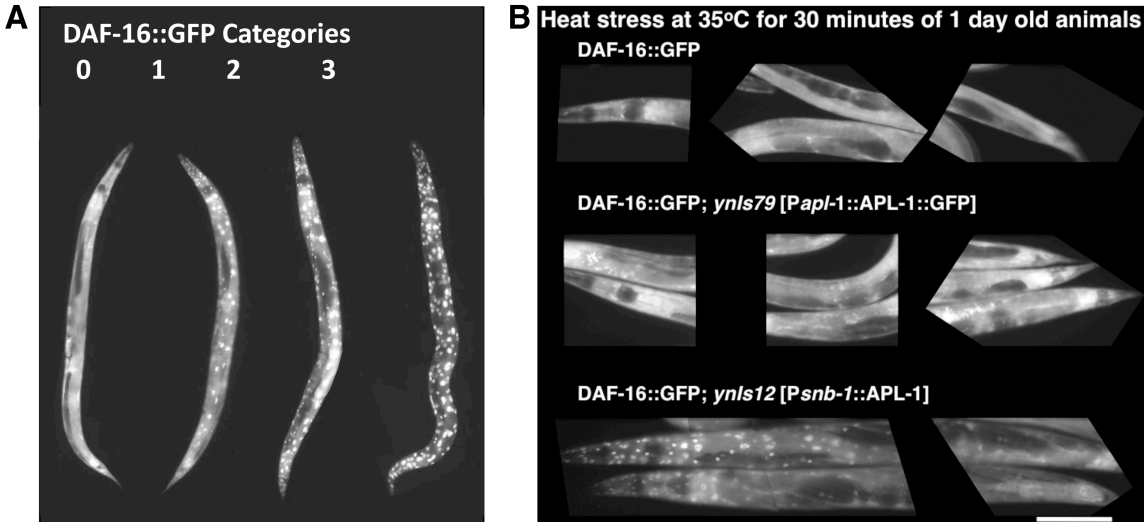

Supporting Figure S4. P*snb-1*::APL-1 expression accelerates DAF-16::GFP nuclear translocation. A. Scoring categories of DAF-16::GFP localization. Category 0: DAF16::GFP showing diffuse localization only in the cytoplasm; category 1: more DAF-16::GFP localized in cytoplasm than in nucleus; category 2: more DAF-16::GFP localized in nucleus than in cytoplasm; category 3: almost all DAF-16::GFP localized in nucleus. Same scoring categories used as described (Curran & Ruvkun 2007). Anterior up, ventral side to the left. B. DAF-16::GFP localization in a wild-type and *ynIs79* [APL-1::GFP] background is mainly in the cytoplasm (category 0), whereas DAF-16::GFP in a *ynIs12* [P*snb-1*::APL-1] animal is already translocating into the nucleus (category 1) after 30 minutes of 35ºC heat-stress. Anterior to the left, ventral side down. Scale bar = 50 μm. *Is*, [], integrated transgene.

Table S1. Autofluorescence of Lipofucins at 20°C

Strain (Genotype)	Intensity of Autoflurescence [mean grey value of pixels] L4 mean ± S.E.M. (N) P-value N2	Day 4 mean ± S.E.M. (N) P-value N2	Day 8 mean ± S.E.M. (N) P-value N2	Day 8 mean ± S.E.M. (N) P-value N2
Controls				
N2 (wild type)	27.3 ± 0.3 (37)	48.5 ± 2.0 (37)	92.7 ± 3.0 (37)	119.5 ± 4.4 (47)
daf-16(mu86)	29.85 ± 0.2 (34)	60.7 ± 1.1 (47)	102.1 ± 3.4 (35)	134.2 ± 8.2 (34)
Endogenous Overexpression of Full-Length APL-1				
ynIs79 [P*apl-1*::APL-1::GFP]	29.5 ± 0.3 (31)	61.1 ± 1.2 (43)	95.1 ± 4.3 (31)	113.3 ± 7.5 (38)
Endogenous Overexpression of the Extracellular Domain of APL-1 (APL-1EXT)				
apl-1(yn5)	27.9 ± 0.3 (77)	45.7 ± 1.0 (38)	81.8 ± 2.3 (51)	106.5 ± 5.2 (46)
Overexpression of APL-1 driven by* snb-1 *promoter				
ynIs12 [P*snb-1*::APL-1]	27.0 ± 0.2 (83)	46.0 ± 1.6 (32)	68.8 ± 2.8 (30) <0.0001	84.2 ± 2.2 (34) <0.0001
ynIs13 [P*snb-1*::APL-1]	28.0 ± 0.4 (56)	49.4 ± 1.7 (30)	71.0 ± 1.5 (31) <0.0001	81.6 ± 2.5 (49) <0.0001

N= number of worms scored; P= P-values against N2 for the corresponding age were determined by one-way ANOVAs with Tukey post-test (95% confidence intervals). Average of 3 independent trials are shown. *Is*, (), integrated transgene, *Ex*, {}, non-integrated transgene.

Table S2. DAF-16::GFP nuclear translocation upon 35°C heat stress

Strains	Cumulative distribution [%] in categories				
	0	1	2	3	N (T)
0 minutes at 35°C					
zIs356 [DAF-16::GFP]	100	0	0	0	176 (7)
zIs356; *ynIs79* [P*apl-1*::APL-1::GFP]	100	0	0	0	264 (4)
zIs356; *ynIs12* [P*snb-1*::APL-1]	93	7	0	0	252 (5)
zIs356; *ynIs107* [P*apl-1*::APL-1mut]	100	0	0	0	44 (1)
zIs356; *vsIs13* [lin-15(+)]	100	0	0	0	120 (3)
30 minutes at 35°C					
zIs356 [DAF-16::GFP]	93	7	0	0	329 (12)
zIs356; *ynIs79* [P*apl-1*::APL-1::GFP]	94	6	0	0	155 (5)
zIs356; *ynIs12* [P*snb-1*::APL-1]	1	96	3	0	343 (6)
zIs356; *ynIs107* [P*apl-1*::APL-1mut]	97.5	2.5	0	0	80 (1)
zIs356; *vsIs13* [lin-15(+)]	96	4	0	0	104 (3)
60 minutes at 35°C					
zIs356 [DAF-16::GFP]	0	100	0	0	245 (10)
zIs356; *ynIs79* [P*apl-1*::APL-1::GFP]	63	37	0	0	112 (4)
zIs356; *ynIs12* [P*snb-1*::APL-1]	0	18	82	0	148 (4)
zIs356; *ynIs107* [P*apl-1*::APL-1mut]	0	100	0	0	57 (1)
zIs356; *vsIs13* [lin-15(+)]	0	100	0	0	133 (3)
90 minutes at 35°C					
zIs356 [DAF-16::GFP]	0	7	91	2	255 (9)
zIs356; *ynIs79* [P*apl-1*::APL-1::GFP]	0	92	8	0	162 (4)
zIs356; *ynIs12* [P*snb-1*::APL-1]	0	1	12	87	210 (3)
zIs356; *ynIs107* [P*apl-1*::APL-1mut]	0	0	100	0	61 (1)
zIs356; *vsIs13* [lin-15(+)]	0	3	97	0	136 (3)
120 minutes at 35°C					
zIs356 [DAF-16::GFP]	0	0	84	16	445 (8)
zIs356; *ynIs79* [P*apl-1*::APL-1::GFP]	0	56	37	7	75 (3)
zIs356; *ynIs12* [P*snb-1*::APL-1]	0	0	8	92	116 (3)
zIs356; *ynIs107* [P*apl-1*::APL-1mut]	0	0	7	93	27 (1)
zIs356; *vsIs13* [lin-15(+)]	0	0	76	24	92 (3)
150 minutes at 35°C					
zIs356 [DAF-16::GFP]	0	0	13	87	518 (9)
zIs356; *ynIs79* [P*apl-1*::APL-1::GFP]	0	0	94	6	127 (3)
zIs356; *ynIs12* [P*snb-1*::APL-1]	0	0	1	99	98 (3)
zIs356; *ynIs107* [P*apl-1*::APL-1mut]	0	0	3	97	61 (1)
zIs356; *vsIs13* [lin-15(+)]	0	0	27	73	72 (3)
180 minutes at 35°C					
zIs356 [DAF-16::GFP]	0	0	1	99	118 (2)
zIs356; *ynIs79* [P*apl-1*::APL-1::GFP]	0	0	79	21	100 (1)
zIs356; *ynIs12* [P*snb-1*::APL-1]	0	0	0	100	41 (1)
210 minutes at 35°C					
zIs356 [DAF-16::GFP]	0	0	0	100	46 (1)
zIs356; *ynIs79* [P*apl-1*::APL-1::GFP]	0	0	43	56	90 (1)
240 minutes at 35°C					
zIs356 [DAF-16::GFP]	0	0	0	100	107 (2)
zIs356; *ynIs79* [P*apl-1*::APL-1::GFP]	0	0	5	95	200 (2)
zIs356; *ynIs12* [P*snb-1*::APL-1]	0	0	0	100	77 (1)

DAF-16::GFP localization was scored on synchronized 1 day old adults. N corresponds to number of worms observed. T corresponds to number of independent trials. The rate of DAF-16::GFP nuclear translocation was scored as described (Curran & Ruvkun 2007): category 0: all DAF-16::GFP showing diffuse localization in the cytoplasm; category 1: more DAF-16::GFP localized in cytoplasm than in nucleus; category 2: more DAF-16::GFP localized in nucleus than in cytoplasm; category 3: almost all DAF-16::GFP localized in nucleus. *ynIs107* is a transgene that contains the missense mutation *yn32* in *apl-1*; this transgene does not rescue *apl-1(yn10)* null lethality and is considered a non-functional APL-1 control. *vsIs13* [lin-15(+)] transgene served as a co-injection marker control for *ynIs12* [P*snb-1*::APL-1] carrying animals.

Chapter IV: The extracellular domain of APL-1, an APP-related protein, acts via DAF-16/FOXO and DAF-12 to slow developmental progression in *C. elegans*

Collin Y. Ewald and Chris Li

IV.1 Abstract

Alzheimer's disease is the most common form of dementia and affects about 5 million Americans. Mutations in the amyloid precursor protein (*APP*) gene or in genes that process APP are correlated with familial Alzheimer's disease. The biological function of APP remains unclear. APP is a transmembrane protein that can be sequentially cleaved by different secretases to yield multiple fragments, which can potentially act as a signaling molecule. *Caenorhabditis elegans* encodes one APP-related protein, APL-1. Release of an extracellular fragment of APL-1 is essential for viability. However, the downstream components of the APL-1 signaling pathway and the function of *apl-1* at later stages of development are unknown. Here, we show that the released APL-1 fragment signals through the FOXO transcription factor DAF-16 and the nuclear hormone receptor DAF-12 to influence developmental progression, body size, and egg-laying rate. Furthermore, high levels of the released APL-1 fragment can be harmful during early embryonic development. In a genetic screen to identify modifiers that influence the effects of APL-1 during embryonic development, we have identified two mutants, *yn38* and

***yn39*. Knockdown of *apl-1* in an *apl-1* mutant background caused lethality and molting defects at all larval stages, suggesting that *apl-1* is required for each transitional molt. We suggest that signaling of the released APL-1 fragment modulates multiple metabolic states and that APL-1 is required throughout development.**

IV.2. Introduction

Alzheimer's disease (AD) is a neurodegenerative disorder that leads to cognitive decline (Alzheimer's Association 2010). One postmortem criterion in the diagnosis of AD is the presence of senile plaques in AD patients (Kidd 1964; Luse & Smith 1964; Terry *et al*. 1964; Krigman *et al*. 1965). The major component of the senile plaques is the β-amyloid peptide, which is a cleavage fragment of the amyloid precursor protein (APP) (Kang *et al*. 1987). Mutations and duplications of APP have been correlated with familial Alzheimer's disease (Chartier-Harlin *et al*. 1991; Goate *et al*. 1991; Murrell *et al*. 1991; Cabrejo *et al*. 2006; Rovelet-Lecrux *et al*. 2006; Sleegers *et al*. 2006). APP is a single transmembrane domain protein (Kang *et al*. 1987), which can be cleaved by either α- or β-secretase to release a large extracellular fragment (sAPPα or sAPPβ), and subsequently cleaved by the γ-secretase to release a small intracellular fragment (AICD) and, in the case of a previous β-secretase cleavage, the β-amyloid peptide (reviewed in (Gralle & Ferreira 2007). The biological functions of the cleaved APP fragments, sAPPα/β and AICD, remain unclear. Determining the function of APP in mammals is complicated by two functionally redundant proteins, APLP1 and APLP2. In mice, knockout of *APP* leads to mild deficits (Zheng *et al*. 1995), while double knockouts of *APP* and *APLP2* or

triple knockouts of *APP*, *APLP1*, and *APLP2* leads to postnatal lethality (Heber *et al*. 2000; Herms *et al*. 2004). The nematode *C. elegans* encodes only one APP-related gene, *apl-1* (Daigle & Li 1993). Like the APP family in mice, *apl-1* has an essential function: knockout of *apl-1* results in a molting defect during the first to the second larval transition, resulting in larval lethality. Like mammalian APP, APL-1 could function as a receptor and/or its cleaved fragments could function as signaling molecules (reviewed in (Ewald & Li 2010)). Re-introducing an extracellular domain of APL-1 rescues the molting defect of *apl-1* knockouts (Hornsten *et al*. 2007), suggesting that APL-1EXT acts during early development, but it remains unclear whether APL-1EXT acts later in development.

C. elegans eggs hatch and develop through four larval stages (L1-L4) before reaching adulthood (Sulston & Horvitz 1977). The timing of postembryonic developmental programs is regulated by the heterochronic genes in *C. elegans* (reviewed in (Ambros 2000)). For the last molt of L4 to adulthood, *let-7* miRNA binds 3' UTR of *lin-41* (Slack *et al*. 2000), *hbl-1* (Abrahante *et al*. 2003) and *daf-12* (Grosshans *et al*. 2005) to prevent their translation. However, the *let-7* targets, *daf-12* and *hbl-1,* negatively feedback to regulate *let-7* (Bethke *et al*. 2009; Hammell *et al*. 2009; Roush & Slack 2009). During late L4 development, *let-7* also regulates expression of *apl-1* via *hbl-1*, *lin-41*, *lin-42* and *nhr-25* (Niwa *et al*. 2008; Hada *et al*. 2010). RNAi of *apl-1* rescues *let-7* vulva bursting, extra molt and lethality (Niwa *et al*. 2008), suggesting that *apl-1* acts downstream of *let-7*. Although *let-7* regulates transcription of *apl-1*, no *let-7* binding sites are present in the 3'UTR of *apl-1*; however, other *let-7*-family could also regulate

apl-1 and other miRNA binding sites have been found in the 3'UTR of *apl-1* (miR-284, miR-48, miR-67, miR-2, miR-60 (Niwa *et al*. 2008)).

We have isolated an *apl-1(yn5)* deletion allele in which the deletion removes the coding region for the transmembrane and cytoplasmic portions of the APL-1 protein and a large portion of the 3'UTR (Hornsten *et al*. 2007). Intriguingly, *apl-1(yn5)* mutants are viable, show a 16 times overexpression of the extracellular domain of APL-1 on western blots and show a slowed development compared to wild-type animals (Hornsten *et al*. 2007). In this study we investigate the function of APL-1 during development.

IV.3. Results

IV.3.1. Overexpression of the extracellular domain of APL-1 is sufficient to slow developmental progression of *apl-1(yn5)* animals

Wild-type animals have a very stereotyped pattern of cell divisions. Synchronized eggs develop into L4 larva within 65 hours and into adults by 72 hours at 20ºC (Ailion & Thomas 2000). By contrast, *apl-1(yn5)* animals are found mostly in L4 or earlier larval stages at 72 hours (Table 1; (Hornsten *et al*. 2007)). The *apl-1(yn5)* mutation deletes not only the transmembrane and cytoplasmic domains of APL-1, but also a large portion of the 3' UTR. *apl-1(yn5)* mutants express high levels of an extracellular fragment of APL-1 (APL-1EXT), which is slightly larger than sAPPα. The slowed developmental progression can be phenocopied by microinjection of APL-1EXT (*ynIs71*) (Table 1). As a control, we generated an APL-1EXT transgene that contained a mutation corresponding to the *apl-1*(*yn32*) null mutation (APL-1(*yn32)*EXT); this transgene did not rescue the *apl-1* knockouts and animals carrying this transgene (*ynIs106*) developed at the same rate

as wild-type animals (Table 1). These results indicate that overexpression of APL-1EXT is sufficient to slow developmental progression.

Although it appears that the *apl-1(yn5)* mutation delays developmental progression by one larval stage, in actuality the delay is more significant. After fertilization, wild-type eggs develop and are laid when they reach about the 30-cell stage of division (Sulston *et al*. 1983). *apl-1(yn5)* mutants retain eggs in the uterus longer than wild-type animals; hence, eggs laid by *apl-1(yn5)* mutants are chronologically older than eggs laid by wild-type animals. For instance, at 15ºC most wild-type eggs were at the 30-100 cells stage after 30 minutes or at the comma stage after 6 hours after being laid. By contrast, most *apl-1(yn5)* eggs were already in the comma stage after 30 minutes or the 3-fold (pretzel) stage after 6 hours after being laid at 15ºC; the time to progress from the comma stage to the pretzel stage is about half the time to progress from the 30-100 cell stage to the comma stage. Hence, the *apl-1(yn5)* mutation causes a severe delay in developmental progression.

IV.3.2. The slowed development of *apl-1(yn5)* animals is rescued by RNAi knock down of *daf-12*

To determine the pathway in which APL-1EXT slows development, we screened candidate genes that have been identified to regulate development. The *daf-12* gene encodes a nuclear hormone receptor (NHR) that determines whether animals go through reproductive growth or an alternative life cycle, called dauer, whereby second larval stage animals become a dauer larva rather than a third stage larva; when animals are returned to favorable environments, dauer animals enter the fourth larval stage (Riddle & Albert

1997)(Antebi et al. 2000). The slowed development of *apl-1(yn5)* mutants was suppressed by knockdown by RNAi of *daf-12* NHR, whereas *daf-12* RNAi had no effect on developmental progression of wild type or *daf-12(m20)* mutant animals (Table 1). Similarly, the slowed development of *ynIs71* [APL-1EXT] overexpression animals was rescued in a *daf-12(m20)* mutant background (Table 1), excluding an RNAi off-target effect of *daf-12* RNAi. Hence, decreased DAF-12 NHR activity influences the function of *apl-1*.

IV.3.3. *Daf-16* FOXO activity is required for the slowed development of *apl-1(yn5)* animals

Several pathways converge on DAF-12 NHR during the developmental decision to enter reproductive growth or dauer formation. One such pathway is the insulin signaling pathway. Signaling through the DAF-2 insulin/IGF-1 receptor leads to the phosphorylation of the FOXO transcription factor DAF-16 (Kenyon 2005). Phosphorylated DAF-16 is retained in the cytoplasm, whereas non-phosphorylated DAF-16/FOXO enters the nucleus to activate target genes involved in longevity, stress resistance, and dauer formation (Kenyon 2005). To determine whether the insulin signaling pathway was involved in the slowed growth of *apl-1(yn5)* mutants, we constructed double mutants with *apl-1(yn5)*. Mutations in *daf-16*, such as the *daf-16(mu86)* null allele, lead to dauer defective animals; in addition, *daf-16* genetically interacts with *daf-12* to induce dauer formation (Larsen *et al*. 1995). *daf-16*/FOXO is expressed ubiquitously in all developmental stages and adults (Henderson & Johnson 2001; Lee *et al*. 2001; Lin *et al*. 2001). *daf-16(mu86)* mutants showed a similar

developmental progression pattern as wild-type animals, whereas overexpression of *daf-16* with a translational fusion DAF-16::GFP slows developmental progression, such that most animals are in the L4 stage after 72 hours (Table 1; (Henderson & Johnson 2001)). Double mutants of *apl-1(yn5); daf-16(mu86)* showed a similar developmental progression as *daf-16(mu86)* or wild-type animals (Table 1), suggesting that the *daf-16(mu86)* mutation rescues the slowed development of *apl-1(yn5)* animals. By contrast, the *apl-1(yn5)* mutation were additive to the effects of DAF-16 overexpression: after 72 hours DAF-16::GFP; *apl-1(yn5)* animals are mostly found in the L2-L3 stage. These results suggest that APL-1EXT signals to increase the activity of DAF-16 to affect developmental progression.

IV.3.4. *apl-1(yn5)* slows DAF-16 nuclear localization under heat-shock conditions

Because APL-1EXT is a released fragment, APL-1EXT signaling will influence DAF-16 activity indirectly. Since *C. elegans* is transparent, DAF-16 localization can be monitored by using a translational fusion of DAF-16 with GFP (Green Fluorescent Protein; (Henderson & Johnson 2001)). Under well fed, non-crowded and unstressed laboratory conditions, DAF-16::GFP is predominantly found diffuse in the cytoplasm of all cells in wild-type (Henderson & Johnson 2001) and *apl-1(yn5)* animals (Table S1). DAF-16::GFP nuclear localization can be induced by putting animals under a heat stress (Henderson & Johnson 2001). When DAF-16::GFP animals were shifted from 20ºC to 35ºC, DAF-16::GFP translocates into the nucleus within 3 hours (Table S1; (Henderson & Johnson 2001)). DAF-16::GFP; *apl-1(yn5)* animals showed a delayed DAF-16::GFP nuclear translocation compared to DAF-16::GFP animals at 35ºC (Table S1). As a

control, non-functional APL-1EXT(mut) did not alter the timing of DAF-16::GFP nuclear translocation (DAF-16::GFP; *ynIs106*, Table S1). These results indicate that APL-1EXT activity slows DAF-16 nuclear translocation and presumably decreases its activity. Hence, *apl-1* acts in multiple pathways to affect DAF-16/FOXO activity.

IV.3.5. *apl-1(yn5)* enhances *daf-2*-induced L1 arrest but not dauer formation

If first larval stage (LI) animals hatch in the absence of food, development halts and animals enter and remain in L1 arrest until food becomes available (Baugh & Sternberg 2006). In addition, even in the presence of food, strongly reducing *daf-2* insulin/IGF-1 receptor activity induces L1 arrest (Gems et al. 1998; Baugh and Sternberg 2006), while slightly reducing *daf-2* activity induces dauer formation (Kimura et al., 1997); both L1 arrest (Baugh & Sternberg 2006) and dauer formation (Lin *et al*. 1997; Ogg *et al*. 1997) require DAF-16/FOXO activity (Henderson & Johnson 2001; Lee *et al*. 2001; Lin *et al*. 2001). Animals with a weak temperature sensitive *daf-2(e1370)* mutation have a slowed progression through all larval stages at the 20ºC permissive temperature (Table 1); in addition, about 3% of the animals (23 dauers/748 total) enter the dauer stage compared to none of the wild-type (0 dauers/3572 total) or *apl-1(yn5)* animals (0 dauers/943 total)). When combined with *apl-1(yn5)* at 20ºC, *daf-2(e1370); apl-1(yn5)* double mutants showed an even slower developmental progression than *daf-2(e1370)* or *apl-1(yn5)* single mutants, but the rate of dauer formation was not increased in the double mutants (Table 1). Further reducing DAF-2 activity by raising animals to the restrictive temperature of 25ºC caused 10% of the *daf-2(e1370)* mutants to enter L1 arrest and the residual 90% of the *daf-2(e1370)* mutants to enter dauer (Figure 1, (Kimura *et al*. 1997; Gems *et al*.

1998)), while all wild-type animals at 25ºC develop into adults (Figure 1; (Kimura *et al*. 1997; Gems *et al*. 1998)). The percentage of *daf-2(e1370)* animals entering L1 arrest at 25ºC was greatly enhanced by *apl-1(yn5)*: almost 90% of *daf-2(e1370); apl-1(yn5)* entered L1 arrest while the residual 10% entered into dauer diapause (Figure 1). Thus, *apl-1(yn5)* reduces the activity of the insulin/IGF-1 signaling pathway specifically at the L1 stage to enhance L1 arrest.

IV.3.6. Several *apl-1(yn5)* induced phenotypes require *daf-16*/FOXO and *daf-12* NHR activity

Our results suggest that *apl-1(yn5)* acts in multiple pathways that converge on *daf-16*/FOXO. For instance, *apl-1(yn5)* activity decreased *daf-2* insulin/IGF-1 receptor signaling, which presumably resulted in more DAF-16 entering the nucleus, whereas *apl-1(yn5)* delayed DAF-16 nuclear localization under stress conditions (35ºC). We examined whether *daf-16*/FOXO mediates other a*pl-1(yn5)* phenotypes. Wild-type adult animals are 1225 ± 6.6 mm (n=172) in length. *apl-1(yn5)* mutants and transgenic animals carrying an APL-1EXT transgene (*ynIs71*) were 15% (1047 ± 11.6 mm, n=63) or 27% (894 ± 28.2 mm, n=33) shorter, respectively, than wild-type animals (Figure 2A, Table S2). Similarly, animals that overexpress full-length of APL-1 (*ynIs86* and *ynIs79*) were 12-20% shorter than wild-type animals, whereas animals that carry a transgene with a mutated APL-1 (*ynIs100*) were wild type in length (Figure 2A, Table S2). Furthermore, animals that overexpress either full-length or extracellular APL-1 driven ectopically by the *snb-1* promoter, which drives expression in supporting cells, the somatic gonad, and

all neurons, were 17-30% shorter than wild-type animals (Figure 2A, Table S2). Thus, *apl-1* activity affects body length.

daf-16(mu86) animals were slightly (3%) longer and DAF-16::GFP animals were slightly shorter, although both not significantly, than wild-type animals; similarly, *daf-12(mu20)* mutants were similar in length as wild-type animals (Figure 2A, Table S2). In a *daf-16(mu86)* background, *apl-1(yn5)* mutants and transgenic APL-1 overexpression lines were the same length as *daf-16(mu86)* mutants (Figure 2A, Table S2), suggesting a complete rescue of the shorter body length due to APL-1EXT or APL-1 overexpression. Similarly, in a *daf-12(mu20)* background, transgenic lines APL-1 overexpression lines were the same length as *daf-12(m20)* mutants (Figure 2A, Table S2). Furthermore, knocking down *daf-12* levels in *apl-1(yn5)* animals was sufficient to rescue the *apl-1(yn5)* shortened body length (Table S2). Hence, both *daf-16*/FOXO and *daf-12* NHR activity are required for the shortened body length of *apl-1(yn5)* animals. By contrast, decreased *daf-2* activity or DAF-16 overexpression enhanced the shortened body length of transgenic APL-1 overexpression lines (Table S2), suggesting that the decreased body length is not due to higher *daf-16* activity or higher DAF-16 protein levels.

apl-1(yn5) mutants, as well as transgenic APL-1 or APL-1EXT overexpression lines, show a decreased egg-lying rate (Hornsten et al., 2007). Wild-type animals lay about 7 eggs per hour, whereas *apl-1(yn5)* mutants lay about 4 eggs per hour (Figure 2B, Table S3; Hornsten et al., 2007). Transgenic animals overexpressing either full-length APL-1 (*ynIs86* and *ynIs79*) or APL-1EXT (*ynIs71*) laid about 5 eggs an hour (Figure 2B, Table S3; Hornsten et al., 2007). *daf-16(mu86)* mutants laid significantly more eggs, about 9 eggs per hour, than wild-type animals (Figure 2B, Table S3). Transgenic APL-1

overexpression lines and *apl-1(yn5)* mutants carrying the *daf-16(mu86)* mutation laid eggs at the same rate as *daf-16(mu86)* mutants (Figure 2B, Table S3), suggesting a complete rescue of the egg-laying defect. Conversely, animals that overexpress DAF-16 showed a dramatic decrease in egg-laying rate to about 1-2 eggs per hour (Table S3). Overexpression of full-length APL-1 (*ynIs79*) or *apl-1(yn5)* mutation had no effect on the decreased egg-laying rate of DAF-16 overexpression animals (Table S3). *daf-12(m20)* mutants showed a similar egg-laying rate as wild-type animals (Figure 2B, Table S3). The decreased egg-laying rate of APL-1EXT overexpression animals (*ynIs71*) was completely rescued to *daf-12(m20)* levels (Figure 2B, Table S3). Collectively, these results suggest that APL-1EXT requires *daf-16*/FOXO and *daf-12* NHR activity to decrease body length and egg-laying rate.

IV.3.7. A mild increase in temperature increases the *apl-1(yn5)* lethality

As discussed above, at 20ºC and 25ºC wild-type animals hatch and develop into adults. At 27ºC, however, although all wild-type eggs hatch and animals survive (Table S4, (Ailion & Thomas 2000)), about 10% of developing animals enter the dauer life cycle (Ailion & Thomas 2000). At 20ºC, 86% of the *apl-1(yn5)* mutants survived and 14% remained either arrested in L1 or died (Table S4). This lethality was enhanced at slightly higher temperatures: 75% and 47% of the *apl-1(yn5)* mutants survived at 25ºC and 27ºC, respectively (Table S4). In addition, among the *apl-1(yn5)* mutants that survived, 46% remained in L1 arrest compared to only 1% of wild-type animals after 44 hours at 27ºC (Table S4); most of these *apl-1(yn5)* L1 arrested animals died within five days and only a few developed into gravid adults (data not shown). Hence, the *apl-1(yn5)* mutation

causes a temperature-sensitive lethality and developmental progression block. To determine whether this lethality could be phenocopied, we examined transgenic APL-1EXT animals (*ynIs71*). 82% of *ynIs71* [APL-1EXT] animals survived at 20ºC, 64% at 25ºC, and 54% at 27ºC (Table S4). Similarly, transgenic expression of APL-1EXT with the *snb-1* promoter (*ynIs105* [P*snb-1*::APL-1EXT]) resulted in 78% survival at 20ºC and 34% survival at 27ºC (Table S4). Animals carrying the mutated transgene APL-1*(yn32)*EXT (*ynIs106*) survived at similar rates as wild-type animals at 20ºC and 27ºC (Table S4). Hence, APL-1EXT activity is sufficient to cause a temperature-sensitive lethality and L1 arrest.

IV.3.8. The critical period for APL-1 induced lethality is during embryogenesis

Because APL-1 overexpression animals characteristically die after L1 arrest at 27ºC, we determined the critical time period of this APL-1 overexpression induced-lethality. Wild-type animals and *apl-1(yn5)* mutants were allowed to lay eggs at 15ºC. Eggs were shifted to 27ºC at 30 minute intervals and scored for survival 44 hours later. All wild-type eggs hatched and all animals survived from the different times (Figure 3). By contrast, the fraction of *apl-1(yn5)* eggs that hatched and survived increased linearly. At 30 minutes, 30% of *apl-1(yn5)* animals survived, whereas shifting the eggs to 27ºC at 6 hours resulted in nearly 100% survival (Figure 3), suggesting a critical time window of APL-1EXT-induced lethality during embryogenesis. *apl-1(yn5)* eggs that developed past the 3-fold (pretzel) embryonic stage at 15ºC survived the 27ºC shift (Figure 3), suggesting that the critical time period for APL-1 overexpression lethality is before and during elongation of the embryo development. These results would predict that all L1 APL-1 overexpression

animals shifted to 27ºC should survive. Indeed, all *apl-1(yn5)* L1 mutants (N=562, T=5) and 98% of transgenic *ynIs79* [APL-1::GFP] L1 animals shifted to 27ºC survived (N=377, T=4), again restricting the APL-1 induced lethality to embryogenesis.

IV.3.9. Identification of suppressors and enhancers of the APL-1EXT-induced lethality

To identify genes in the pathway of *apl-1*, we performed a forward genetic screen for modifiers of the APL-1EXT-induced lethality. The *apl-1(yn5)* mutants have a 53% lethality rate at 27ºC (Figure 4, Table S4). Mutagenized L4 animals were singly plated and 10 F1 adults were allowed to lay F2 eggs, which were then shifted to 27ºC. Plates on which the number of F2 progeny was greater or smaller than the number of progeny from non-mutagenized *apl-1(yn5)* mutants were selected for further analysis. In a screen of 200 haploid genomes, we isolated one mutant, *yn39*, that enhanced and one mutant, *yn38*, that suppressed the lethality rate. The survival rate was of those mutants was determined after several generations. For the enhancer strain only 18% of its progeny survived at 27ºC, while the suppressor strain showed a 96% survival rate (Figure 4, Table S4). These modifying effects were not temperature dependent. At 20ºC *apl-1(yn5)* animals have a lethality rate of 14%, whereas *yn39; apl-1(yn5)* and *yn38; apl-1(yn5)* double mutants showed a lethality rate of 31% and 4%, respectively (Table S4). To determine whether the *yn39* enhancement of lethality is dependent on *apl-1(yn5)*, we outcrossed *yn39* from the *apl-1(yn5)* background, allowed F2 animals to lay eggs, shifted F3 eggs to 27ºC, and scored for survival after 44 hours. All eggs developed into L4 animals, suggesting that the *yn39* mutation by itself does not cause lethality but rather enhances the *apl-1(yn5)*

lethality. As a control, from the same cross, 40 F2 *apl-1(yn5)* heterozygous animals were also picked at 20ºC. Of the F3 progeny, about 25% were homozygous for the *yn39* mutation (9/40=0-33% survival), while the rest of the animals showed a similar survival rate (40-60%) as *apl-1(yn5)* animals, except for one where 100% F3 progeny survived, presumably due to recombination

Both *yn38* and *yn39* are recessive alleles. *yn38* was mapped by conventional methods (Brenner, 1974) to chromosome III and *yn39* was mapped using SNPs to chromosome II. The DNA from both mutants was isolated and used for whole genome deep sequencing. Both strains were outcrossed for phenotypic characterization.

To determine whether the mutations suppressed or enhanced other *apl-1(yn5)* phenotypes, we examined L1 arrest. The *yn38* mutation partially suppressed the L1 arrest, while the *yn39* enhanced the L1 arrest at 27ºC: *apl-1(yn5)* animals have an L1 arrest rate of 46%, whereas *yn39; apl-1(yn5)* and *yn38; apl-1(yn5)* double mutants showed L1 arrest rates of 69% and 23%, respectively (Figure S2, Table S4). Hence, the *yn38* and *yn39* mutations regulate at least two phenotypes resulting from the *apl-1(yn5)* mutation.

IV.3.10. Knockdown of *apl-1* by RNAi on *apl-1(yn5)* mutants causes molting defect

Since *apl-1(yn5)* mutants overexpress APL-1EXT (Hornsten *et al*. 2007), we hypothesized that *apl-1* knock down by RNAi could rescue the *apl-1(yn5)*-induced overexpression lethality. Surprisingly, feeding double stranded *apl-1* RNA to L4 *apl-1(yn5)* animals resulted in dead L1-L4 animals in the next generation (F1). These F1 animals showed severe molting defects, similar to those seen in *apl-1(yn10)* mutants,

during the first to second larval transition (L1/L2). Complete loss of *apl-1*, as in *apl-1(yn10)* animals, leads to 100% L1/L2 lethality because mutants are unable to shed their old cuticle during the L1/L2 molt. However, the RNAi *apl-1*-induced molting defect of *apl-1(yn5)* animals occurred through all larval stages, suggesting that *apl-1* is required for molting not only during the L1/L2 transition, but during all larval transitions. Interestingly, *yn38* mutants partially rescued the molting defect resulting from *apl-1* knockdown of *apl-1(yn5)* animals (3/4 trials), suggesting a common mechanism of *apl-1(yn5)* 27ºC induced lethality and the molting defect.

IV.4. Discussion

Our results demonstrate that *apl-1* influences the *daf-16*/FOXO and *daf-12* NHR pathways to regulate multiple processes. Although the molecular mechanism of how APL-1 affects DAF-16 and DAF-12 activity is unclear, APL-1EXT activity is sufficient to affect developmental progression, viability, body length, and egg laying. These results suggest that after APL-1 cleavage, sAPL-1α signals to alter DAF-16 and DAF-12 activity. Hence, sAPL-1α might act as a modulator of DAF-16 and DAF-12 function. One possibility is that *apl-1(yn5)* animals are slowed during the molting transitions from one larval stage to the next. *apl-1(yn10)* null animals fail to shed their cuticle during the L1/L2 transition; this molting defect is rescued by APL-1EXT (Hornsten *et al*. 2007). *apl-1* knockdown leads to a molting defect during all four larval stages (Wiese *et al*. 2010), suggesting that APL-1 is required during each molt. Hence, overexpression of sAPL-1α could lead to a delay of the larval transitions. Thus far, *daf-2* insulin/IGF-1 receptor, *daf-12* NHR and *daf-16*/FOXO activity have not been implicated in the molting

process. However, *daf-12* NHR has been implicated in the heterochronic feedback loop of *let-7* miRNA, which regulates late developmental progression from L4 to adults (Bethke *et al*. 2009; Hammell *et al*. 2009) and *apl-1* expression in seam cells (Niwa *et al*. 2008). However, RNAi knockdown of *daf-12* did not alter *apl-1* expression in seam cells during the late L4 stage (Hada *et al*. 2010) and possible miRNA binding sites in the 3' UTR were deleted by the *apl-1(yn5)* mutation. Nevertheless, *daf-12* knockdown completely suppressed the developmental delay in *apl-1(yn5)* mutants, suggesting that sAPL-1α would signal through *daf-12* NHR earlier than the L1/L2 transition. By contrast, the *daf-16(mu86)* null mutation did not completely rescue the slowed development of *apl-1(yn5)* mutants, since a low percentage of *apl-1(yn5); daf-16(mu86)* animals were still found in L1-L4 stages. *apl-1* either signals through the *daf-2* pathway and/or in parallel to the *daf-16* and *daf-12* pathways. Interestingly, this signaling pathway is observed to regulate different modalities, such as egg-laying behavior and body-size. Similarly, transgenic *APP* mice show impairments in behavior, are lighter, and show reduced body weight gain compared to their wild-type littermates (Pugh *et al*. 2007; Codita *et al*.). Weight loss is also associated with patients with Alzheimer's disease, despite patients consuming more calories than age-matched non-AD controls (reviewed in (Aziz *et al*. 2008)). Hence, AD patients may have altered metabolic rates (Wang *et al*. 2004). Our results might suggest that metabolic rate changes could be mediated by secreted sAPP, which alters hormonal and insulin signaling pathways.

IV.5. Materials and Methods

IV.5.1. Strains

Caenorhabtitis elegans strains were grown and maintained on MYOB plates (Church *et al*. 1995) containing OP50 Escherichia coli bacteria at 20ºC using methods as described (Brenner 1974), unless noted. All mutations used are described in Wormbase (www.wormbase.org) and include: LGI: *daf-16(mu86)* (Lin *et al*. 1997); LGII: *yn38*; LGIII: *yn39, daf-2(e1370)* (Kimura *et al*. 1997); LGX: *daf-12(m20)* (Larsen *et al*. 1995), *apl-1(yn5* and *yn10)* (Hornsten *et al*. 2007). Construction of the APL-1 transgenes and the resulting transgenic lines are described (Hornsten *et al*. 2007). Integrated transgenic lines used were: *ynIs106* (P*apl-1*::APL-1(*yn32 yn5*), P*myo-2*::GFP); LGI: *ynIs109* (P*snb-1*::APL-1(cDNA)::GFP); LGII: *ynIs105* (P*snb-1*::APL-1(*yn5*)(cDNA), P*sur-5*::GFP); LGIII: *ynIs12* (P*snb-1*::APL-1(cDNA), *lin-15B*(+)); LGIV: *ynIs104* (P*rab-3*::APL-1(cDNA)::GFP, P*myo-2*::GFP), *zIs356* (P*daf-16*::DAF-16::GFP, pRF4 *rol-6(su1006gf)*) (Henderson & Johnson 2001); LGV: *ynIs13* (P*snb-1*::APL-1(cDNA), *lin-15B*(+)), *ynIs71* (P*apl-1*::APL-1(*yn5*), P*sur-5*::GFP), *ynIs79* (P*apl-1*::APL-1::GFP), *ynIs100* (P*apl-1*::APL-1(*yn32*)::GFP, pRF4 *rol-6(su1006gf)*); and LGX: *ynIs86* (P*apl-1*::APL-1, P*sur-5*::GFP), and *ynIs107* (P*apl-1*::APL-1(*yn32* E71K/D342C/S362C)::GFP, P*myo-2*::GFP) (Hoopes *et al*. 2010).

IV.5.2. Developmental timing and egg-laying rate assays

To synchronize worm populations ~15 gravid adult worms were placed into a bleach solution to release the eggs. Hatched worms were raised at 20ºC. Four days later [or five days for slower developing strains such as *apl-1(yn5)* and *zIs356*(DAF-16::GFP)], 10

synchronized adults were placed onto a fresh plate and allowed to lay eggs for 1-1.5 hours at room temperature (22-24ºC). Eggs were counted to determine an egg-laying rate; F1 progeny were placed at 20ºC to allow development. After 70-72 hours, the developmental stages of the animals at 20ºC were scored. For development at 25ºC, animals were scored after 48 hours. Each individual trial was performed with at least 3 plates of synchronized eggs for each strain and always included wild-type animals as a control. For statistical analysis one-way ANOVAs with Tukey post-test (95% confidence intervals) were performed to assess similarity between groups using Prism 4.0a software (GraphPad).

IV.5.3. Body length measurements

For each individual trial, 30 L4 animals (10 L4 per plate) for each strain were picked and allowed to develop for 3 days at room temperature (22-24ºC). Animals were mounted onto 2% agar pads containing a drop of 10 mM NaN_3 and pictures of the animals were taken at 10x magnification on a confocal microscope (Zeiss LSM 510 Confocal Laser Scanning System). The lengths of the worms were determined by drawing a line along the midline of the animals from the tip of the mouth to the tail. For statistical analysis one-way ANOVAs with Tukey post-test (95% confidence intervals) was performed to assess similarity between groups using Prism 4.0a software (GraphPad Software).

IV.5.4. Critical period assays

10 synchronized gravid adults were placed onto a fresh plate and allowed to lay eggs for 0.5, 1 or maximum of 1.5 hours at 15ºC. Eggs were counted and adult P_o were killed; F1

progeny were either shifted to 27 ºC or placed back at 15ºC to allow development, so that eggs in intervals of 30 minutes were shifted to 27 ºC up to 6 hours. After 44 hours at 27 ºC, the developmental stages and number of surviving animals were scored. Each individual trial was performed with at least 3 plates of synchronized eggs for each strain and always included wild type as a control. For statistical analysis one-way ANOVAs with Tukey post-test (95% confidence intervals) was performed to assess similarity between groups using Prism 4.0a software (GraphPad).

IV.5.5. RNA interference assays

RNAi by feeding: day -1, a single RNAi clone (bacteria HT115) was picked from the Ahringer library (Kamath *et al*. 2001) (Geneservice), which is maintained at -80ºC on Luria broth medium (LB) agar plates with 25 μg/ml carbenicillin and 12.5 μg/ml tetracycline), and incubated in 1 ml LB containing 100 μg/ml ampicillin (at 37°C, 280 rpm) overnight; day 0, the 1 ml bacterial culture was transferred into 10 ml LB containing 100 μg/ml ampicillin and incubated for another 4-6 hours at 37°C at 280 rpm. 450 μl of the bacteria culture was spread onto MYOB plates containing 400 mM of βD-isothiogalactopyranoside (IPTG) and 50 μg/ml ampicillin and these RNAi plates were placed in 37°C overnight; day 1, eight L4 animals (P_o) were placed on bacteria lawn that express double-stranded RNA (dsRNA) of *apl-1, daf-12* or empty vector control (L4440) to knock down expression levels of the targeted gene; day 4, about 50 F1 L4 animals were transferred onto new plates containing the same dsRNA expressing bacteria; day 5, about 10 F1 one day adults were transferred onto new plates containing the same dsRNA

expressing bacteria to lay eggs for 1-1.5 hours at 20ºC; day 8, the F2 population was scored for developmental progression.

IV.5.6. DAF-16::GFP nuclear translocation assays

L4 animals were placed onto new plates and grown at 20ºC. One day later, animals were placed at 35ºC and scored at different times (T=0, 30, 60, 90, 120, and 150 minutes) by mounting the animals onto 2% agar pads containing a drop of M9 physiological buffer (M9 is defined (Brenner 1974)) and looking at the worms at 100x magnification on a Zeiss Axioplan microscope. To ensure exact timing, the individual strains were placed at 35ºC in five minutes intervals. Upon 35ºC heat stress, DAF-16::GFP translocates from the cytoplasm into the nucleus (Henderson & Johnson 2001). The rate of DAF-16::GFP nuclear translocation was scored as described (Curran & Ruvkun 2007): category 0: all DAF-16::GFP showing diffuse localization in the cytoplasm; category 1: more DAF-16::GFP localized in cytoplasm than in nucleus; category 2: more DAF-16::GFP localized in nucleus than in cytoplasm; category 3: almost all DAF-16::GFP localized in nucleus.

IV.5.7. Mutagenesis screen and mapping

Worms were mutagenized with 50 mM EMS, as described (Brenner 1974). Mutagenized L4 animals (P_o) were singly plated and placed at 20ºC to develop until F1 animals reached adulthood. 10 F1 adults were allowed to lay F2 eggs, which were then shifted to 27ºC. Plates on which the number of F2 progeny was greater or smaller than the number of progeny from non-mutagenized *apl-1(yn5)* mutants were selected for further analysis.

We isolated 5 mutant alleles out of 200 haploid genomes screened. The strongest suppressor (*yn39*) and enhancer (*yn38*) of *apl-1(yn5)* lethality at 27 ºC were selected for mapping. *yn38* was mapped by conventional methods (Brenner 1974) to chromosome III and *yn39* was mapped using SNP to chromosome II as described (Davis *et al*. 2005). The DNA from both mutants was isolated and used for whole genome deep sequencing as described (Sarin *et al*. 2010).

IV.6. Acknowledgments

We wish to thank Cathy Savage-Dunn's group for kindly providing their N2, Oliver Hobert's lab for whole genome sequencing of *yn38* and *yn39,* lab members for helpful discussions, Sarah Tichelli and Casey Brander for help with the length measurements, Mboutidem Etokakpan for help in the genetic screen, and CGC for providing *daf-16,* DAF-16::GFP, and *daf-12* worms. This work was supported by grants from the Alzheimer's Association, National Institutes Health (R21AG0339 and R01AG32042), and National Science Foundation (IOS08207) (CL) and a National Institutes of Health RCMI grant to City College.

IV.7. References

Abrahante JE, Daul AL, Li M, Volk ML, Tennessen JM, Miller EA , Rougvie AE (2003). The *Caenorhabditis elegans* hunchback-like gene *lin-57/hbl-1* controls developmental time and is regulated by microRNAs. *Dev Cell*. **4**, 625-637.

Ailion M , Thomas JH (2000). Dauer formation induced by high temperatures in *Caenorhabditis elegans*. *Genetics*. **156**, 1047-1067.

Alzheimer's Association KM (2010). 2010 Alzheimer's disease facts and figures. *Alzheimer's and Dementia*. **6**, 158-194.

Ambros V (2000). Control of developmental timing in *Caenorhabditis elegans*. *Curr Opin Genet Dev*. **10**, 428-433.

Aziz NA, van der Marck MA, Pijl H, Olde Rikkert MG, Bloem BR , Roos RA (2008). Weight loss in neurodegenerative disorders. *J Neurol*. **255**, 1872-1880.

Baugh LR , Sternberg PW (2006). DAF-16/FOXO regulates transcription of *cki-1*/Cip/Kip and repression of *lin-4* during *C. elegans* L1 arrest. *Curr Biol*. **16**, 780-785.

Bethke A, Fielenbach N, Wang Z, Mangelsdorf DJ , Antebi A (2009). Nuclear hormone receptor regulation of microRNAs controls developmental progression. *Science*. **324**, 95-98.

Brenner S (1974). The Genetics of *Caenorhabditis elegans*. *Genetics*. **77**, 71-94.

Cabrejo L, Guyant-Marechal L, Laquerriere A, Vercelletto M, De la Fourniere F, Thomas-Anterion C, Verny C, Letournel F, Pasquier F, Vital A, Checler F, Frebourg T, Campion D , Hannequin D (2006). Phenotype associated with APP duplication in five families. *Brain*. **129**, 2966-2976.

Chartier-Harlin MC, Crawford F, Houlden H, Warren A, Hughes D, Fidani L, Goate A, Rossor M, Roques P, Hardy J , et al. (1991). Early-onset Alzheimer's disease caused by mutations at codon 717 of the beta-amyloid precursor protein gene. *Nature*. **353**, 844-846.

Church DL, Guan KL , Lambie EJ (1995). Three genes of the MAP kinase cascade, *mek-2*, *mpk-1/sur-1* and *let-60 ras*, are required for meiotic cell cycle progression in *Caenorhabditis elegans*. *Development*. **121**, 2525-2535.

Codita A, Gumucio A, Lannfelt L, Gellerfors P, Winblad B, Mohammed AH , Nilsson LN (2010). Impaired behavior of female tg-ArcSwe APP mice in the IntelliCage: A longitudinal study. *Behav Brain Res*. **215**, 83-94.

Curran SP , Ruvkun G (2007). Lifespan regulation by evolutionarily conserved genes essential for viability. *PLoS Genet*. **3**, e56.

Daigle I , Li C (1993). *apl-1*, a *Caenorhabditis elegans* gene encoding a protein related to the human beta-amyloid protein precursor. *Proc Natl Acad Sci USA*. **90**, 12045-12049.

Davis MW, Hammarlund M, Harrach T, Hullett P, Olsen S , Jorgensen EM (2005). Rapid single nucleotide polymorphism mapping in *C. elegans*. *BMC Genomics*. **6**, 118.

Ewald CY , Li C (2010). Understanding the molecular basis of Alzheimer's disease using a *Caenorhabditis elegans* model system. *Brain Struct Funct*. **214**, 263-283.

Gems D, Sutton AJ, Sundermeyer ML, Albert PS, King KV, Edgley ML, Larsen PL , Riddle DL (1998). Two pleiotropic classes of *daf-2* mutation affect larval arrest,

adult behavior, reproduction and longevity in *Caenorhabditis elegans*. *Genetics*. **150**, 129-155.

Goate A, Chartier-Harlin MC, Mullan M, Brown J, Crawford F, Fidani L, Giuffra L, Haynes A, Irving N, James L , et al. (1991). Segregation of a missense mutation in the amyloid precursor protein gene with familial Alzheimer's disease. *Nature*. **349**, 704-706.

Gralle M , Ferreira ST (2007). Structure and functions of the human amyloid precursor protein: the whole is more than the sum of its parts. *Prog Neurobiol*. **82**, 11-32.

Grosshans H, Johnson T, Reinert KL, Gerstein M , Slack FJ (2005). The temporal patterning microRNA *let-7* regulates several transcription factors at the larval to adult transition in *C. elegans*. *Dev Cell*. **8**, 321-330.

Hada K, Asahina M, Hasegawa H, Kanaho Y, Slack FJ , Niwa R (2010). The nuclear receptor gene *nhr-25* plays multiple roles in the *Caenorhabditis elegans* heterochronic gene network to control the larva-to-adult transition. *Dev Bio*. **344**, 1100-1109.

Hammell CM, Karp X , Ambros V (2009). A feedback circuit involving *let-7*-family miRNAs and DAF-12 integrates environmental signals and developmental timing in *Caenorhabditis elegans*. *Proc Natl Acad Sci USA*. **106**, 18668-18673.

Heber S, Herms J, Gajic V, Hainfellner J, Aguzzi A, Rulicke T, von Kretzschmar H, von Koch C, Sisodia S, Tremml P, Lipp HP, Wolfer DP , Muller U (2000). Mice with combined gene knock-outs reveal essential and partially redundant functions of amyloid precursor protein family members. *J Neurosci*. **20**, 7951-7963.

Henderson ST , Johnson TE (2001). *daf-16* integrates developmental and environmental inputs to mediate aging in the nematode *Caenorhabditis elegans*. *Curr Biol*. **11**, 1975-1980.

Herms J, Anliker B, Heber S, Ring S, Fuhrmann M, Kretzschmar H, Sisodia S , Muller U (2004). Cortical dysplasia resembling human type 2 lissencephaly in mice lacking all three APP family members. *Embo J*. **23**, 4106-4115.

Hoopes JT, Liu X, Xu X, Demeler B, Folta-Stogniew E, Li C , Ha Y (2010). Structural characterization of the E2 domain of APL-1, a *Caenorhabditis elegans* homolog of human amyloid precursor protein, and its heparin binding site. *The Journal of biological chemistry*. **285**, 2165-2173.

Hornsten A, Lieberthal J, Fadia S, Malins R, Ha L, Xu X, Daigle I, Markowitz M, O'Connor G, Plasterk R , Li C (2007). APL-1, a *Caenorhabditis elegans* protein related to the human beta-amyloid precursor protein, is essential for viability. *Proc Natl Acad Sci USA*. **104**, 1971-1976.

Kamath RS, Martinez-Campos M, Zipperlen P, Fraser AG , Ahringer J (2001). Effectiveness of specific RNA-mediated interference through ingested double-stranded RNA in *Caenorhabditis elegans*. *Genome Biol*. **2**, RESEARCH0002.

Kang J, Lemaire HG, Unterbeck A, Salbaum JM, Masters CL, Grzeschik KH, Multhaup G, Beyreuther K , Muller-Hill B (1987). The precursor of Alzheimer's disease amyloid A4 protein resembles a cell-surface receptor. *Nature*. **325**, 733-736.

Kenyon C (2005). The plasticity of aging: insights from long-lived mutants. *Cell*. **120**, 449-460.

Kidd M (1964). Alzheimer's Disease--an Electron Microscopical Study. *Brain*. **87**, 307-320.

Kimura KD, Tissenbaum HA, Liu Y , Ruvkun G (1997). *daf-2*, an insulin receptor-like gene that regulates longevity and diapause in *Caenorhabditis elegans*. *Science*. **277**, 942-946.

Krigman MR, Feldman RG , Bensch K (1965). Alzheimer's Presenile Dementia. A Histochemical and Electron Microscopic Study. *Lab Invest*. **14**, 381-396.

Larsen PL, Albert PS , Riddle DL (1995). Genes that regulate both development and longevity in *Caenorhabditis elegans*. *Genetics*. **139**, 1567-1583.

Lee RY, Hench J , Ruvkun G (2001). Regulation of *C. elegans* DAF-16 and its human ortholog FKHRL1 by the *daf-2* insulin-like signaling pathway. *Curr Biol*. **11**, 1950-1957.

Lin K, Dorman JB, Rodan A , Kenyon C (1997). *daf-16*: An HNF-3/forkhead family member that can function to double the life-span of *Caenorhabditis elegans*. *Science*. **278**, 1319-1322.

Lin K, Hsin H, Libina N , Kenyon C (2001). Regulation of the *Caenorhabditis elegans* longevity protein DAF-16 by insulin/IGF-1 and germline signaling. *Nature genetics*. **28**, 139-145.

Luse SA , Smith KR, Jr. (1964). The ultrastructure of senile plaques. *Am J Pathol*. **44**, 553-563.

Murrell J, Farlow M, Ghetti B , Benson MD (1991). A mutation in the amyloid precursor protein associated with hereditary Alzheimer's disease. *Science*. **254**, 97-99.

Niwa R, Zhou F, Li C , Slack FJ (2008). The expression of the Alzheimer's amyloid precursor protein-like gene is regulated by developmental timing microRNAs and their targets in *Caenorhabditis elegans*. *Dev Bio*. **315**, 418-425.

Ogg S, Paradis S, Gottlieb S, Patterson GI, Lee L, Tissenbaum HA , Ruvkun G (1997). The Fork head transcription factor DAF-16 transduces insulin-like metabolic and longevity signals in *C. elegans*. *Nature*. **389**, 994-999.

Pugh PL, Richardson JC, Bate ST, Upton N , Sunter D (2007). Non-cognitive behaviours in an APP/PS1 transgenic model of Alzheimer's disease. *Behav Brain Res*. **178**, 18-28.

Riddle DL , Albert PS (1997). Genetic and Environmental Regulation of Dauer Larva Development. In *C. elegans II*. (DL Riddle, T Blumenthal, BJ Meyer , JR Priess, eds). New York: Cold Spring Harbor Laboratory Press, pp. 739–768.

Roush SF , Slack FJ (2009). Transcription of the *C. elegans let-7* microRNA is temporally regulated by one of its targets, *hbl-1*. *Dev Bio*.

Rovelet-Lecrux A, Hannequin D, Raux G, Le Meur N, Laquerriere A, Vital A, Dumanchin C, Feuillette S, Brice A, Vercelletto M, Dubas F, Frebourg T , Campion D (2006). APP locus duplication causes autosomal dominant early-onset Alzheimer disease with cerebral amyloid angiopathy. *Nature genetics*. **38**, 24-26.

Sarin S, Bertrand V, Bigelow H, Boyanov A, Doitsidou M, Poole RJ, Narula S , Hobert O (2010). Analysis of multiple ethyl methanesulfonate-mutagenized *Caenorhabditis elegans* strains by whole-genome sequencing. *Genetics*. **185**, 417-430.

Slack FJ, Basson M, Liu Z, Ambros V, Horvitz HR , Ruvkun G (2000). The *lin-41* RBCC gene acts in the *C. elegans* heterochronic pathway between the *let-7* regulatory RNA and the LIN-29 transcription factor. *Mol Cell*. **5**, 659-669.

Sleegers K, Brouwers N, Gijselinck I, Theuns J, Goossens D, Wauters J, Del-Favero J, Cruts M, van Duijn CM , Van Broeckhoven C (2006). APP duplication is sufficient to cause early onset Alzheimer's dementia with cerebral amyloid angiopathy. *Brain*. **129**, 2977-2983.

Sulston JE , Horvitz HR (1977). Post-embryonic cell lineages of the nematode, *Caenorhabditis elegans*. *Dev Bio*ed. **56**, 110-156.

Sulston JE, Schierenberg E, White JG , Thomson JN (1983). The embryonic cell lineage of the nematode *Caenorhabditis elegans*. *Dev Bio*. **100**, 64-119.

Terry RD, Gonatas NK , Weiss M (1964). Ultrastructural Studies in Alzheimer's Presenile Dementia. *Am J Pathol*. **44**, 269-297.

Wang PN, Yang CL, Lin KN, Chen WT, Chwang LC , Liu HC (2004). Weight loss, nutritional status and physical activity in patients with Alzheimer's disease. A controlled study. *J Neurol*. **251**, 314-320.

Wiese M, Antebi A , Zheng H (2010). Intracellular trafficking and synaptic function of APL-1 in *Caenorhabditis elegans*. *PLoS One*. **5**.

Zheng H, Jiang M, Trumbauer ME, Sirinathsinghji DJ, Hopkins R, Smith DW, Heavens RP, Dawson GR, Boyce S, Conner MW, Stevens KA, Slunt HH, Sisoda SS, Chen HY , Van der Ploeg LH (1995). beta-Amyloid precursor protein-deficient mice show reactive gliosis and decreased locomotor activity. *Cell*. **81**, 525-531.

IV.8. Figures and Tables

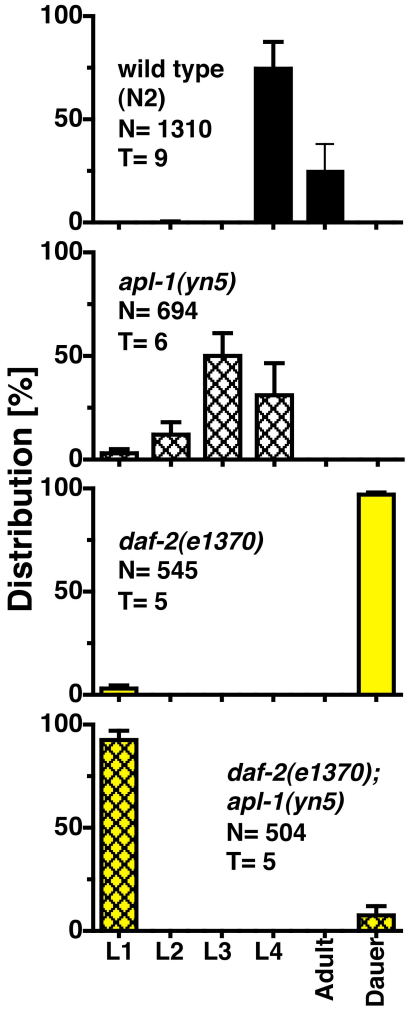

Figure 1. APL-1EXT expression slows developmental progression of wild-type and *daf-2* animals at 25ºC. After 48 hours at 25ºC, all eggs from wild-type N2 animals developed into L4 or adult animals and *apl-1(yn5)* mutants developed mostly into L3 to L4 animals, whereas almost all *daf-2(e1370)* transitioned into an alternative dauer stage. Most *daf-2(e1370); apl-1(yn5)* double mutants, however, arrest in the L1 stage at 25ºC. N= number of animals, T= number of independent trials.

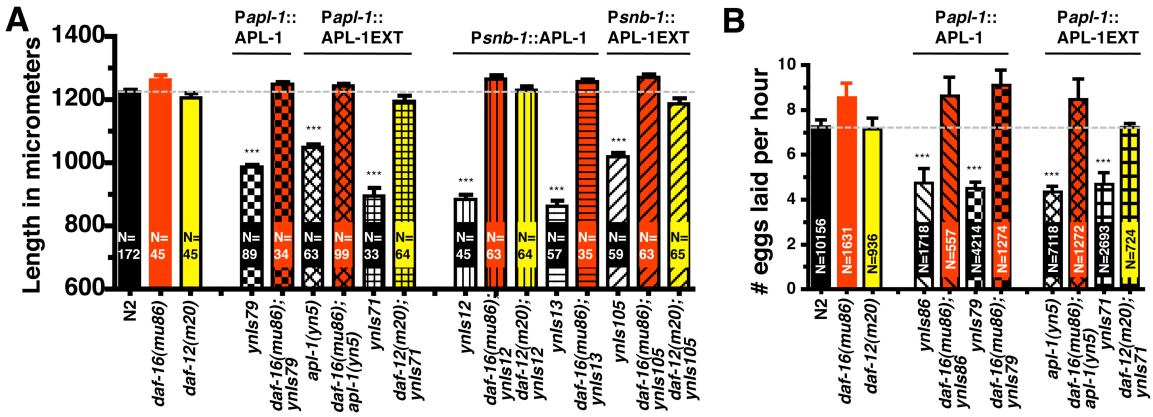

Figure 2. Decreased DAF-16/FOXO and DAF-12 NHR activity is required for APL-1 signaling to modulate body-size and egg-laying rate. Overexpression of APL-1 or APL-1EXT under either the endogenous or *snb-1* promoter caused a shortened the body length of the animal (A; black). This shortened body length was abolished in a *daf-16* null background (A; red) or in a *daf-12(m20)* mutant background (A; yellow). Similarly, overexpression of APL-1 or APL-1EXT caused a reduction in the egg-laying rate (B; black); an egg-laying rate higher than wild type was restored in a *daf-16* null background (B; red) or in a *daf-12(m20)* mutant background (B; yellow). Tables S2 and S3 show detailed statistical analysis and results of additional strains. Each APL-1 transgene indicated with a different cross hatching; *daf-16* null background is indicated in red; *daf-12(m20)* mutant background is indicated in yellow; *Is*, indicates integrated transgene. ***=P<0.001 determined by one-way ANOVA with Tukey post-test.

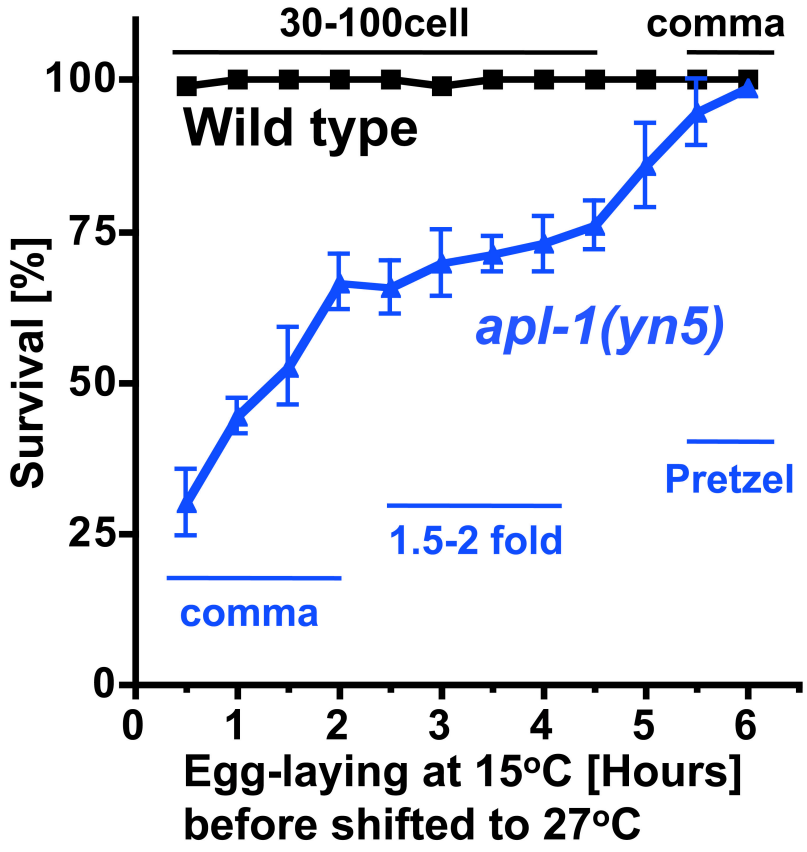

Figure 3. Critical time period for APL-1 lethality.

Eggs were laid at 15ºC and shifted at intervals of 30 minutes to 27ºC: plotted is the survival rate of those eggs after 44 hours at 27ºC. All wild-type eggs survive the 27ºC shifted, whereas at 30 minutes only 30% of the *apl-1(yn5)* eggs survived into larval stages. However, by letting the *apl-1(yn5)* eggs develop at 15ºC for 6 hours, all eggs survived and developed into larval animals. The developmental stage of eggs (30-100 cell, comma, 1.5-2 fold embryo, 3-fold embryo, pretzel) was scored at various time points. *apl-1(yn5)* eggs were chronologically further developed when laid compared to wild type, because *apl-1(yn5)* animals retained eggs longer in the uterus than wild-type animals. At least 3 trials for each time point (N>300).

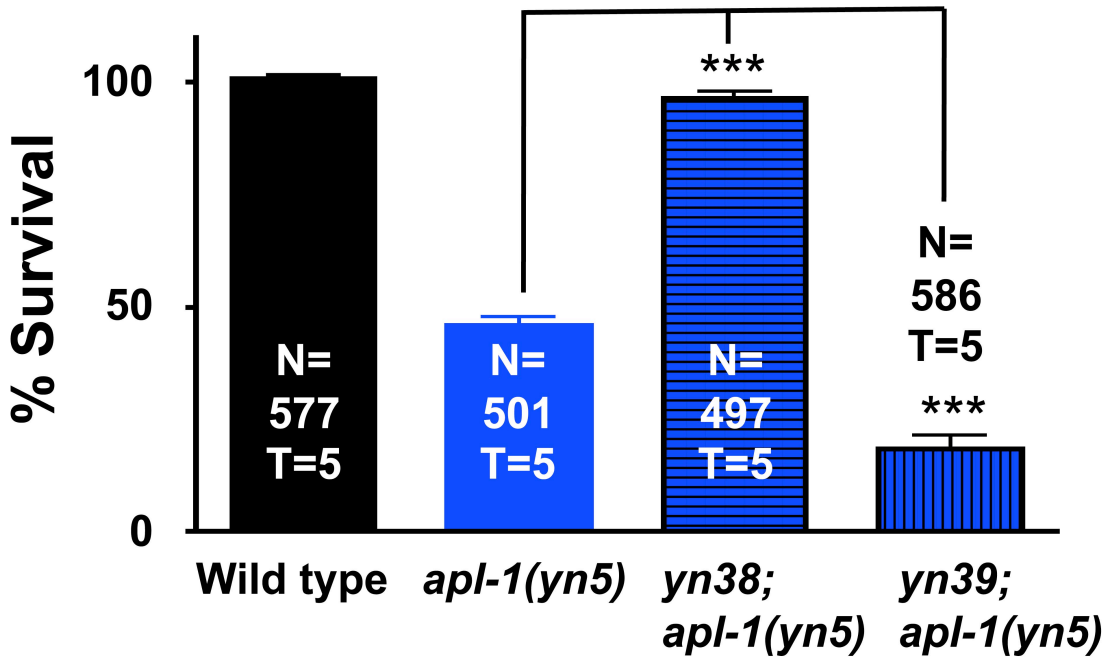

Figure 4. Suppressor and enhancer of APL-1 induced lethality

All wild-type eggs survived and developed into larval animals, whereas only 45% of *apl-1(yn5)* eggs survived and developed at 27ºC. From the mutagenesis screen, 96% of the *yn38; apl-1(yn5)* and 18% of the *yn3; apl-1(yn5)* double mutant animals survived. *** P<0.001 to *apl-1(yn5)* determined with One-way ANOVA post hoc Tukey.

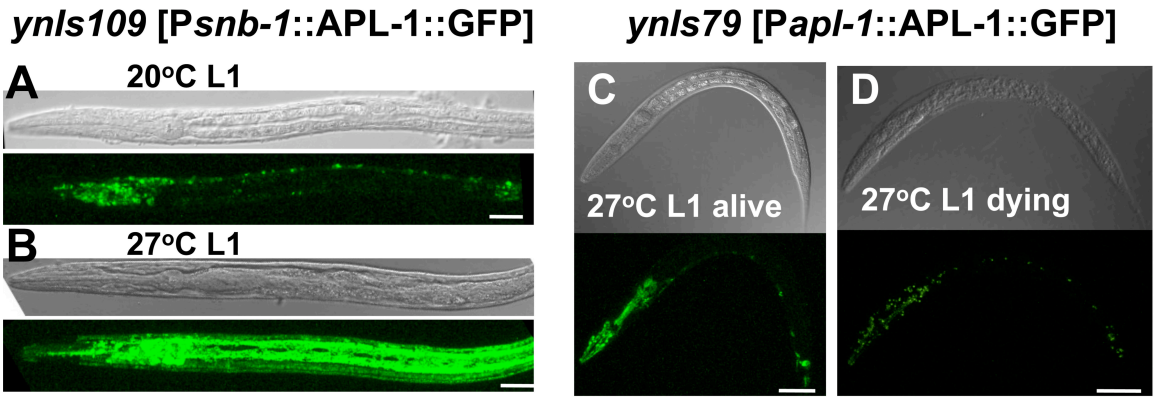

Supplement Figure S1. Higher temperature increases APL-1::GFP fluorescence in L1 animals

The APL-1::GFP fluorescence of *ynIs109* [P*snb-1*::APL-1::GFP] L1 animals is increased at 27ºC (**B**) compared at 20ºC (**A**). APL-1::GFP fluorescence of *ynIs79* [P*apl-1*::APL-1::GFP] L1 animals alive (**C**) or dying (**D**) at 27ºC. Scale bars in all pictures are 50 μm.

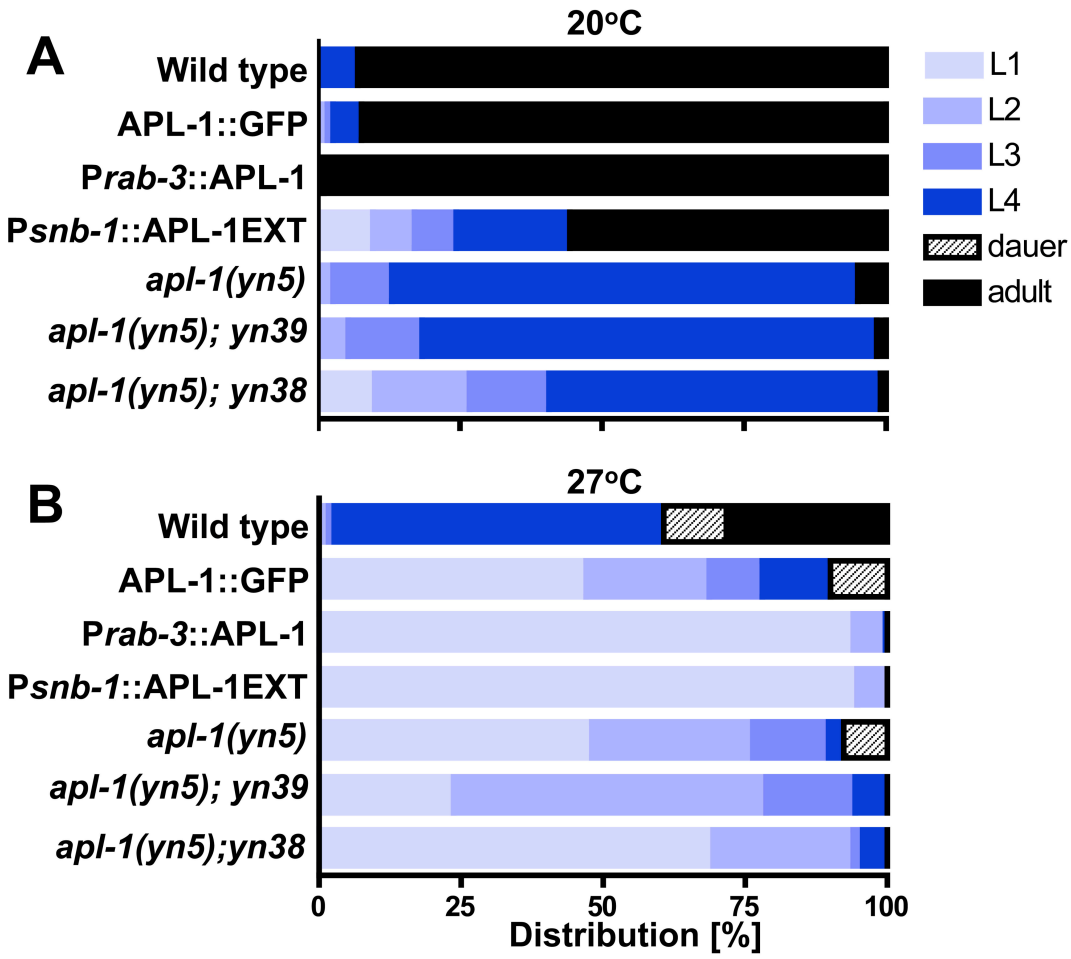

Supplement Figure S2. APL-1 overexpression animals retard in L1 at higher temperature.

A. At 20ºC, most wild-type eggs developed into adults after 72 hours. By contrast, the surviving *apl-1(yn5)* animals are found in earlier larval stages. **B**. At 27ºC, most wild-type eggs developed into L4 or adults and about 10% went into dauer diapause after 44 hours. By contrast, 50% the surviving *apl-1(yn5)* or transgenic *ynIs79* [APL-1::GFP] animals were found retarded in L1 and the remaining in L2-L4 with about 10% dauers. Strikingly, about 90% animals overexpressing APL-1 in all neurons are found in L1 stage. For N values see Table S4.

Table 1. Developmental stage after 72 hours at 20°C(cumulative)

Strain (Genotype)	N_{eggs}	L1 [%]	L2 [%}	L3 [%]	L4 [%]	Adult [%]	N_{worms} (T)	Average Survival 20°C[%]
Controls								
N2 (wild type)	3462	0	0	0	3	97	3572 (30)	100'
ynIs106 [P*apl-1*::APL-1EXT(*yn32*)]	256	0	0	0	0	100	259 (3)	100'
Endogenous Overexpression of the Extracellular Domain of APL-1 (APL-1EXT)								
apl-1(yn5)	943	1	2	10	82	5	826 (11)	86
ynIs71 [P*apl-1*::APL-1EXT]	488	1	1	2	37	59	397 (6)	82
Overexpression of APL-1 in a* daf-12(m20) *mutant background								
daf-12(m20)	936	0	0	0	1	99	921 (7)	97
daf-12(m20); ynIs71	244	0	0	0	7	93	197 (3)	80
RNAi* daf-12 *on apl-1(yn5)								
N2 grown on L4440 RNAi	320	0	0	0	0	100	323 (3)	100'
N2 grown on *daf-12* RNAi	766	0	0	0	0	100	733 (3)	95
daf-12(m20) grown on L4440 RNAi	366	0	0	0	0	100	332 (3)	91
daf-12(m20) grown on *daf-12* RNAi	460	0	0	0	0	100	404 (3)	89
apl-1(yn5) grown on L4440 RNAi	683	1	0	4	95	0	538 (3)	78
apl-1(yn5) grown on *daf-12* RNAi	743	0	0	0	0	100	608 (3)	81
Overexpression of APL-1 in a* daf-16(mu38) *null background								
daf-16(mu86)	579	0	0	0	1	99	597 (5)	100'
daf-16(mu86); yn5	1272	8	5	3	11	73	1115 (4)	85
Overexpression of APL-1 and overexpression of DAF-16								
zIs356 [DAF-16::GFP]	2241	0	1	9	90	0	2236 (12)	99
zIs356; *apl-1(yn5)*	1165	1	26	60	13	0	1031 (3)	90
Overexpression of APL-1 in a* daf-2(e1370) *reduction-of-function background								
daf-2(e1370) *[1]	748	1	0	2	93	1	691(4)	92
daf-2(e1370); apl-1(yn5) *[2]	416	10	13	77	0	0	283 (3)	69

All developmental distributions are shown in cumulative form. *Is*, [] integrated transgene. *Ex*, {} non-integrated transgene. (N) corresponds to the number of animals observed. (T) corresponds to the number of independent times experiment was performed. *[1]=form on average 3% dauers; *[2] =no dauers observed at 20°C. L4440 RNAi = empty vector control

Table S1. DAF-16::GFP nuclear translocation upon 35°C heat stress

Strains	Cumulative distribution [%] in categories				
	0	1	2	3	N (T)
0 minutes at 35°C					
zIs356 [DAF-16::GFP]	100	0	0	0	176 (7)
zIs356; *apl-1(yn5)*	100	0	0	0	107 (1)
zIs356; *ynIs106* [P*apl-1*::APL-1EXTnull]	100	0	0	0	32 (1)
zIs356; *flp-1(ok2781)*	100	0	0	0	27 (1)
30 minutes at 35°C					
zIs356 [DAF-16::GFP]	93	7	0	0	329 (12)
zIs356; *apl-1(yn5)*	100	0	0	0	127 (4)
zIs356; *ynIs106* [P*apl-1*::APL-1EXTnull]	97.5	2.5	0	0	61 (1)
zIs356; *flp-1(ok2781)*	97	3	0	0	33 (1)
60 minutes at 35°C					
zIs356 [DAF-16::GFP]	0	100	0	0	245 (10)
zIs356; *apl-1(yn5)*	11	89	0	0	141 (4)
zIs356; *ynIs106* [P*apl-1*::APL-1EXTnull]	0	100	0	0	33 (1)
zIs356; *flp-1(ok2781)*	0	100	0	0	63 (1)
90 minutes at 35°C					
zIs356 [DAF-16::GFP]	0	7	91	2	255 (9)
zIs356; *apl-1(yn5)*	0	93	7	0	150 (4)
zIs356; *ynIs106* [P*apl-1*::APL-1EXTnull]	0	0	100	0	53 (1)
zIs356; *flp-1(ok2781)*	0	0	100	0	30 (1)
120 minutes at 35°C					
zIs356 [DAF-16::GFP]	0	0	84	16	445 (8)
zIs356; *apl-1(yn5)*	0	84	16	0	141 (3)
zIs356; *ynIs106* [P*apl-1*::APL-1EXTnull]	0	0	7	93	40 (1)
zIs356; *flp-1(ok2781)*	0	0	39	61	41 (1)
150 minutes at 35°C					
zIs356 [DAF-16::GFP]	0	0	13	87	518 (9)
zIs356; *apl-1(yn5)*	0	0	97	3	156 (3)
zIs356; *ynIs106* [P*apl-1*::APL-1EXTnull]	0	0	3	97	38 (1)
zIs356; *flp-1(ok2781)*	0	0	9	91	12 (1)

DAF-16::GFP localization was scored on synchronized 1 day old adults. N corresponds to number of worms observed. T corresponds to number of independent trials. The rate of DAF-16::GFP nuclear translocation was scored as described (Curran & Ruvkun 2007): category 0: all DAF-16::GFP showing diffuse localization in the cytoplasm; category 1: more DAF-16::GFP localized in cytoplasm than in nucleus; category 2: more DAF-16::GFP localized in nucleus than in cytoplasm; category 3: almost all DAF-16::GFP localized in nucleus. *ynIs106* is a transgene that contains the missense mutation *yn32* in APL-1EXT; this transgene does not rescue *apl-1(yn10)* null lethality and is considered a non-functional APL-1EXT control. *flp-1(ok2781)* was used as another control.

Table S2. Body Size of 3 Days old Adults

Strain (Genotype)	Length ± S.E.M. [μm]	N	% N2	P-Value against N2	P-Value against control ($^{\lozenge,\wedge,\#,@}$)
Controls					
N2 (wild type)	1225 ± 6.6	172			>0.05$^{\lozenge}$
ynIs100 [P*apl-1*::APL-1(mut)::GFP]*	1200 ± 21.3	20	-2%	>0.05	>0.05$^{\lozenge}$
Endogenous Overexpression of Full Length APL-1					
ynIs86 [P*apl-1*::APL-1]	1074 ± 11.9	59	-12%	<0.001	<0.001$^{\lozenge}$
ynIs79 [P*apl-1*::APL-1::GFP]	986 ± 9.6	89	-20%	<0.001	<0.001$^{\lozenge}$
apl-1(yn10) {P*apl-1*::APL-1}	1016 ± 19.3	46	-17%	<0.001	<0.001$^{\lozenge}$
Endogenous Overexpression of the Extracellular Domain of APL-1 (APL-1EXT)					
apl-1(yn5)	1047 ± 11.6	63	-15%	<0.001	<0.001$^{\lozenge}$
ynIs71 [P*apl-1*::APL-1EXT]	894 ± 28.2	33	-27%	<0.001	<0.001$^{\lozenge}$
Overexpression of APL-1 driven by* snb-1 *promoter					
ynIs12 [P*snb-1*::APL-1]	884 ± 14.36	45	-28%	<0.001	<0.001$^{\lozenge}$
ynIs13 [P*snb-1*::APL-1]	861 ± 19.5	57	-30%	<0.001	<0.001$^{\lozenge}$
ynIs109 [P*snb-1*::APL-1::GFP]	919 ± 19.5	52	-25%	<0.001	<0.001$^{\lozenge}$
ynIs12; ynIs86	1073 ± 8.6	117	-12%	<0.001	<0.001$^{\lozenge}$
Overexpression of the Extracellular Domain of APL-1 driven by* snb-1 *promoter					
ynIs105 [*Psnb-1*::APL-1EXT]	1018 ± 13.1	59	-17%	<0.001	<0.001$^{\lozenge}$
Overexpression of APL-1 in a* daf-16(mu38) *null background					
daf-16(mu86)	1263 ± 15.8	45	+3%	>0.05	
daf-16(mu86); ynIs79	1247 ± 10.2	34	+2%	>0.05	>0.05$^{\lozenge}$
daf-16(mu86); apl-1(yn5)	1243 ± 9.0	99	+1%	>0.05	>0.05$^{\lozenge}$
daf-16(mu86); ynIs12	1265 ± 12.9	63	+3%	>0.05	>0.05$^{\lozenge}$
daf-16(mu86); ynIs13	1256 ± 8.7	35	+3%	>0.05	>0.05$^{\lozenge}$
daf-16(mu86); ynIs105	1271 ± 10.8	63	+4%	>0.05	>0.05$^{\lozenge}$
Overexpression of APL-1 in a* daf-2(e1370) *reduction-of-function background					
daf-2(e1370)	1131 ± 9.4	44	-8%	<0.001	<0.001$^{\lozenge}$
daf-2(e1370); ynIs79	1037 ± 12.0	51	-15%	<0.001	<0.01$^{\wedge}$
daf-2(e1370); apl-1(yn10) {*Papl-1*::APL-1}	1228 ± 15.8	17	0%	>0.05	>0.05$^{\wedge}$
Overexpression of APL-1 and overexpression of DAF-16					
zIs356 [DAF-16::GFP]*	1124 ± 20.8	15	-8%	>0.05	<0.01$^{\lozenge}$
zIs356; *ynIs79**	1034 ± 12.2	29	-16%	<0.001	>0.05$^{\#}$
Overexpression of APL-1 in a* daf-12(m20) *mutant background					
daf-12(m20)	1173 ± 11.8	45	-4%	>0.05	<0.05$^{\lozenge}$
daf-12(m20); ynIs71	1196 ± 16.8	64	-2%	>0.05	>0.05$^{@}$
daf-12(m20); ynIs12	1231 ± 12.7	64	0.5%	>0.05	>0.05$^{@}$
daf-12(m20); ynIs105	1187 ± 18.6	65	-3%	>0.05	>0.05$^{@}$
RNAi* daf-12 *on apl-1(yn5)					
N2 grown on L4440 RNAi	1345 ± 15.2	51			
N2 grown on *daf-12* RNAi	1337 ± 14.6	28	-1%$^{\infty}$	>0.05$^{\infty}$	<0.05$^{»}$
apl-1(yn5) grown on L4440 RNAi	1254 ± 18.3	35	-7%$^{\infty}$	<0.01$^{\infty}$	
apl-1(yn5) grown on *daf-12* RNAi	1476 ± 20.9	36	+10%$^{\infty}$	<0.001$^{\infty}$	<0.001$^{»}$

*animals carry pRF4 *rol-6 (su1006)* co-injection marker. *Is*, [] integrated transgene. *Ex*, {} non-integrated transgene. (N) corresponds to the number of animals observed. L4440 RNAi = empty vector control. P-values were determined by one-way ANOVAs with Tukey post-test (95% confidence intervals). P values against controls: ◊ = *daf-16(mu86)*, **^** = *daf-2(e1370)*, **#** = DAF-16::GFP*(zIs356)*, @ = *daf-12(m20)*, ∞ = N2 grown on L4440 RNAi, » = *apl-1(yn5)* grown on L4440 RNAi. Because data from the N2 strains from our lab and those from the lab of Cathy Savage-Dunn showed no statistical difference, the N2 body size statistics were combined.

Table S3. Egg-Laying-Rate of 2 Days old Adults at Room Temperature 22-24°C

Strain (Genotype)	N_{Po}	T	N_{eggs}	Average Egg/1h/1Po ± S.E.M.	% N2	P-value against N2	P-value against control ($^{\lozenge,\wedge,\#,@}$)
Controls							
N2 (wild type)	988	38	10156	7.3 ± 0.3			>0.05$^{\lozenge}$
lon-2(e678) apl-1(yn10)/dpy-8(e130)	52	4	113	3.4 ± 1.3	-53%	>0.05	0.0084
ynIs100 [P*apl-1*::APL-1(mut)::GFP]*	83	3	575	5.4 ± 0.9	-26%	>0.05	0.0188
ynIs107 [P*apl-1*::APL-1(mut)]	118	6	994	7.9 ± 1.0	+8%	>0.05	0.5892
Endogenous Overexpression of Full Length APL-1							
ynIs86 [P*apl-1*::APL-1]	173	5	1718	4.7 ± 0..6	-36%	<0.05	0.0017
ynIs79 [P*apl-1*::APL-1::GFP]	609	16	4214	4.5 ± 0.3	-38%	<0.001	<0.0001
Endogenous Overexpression of the Extracellular Domain of APL-1 (APL-1EXT)							
apl-1(yn5)	1055	34	7118	4.3 ± 0.2	-41%	<0.001	<0.0001
ynIs71 [P*apl-1*::APL-1EXT]	291	6	2693	4.7 ± 0.5	-36%	<0.05	0.0008
Overexpression of APL-1 in a* daf-16(mu38) *null background							
daf-16(mu86)	136	10	1631	8.5 ± 0.6	+16%	>0.05	
daf-16(mu86); ynIs86	78	4	557	8.6 ± 0.8	+18%	>0.05	>0.05$^{\lozenge}$
daf-16(mu86); ynIs79	92	4	1274	9.1 ± 0.7	+25%	<0.05	>0.05$^{\lozenge}$
daf-16(mu86); yn5	199	4	1272	8.5 ± 0.9	+16%	>0.05	>0.05$^{\lozenge}$
Overexpression of APL-1 and overexpression of DAF-16							
zIs356 [DAF-16::GFP]*	276	9	2092	1.4 ± 0.1	-81%	<0.001	<0.001$^{\lozenge}$
zIs356; *ynIs79**	295	7	2633	1.5 ± 0.1	-79%	<0.001	>0.05$^{\#}$
zIs356; *apl-1(yn5)**	121	3	1165	2.9 ± 0.3	-60%	<0.001	>0.05$^{\#}$
Overexpression of APL-1 in a* daf-12(m20) *mutant background							
daf-12(m20)	86	7	936	7.1 ± 0.5	-3%	>0.05	>0.05$^{\lozenge}$
daf-12(m20); ynIs71	53	5	724	7.2 ± 0.2	-1%	>0.05	>0.05$^{@}$

All developmental distributions are shown in cumulative form. *animals carry pRF4 *rol-6 (su1006)* co-injection marker. *Is*, [] integrated transgene, *Ex*, {} non-integrated transgene. (N) corresponds to the number of animals observed. (T) corresponds to the number of independent times experiment was performed. P-values were determined by one-way ANOVAs with Tukey post-test (95% confidence intervals). P values against controls: ◊ = *daf-16(mu86)*, **#** = DAF-16::GFP*(zIs356), @ = daf-12(m20).* Because data from the N2 strains from our lab and those from the lab of Cathy Savage-Dunn showed no statistical difference, the N2 egg-laying rate statistics were combined.

Table S4. APL-1 overexpression induced lethality increases with higher temperature from 20°C to 27°C

Strain (Genotype)	20°C N_{eggs}	N_{worms}	T	Ave % Survival STE	% L1	25°C N_{eggs}	N_{worms}	T	Ave % Survival STE	% L1	27°C N_{eggs}	N_{worms}	T	Ave % Survival STE	% L1
Controls															
N2 (wild type)	3462	3572	30	103±0.7	0	1310	1351	12	104±3.0	0	5633	6006	50	106±1.6	1
ynIs107 [*Papl-1*::APL-1(*yn32*)D342C/S362C::GFP]	518	528	4	102±1.4	0						810	816	8	100±1.9	1
ynIs100 [*Papl-1*::APL-1(*yn32*)::GFP]	386	394	4	102±2.3	0						575	621	6	106±2.3	1
ynIs106 [*Papl-1*::APL-1EXT(*yn32*)]	256	259	3	98±10.7	0						316	311	3	98±1.4	0
vsIs13 [*lin-15*(+) co-inj.marker]	1236	1277	10	105±3.6	0						451	455	4	101±1.2	0
Endogenous Overexpression of full-length APL-1															
ynIs86 [P*apl-1*::APL-1]	455	404	5	88±4.5	0	420	315	4	77±4.7	0	449	265	4	60±3.5	31
ynIs79 [P*apl-1*::APL-1::GFP]	1015	639	10	63±5.6	1	494	266	5	34±10.8	3	1690	64	14	4.3±0.9	47
Endogenous Overexpression of the Extracellular Domain of APL-1 (APL-1EXT)															
ynIs71 [P*apl-1*::APL-1EXT]	488	397	6	82±4.5	1	283	180	3	64±8.6	9	484	261	5	54±2.9	72
apl-1(yn5)	943	826	11	86±1.7	2	694	512	6	75±2.1	3	3737	1841	41	47±1.9	46
apl-1(yn5); yn39	668	635	5	95±4.8	2						497	480	5	96±1.4	23
apl-1(yn5); yn38	364	237	3	69±10.9	8						586	117	5	18±2.9	69
Pan-neural expression of APL-1 driven by* rab-3 *promoter															
ynIs104 [P*rab-3::*APL-1]	304	274	4	91±3.8	0	372	205	4	55±9.3	2	779	366	8	38±5.4	96
ynIs91 [P*rab-3::*APL-1]	382	320	3	83±3.5	0						564	124	5	22±4.4	91
Overexpression of APL-1 driven by* snb-1 *promoter															
ynIs12 [P*snb-1::*APL-1]	1007	919	10	92±1.9	0	326	291	4	91±3.6	0	1408	1047	12	75±3.8	53
ynIs13 [P*snb-1::*APL-1]	564	465	5	83±5.6	0	315	228	3	75±10.4	0	1105	746	10	68±3.2	73
ynIs109 [P*snb-1::*APL-1::GFP]	556	328	5	59±7.6	24						1317	0	12	0	-
Overexpression of the Extracellular Domain of APL-1 driven by* snb-1 *promoter															
ynIs105 [P*snb-1::*APL-1EXT]	358	307	3	78±11.2	1						822	274	8	32±4.5	95
Overexpression of BEC-1															
ynIs110 [RFP::BEC-1]	298	237	3	79±5.5											
ynIs110; ynIs79	890	308	9	28±8.0							180	0	3	0	0

Chapter V: Pan-neuronal expression of APL-1, an APP-related protein, disrupts olfactory, gustatory and touch learning in *C. elegans*

Collin Y. Ewald, Ruby Cheng, Vishal Shah, Lana Tolen, Aneela Gillani, Afsana Nasrin and Chris Li

V.1. Abstract

Patients with Alzheimer's disease show age-related cognitive decline. Post-mortem autopsy of their brains shows the presence of large numbers of amyloid peptide aggregates, whose major component is the β-amyloid peptide. The β-amyloid peptide is a cleavage product of the amyloid precursor protein (APP). In addition to the neurodegeneration associated with Alzheimer's disease patients, APP has also been shown to disrupt several behaviors independent of amyloid peptide aggregation. However, the pathways in which APP function to disrupt these behaviors are unknown. Here we show that pan-neuronal expression of APL-1, the *Caenorhabdtitis elegans* orthologue of APP, disrupts several behaviors, such as olfactory and gustatory avoidance learning and touch habituation. These behaviors are mediated by distinct neuronal circuits, suggesting a broad function of APL-1. Furthermore, we found that disruption of these three behaviors is mediated via the insulin/IGF-1 and TGF-β pathways. These results suggest pathways and molecular components that may underlie memory defects in patients with Alzheimer's disease.

V.2. Introduction

Alzheimer's disease (AD) is the most common form of dementia (Alzheimer's Association 2010) and has been associated with type 2 diabetes (Ott *et al*. 1999; Luchsinger *et al*. 2004; Alzheimer's Association 2010); however, the underlying cellular mechanism that connects the association is unknown. In addition to the amyloid plaque depositions that are a hallmark in the diagnosis of AD, the levels of insulin and IGF-1 receptors have also been shown to be lower in brains of AD patients (Steen *et al*. 2005). The amyloid plaques contain aggregations of the β-amyloid peptide, which is a cleavage product of the amyloid precursor protein (APP) (Glenner & Wong 1984; Masters *et al*. 1985; Kang *et al*. 1987). Families with an extra copy of the APP locus on chromosome 21 have been correlated with AD (Cabrejo *et al*. 2006; Rovelet-Lecrux *et al*. 2006; Sleegers *et al*. 2006) and the incidence of AD among Down syndrome patients, who have a trisomy of chromosome 21, is extremely high (Mann & Esiri 1989; Schupf *et al*. 1998; Korbel *et al*. 2009). These findings suggest that higher levels of APP could contribute to the development of AD. Overexpression of APP in mice leads to lethality and learning defects independent of amyloid peptide aggregation (Hsiao *et al*. 1995; Simon *et al*. 2009). Similarly, overexpression of APL-1, the *Caenorhabdtitis elegans* orthologue of APP, leads to lethality (Hornsten *et al*. 2007). However, whether overexpression of APL-1 leads to learning defects is unknown.

The nematode *C. elegans* offers a variety of well-studied behaviors, such as olfactory and gustatory plasticity and touch habituation. These behaviors are generated by distinct neuronal circuits (Bargmann 2006; Giles & Rankin 2009). Conceptually, it is

advantageous for *C. elegans* to adapt to persistent stimuli. For instance, to navigate through the environment *C. elegans* has to constantly monitor its surroundings to respond to novel stimuli and ignore non-threatening persistent stimuli (Lee *et al*. 2010). In addition, *C. elegans* is attracted to odorants that resemble food odorants or byproducts. However, after crawling towards an attractive odorant without finding food, *C. elegans* no longer responds to or avoids the odorant (Yamada *et al*. 2010). This situation can be mimicked in the laboratory by exposing *C. elegans* for an hour to an attractive volatile chemical (olfactory), such as benzaldehyde, or to an attractive water-soluble chemical (gustatory), such as sodium, in the absence of food; animals will show associative learning and decrease its response or avoid the attractive chemical (Colbert & Bargmann 1995; Tomioka *et al*. 2006). This plasticity in response is achieved by uncoupling the olfactory receptor response from its downstream signaling pathway.

Odorants are detected by chemosensory neurons that also control developmental decisions (Bargmann & Horvitz 1991b). Under harsh environmental conditions, developing *C. elegans* enter an alternative stress-resistant larval stage, called dauer (Riddle & Albert 1997). Activity of *daf-16*, which encodes a FOXO transcription factor, and *daf-12*, which encodes a nuclear hormone receptor (NHR) are required for dauer formation, whereas reduced *daf-2* insulin-IGF-1 receptor signaling is also necessary for dauer formation (Bargmann & Horvitz 1991b; Lin *et al*. 1997; Ogg *et al*. 1997; Antebi *et al*. 2000). The reduction of *daf-2*/insulin/IGF-1 receptor function has also been shown to impair sodium chloride and benzaldehyde plasticity (Tomioka *et al*. 2006; Lin *et al*. 2010). Because altered insulin signaling is associated with Alzheimer's disease, we

determined whether altered insulin signaling and overexpression of APL-1 could have a similar affect on the simple *C. elegans* learning behaviors.

V.3. Results

V.3.1. Reduced or increased levels of APL-1 disrupts olfactory chemotaxis

C. elegans is attracted or repulsed to certain volatile and water-soluble chemicals. This chemosensory behavior is mediated by 22 amphidial neurons (Ward *et al*. 1975). To determine whether a chemical is attractive or repulsive to *C. elegans*, animals are placed onto an agar plate that contains a spot with the test chemical and a control spot (Fig. 1A). Both spots also contain sodium azide to anesthetize the animal whenever it reaches either spot. A chemotaxis index (CI) is determined by calculating (number of animals on the test spot – number of the animals on the control spot)/total number of animals on the plate. A CI of 1 indicates a strong attractive test chemical, a CI of -1 a repulsive test chemical, and a CI of 0 no preference. Wild-type animals chemotax towards the volatile odorant benzaldehyde (CI=0.77±0.02; N>3000) and the water-soluble chemical sodium acetate (CI=0.77±0.01, N>3000) (Figs. 1B and 1D). Hence, benzaldehyde and sodium acetate are considered strong attractants. Benzaldehyde is sensed by two bilaterally symmetric AWC neurons (Bargmann *et al*. 1993), while sodium is mainly sensed by the pair of ASE neurons (Bargmann & Horvitz 1991a). Heterozygous *apl-1(yn10)* animals showed a reduced chemotaxis response towards both benzaldehyde (CI=0.43±0.09; N>800) and sodium acetate (CI=0.34±0.05; N>1500), although both chemicals were still attractive to the heterozygous animals (Figs. 1B and 1D). Hence, decreasing APL-1 levels lowers the chemosensory response without affecting chemical preference.

Transgenic animals in which APL-1 is overexpressed in different cell types were generally attracted to benzaldehyde and sodium acetate, but as with the heterozygous animals, the response was much reduced compared to wild type (Figs. 1B and 1D). For example, animals with endogenous overexpression of APL-1 (*ynIs86* [P*apl-1*::APL-1], *ynIs79* [P*apl-1*::APL-1::GFP], and *apl-1(yn10); ynEx1130* [P*apl-1*::APL-1]) showed a positive chemotaxis response to benzaldehyde and sodium acetate, but the chemotaxis indices were lower than wild type, and in the case of high levels of APL-1 overexpression, the chemotaxis index was only 40% of wild type (Figs. 1B and 1D). Control animals in which a mutation or deletion was introduced into the transgene (APL-1(mut)::GFP or APL-1Δ::GFP) or transgenic animals that carried the same co-injection marker (e.g., *lin-15*(+)) showed wild-type responses (Figs. 1B and 1D). Hence, overexpression of APL-1, as with decreased levels of APL-1, decreases the overall chemotaxis response, but does not change the preference to the chemical. *apl-1* is expressed in many cell types, including several amphidial chemosensory neurons, such as ASJ, amphidial sheath cells, and several interneurons that are downstream of the chemosensory neurons (Hornsten *et al*. 2007), suggesting that APL-1 exerts its effects on chemotaxis indirectly.

To determine whether the decreased chemotaxis response is due to defects in the chemosensory neurons, we examined the morphology of the chemosensory neurons by staining with a lipophilic dye, DiI. The ciliary endings of the chemosensory neurons are exposed to the extracellular milieu through the amphidial pore, through which DiI can be taken up by the ciliated dendritic endings of a subset of chemosensory neurons (Perkins *et al*. 1986). In all strains, the morphology of the labeled chemosensory neurons

appeared wild type (Fig. S1). Furthermore, when an RFP marker is expressed in AWC (P*odr-1*::dsRED), the morphology of AWC in these strains appeared wild type (data not shown).

Like mammalian APP, *C. elegans* APL-1 is cleaved to release a large extracellular domain (sAPL-1α) and a small cytoplasmic domain (reviewed in (Ewald & Li 2010)). The *apl-1(yn5)* mutation deletes the region encoding the transmembrane and cytoplasmic domains; these animals produce high levels of an extracellular fragment (APL-1EXT) that is slightly larger than sAPL-1α (Hornsten *et al*. 2007). *apl-1(yn5)* mutants have a wild-type response to benzaldehyde, but a reduced attractive response to sodium acetate (Fig. 1, Table 1). Similarly, transgenic animals that carry the APL-1EXT transgene (*ynIs71*) and produce high levels of APL-1EXT (Hornsten *et al*. 2007) also showed a wild-type response to benzaldehyde, but a reduced attractive response to sodium acetate (Figs. 1B and 1D). The chemosensory neurons of transgenic animals carrying APL-1EXT and *apl-1(yn5)* mutants have wild-type morphologies, as determined by DiI labeling or by driving RFP expression in AWC (P*odr-1*::dsRED; not shown). Hence, APL-1EXT overexpression appears to differentially affect the chemosensory responses: the response to sodium acetate is compromised, whereas the response to benzaldehyde is unaffected. These results suggest that components mediating response to sodium acetate may be more sensitive to high levels of APL-1 than those mediating the response to benzaldehyde.

V.3.2. Ectopic expression of APL-1 disrupts chemotaxis

apl-1 is expressed in a subset of neurons that does not include the chemosensory neurons AWC and ASE that mediate the initial sensory responses to benzaldehyde and sodium acetate, respectively (Bargmann & Horvitz 1991a; Bargmann *et al*. 1993). To determine whether ectopic *apl-1* expression in these neurons would affect the chemotaxis response, we used a pan-neuronal promoter, *rab-3*, to drive APL-1 expression in all neurons. These transgenic animals, *ynIs104* [P*rab-3*::APL-1::GFP], showed wild-type chemotaxic responses to benzaldehyde and sodium acetate, indicating that *apl-1* expression in the chemosensory neurons does not disrupt their function (Figs. 1B and 1D). By contrast, when *apl-1* is expressed not only pan-neuronally, but also in numerous other cell types with the *snb-1* promoter, the transgenic *ynIs12* [P*snb-1*::APL-1], *ynIs13* [P*snb-1*::APL-1], and *ynIs109* [P*snb-1*::APL-1::GFP] lines showed poor chemotaxic responses to benzaldehyde and slightly better responses to sodium acetate (Figs. 1B and 1D). Again, the chemosensory neurons showed wild-type morphologies as assayed by DiI staining (Figure S1) or by driving RFP expression in AWC (P*odr-1*::dsRED; not shown). Collectively, these results indicate that the decreased chemotaxic responses seen in animals overexpressing APL-1 do not appear to be due to structural defects in the neurons, but in signaling within the neurons or in cells outside the nervous system. Alternatively, the *rab-3* promoter may drive lower levels of expression than the *snb-1* and *apl-1* promoters, and hence, the P*rab-3*::APL-1::GFP expression does not disrupt neuronal function. Because western blot analysis cannot distinguish between these possibilities, we examined the levels of tagged APL-1::GFP expression in the different transgenic lines. The level of neuronal APL-1::GFP expression was consistently much

lower in transgenic animals with P*rab-3*::APL-1::GFP expression compared to that in transgenic animals with P*snb-1*::APL-1::GFP or P*apl-1*::APL-1 expression. Indeed, APL-1::GFP was only detected faintly in a few neurons from the first larval stage (L1) throughout adulthood in P*rab-3*::APL-1::GFP animals (*ynIs104*; Fig. S2). Hence, the level of APL-1 expression driven pan-neuronally by the *rab-3* promoter may be low enough to preserve the chemotaxic response.

V.3.3. Pan-neuronal APL-1 expression disrupts avoidance behavior

As with other organisms, *C. elegans* shows associative plasticity (Nuttley *et al*. 2002). Wild-type animals exposed to benzaldehyde (or sodium acetate) for 60 minutes in the absence of food showed significantly reduced chemotaxic responses, which we will hereafter refer to as avoidance responses, such that the chemotaxic indices were now much lower than those of naïve animals (Figs. 1B and 1D; (Tomioka *et al*. 2006; Lin *et al*. 2010). The avoidance response was detected with as little as 30 minutes pairing of benzaldehyde (or sodium acetate) and starvation, and the avoidance response was greater as the exposure time was increased from 30 to 150 minutes (Figs. 1F and 1H). Hence, pairing of a chemoattractant with starvation changes chemical preference, demonstrating that *C. elegans* displays behavioral plasticity towards benzaldehyde and sodium acetate (Tomioka *et al*. 2006; Lin *et al*. 2010).

To determine how long the association between the chemoattractant and starvation persists, wild-type animals were exposed for 60 minutes to benzaldehyde or sodium acetate under starvation conditions, and transferred to plates without a food source or test chemical for 30-minute intervals up to 240 minutes before assaying for

chemotaxis. The animals continued to show the avoidance response for 120 minutes, after which point the animals began to show an increased attraction towards the chemicals (Figs. 2B and 2D). Hence, this avoidance response appears to correspond to a short-lasting memory of about two hours.

We examined the avoidance response in transgenic APL-1 overexpression animals that showed a chemotaxis response. Animals that overexpress APL-1 under its endogenous promoter (*ynIs86*, *ynIs79*) showed avoidance to benzaldehyde, but not to sodium acetate (Figs. 1B and 1D). Similarly, animals that overexpressed only APL-1EXT, *apl-1(yn5)* and *ynIs71* (Figs. 1B and 1D), showed avoidance to benzaldehyde, but not to sodium acetate. Hence, endogenous overexpression of APL-1 or APL-1EXT disrupts avoidance behavior to sodium acetate.

Surprisingly, after pairing benzaldehyde or sodium acetate to starvation, animals with pan-neuronal APL-1 expression (*ynIs104* [P*rab-3*::APL-1::GFP]) showed no avoidance response to either benzaldehyde or sodium acetate for at least 150 minutes after exposure (Figs. 2B, 2D). Indeed, only when pairing times of benzaldehyde (or sodium acetate) with starvation was increased to 120 minutes did *ynIs104* [P*rab-3*::APL-1::GFP] animals start to show an avoidance response (Figs. 1F and 1H). To confirm that the avoidance behaviors towards benzaldehyde and sodium acetate were due to pairing of the chemical with starvation, we exposed wild-type animals to sodium acetate in the absence of food for 60 minutes and assayed their response to benzaldehyde. Wild-type animals were attracted to benzaldehyde (Figure S3), indicating that the starvation state of the animal does not affect chemotaxis responses. Hence, although pan-neuronal APL-1

expression does not disrupt chemotaxis, this expression disrupts the avoidance response to both benzaldehyde and sodium acetate.

V.3.4. Pan-neuronal APL-1 expression disrupts associative learning

To determine whether pan-neuronal APL-1 expression disrupts receptor desensitization or associative avoidance, we tested *ynIs104* [P*rab-3*::APL-1::GFP] animals under different conditions (Figs. 2F and 2G). If the avoidance response is due to receptor desensitization, then the environment in which the animal is exposed to the chemical should not affect the avoidance response. Hence, exposure to the test chemical with food should still reveal a diminished chemotaxis response. When wild-type animal were treated as such, there was only a slight decrease in the chemotaxis response compared to naïve animals (Figs. 2F, G), suggesting that there is little receptor desensitization. Similarly, *ynIs104* [P*rab-3*::APL-1::GFP] animals showed only a slight decrease in chemotaxis response. Alternatively, if the avoidance response occurs through association of starvation with the test chemical, then placing the animals on food without the tested chemical for a short period of time before testing for chemotaxis should also not affect their diminished chemotaxis response, as animals on empty plates displayed the avoidance response for at least two hours (Figs. 2B and 2D). Wild-type animals tested under these conditions still showed the avoidance response to sodium acetate, but only partially for benzaldehyde (Figure 2F and 2G condition: + → 15' or 30' food), suggesting that the avoidance response is the result of an association between the chemical and starvation. Under these conditions, *ynIs104* [P*rab-3*::APL-1::GFP] animals showed

similar responses as naïve animals (Figs. 2F and 2G). Hence, *ynIs104* [P*rab-3*::APL-1::GFP] animals are defective in associative learning.

V.3.5. Impaired chemotaxis responses due to activation of the insulin/IGF-1 and TGF-β signaling pathways

In *C. elegans* the absence of food or overpopulation induces animals to undergo an alternative life cycle and form dauer larva. At least three pathways act in parallel to integrate sensory information, such as starvation, with developmental decisions: (I) insulin/IGF-1 receptor (*daf-2*) signaling, which inhibits the phosphorylation of a FOXO transcription factor DAF-16 and movement of DAF-16 into the nucleus to activate target genes that regulate dauer formation, stress resistance, and longevity; (II) TGFβ (*daf-7*) signaling; and (III) cyclic GMP (*daf-11*) signaling. All three pathways converge on the nuclear hormone receptor (NHR) *daf-12*, which acts as a switch between reproductive growth and dauer formation (Daniels et al., 2000). Reducing the activity of any one of the three pathways can induce dauer formation (Daniels *et al*. 2000). To determine whether the impaired chemotaxis response in transgenic animals carrying the P*snb-1*::APL-1 or P*apl-1*::APL-1 transgenes was due to reduced signaling from one of these pathways, we first characterized the chemotaxis and avoidance responses of mutants from two of the pathways, as mutants in the *daf-11* cGMP branch are completely chemotaxis defective. Although *daf-12(m20)* NHR mutants show an impaired chemotaxis response towards butanone (Daniels *et al*. 2000), *daf-12(m20)* mutants showed wild-type chemoattractive responses to benzaldehyde and sodium acetate. Similarly, *daf-2(e1370)* reduction of function mutants and *daf-16(mu86)* null mutants showed wild-type chemoattractive

responses, while *daf-7(e1372)* mutants showed slightly lowered chemoattractive responses to benzaldehyde (Fig. 3). For sodium acetate, *daf-2(e1370)* and *daf-16(mu86)* showed decreased chemoattraction, whereas *daf-7(e1372)* showed wild-type chemoattraction. Collectively, these results suggest that *daf-2*, *daf-7*, and *daf-12* are not required for chemoattraction to benzaldehyde or sodium acetate. Although transgenic animals carrying the P*snb-1*::APL-1 transgene did not show a chemotaxis response in a wild-type background, these animals (*ynIs12* [P*snb-1*::APL-1]) did show a robust chemotaxis response to benzaldehyde when *daf-7* TGFβ signaling and *daf-12* NHR activity were decreased, but not when *daf-16*/FOXO activity was decreased. By contrast, *ynIs79* [P*apl*-1::APL-1::GFP] animals showed a chemotaxis response to benzaldehyde when *daf-2* insulin/IGF-1 receptor activity was decreased, but not when the activity of *daf-16*/FOXO and *daf-7* TGFβ were decreased (Fig. 3). These results indicate that the impaired ability to chemotax when APL-1 is overexpressed is not due to defects in chemosensory function, but rather to disruption of downstream signaling.

V.3.6. The avoidance response in P*rab-3*::APL-1 animals is mediated by *daf-16*/FOXO and *daf-12* NHR

daf-16(mu86) and *daf-7(e1372)* mutants showed wild-type avoidance responses to benzaldehyde and sodium acetate, whereas *daf-2(e1370)* and *daf-12(m20)* reduction of function mutants showed impaired avoidance responses (Fig. 3; (Tomioka *et al*. 2006; Lin *et al*. 2010)). *daf-2* insulin/IGF-1 receptor activity negatively regulates *daf-16*/FOXO; in addition, the longevity and dauer phenotypes of *daf-2* mutants require *daf-16*/FOXO activity (Lin *et al*. 1997; Ogg *et al*. 1997). Similarly, *daf-2(e1370); daf-*

16(mu86) double mutants showed a wild-type or *daf-16(mu16)* avoidance behavior (Fig. 3), suggesting that *daf-16*/FOXO is required for the impaired avoidance response of *daf-2* insulin/IGF-1 receptor mutants. To investigate whether signaling in the dauer pathways also affects the avoidance response, we examined transgenic *ynIs104* animals with pan-neuronal expression of APL-1; these animals showed a wild-type chemotaxis response to benzaldehyde, but did not show the avoidance response. In a *daf-16(mu86)* background, transgenic P*rab-3*::APL-1 animals showed wild-type avoidance responses towards benzaldehyde and sodium acetate. Similarly, in *daf-12(m20)* NHR and *daf-7(e1372*) TGFβ mutant backgrounds, P*rab-3*::APL-1 animals showed avoidance responses to benzaldehyde and sodium acetate similar to or stronger than those of *daf-12(mu20)* and *daf-7(e1372)* mutants alone. These results suggest that pan-neuronal APL-1 expression signals upstream of the insulin/IGF-1 and TGFβ pathways.

V.3.7. Neuronal overexpression of APL-1 diminishes touch habituation

The avoidance impairment in animals with pan-neuronal APL-1 expression may be restricted to chemosensation or may represent a general impairment with learning of other behaviors as well. To distinguish between these alternatives, we examined a different sensory modality, gentle body touch. A gentle touch to the animal's head causes the animal to reverse, whereas a gentle touch to the animal's posterior causes it to move forward (Chalfie & Sulston 1981). This response is mediated by six mechanosensory neurons (Chalfie *et al*. 1985). When wild-type animals are repeatedly touched, they no longer respond, but habituate to the touch stimulus (Chalfie & Sulston 1981). We designed a paradigm whereby animals were touched on the head, allowed to

move backwards, and then touched on the tail, which caused the animal to move forward. The inter-stimulus interval averaged 1.3±0.15 seconds (N=10). After five consecutive head-touch stimuli, the animals habituated and no longer responded (Fig. 4). Heterozygous *apl-1* mutants and transgenic animals that have increased endogenous levels of APL-1 (*ynIs86* and *ynIs79*) showed wild-type habituation (Fig. 4), indicating that APL-1 overexpression does not disrupt this sensory modality. Endogenous promoter driven APL-1::GFP expression is not detected in the six mechanosensory neurons. By contrast, transgenic animals with pan-neuronal APL-1 expression (*ynIs91, ynIs104*) or ectopic expression with the *snb-1* promoter (*ynIs12, ynIs13, ynIs109*) needed significantly more head-tail stimuli before they habituated (Fig. 4). These results indicate that pan-neuronal APL-1 expression disrupts learning responses to multiple behaviors. *daf-16(mu86)* or *daf-12(m20)* mutants showed wild-type habituation (Fig. 4). The impaired habituation response of transgenic animals with pan-neuronal APL-1 expression is suppressed in a *daf-16(mu86)* or *daf-12(m20)* mutant background (Fig. 4), suggesting that *daf-16*/FOXO and *daf-12* NHR are required downstream of APL-1 signaling to inhibit touch habituation.

V.4. Discussion

Avoidance learning to benzaldehyde and sodium acetate and touch habituation do not require the activity of DAF-16/FOXO or DAF-12 NHR (Fig. 3). Reducing *daf-2* activity, however, caused disruption of avoidance behavior to benzaldehyde and sodium acetate (Fig. 3). Signaling through the DAF-2 insulin/IGF-1 receptor negatively regulates DAF-16/FOXO activity for longevity, dauer formation, and stress resistance (reviewed in

(Kenyon 2005)). The disrupted avoidance behavior towards benzaldehyde and sodium acetate of *daf-2(e1370)* mutants is restored in a *daf-16(mu86)* null background (Figure 3). These results are in contrast with those of Tomioka *et al*. (2006), who reported that the impaired avoidance behavior towards sodium chloride of *daf-2(e1370)* mutants was not restored in a *daf-16(m26)* reduction-of-function or *daf-16(mgDf47)* deficiency background (Tomioka *et al*. 2006). The difference could result either from using different *daf-16* alleles or by pairing with sodium acetate rather than sodium chloride (Tomioka *et al*. 2006). Sodium is preferentially sensed by ASEL and chloride by ASER (Pierce-Shimomura *et al*. 2001); hence, pairing with sodium chloride excites both ASE neurons, whereas sodium acetate preferentially excites ASEL.

Loss of DAF-16/FOXO or DAF-12 NHR activity is required for associative learning in transgenic animals with pan-neuronal APL-1 expression. DAF-16/FOXO or DAF-12 NHR activity might activate genes that interfere with learning (see Figure 5). Similarly, reduced *daf-2* insulin/IGF-1 receptor activity did not restore avoidance behavior in transgenic animals with pan-neuronal APL-1 expression. The neurons in which APL-1 expression is required to disrupt avoidance behavior are unknown. Pre-exposing wild-type animals to sodium acetate did not change their attraction towards benzaldehyde, suggesting that the association between starvation and the test chemical is specific for the avoidance behavior.

Neuronal APL-1 expression also disrupts touch habituation. Touch habituation is probably mediated by a different neuronal circuit than benzaldehyde and sodium associative learning. Surprisingly, the neuronal APL-1 expression induced disruption of habituation is restored when *daf-16*/FOXO and *daf-12* NHR activity is decreased.

Expression of APL-1 in all neurons by the *rab-3* or *snb-1* promoter similarly leads to disrupted habituation, suggesting that APL-1 expression in neurons is a pre-requisite in the disruption of touch habituation. Because endogenous APL-1 is not expressed in the six touch cells that mediate the touch response, those transgenic animals showed wild-type habituation.

Interestingly, APL-1 overexpression by either its endogenous or *snb-1* promoter diminished the chemotaxis response to both sodium acetate and benzaldehyde, whereas animals with APL-1 expression driven by the pan-neuronal *rab-3* promoter showed wild-type chemotaxis responses. These results suggest that APL-1 expression in non-neuronal cells decreases or disrupts chemotaxis. Strikingly, the chemotaxis impairments of transgenic animals with endogenous and *snb-1* driven APL-1 were fully or partially restored by decreased *daf-2* insulin-IGF-1 receptor, *daf-7* TGFβ, or *daf-12* NHR signaling. Hence, the effects of APL-1 on chemotaxis and learning are unlikely due to neurodegeneration.

Taken together, these results suggest novel interactions of *daf-16*/FOXO, *daf-12*, NHR, and *apl-1* in learning. In mammals, overexpression of APP shows impairments of several behaviors independent of plaque formation (Hsiao *et al*. 1995; Simon *et al*. 2009). Our results suggest that APP is not directly involved in forming those behaviors, but indirectly affect them via the insulin/IGF-1 pathway.

V.5. Materials and methods

V.5.1. Strains

Caenorhabtitis elegans strains were grown and maintained on MYOB plates (Church *et al*. 1995) containing OP50 Escherichia coli bacteria at 20ºC using methods as described (Brenner 1974), unless noted. All mutations used are described in Wormbase (www.wormbase.org) and include: LGI: *daf-16(mu86)*; LGIII: *daf-2(e1370)*, *daf-7(e1372)*; LGX: *daf-12(m20)*, *lon-2(e678)*, *apl-1(yn5* and *yn10)*, and *dpy-8(e130)*. Construction of the APL-1 transgenes and the resulting transgenic lines are described (Hornsten *et al*. 2007). Non-integrated transgenic lines used were: *ynEx1130* (P*apl-1*::APL-1, P*sur-5*::GFP). Integrated transgenic lines used were: LGI: *ynIs109* (P*snb-1*::APL-1(cDNA)::GFP); LGIII: *ynIs12* (P*snb-1*::APL-1(cDNA), *lin-15B*(+)), *jsIs682* (Prab-3::GFP::RAB-3) (Mahoney *et al*. 2006); LGIV: *vsIs13* (*lin-11*::*pes-10*::GFP, *lin-15*(+))(Bany *et al*. 2003), *ynIs104* (P*rab-3*::APL-1(cDNA)::GFP, P*myo-2*::GFP); LGV: *ynIs13* (P*snb-1*::APL-1(cDNA), *lin-15B*(+)), *ynIs79* (P*apl-1*::APL-1::GFP), *pyIs500* [P*odr-1*::dsRED; P*odr-3*::GFP::EGL-4] (Lee *et al*. 2010); and LGX: *ynIs86* (P*apl-1*::APL-1, P*sur-5*::GFP), *ynIs91* (P*rab-3*::APL-1, pRF4 *rol-6(su1006gf)*), *ynIs108* (P*apl-1*::APL-1(Δheparin ΔE2 domain)::GFP; P*sur-5*::GFP), and *ynIs107* (P*apl-1*::APL-1(*yn32* E71K/D342C/S362C)::GFP, P*myo-2*::GFP) (Hoopes *et al*. 2010).

V.5.2. Chemotaxis and adaptation assays

Chemotaxis and adaptation assays were performed at the same time and as described (Colbert & Bargmann 1995; Tomioka *et al*. 2006). For each strain, worms were grown in duplicates, one set for chemotaxis and one for adaptation assays. To synchronize worm populations, ~15 gravid adult worms were placed into a hypochlorite solution to release

the eggs. Hatched worms were grown at 20ºC (unless noted). Four days later, animals were washed off the growing plate with water into a 1.5 ml microfuge tube and washed an additional three times with water. ***For benzaldehyde assays***: for each strain, three 10 cm plates were poured with 10 ml of 2% agar; two were used for chemotaxis and one for pre-exposure to benzaldehyde. On the back of the chemotaxis plates, an equilateral triangle with 4 cm sides was drawn: the first corner was defined as starting point for the worms, on the second corner 1 µl of 1:200 benzaldehyde diluted in ethanol together with 1 µl of 1 M sodium azide was placed on the agar and on the last corner 1 µl of ethanol together with 1 µl of 1 M sodium azide was placed on the agar as a control. For the pre-exposure plate: 5 molten plugs of 2% agar were placed on the lid; when solidified 0.6 µl of undiluted benzaldehyde was placed on each plug (total of 3 µl benzaldehyde). Of the two batches of washed worms per strain: one batch of worms was placed on the starting point of the chemotaxis plate, the other batch was placed on an empty plate and covered with the benzaldehyde pre-exposure lid; the plate was sealed with parafilm. Plates were maintained in a 20ºC incubator for 60 minutes, after which animals were washed three times and assayed for chemotaxis (unless indicated). The CI was determined after 60 minutes (CI=number of worms on the test point - number of worms on control point / total number of worms on the plate). ***For salt assays***: The night before the assay for each strain two 10 cm plates were poured with 10 ml of 2% agar for chemotaxis. When the molten agar solidified, an equilateral triangle with 4 cm sides was drawn on the back of the chemotaxis plates: the first corner was defined as starting point for the worms, on the second corner a hole of 0.8 cm diameter was punched and filled with 2% agar containing 400 mM sodium acetate, on the third corner a hole of 0.8 cm diameter was punched and

filled with 2% agar as a control. The sodium acetate was allowed to form a gradient overnight. Before the chemotaxis assay, 1 µl of 1 M sodium azide was placed on the test and control spot. Of the two batches of washed worms per strain: one batch of worms was placed on the starting point of the chemotaxis plate, the other batch was incubated in 1 mL of 100 mM sodium acetate in a microfuge tube. After 60 minutes at 20ºC, the CI was scored for the chemotaxis plate and the pre-exposed worms were washed three times with water and then placed on the chemotaxis plate. After 60 minutes at 20ºC, the CI was scored. For statistical analysis, repeated measures (mixed model) two-way ANOVAs with Bonferroni post-tests to compare replicate means (95% confidence intervals) were performed to assess similarity between groups using Prism 4.0a software (GraphPad).

V.5.3. Dye fill assays

Worms were washed off plates with M9 and washed two additional times with M9 (M9 is defined in (Brenner 1974)). Worms were incubated for two hours in M9 containing 100 ng/µl DiI. Animals were mounted onto 2% agar pads containing a drop of 10 mM sodium azide and amphidial neuronal morphology was scored at 400x magnification on a Zeiss Axioplan microscope. Images and z-stacks of the animals were taken at 400x magnification on a confocal microscope (Zeiss LSM 510 Confocal Laser Scanning System; slice thickness 0.49 µm; for GFP: excitation wavelength 488 nm, Laser intensity 5%, Filter BP505-530; pinhole 80 µm; for DiI: excitation wavelength 514 nm, Laser intensity 66%, Filter LP560; pinhole 78 µm). The co-localization of the GFP and DiI fluorescence for z-stacks of each worm was determined by Image J's "Colocalisation analysis (test and highlighter)".

V.5.4. Touch habituation assays

One day before the assay, three L4 animals were placed into a fresh plate with bacteria. One-day adult animals were lightly touched with an eyebrow hair on the side of the head, which caused a backwards movement and then at the side of the tail, which caused a forward movement. The touch assay was videotaped for xx animals on a Leica xx using xx software. The inter-stimulus interval was determined by viewing the videotapes. For statistical analysis, a one-way ANOVA with post hoc Tukey was used for comparison.

V.6. Acknowledgments

We wish to thank Noelle L'Etoile for kindly *pyIs500* strains, lab members for helpful discussions, Sarah Tichelli help with statistical analysis, and CGC, which is supported by the NIH National Center for Research Resources, for providing strains. This work was supported by grants from the Alzheimer's Association, National Institutes Health (R21AG0339 and R01AG32042), and National Science Foundation (IOS08207) (CL) and a National Institutes of Health RCMI grant (G12-RR03060-25) to City College.

V.7. Author's contribution

Benzaldehyde assays: RC, VS, LT, AG, AN and CE

Sodium acetate assays: LT, RC, VS and CE

Touch habituation: CE, RC, LT and AN

Dye filling: CE, LT, RC and VS

Confocal imaging: CE

Generation of transgenic strains: CE and CL

Designing experiments: CE and CL

Manuscript: CE and CL

V.8. References

Alzheimer's Association KM (2010). 2010 Alzheimer's disease facts and figures. *Alzheimer's and Dementia*. **6**, 158-194.

Antebi A, Yeh WH, Tait D, Hedgecock EM , Riddle DL (2000). *daf-12* encodes a nuclear receptor that regulates the dauer diapause and developmental age in *C. elegans*. *Genes Dev*. **14**, 1512-1527.

Bany IA, Dong MQ , Koelle MR (2003). Genetic and cellular basis for acetylcholine inhibition of *Caenorhabditis elegans* egg-laying behavior. *J Neurosci*. **23**, 8060-8069.

Bargmann CI (2006). Chemosensation in *C. elegans*. *WormBook*, 1-29.

Bargmann CI, Hartwieg E , Horvitz HR (1993). Odorant-selective genes and neurons mediate olfaction in *C. elegans*. *Cell*. **74**, 515-527.

Bargmann CI , Horvitz HR (1991a). Chemosensory neurons with overlapping functions direct chemotaxis to multiple chemicals in *C. elegans*. *Neuron*. **7**, 729-742.

Bargmann CI , Horvitz HR (1991b). Control of larval development by chemosensory neurons in *Caenorhabditis elegans*. *Science*. **251**, 1243-1246.

Brenner S (1974). The Genetics of *Caenorhabditis elegans*. *Genetics*. **77**, 71-94.

Cabrejo L, Guyant-Marechal L, Laquerriere A, Vercelletto M, De la Fourniere F, Thomas-Anterion C, Verny C, Letournel F, Pasquier F, Vital A, Checler F, Frebourg T, Campion D , Hannequin D (2006). Phenotype associated with APP duplication in five families. *Brain*. **129**, 2966-2976.

Chalfie M , Sulston J (1981). Developmental genetics of the mechanosensory neurons of *Caenorhabditis elegans*. *Developmental biology*. **82**, 358-370.

Chalfie M, Sulston JE, White JG, Southgate E, Thomson JN , Brenner S (1985). The neural circuit for touch sensitivity in *Caenorhabditis elegans*. *J Neurosci*. **5**, 956-964.

Church DL, Guan KL , Lambie EJ (1995). Three genes of the MAP kinase cascade, *mek-2*, *mpk-1/sur-1* and *let-60 ras*, are required for meiotic cell cycle progression in *Caenorhabditis elegans*. *Development*. **121**, 2525-2535.

Colbert HA , Bargmann CI (1995). Odorant-specific adaptation pathways generate olfactory plasticity in *C. elegans*. *Neuron*. **14**, 803-812.

Daniels SA, Ailion M, Thomas JH , Sengupta P (2000). *egl-4* acts through a transforming growth factor-beta/SMAD pathway in *Caenorhabditis elegans* to regulate multiple neuronal circuits in response to sensory cues. *Genetics*. **156**, 123-141.

Ewald CY , Li C (2010). Understanding the molecular basis of Alzheimer's disease using a *Caenorhabditis elegans* model system. *Brain Struct Funct*. **214**, 263-283.

Fielenbach N , Antebi A (2008). *C. elegans* dauer formation and the molecular basis of plasticity. *Genes Dev*. **22**, 2149-2165.

Giles AC , Rankin CH (2009). Behavioral and genetic characterization of habituation using *Caenorhabditis elegans*. *Neurobiol Learn Mem*. **92**, 139-146.

Glenner GG , Wong CW (1984). Alzheimer's disease and Down's syndrome: sharing of a unique cerebrovascular amyloid fibril protein. *Biochem Biophys Res Commun*. **122**, 1131-1135.

Hoopes JT, Liu X, Xu X, Demeler B, Folta-Stogniew E, Li C , Ha Y (2010). Structural characterization of the E2 domain of APL-1, a *Caenorhabditis elegans* homolog of human amyloid precursor protein, and its heparin binding site. *The Journal of biological chemistry*. **285**, 2165-2173.

Hornsten A, Lieberthal J, Fadia S, Malins R, Ha L, Xu X, Daigle I, Markowitz M, O'Connor G, Plasterk R , Li C (2007). APL-1, a *Caenorhabditis elegans* protein related to the human beta-amyloid precursor protein, is essential for viability. *Proc Natl Acad Sci USA*. **104**, 1971-1976.

Hsiao KK, Borchelt DR, Olson K, Johannsdottir R, Kitt C, Yunis W, Xu S, Eckman C, Younkin S , Price D (1995). Age-related CNS disorder and early death in transgenic FVB/N mice overexpressing Alzheimer amyloid precursor proteins. *Neuron*. **15**, 1203-1218.

Kang J, Lemaire HG, Unterbeck A, Salbaum JM, Masters CL, Grzeschik KH, Multhaup G, Beyreuther K , Muller-Hill B (1987). The precursor of Alzheimer's disease amyloid A4 protein resembles a cell-surface receptor. *Nature*. **325**, 733-736.

Kenyon C (2005). The plasticity of aging: insights from long-lived mutants. *Cell*. **120**, 449-460.

Korbel JO, Tirosh-Wagner T, Urban AE, Chen XN, Kasowski M, Dai L, Grubert F, Erdman C, Gao MC, Lange K, Sobel EM, Barlow GM, Aylsworth AS, Carpenter NJ, Clark RD, Cohen MY, Doran E, Falik-Zaccai T, Lewin SO, Lott IT, McGillivray BC, Moeschler JB, Pettenati MJ, Pueschel SM, Rao KW, Shaffer LG, Shohat M, Van Riper AJ, Warburton D, Weissman S, Gerstein MB, Snyder M , Korenberg JR (2009). The genetic architecture of Down syndrome phenotypes revealed by high-resolution analysis of human segmental trisomies. *Proc Natl Acad Sci USA*. **106**, 12031-12036.

Lee JI, O'Halloran DM, Eastham-Anderson J, Juang BT, Kaye JA, Scott Hamilton O, Lesch B, Goga A , L'Etoile ND (2010). Nuclear entry of a cGMP-dependent kinase converts transient into long-lasting olfactory adaptation. *Proc Natl Acad Sci USA*. **107**, 6016-6021.

Lin CH, Tomioka M, Pereira S, Sellings L, Iino Y , van der Kooy D (2010). Insulin signaling plays a dual role in *Caenorhabditis elegans* memory acquisition and memory retrieval. *J Neurosci*. **30**, 8001-8011.

Lin K, Dorman JB, Rodan A , Kenyon C (1997). *daf-16*: An HNF-3/forkhead family member that can function to double the life-span of *Caenorhabditis elegans*. *Science*. **278**, 1319-1322.

Luchsinger JA, Tang MX, Shea S , Mayeux R (2004). Hyperinsulinemia and risk of Alzheimer disease. *Neurology*. **63**, 1187-1192.

Mahoney TR, Liu Q, Itoh T, Luo S, Hadwiger G, Vincent R, Wang ZW, Fukuda M , Nonet ML (2006). Regulation of synaptic transmission by RAB-3 and RAB-27 in *Caenorhabditis elegans*. *Mol Biol Cell*. **17**, 2617-2625.

Mann DM , Esiri MM (1989). The pattern of acquisition of plaques and tangles in the brains of patients under 50 years of age with Down's syndrome. *J Neurol Sci*. **89**, 169-179.

Masters CL, Simms G, Weinman NA, Multhaup G, McDonald BL , Beyreuther K (1985). Amyloid plaque core protein in Alzheimer disease and Down syndrome. *Proc Natl Acad Sci USA*. **82**, 4245-4249.

Nuttley WM, Atkinson-Leadbeater KP , Van Der Kooy D (2002). Serotonin mediates food-odor associative learning in the nematode *Caenorhabditis elegans*. *Proc Natl Acad Sci USA*. **99**, 12449-12454.

Ogg S, Paradis S, Gottlieb S, Patterson GI, Lee L, Tissenbaum HA , Ruvkun G (1997). The Fork head transcription factor DAF-16 transduces insulin-like metabolic and longevity signals in *C. elegans*. *Nature*. **389**, 994-999.

Ott A, Stolk RP, van Harskamp F, Pols HA, Hofman A , Breteler MM (1999). Diabetes mellitus and the risk of dementia: The Rotterdam Study. *Neurology*. **53**, 1937-1942.

Perkins LA, Hedgecock EM, Thomson JN , Culotti JG (1986). Mutant sensory cilia in the nematode *Caenorhabditis elegans*. *Developmental biology*. **117**, 456-487.

Pierce-Shimomura JT, Faumont S, Gaston MR, Pearson BJ , Lockery SR (2001). The homeobox gene *lim-6* is required for distinct chemosensory representations in *C. elegans*. *Nature*. **410**, 694-698.

Riddle DL , Albert PS (1997). Genetic and Environmental Regulation of Dauer Larva Development. In *C. elegans II*. (DL Riddle, T Blumenthal, BJ Meyer , JR Priess, eds). New York: Cold Spring Harbor Laboratory Press, pp. 739–768.

Rovelet-Lecrux A, Hannequin D, Raux G, Le Meur N, Laquerriere A, Vital A, Dumanchin C, Feuillette S, Brice A, Vercelletto M, Dubas F, Frebourg T , Campion D (2006). APP locus duplication causes autosomal dominant early-onset Alzheimer disease with cerebral amyloid angiopathy. *Nature genetics*. **38**, 24-26.

Schupf N, Kapell D, Nightingale B, Rodriguez A, Tycko B , Mayeux R (1998). Earlier onset of Alzheimer's disease in men with Down syndrome. *Neurology*. **50**, 991-995.

Simon AM, Schiapparelli L, Salazar-Colocho P, Cuadrado-Tejedor M, Escribano L, Lopez de Maturana R, Del Rio J, Perez-Mediavilla A , Frechilla D (2009). Overexpression of wild-type human APP in mice causes cognitive deficits and pathological features unrelated to Abeta levels. *Neurobiol Dis*. **33**, 369-378.

Sleegers K, Brouwers N, Gijselinck I, Theuns J, Goossens D, Wauters J, Del-Favero J, Cruts M, van Duijn CM , Van Broeckhoven C (2006). APP duplication is sufficient to cause early onset Alzheimer's dementia with cerebral amyloid angiopathy. *Brain*. **129**, 2977-2983.

Steen E, Terry BM, Rivera EJ, Cannon JL, Neely TR, Tavares R, Xu XJ, Wands JR , de la Monte SM (2005). Impaired insulin and insulin-like growth factor expression and signaling mechanisms in Alzheimer's disease--is this type 3 diabetes? *J Alzheimers Dis*. **7**, 63-80.

Tomioka M, Adachi T, Suzuki H, Kunitomo H, Schafer WR , Iino Y (2006). The insulin/PI 3-kinase pathway regulates salt chemotaxis learning in *Caenorhabditis elegans*. *Neuron*. **51**, 613-625.

Ward S, Thomson N, White JG , Brenner S (1975). Electron microscopical reconstruction of the anterior sensory anatomy of the nematode *Caenorhabditis elegans*. *J Comp Neurol*. **160**, 313-337.

Yamada K, Hirotsu T, Matsuki M, Butcher RA, Tomioka M, Ishihara T, Clardy J, Kunitomo H , Iino Y (2010). Olfactory plasticity is regulated by pheromonal signaling in *Caenorhabditis elegans*. *Science*. **329**, 1647-1650.

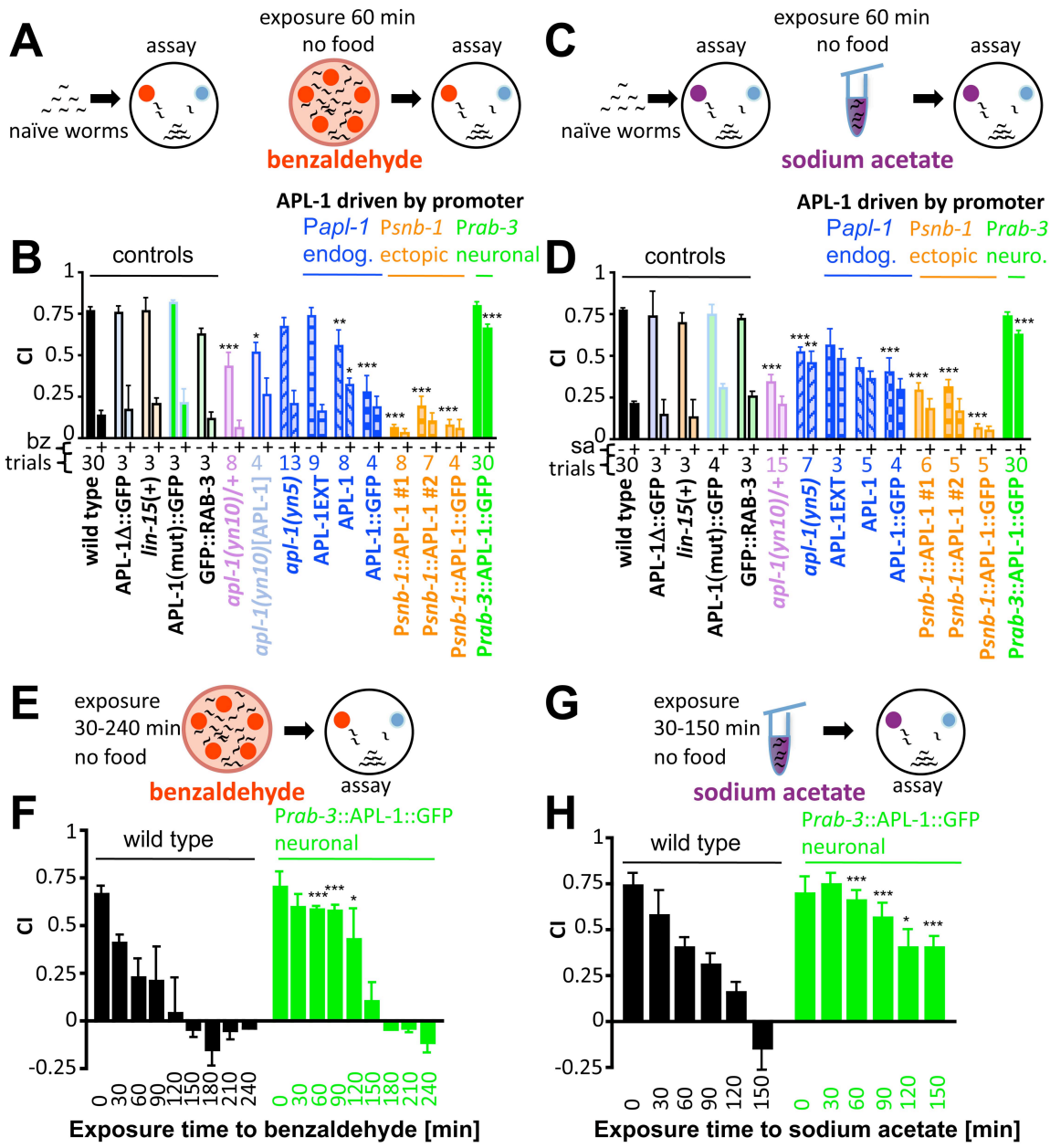

Figure 1. Increased APL-1 activity disrupts chemotaxis and avoidance behavior

A and **C**. Schematic of how naïve worms (A) and worms paired with a test chemical and starvation (B, C) were tested for chemotaxis towards benzaldehyde (B) or sodium acetate (C). **B** and **D**. CI of naïve worms (-) and pre-exposed worms (+) of each strain are represented by bars. Heterozygous *apl-1*, endogenous or ectopic APL-1 overexpression lines showed diminished chemotaxis. Pan-neuronal APL-1 expression lines had wild-

type chemotaxis, but showed no avoidance response towards benzaldehyde or sodium acetate. **E.** and **G.** Schematic representation of different pairing times of test chemical and absence of food (30-240 min). **F**. and **H.** Wild-type animals started to show an avoidance response after 30 minutes and increased avoidance to the test chemicals as the pairing time with starvation increased. At 150 minutes, the test chemicals became repulsive. *ynIs104* [P*rab-3*::APL-1::GFP] animals started to show an avoidance response at 150 minutes. Each trial consisted of about 100-200 worms. bz=benzaldehyde and sa=sodium acetate. For F and H trials > 5. *<0.05; **<0.01; ***<0.001 to wild type, two-way ANOVA repeated measure with post hoc Bonferroni was used.

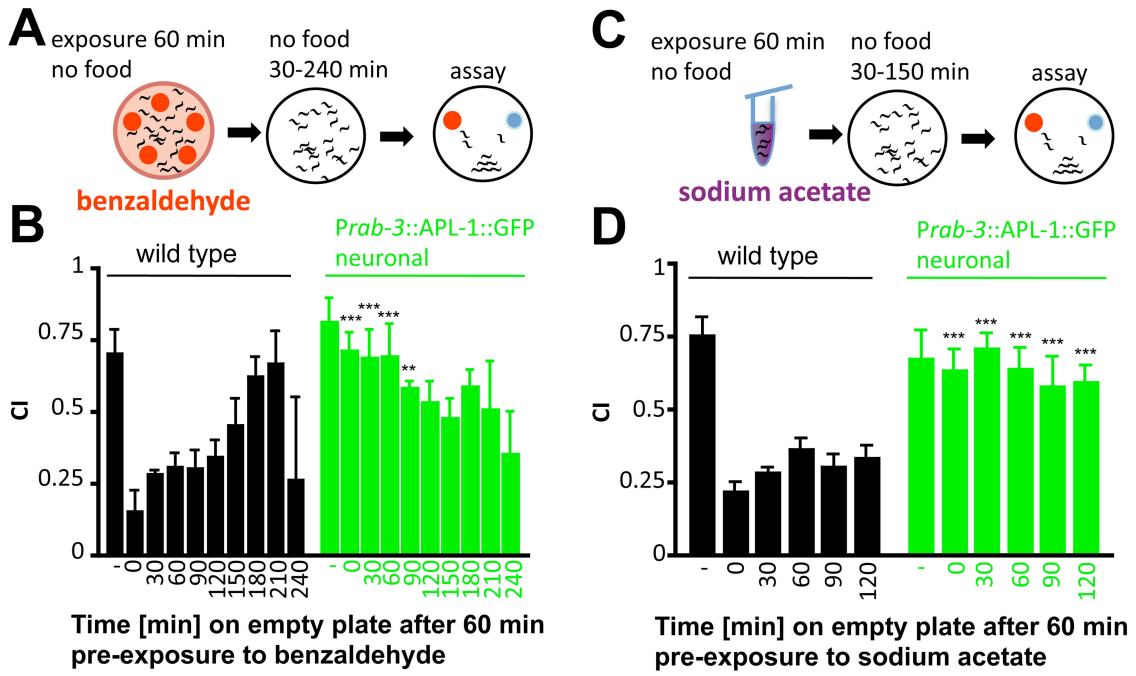

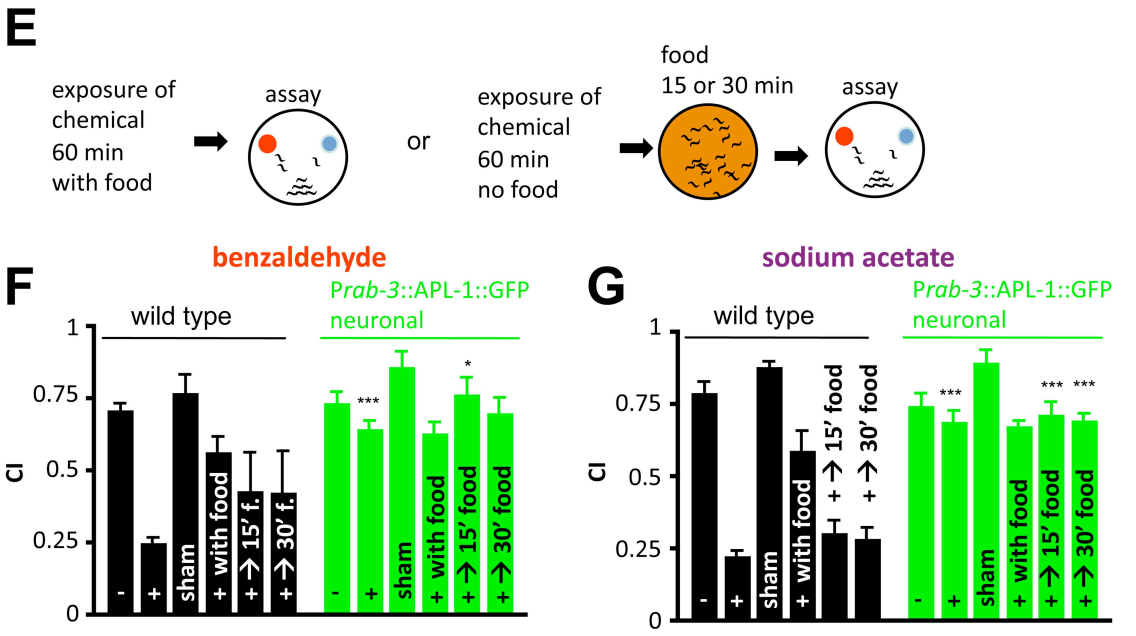

Figure 2. Wild-type animals maintain the avoidance response for two hours, whereas *ynIs104* [P*rab-3*::APL-1::GFP] animals show little associative learning. A and **C**. Animals were pre-exposed for one hour to the test chemical, washed and placed on empty agar plates for 30-240 minutes before their chemotaxis response was measured.

B and **D**. Wild-type animals maintained the avoidance response for at least for two hours, whereas *ynIs104* [P*rab-3*::APL-1::GFP] animals did not show a strong avoidance response for the entire time. **E**. The chemotaxis response was measured for five different conditions (two of them shown in the schematic). **F** and **G**. Chemotaxis response of naïve worms (-), worms that were pre-exposed to test chemical without food (+) for 60 minutes, worms that were placed on an empty plate (sham) for 60 minutes, worms that were pre-exposed to test chemical with food (+ with food) for 60 minutes, worms that were pre-exposed to test chemical without food for 60 minutes and then placed on a plate with food for 15 or 30 minutes (+ → 15' or 30' food (f.)). Each trial consisted of about 100-200 worms. B=5 trials, D=3trials, F=10trials, and G= 7trials. *<0.05; **<0.01; ***<0.001 to wild type, two-way ANOVA repeated measure with post hoc Bonferroni was used.

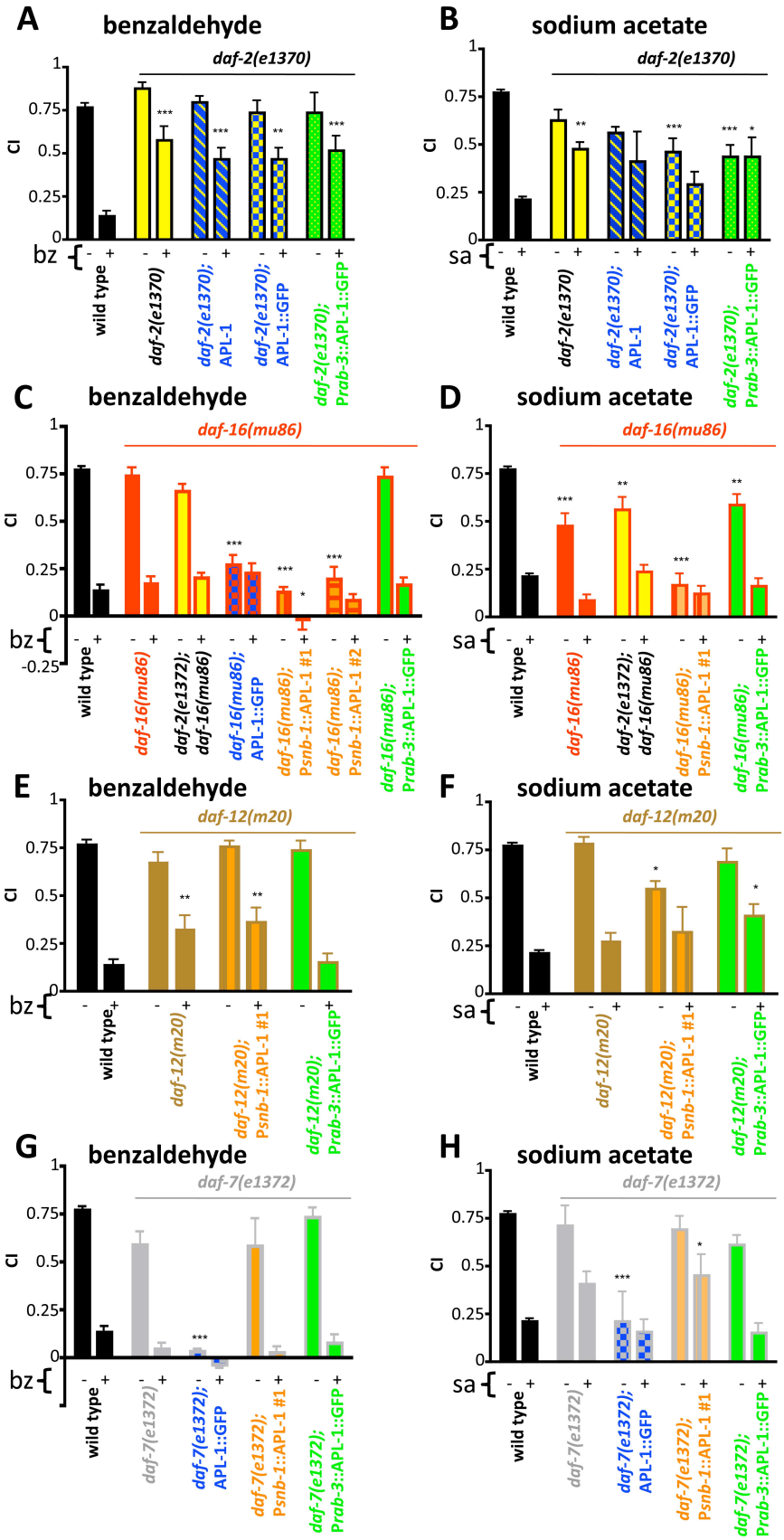
A
benzaldehyde
daf-2(e1370)
CI
bz
wild type
daf-2(e1370)
daf-2(e1370); APL-1
daf-2(e1370); APL-1::GFP
daf-2(e1370); Prab-3::APL-1::GFP
B
sodium acetate
daf-2(e1370)
sa
C
benzaldehyde
daf-16(mu86)
daf-16(mu86)
daf-2(e1372); daf-16(mu86)
daf-16(mu86); APL-1::GFP
daf-16(mu86); Psnb-1::APL-1 #1
daf-16(mu86); Psnb-1::APL-1 #2
daf-16(mu86); Prab-3::APL-1::GFP
D
sodium acetate
daf-16(mu86)
E
benzaldehyde
daf-12(m20)
daf-12(m20)
daf-12(m20); Psnb-1::APL-1 #1
daf-12(m20); Prab-3::APL-1::GFP
F
sodium acetate
daf-12(m20)
G
benzaldehyde
daf-7(e1372)
daf-7(e1372)
daf-7(e1372); APL-1::GFP
daf-7(e1372); Psnb-1::APL-1 #1
daf-7(e1372); Prab-3::APL-1::GFP
H
sodium acetate
daf-7(e1372)

Figure 3. The avoidance response of transgenic animals with pan-neuronal APL-1 expression is dependent on decreased *daf-16*/FOXO, *daf-12* NHR, and *daf-7* TGFβ activity.

A and **B**. *daf-2(e1370)* mutants show no avoidance response towards benzaldehyde or sodium acetate. Decreased *daf-2(e1370)* activity restores the chemotaxis response in APL-1 overexpression lines. **C** and **D**. Loss of *daf-16* activity restores the avoidance response in *daf-2(e1370)* and *ynIs104* [P*rab-3*::APL-1::GFP] animals to wild-type levels. **E** and **F**. Decreased *daf-12(m20)* activity restores the chemotaxis response in *ynIs12* [P*snb-1*::APL-1] animals and the avoidance response in *ynIs104* [P*rab-3*::APL-1::GFP] animals. **G** and **H**. *daf-7(e1372)* mutants showed wild-type chemotaxis towards benzaldehyde and sodium acetate, but had a slightly lower avoidance response to sodium acetate (H). Decreased *daf-7* TGFβ signaling restores the chemotaxis response in *ynIs12* [P*snb-1*::APL-1] animals, but not in *ynIs79* [APL-1::GFP] animals. In addition, the avoidance response is restored in *ynIs104* [P*rab-3*::APL-1::GFP] animals when *daf-7(e1372)* activity is decreased. Each trial consisted of about 100-200 worms. bz=benzaldehyde and sa=sodium acetate. For A-H trials > 5. *<0.05; **<0.01; ***<0.001 to wild type, two-way ANOVA repeated measure with post hoc Bonferroni was used.

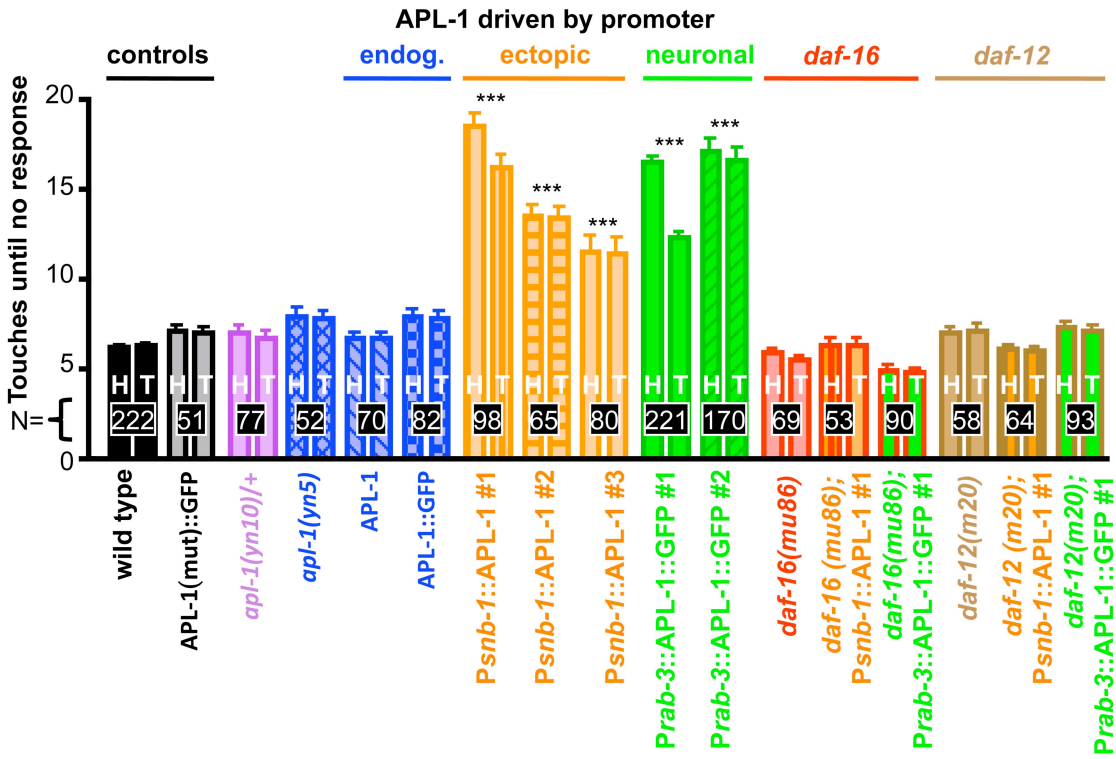

Figure 4. Pan-neuronal APL-1 expression impairs touch habituation.

Animals were touched alternately with an eyebrow hair on the head (H) and tail (T) and the number of touches until the animal stopped responding by moving forward or backwards were counted. After six light touches, wild-type animals no longer responded to the touch stimuli, indicating habituation. Similarly, heterozygous *apl-1*, mutant *apl-1(yn5)*, or animals that overexpress APL-1 under its endogenous promoter, which does not express APL-1 in any of the six touch cells, showed wild-type habituation. By contrast, it took at least twice as many touches for transgenic animals with pan-neuronal APL-1 expression ([P*snb-1*::APL-1] and [P*rab-3*::APL-1::GFP]) to habituate. The wild-type habituation response was restored in a *daf-16(mu86)* null and *daf-12(m20)* mutant background. N=number of animals, trials > 3, ***<0.001 to wild type, one-way ANOVA with post hoc Tukey.

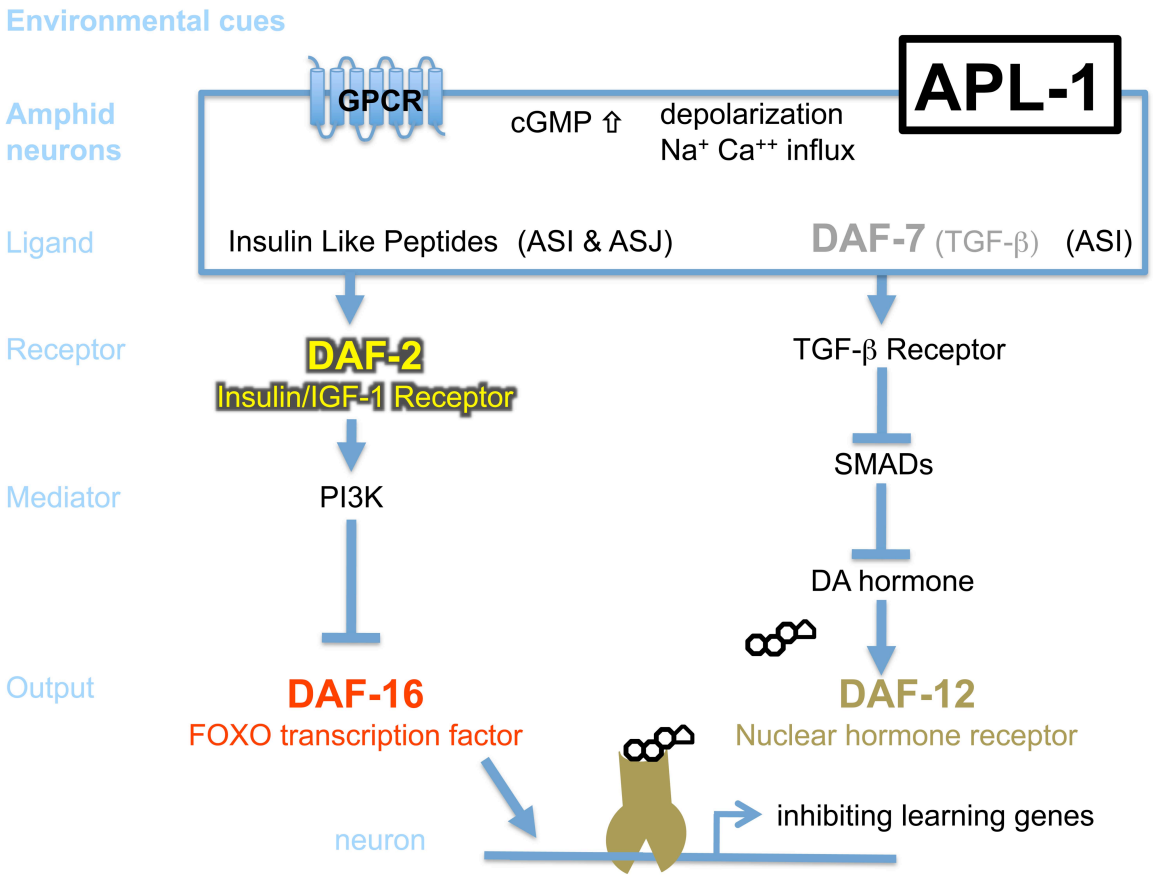

Figure 5. Model for how neuronal APL-1 expression impairs learning

The TGFβ and insulin/IGF-1 pathways for dauer formation regulate olfactory plasticity (Daniels *et al*. 2000; Fielenbach & Antebi 2008). APL-1 modulates the *daf-7* TGFβ and *daf-2* insulin/IGF-1 receptor signaling pathways, thereby regulating olfactory plasticity and touch habituation.

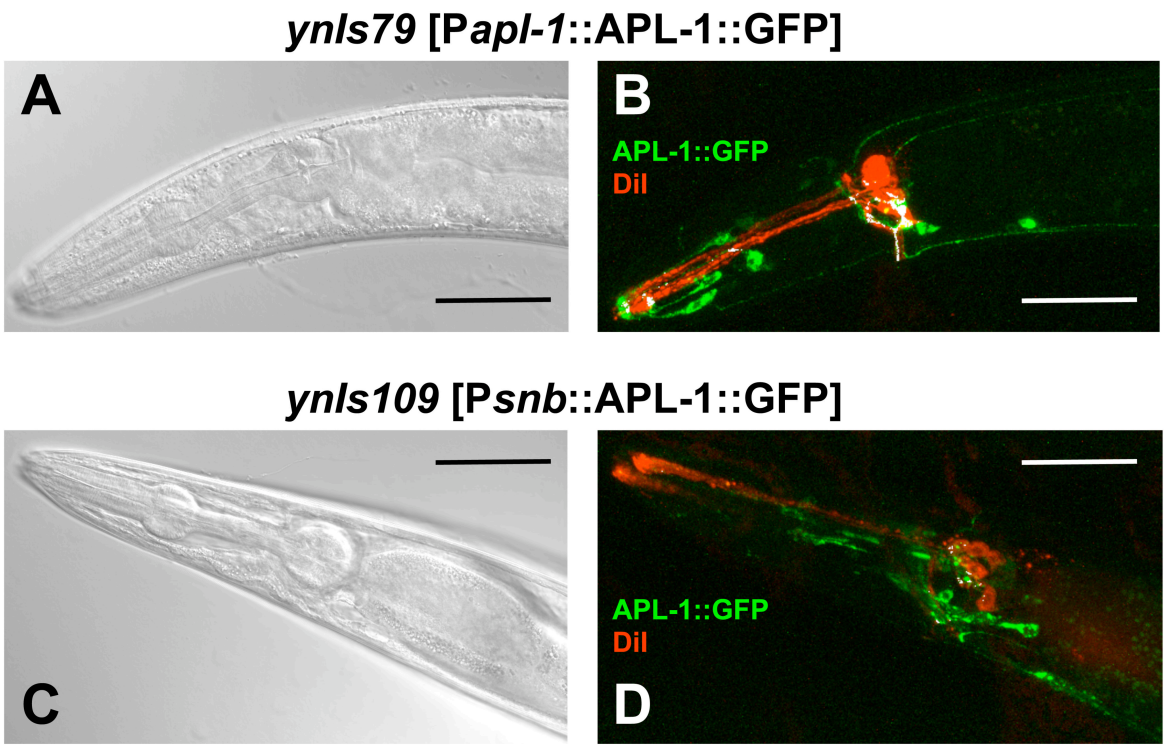

Supplement Figure S1. APL-1 overexpression does not affect amphid neuron morphology

A and **B**. Head region of a *ynIs79* [P*apl-1*::APL-1::GFP] animal. **B**. DiI staining in red, APL-1::GFP expression in green; co-localizations are highlighted in white. The ASJ chemosensory neuron appears to express APL-1::GFP **C** and **D**. Head region of a *ynIs109* [P*snb-1*::APL-1::GFP] animal. **D**. Although the *snb-1* promoter drives GFP expression in all neurons, GFP expression was not readily apparent in many amphid neurons. Anterior to the left. Scale bars = 50 μm.

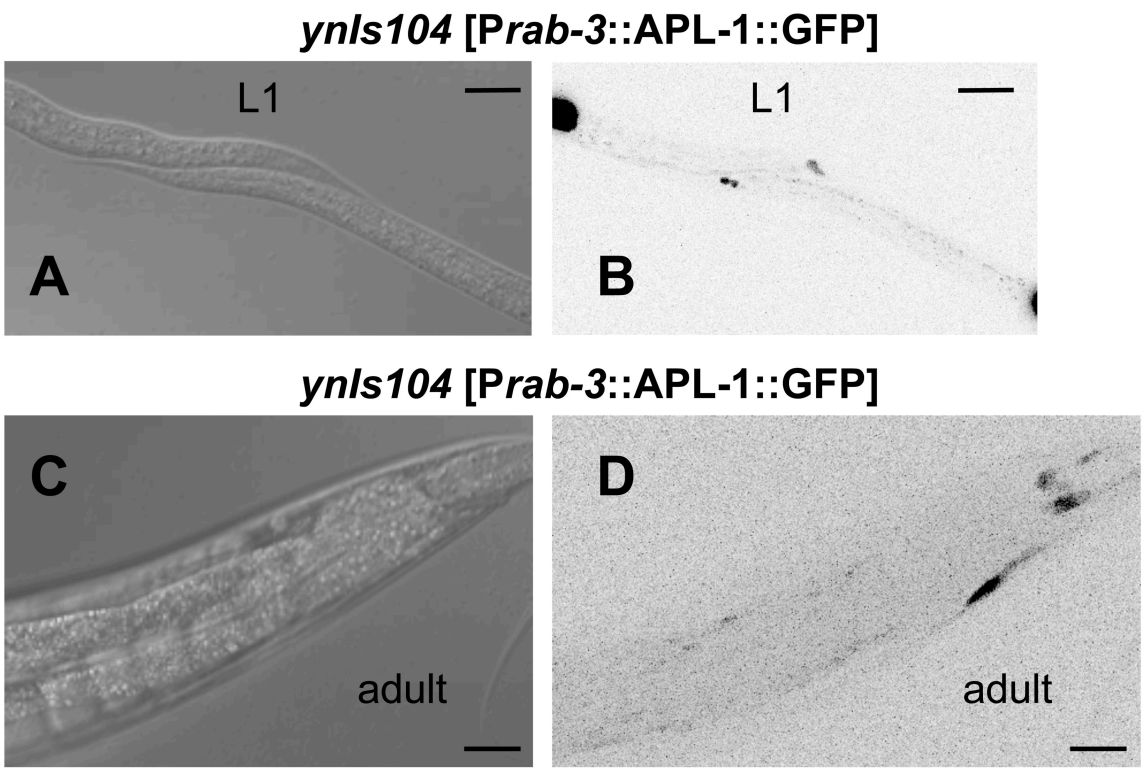

Supplement Figure S2. APL-1::GFP is very faintly expressed by the *rab-3* promoter

A-D. Body region or tail region of L1 (A and B) or adult (C and D) of *ynIs104* [P*rab-3*::APL-1::GFP; P*myo-2*::GFP] animals are shown, since they also express a GFP co-injection marker in the pharynx. **B.** Confocal pictures were inverted and dark black indicates APL-1::GFP. Scale bars = 50 μm.

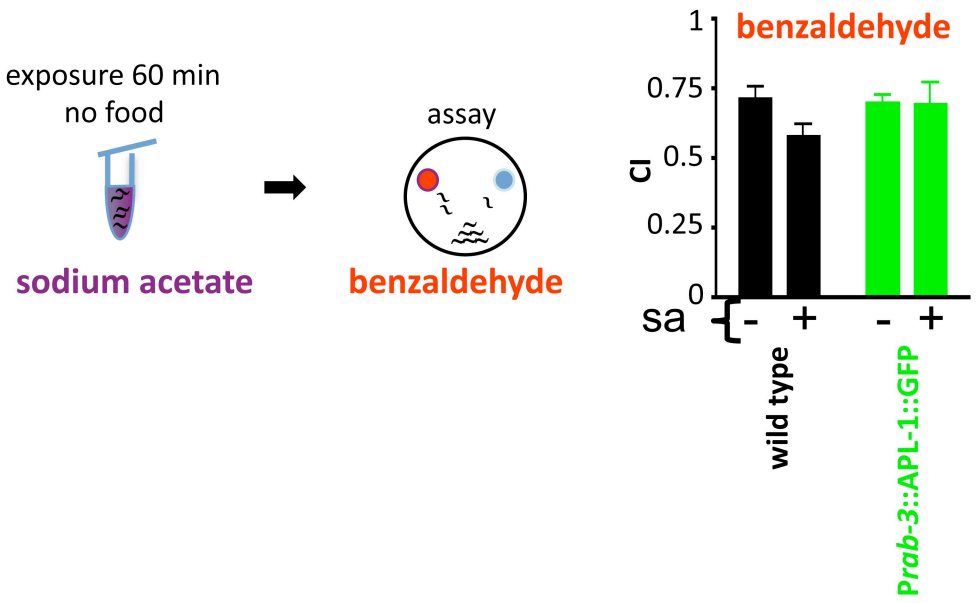

Supplement Figure S3. Pre-exposure to sodium acetate does not affect benzaldehyde chemotaxis.

Wild-type or *ynIs104* [P*rab-3*::APL-1::GFP] animals were pre-exposed for 60 minutes in the absence of food to sodium acetate and their chemotaxic response to benzaldehyde was determined. sa indicates sodium acetate.

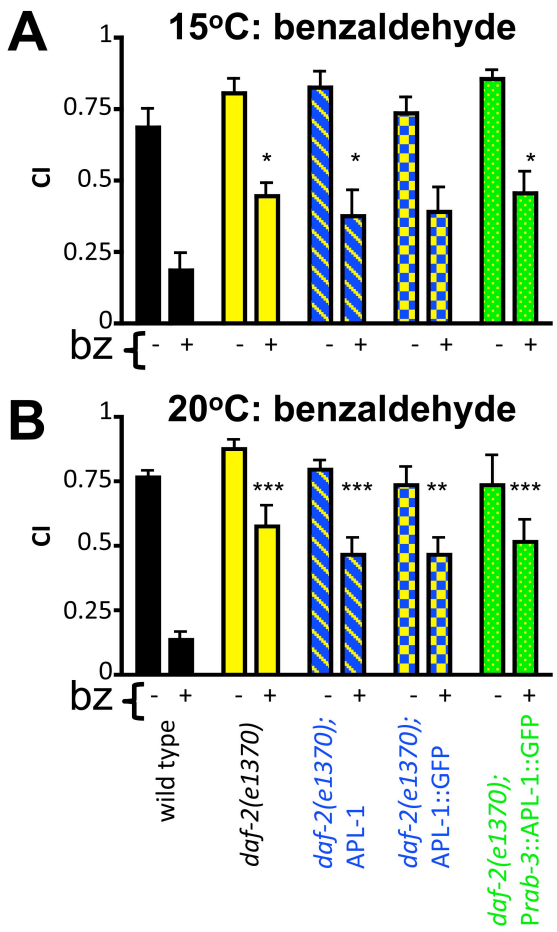

Supplement Figure S4. The *daf-2(e1370)* mutation restores the chemotaxis response in transgenic APL-1 overexpression lines at the permissive temperature (15°C).

Animals with the *daf-2(e1370)* temperature sensitive allele showed partial rescue of the avoidance response at the permissive temperatures of 15°C (A) and 20°C (B). *daf-2(e1370)* mutants that overexpress APL-1 by its endogenous promoter or *rab-3* promoter showed similar chemotaxis and avoidance behavior as *daf-2(e1370)* mutants at 15°C and 20°C. Trials > 5. *<0.05; **<0.01; ***<0.001 to wild type, two-way ANOVA repeated measure with post hoc Bonferroni was used.

Chapter VI: Discussion

APL-1 is a multifunctional protein that regulates several important processes, including viability, mobility, aging, developmental progression, egg-laying rate, body size, touch habituation, and olfactory and gustatory avoidance behavior. Most of these process are mediated via the transcription factor DAF-16/FOXO and the nuclear hormone receptor DAF-12/NHR. APL-1 is likely to act cell-non autonomously to affect *daf-16* or *daf-12* activity.

VI.1. The role of APL-1 during aging

The incidence of Alzheimer's disease (AD) increases with age and modifications in APP is suggested to be a causative factor of AD. However, the role of APP during aging is unclear and difficult to examine. We used *C. elegans* due to its suitably for lifespan experiments to ask how overexpression of APL-1, the *C. elegans* orthologue of human APP, affects aging (Chapter 3). Overexpression of APL-1 driven by its endogenous promoter accelerates aging and shortens lifespan. The shortening of lifespan is not simply caused by an accumulation of APL-1 protein with age. Using a GFP-tagged APL-1 marker, APL-1::GFP fluorescence of the head region only mildly increases with age and not to the level as seen when animals are placed at higher temperature (Appendix Figure 1: compare *ynIs79* [P*apl-1*::APL-1::GFP] day 10 at 20ºC versus day 4 at 27ºC). In addition, *apl-1* is not up-regulated during normal aging (Hill *et al*. 2000; Lund *et al*. 2002; Golden & Melov 2004). As determined by microarray analyses of wild-type animals of different ages (day 3-19), mRNA levels of *apl-1* did not change significantly

(0-1.18 fold) (Lund *et al*. 2002)). Lowering *apl-1* levels either by RNAi or in a heterozygous background had no affect on lifespan (RNAi data not shown; personal comm. with R. Niwa). Similarly, reducing *sel-12* presenilin function, which decreases APL-1 levels and partially rescues lethality of *ynIs79* animals (Hornsten *et al*. 2007), did not affect lifespan (Kitagawa *et al*. 2003).

Overexpression of the extracellular domain of APL-1, as seen by transgenic *ynIs71* or mutant *apl-1(yn5)* animals, was sufficient to decrease lifespan, suggesting that signaling through the released APL-1 fragment modulates longevity (Chapter 3, Figure 1). Although neurons do not age compared to other tissues (Herndon *et al*. 2002), pan-neuronal expression of APL-1 (*ynIs104* [P*rab-3*::APL-1::GFP]) had the most dramatic effect on decreasing lifespan (Chapter 3, Table 1). Interestingly, a very small fraction of the *ynIs104* [P*rab-3*::APL-1::GFP] showed a similar maximum lifespan as wild-type animals (Chapter 3, Figure 1). This fraction might be due to stochastic events during the life history of the animals. For instance, even when the environment is kept constant, isogenic animals show stochastic changes in expression levels of *hsp-16.2* (heat-shock protein), which correlate positively with longevity and stress-resistance (Rea *et al*. 2005). HSP-16.2 and other heat-shock proteins are up-regulated by lower *daf-2*/insulin/IGF-1 receptor activity (Murphy *et al*. 2003). Decreased *daf-2* activity counteracted the shortened lifespan of endogenous APL-1 overexpression lines. By analogy, neuronal specific knockout of IGF-1 receptor or complete knock out of IRS-2, a downstream component of IGF-1 receptor, counteracted the short lifespan of transgenic mice that overexpress human APPswe (swe: double mutation in APP found in familial AD patients from Sweden) (Freude *et al*. 2009). By contrast, decreased *daf-2* activity could only

partially extend the shortened lifespan of animals with pan-neuronal APL-1 expression (*daf-2(e1370)*; *ynIs104* [P*rab-3*::APL-1::GFP]) (Chapter 3, Figure 1).

VI.2. The role of mis-expression of APL-1 during aging

Surprisingly, overexpression of APL-1 with the *snb-1* promoter enhanced lifespan (Chapter 3, Figure 1). Moreover, expression of the extracellular domain of APL-1 with the *snb-1* promoter was sufficient to cause the enhanced lifespan (Chapter 3, Figure 1). We found that the *snb-1* promoter drives APL-1::GFP expression primarily in all neurons and the somatic gonad at 20ºC (Chapter 3, Figure S3). By using a similar length of the 5' promoter region of *snb-1* (~3 kb), other groups have shown that transcriptional fusions of the *snb-1* promoter with GFP showed expression not only in neurons and the somatic gonad, but also in muscle cells (McKay *et al*. 2003; Hunt-Newbury *et al*. 2007) or showed ubiquitous expression (O. Hobert, pers. comm.). As with other promoters, at 27ºC APL-1::GFP expression driven by the *snb-1* promoter was also detected in additional tissues, including body wall muscles, but not in intestinal cells (Appendix Figure 2). Consistent with the P*snb-1*::APL-1 expression patterns are phenotypic observations: driving human Aβ expression with the *snb-1* promoter caused gonadal defects (C. Link, pers. comm.), but did not cause paralysis as seen by Aβ expression in muscles (Link 2006), suggesting that Aβ expression driven by the *snb-1* promoter does not express strongly in muscles and does not cause neurodegeneration that would also result in paralysis or at least severe uncoordination.

Signals from both the somatic gonad as well as the germline have been implicated in the regulation of lifespan (Hsin & Kenyon 1999). In addition, signaling from neurons

and intestinal cells are required to decrease insulin signaling to induce longevity (Wolkow *et al*. 2000; Libina *et al*. 2003). We determined that the enhanced lifespan transgenic animals with *Psnb-1*::APL-1 expression is dependent on signals from the somatic gonad and activity of *daf-16*/FOXO and *daf-12* NHR (Chapter 3, Figure 3). However, this mis-expression of APL-1 by the *snb-1* promoter might not reflect biological function of APL-1. Whether *apl-1* in a biological context affects *daf-12* NHR and *daf-16*/FOXO activity have yet to be determined. Interestingly, ovariectomy of young mice that overexpress human APPswe show a severe shortening in lifespan compared to sham operated APPswe mice (Levin-Allerhand & Smith 2002). However, it remains to be determined whether expression of APL-1 exclusively in the somatic gonad is sufficient to enhance lifespan in *C. elegans*.

VI.3. The role of APL-1 during development

In addition to longevity, *daf-16*/FOXO and *daf-12* NHR are also involved in reproductive growth, stress resistance, and reproduction (Kenyon 2005). However, the rate of developmental progression was not affected by loss or reduction of function of *daf-16*/FOXO or *daf-12* NHR activity in wild-type animals. By contrast, the slowed developmental progression of *apl-1(yn5)* animals was partially in the case of *daf-16* null or completely in the case of *daf-12* rescued to wild-type developmental progression rates (Chapter 4, Table 1), suggesting that *apl-1* modulates *daf-16*/FOXO and *daf-12* NHR activity. Moreover, overexpression of DAF-16 phenocopied the *apl-1(yn5)* slowing of developmental progression and shorter body size ((Henderson & Johnson 2001); (Chapter 4, Tables 1 and S2), suggesting that the *apl-1(yn5)* mutation increases *daf-16*/FOXO

activity. However, *apl-1(yn5)* overexpression had different effects on other processes. For instance, *apl-1(yn5)* overexpression slowed DAF-16::GFP nuclear localization during heat stress (Chapter 4, Table S1), suggesting that the extracellular domain of APL-1 signals to decrease the activity of DAF-16/FOXO during heat stress. By micro-array analysis, *apl-1* mRNA levels did not change by activation of DAF-16 through the insulin/IGF-1 pathway (McElwee *et al*. 2003; Murphy *et al*. 2003). These results suggest that during development APL-1 is cleaved and the released extracellular fragment acts as a signal for proper developmental progression, perhaps by synchronizing molting with developmental timing. Thummel (Thummel 2001) proposed that there are two independent timers: one to control the time of molting via steroid hormones and one to control timing of cell differentiation and division via heterochronic genes. Loss of *apl-1* results in a completely penetrant molting defect from the first to the second larval stage (Hornsten *et al*. 2007), which implicates APL-1 as acting in the first timer. *apl-1* is regulated by heterochonic genes and rescues the *let-7* bursting phenotype (Niwa *et al*. 2008), which implicates APL-1 in the second timer. The release of sAPL-1α might integrate or synchronize both timers. Which genes sAPL-1α activates to control the timing of molting remains to be determined. We have started an RNAi screen to identify such genes (Appendix A.10). In addition, GFP tagging the APL-1 extracellular domain and RFP tagging APL-1 at its C-terminus could reveal the time of APL-1 cleavage and presumably the target cells that sAPL-1α binds. The presence of GFP-tagged sAPL-1 in coelomocytes would suggest that released sAPL-1α acts distantly. The heterochronic timer might be coupled via *daf-12* NHR, which forms a feedback loop with *let-7* (Hammell *et al*. 2009). Although *let-7* acts during late development (Reinhart *et al*.

2000), it is possible that *daf-12* NHR regulates other heterochronic genes that act earlier in development. *apl-1* activity is needed not only for molting for the first to the second larval transition, but for molting during all transitions (Chapter 4). Furthermore, the essential function of sAPL-1α might be conserved, even in mammals that do not molt. In mice, double knockouts of APP-APLP2 results in post-natal lethality and this lethality can be rescued by re-introduction of sAPPα (U. Müller, personal communication).

VI.4. The role of APL-1 during learning

The *apl-1* molting defect is rescued by pan-neuronal expression APL-1 (Hornsten *et al*. 2007), suggesting that APL-1 acts non-cell autonomously as a signal to induce shedding of the old cuticle. However, pan-neuronal expression of APL-1 disrupted learning, such that touch habituation and olfactory and gustatory avoidance behavior were lost. Thus far, APL-1 is the first protein that has been shown to affect all three behaviors in *C. elegans*. In mice, overexpression of APP shows a variety of behavioral defects and several defects are associated with the accumulation of the Aβ peptide, which might cause neurodegeneration (Roskam *et al*. 2010). Driving the human Aβ peptide by the *snb-1* promoter in *C. elegans* leads to impairment in olfactory avoidance behavior to diacetyl (Dosanjh *et al*. 2009). However, whether this is caused by accumulation of human Aβ peptide or neurodegeneration remains to be determined. In all our APL-1 overexpression lines, we did not find any signs of neurodegeneration (Appendix A.7-8). Furthermore, neurodegeneration does not appear to be the cause for learning impairments, since the avoidance and touch habituation responses are restored by decreased activity of *daf-7*/TGFβ, *daf-12*/NHR, and or *daf-16*/FOXO (Chapter 5, Figure 3).

Decreasing *daf-2* insulin/IGF-1 receptor activity has multiple effects, including extending lifespan (Kenyon 2005) and impairing olfactory plasticity towards sodium and benzaldehyde (Chapter 5, Figure 3; (Tomioka *et al*. 2006; Lin *et al*. 2010)). Whether the impairment induced by *daf-2* might be mediated through *daf-16*/FOXO, as our results suggest (Chapter 5, Figure 3), or mediated independently of *daf-16*/FOXO, as Tomioka et al. suggest (Tomioka *et al*. 2006), remains to be reconciled. Yamada et al. (Yamada *et al*. 2010) have demonstrated that pheromone levels regulate olfactory plasticity. Food resources and pheromone levels from crowded conditions are sensed by amphid neurons and external information is integrated via endocrine hormonal signaling by *daf-2* insulin/IGF-1 receptor signaling to *daf-16*/FOXO and/or by *daf-7*/TGF-β to *daf-12* NHR (Fielenbach & Antebi 2008). Hence, the insulin/IGF-1 and DAF-12 NHR pathways are not directly involved in laying down memory, but interact with the pathways to modulate avoidance behavior.

VI.5. Understanding APL-1 function in *C. elegans* might provide insights into APP function in mammals

Collectively, our results reveal the first downstream components of APL-1. Further, our data suggest that APL-1 has multiple roles that are mediated by the same downstream targets, but result in different outcomes depending on the context. First, APL-1 may act to synchronize the timing of molting and developmental progression. The data provided in this study revealed *daf-16*/FOXO and *daf-12* NHR as downstream targets of signaling from the extracellular domain of APL-1 for developmental progression. The ongoing RNAi screen for suppressors of the *apl-1(yn10)* molting defect could reveal proteins

linked to the molting timer. Second, APL-1 may act as a modulator of the insulin/IGF-1 pathway to regulate lifespan and learning. A similar molecular link between APP and the insulin/IGF-1 pathway might exist in mammals. Our results suggest that the shortened lifespan and learning defects in mice in which APP is overexpressed are mediated via the insulin/IGF-1 pathway. Interestingly, AD is strongly associated with type 2 diabetes (Alzheimer's Association 2010) and some AD patients show brain specific diabetes (Steen *et al*. 2005). Our work provides insight into the molecular links and pathways of APL-1 that may translate into understanding the mechanisms of APP action.

VI. 6. References

Alzheimer's Association KM (2010). 2010 Alzheimer's disease facts and figures. *Alzheimer's and Dementia*. **6**, 158-194.

Dosanjh LE, Brown MK, Rao G, Link CD , Luo Y (2009). Behavioral phenotyping of a transgenic *C. elegans* expressing neuronal amyloid-beta. *J Alzheimers Dis*.

Fielenbach N , Antebi A (2008). *C. elegans* dauer formation and the molecular basis of plasticity. *Genes Dev*. **22**, 2149-2165.

Freude S, Hettich MM, Schumann C, Stohr O, Koch L, Kohler C, Udelhoven M, Leeser U, Muller M, Kubota N, Kadowaki T, Krone W, Schroder H, Bruning JC , Schubert M (2009). Neuronal IGF-1 resistance reduces Abeta accumulation and protects against premature death in a model of Alzheimer's disease. *Faseb J*. **23**, 3315-3324.

Golden TR , Melov S (2004). Microarray analysis of gene expression with age in individual nematodes. *Aging Cell*. **3**, 111-124.

Hammell CM, Karp X , Ambros V (2009). A feedback circuit involving *let-7*-family miRNAs and DAF-12 integrates environmental signals and developmental timing in *Caenorhabditis elegans*. *Proc Natl Acad Sci USA*. **106**, 18668-18673.

Henderson ST , Johnson TE (2001). *daf-16* integrates developmental and environmental inputs to mediate aging in the nematode *Caenorhabditis elegans*. *Curr Biol*. **11**, 1975-1980.

Herndon LA, Schmeissner PJ, Dudaronek JM, Brown PA, Listner KM, Sakano Y, Paupard MC, Hall DH , Driscoll M (2002). Stochastic and genetic factors influence tissue-specific decline in ageing *C. elegans*. *Nature*. **419**, 808-814.

Hill AA, Hunter CP, Tsung BT, Tucker-Kellogg G , Brown EL (2000). Genomic analysis of gene expression in *C. elegans*. *Science*. **290**, 809-812.

Hornsten A, Lieberthal J, Fadia S, Malins R, Ha L, Xu X, Daigle I, Markowitz M, O'Connor G, Plasterk R , Li C (2007). APL-1, a *Caenorhabditis elegans* protein related to the human beta-amyloid precursor protein, is essential for viability. *Proc Natl Acad Sci USA*. **104**, 1971-1976.

Hsin H , Kenyon C (1999). Signals from the reproductive system regulate the lifespan of *C. elegans*. *Nature*. **399**, 362-366.

Hunt-Newbury R, Viveiros R, Johnsen R, Mah A, Anastas D, Fang L, Halfnight E, Lee D, Lin J, Lorch A, McKay S, Okada HM, Pan J, Schulz AK, Tu D, Wong K, Zhao Z, Alexeyenko A, Burglin T, Sonnhammer E, Schnabel R, Jones SJ, Marra MA, Baillie DL , Moerman DG (2007). High-throughput in vivo analysis of gene expression in *Caenorhabditis elegans*. *PLoS Biol*. **5**, e237.

Kenyon C (2005). The plasticity of aging: insights from long-lived mutants. *Cell*. **120**, 449-460.

Kitagawa N, Shimohama S, Oeda T, Uemura K, Kohno R, Kuzuya A, Shibasaki H , Ishii N (2003). The role of the presenilin-1 homologue gene *sel-12* of Caenorhabditis elegans in apoptotic activities. *The Journal of biological chemistry*. **278**, 12130-12134.

Levin-Allerhand JA , Smith JD (2002). Ovariectomy of young mutant amyloid precursor protein transgenic mice leads to increased mortality. *J Mol Neurosci*. **19**, 163-166.

Libina N, Berman JR , Kenyon C (2003). Tissue-specific activities of *C. elegans* DAF-16 in the regulation of lifespan. *Cell*. **115**, 489-502.

Lin CH, Tomioka M, Pereira S, Sellings L, Iino Y , van der Kooy D (2010). Insulin signaling plays a dual role in *Caenorhabditis elegans* memory acquisition and memory retrieval. *J Neurosci*. **30**, 8001-8011.

Link CD (2006). *C. elegans* models of age-associated neurodegenerative diseases: lessons from transgenic worm models of Alzheimer's disease. *Experimental gerontology*. **41**, 1007-1013.

Lund J, Tedesco P, Duke K, Wang J, Kim SK , Johnson TE (2002). Transcriptional profile of aging in *C. elegans*. *Curr Biol*. **12**, 1566-1573.

McElwee J, Bubb K , Thomas JH (2003). Transcriptional outputs of the *Caenorhabditis elegans* forkhead protein DAF-16. *Aging Cell*. **2**, 111-121.

McKay SJ, Johnsen R, Khattra J, Asano J, Baillie DL, Chan S, Dube N, Fang L, Goszczynski B, Ha E, Halfnight E, Hollebakken R, Huang P, Hung K, Jensen V, Jones SJ, Kai H, Li D, Mah A, Marra M, McGhee J, Newbury R, Pouzyrev A, Riddle DL, Sonnhammer E, Tian H, Tu D, Tyson JR, Vatcher G, Warner A, Wong K, Zhao Z , Moerman DG (2003). Gene expression profiling of cells, tissues, and developmental stages of the nematode *C. elegans*. *Cold Spring Harb Symp Quant Biol*. **68**, 159-169.

Murphy CT, McCarroll SA, Bargmann CI, Fraser A, Kamath RS, Ahringer J, Li H , Kenyon C (2003). Genes that act downstream of DAF-16 to influence the lifespan of *Caenorhabditis elegans*. *Nature*. **424**, 277-283.

Niwa R, Zhou F, Li C , Slack FJ (2008). The expression of the Alzheimer's amyloid precursor protein-like gene is regulated by developmental timing microRNAs and their targets in *Caenorhabditis elegans*. *Developmental biology*. **315**, 418-425.

Rea SL, Wu D, Cypser JR, Vaupel JW , Johnson TE (2005). A stress-sensitive reporter predicts longevity in isogenic populations of *Caenorhabditis elegans*. *Nature genetics*. **37**, 894-898.

Reinhart BJ, Slack FJ, Basson M, Pasquinelli AE, Bettinger JC, Rougvie AE, Horvitz HR , Ruvkun G (2000). The 21-nucleotide *let-7* RNA regulates developmental timing in *Caenorhabditis elegans*. *Nature*. **403**, 901-906.

Roskam S, Neff F, Schwarting R, Bacher M , Dodel R (2010). APP transgenic mice: the effect of active and passive immunotherapy in cognitive tasks. *Neurosci Biobehav Rev*. **34**, 487-499.

Steen E, Terry BM, Rivera EJ, Cannon JL, Neely TR, Tavares R, Xu XJ, Wands JR , de la Monte SM (2005). Impaired insulin and insulin-like growth factor expression and signaling mechanisms in Alzheimer's disease--is this type 3 diabetes? *J Alzheimers Dis*. **7**, 63-80.

Thummel CS (2001). Molecular mechanisms of developmental timing in *C. elegans* and *Drosophila*. *Dev Cell*. **1**, 453-465.

Tomioka M, Adachi T, Suzuki H, Kunitomo H, Schafer WR , Iino Y (2006). The insulin/PI 3-kinase pathway regulates salt chemotaxis learning in *Caenorhabditis elegans*. In *Neurone*d^eds), pp. 613-625.

Wolkow CA, Kimura KD, Lee MS , Ruvkun G (2000). Regulation of *C. elegans* life-span by insulinlike signaling in the nervous system. *Science*. **290**, 147-150.

Yamada K, Hirotsu T, Matsuki M, Butcher RA, Tomioka M, Ishihara T, Clardy J, Kunitomo H , Iino Y (2010). Olfactory plasticity is regulated by pheromonal signaling in *Caenorhabditis elegans*. *Science*. **329**, 1647-1650.

Appendix

A.1. Increased temperature increases fluorescence of APL-1::GFP

In addition to the L1 lethality and the morphological defects at 20ºC, we observed higher APL-1::GFP fluorescence in dying or dead L1 *ynIs79* [APL-1::GFP] animals. Although all L1 *ynIs79* [APL-1::GFP] animals shifted to 27ºC survived, their GFP fluorescence increased and those animals became sterile (N=377; T=4). To quantify the APL-1::GFP increase, L4 *ynIs79* [APL-1::GFP] animals were placed at 27ºC and the GFP fluorescence intensity was measured. Transgenic L4 *ynIs79* [APL-1::GFP] animals shifted at 27ºC showed a linear increase in GFP intensity within four days and after two days showed a significant intensity increase compared to age-matched *ynIs79* [APL-1::GFP] animals left at 20ºC. The GFP intensity at 20ºC stayed fairly constant; however, the fluorescence intensity showed a dramatic increase by day 8 (Figure 1) due to autofluorescence of the intestine. Measuring the fluorescence in the head of *ynIs79* [APL-1::GFP] animals at 20ºC showed a minimal increase with age (Figure 1). By contrast, microarray analysis of transcripts from wild-type worms of different ages from 3-19 days did not show any transcriptional up-regulation of *apl-1* (Lund *et al*. 2002). The GFP intensity increase with age at 20ºC or at a mild stress condition of 27ºC suggests that there may be a protein degradation problem rather than a heat-shock response, which usually occurs within hours. Indeed, when *ynIs79* [APL-1::GFP] animals were exposed to a 35ºC heat-shock, the GFP fluorescence did not increase (N=621; T=7), consistent with microarray data that *apl-1* expression did not change after 35ºC heat shock (GuhaThakurta *et al*. 2002). Moreover, animals carrying a transgene that drives APL-1::GFP with the *snb-1* promoter

also showed a slow intensity increase of the GFP fluorescence. Transgenic *ynIs109* [P*snb-1*::APL-1::GFP] animals grown at 20ºC showed GFP expression in neurons, supporting cells, and the somatic gonad, whereas *ynIs109* [P*snb-1*::APL-1::GFP] animals shifted at 27ºC after three days showed high GFP fluorescence not only in neurons and the somatic gonad, but also in body wall muscles and hypodermis (Figure 2). These results indicate that the *snb-1* promoter expresses APL-1::GFP in more tissues than is visible at 20ºC and that those tissues might be better at degrading excess APL-1::GFP protein. At 20ºC, GFP intensity of three-day adults seemed to be higher compared to the one-day adult transgenic *ynIs109* [P*snb-1*::APL-1::GFP] animals (Figure 2). Taken together, these results indicate that the slow increase of APL-1::GFP at 27ºC is not due to a heat-shock response, but may be caused by a degradation problem to eliminate APL-1::GFP protein. In addition, tissues such as body wall muscles and hypodermis cells might be better at degrading excess APL-1 protein than neurons and the somatic gonad.

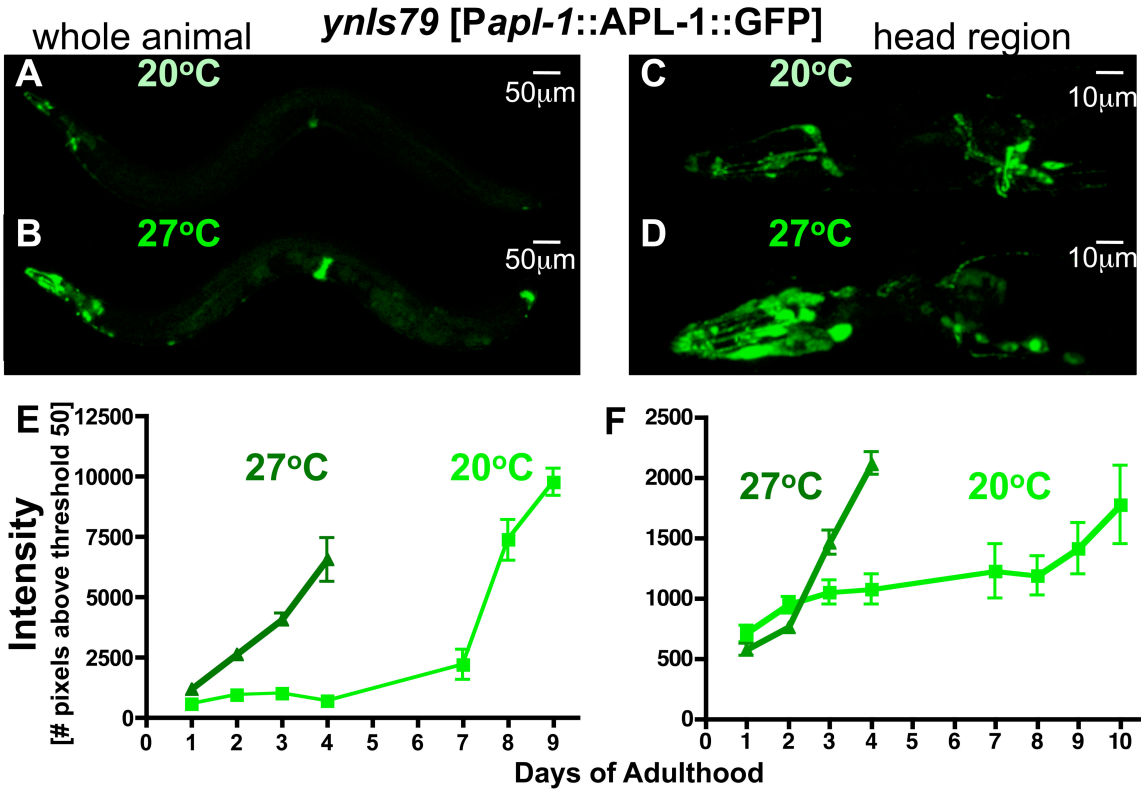

Figure 1. APL-1::GFP fluorescence increases slowly with age and at a higher temperature. Transgenic *ynIs79* [Papl-1::APL-1::GFP] animals were grown at 20ºC and L4 animals (Day 0) were picked and either kept at 20ºC or shifted to 27ºC. Fluorescence intensity was measured on subsequent days. APL-1::GFP fluorescence of whole animals at day 3 at 20ºC (A) or 27ºC (B). Z-stack projection of APL-1::GFP fluorescence of head region of animals at day 3 at 20ºC (C) or 27ºC (D). Quantification of APL-1::GFP intensity from day 1 until day 10 of adulthood at 20ºC and 27ºC for whole animals or only the head region of the same animals (at least 3 trials, N>15 per data point).

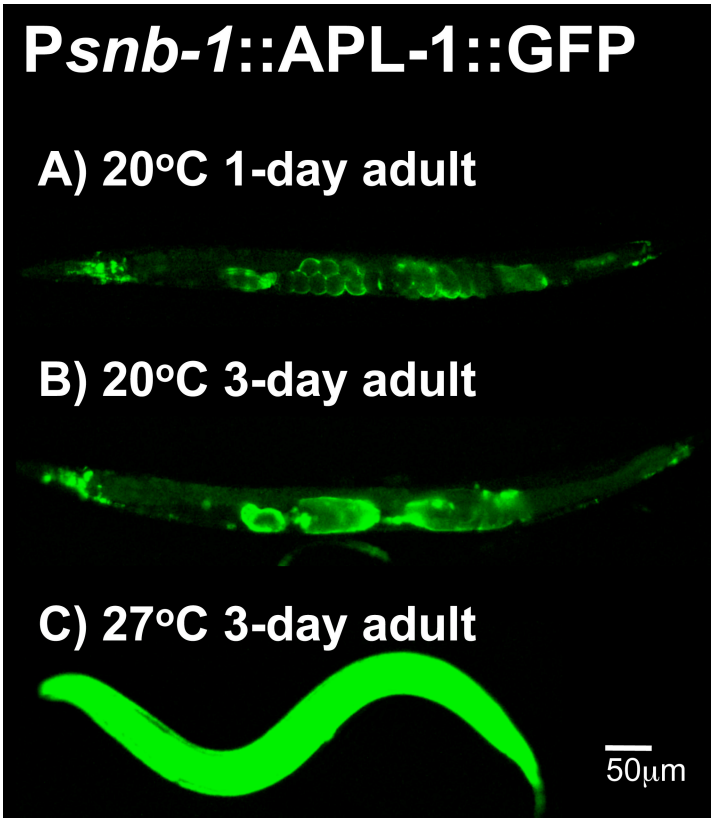

Figure 2. APL-1::GFP driven by the *snb-1* promoter is visible in many tissues at higher temperature.

APL-1::GFP fluorescence of *ynIs109* [P*snb-1*::APL-1::GFP] is increased at day 3 (**B**) compared to day 1 (**A**) of adulthood at 20ºC. While *snb-1* driven APL-1::GFP is only visible in neurons, supporting cells and somatic gonad at 20ºC (**B**), APL-1::GFP at 27ºC is visible also in other tissues, such as muscles and hypodermis (see z-stack movie). Scale bars = 50 μm.

A.2. Increased temperature increases APL-1 protein levels

The increased APL-1::GFP fluorescence could reflect either higher APL-1 protein levels, aggregates of the cleaved cytoplasmic APL-1 fragment onto which the GFP is tagged, or better GFP visibility in degradation lysosomes. To determine whether the increased GFP

intensity at 27ºC reflects higher protein levels, we analyzed western blots with an antibody against the extracellular domain of APL-1 (αAPL-1EXT). *ynIs79* [APL-1::GFP] animals were grown either at 15ºC, 20ºC, 25ºC or 27ºC and their lysates were probed with αAPL-1EXT antibody (Figure 3). Both full-length APL-1 and APL-1EXT protein levels increased at higher temperatures in a temperature-dependent manner, suggesting that the increased GFP fluorescence represents an increase of overall APL-1 protein levels. Similarly, animals that drive APL-1::GFP with the *snb-1* promoter showed an increase in GFP fluorescence at 27ºC compared to 20ºC: their APL-1 protein levels were also dramatically increased at 27ºC compared to 20ºC as determined by western blot analysis (Figure 4). However, wild-type and *apl-1(yn5)* mutant animals grown at 27ºC showed a milder increase of APL-1 protein levels compared to animals grown at 20ºC (Figure 4). These results suggest that *C. elegans* handles lower levels of excess APL-1 better than higher levels. One way for an organism to cope with excess proteins is through autophagy.

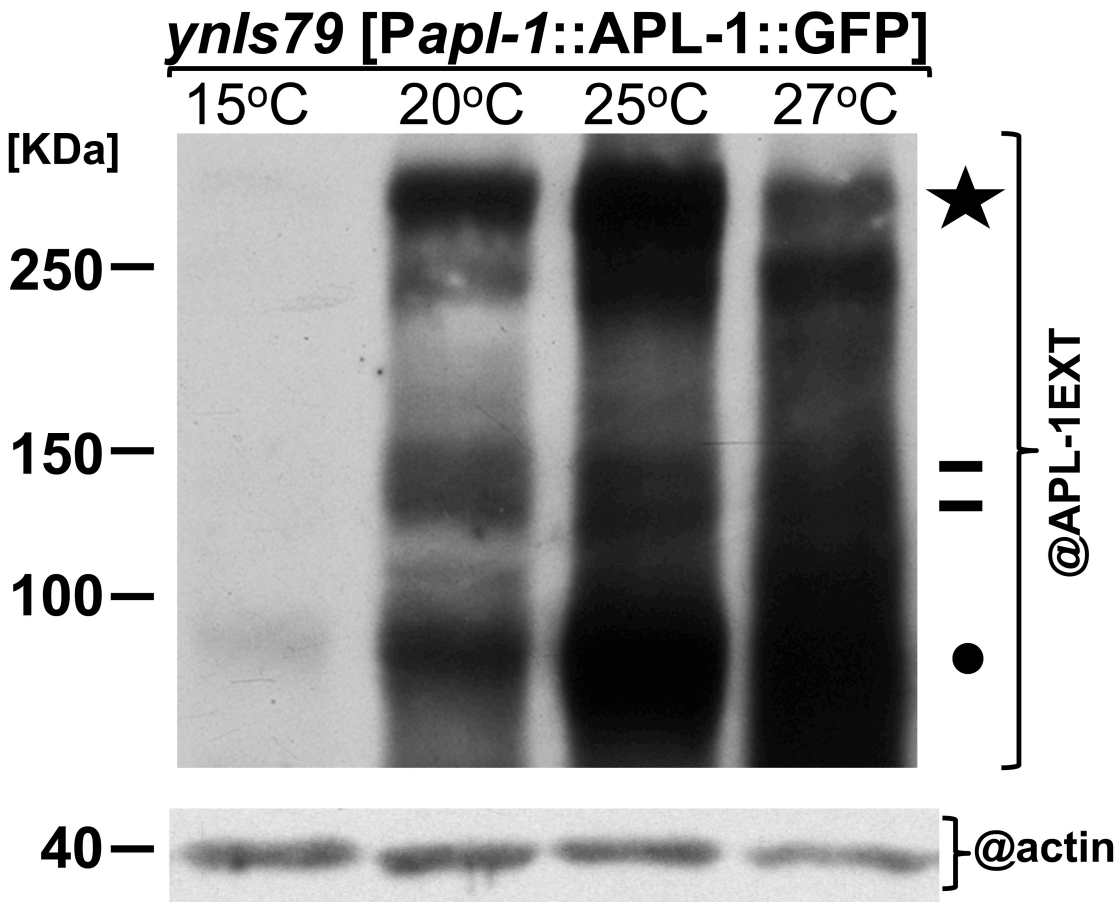

Figure 3. APL-1 protein levels increase in extracts from animals cultivated at higher temperatures.

Transgenic *ynIs79* [P*apl-1*::APL-1::GFP] animals were grown either at 15 ºC, 20ºC, 25 ºC, or 27ºC. Protein levels of in lysates were first normalized to their actin levels (lower panel: @actin). Normalized amounts of lysates were electrophoresed, blotted, and probed with an antibody against the extracellular domain of APL-1 (upper panel: @APL-1EXT). Levels of full-length (bars), cleaved (dot), or dimers (star) of APL-1::GFP protein are increased as the cultivation temperature of the animals is increased.

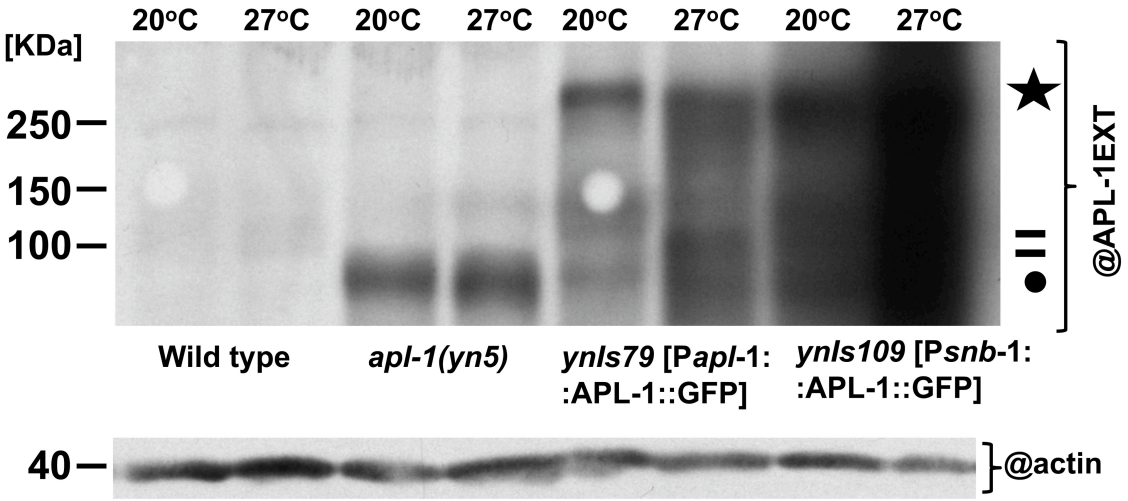

Figure 4. APL-1 protein levels are mildly increased in wild-type animals cultivated at higher temperature.

Animals were grown either at 20ºC or 27 ºC. Protein levels of lysates were first normalized to actin levels (lower panel: @actin). Normalized lysate levels were electrophoresed, blotted, and probed with an antibody against the extracellular domain of APL-1 (upper panel: @APL-1EXT). Levels of APL-1 protein are mildly increased in lysates from animals cultivated at 27ºC compared to 20ºC for wild-type or *apl-1(yn5)* mutant animals. By contrast, levels of full-length (bars), cleaved (dot), or dimers (star) of APL-1::GFP protein are dramatically increased in lysates from *ynIs79* [P*apl-1*::APL-1::GFP] or *ynIs109* [P*snb-1*::APL-1::GFP] animals cultivated at 27ºC compared to 20ºC.

A.3. Reduced autophagy leads to higher APL-1 overexpression lethality

Autophagy is a general degradation process, whereby misfolded, excessive, or used proteins are engulfed into a double membrane organelle to form autophagic vesicles, which fuse with lysosomes to degrade engulfed proteins (reviewed in (Melendez & Neufeld 2008)). For the formation of autophagic vesicles, BEC-1 /Apg6/Vps30p/beclin1

is required (Meléndez *et al*. 2003). To determine whether increased APL-1 levels and lethality are due to autophagic degradation problems, we placed APL-1 overexpression lines in two *bec-1* mutant backgrounds. 90% of animals carrying the homozygous *bec-1(ok691)* or *bec-1(ok700)* alleles die during embryonic development; the *ok691* mutation represents a larger deletion than the *ok700* mutation and both mutations also delete the non-coding RNA T19E7.24. The remaining animals fail to shed their cuticles during all larval molts and only a few make it into adulthood, whereupon they die during the first day of adulthood (Takacs-Vellai *et al*. 2005). Hence, these *bec-1* alleles are maintained over a balancer (nT1), where most heterozygous *bec-1* animals are viable (kindly provided by A. Meléndez lab). Crossing *ynIs79* [APL-1::GFP] with *bec-1(ok691)*/nT1 or crossing *ynIs79*; nT1 with *bec-1(ok691)* never yielded heterozygous *bec-1(ok691); ynIs79* transgenic animals, suggesting a synthetic lethality (T=7). By contrast, *bec-1(ok700)*/nT1; *ynIs79* animals were viable, but very sick and grew extremely slow (it took over one month to grow a full plate of animals at 15ºC, whereas *ynIs79* or *bec-1(ok700)*/nT1 plates were overgrown within a week). On these plates, the number of characteristically dead L1 induced by APL-1 overexpression outnumbered the number of animals that survived into adulthood (Table 1). None of the *bec-1* mutant plates showed any characteristically dead L1 as seen on the APL-1 overexpression plates (Table 1). On plates with APL-1 overexpression worms (*ynIs86* or *ynIs79*), the ratio of dead L1 to adults was much lower compared to plates with animals that overexpressed APL-1 and carried the *bec-1(ok700)* allele (*bec-1(ok700)*/nT1; *ynIs86* or *bec-1(ok700)*/nT1; *ynIs79*) (Table 1). *ynIs79*; *bec-1(ok700)*/nT1 or *ynIs79*; *bec-1(ok700)* that made it to adulthood showed higher APL-1::GFP fluorescence than *ynIs79* [APL-1::GFP] grown at 15ºC

(Figure 5), suggesting that the double mutants have higher APL-1 protein levels. In addition to the enhanced APL-1 induced lethality and APL-1::GFP fluorescence, *bec-1(ok700)* also enhanced the short body length of APL-1 overexpression animals (Figure 5). Heterozygous *bec-1(ok700)*/nT1 animals are slightly longer than wild-type animals (Figure 5). By contrast, *ynIs79; bec-1(ok700)*/nT1 and *ynIs79; bec-1(ok700)* animals are shorter than *bec-1(ok700)*/nT1 and *ynIs79* animals (Figure 5). Hence, the L1 lethality, short body length, and increased APL-1::GFP fluorescence in APL-1 overexpression animals are enhanced by impairing the autophagy process, suggesting that higher APL-1 protein levels are swamping the autophagic degradation process. To determine whether APL-1 accumulates in autophagic vesicles, we used RFP-tagged BEC-1 transgenic animals (kindly provided by A. Melendez lab) to assay co-localization with GFP-tagged APL-1. As determined by confocal microscopy, we did not see any co-localization of RFP::BEC-1 with APL-1::GFP (Figure 5). Although RFP::BEC-1 is functional and rescues the *bec-1(ok691)* maternal and adult lethality, only 79% of animals that overexpress RFP::BEC-1 in a wild-type background survived at 20ºC (Table S1 Chapter 4). However, the lethality of *ynIs79* [APL-1::GFP] was increased from 37% to 72% when RFP::BEC-1 was also expressed (*ynIs110*; Table S1 Chapter 4), suggesting that overexpression of RFP::BEC-1 may itself be toxic. We hypothesize that APL-1 is degraded through multiple mechanisms, including autophagy. However, autophagy may not be the primary degradation pathway.

Table 1. Reduction of *bec-1* increases APL-1 induced L1 lethality at 15°C			
	No. of observed incidences		
Strain/Genotype	dead L1 [mean±SEM]	adults [mean±SEM]	Trials
Wild type (N2)	0	293±31	7
bec-1(ok691)/nT1	0	234±37	3
bec-1(ok700)/nT1	0	242±36	4
ynIs86 [APL-1]	3±1	216±30	3
ynIs86 [APL-1]; *bec-1(ok700)*/nT1	53±5	187±21	4
ynIs79 [APL-1::GFP]	39±7	159±38	4
ynIs79 [APL-1::GFP]; *bec-1(ok700)*/nT1	99±31	48±14	7

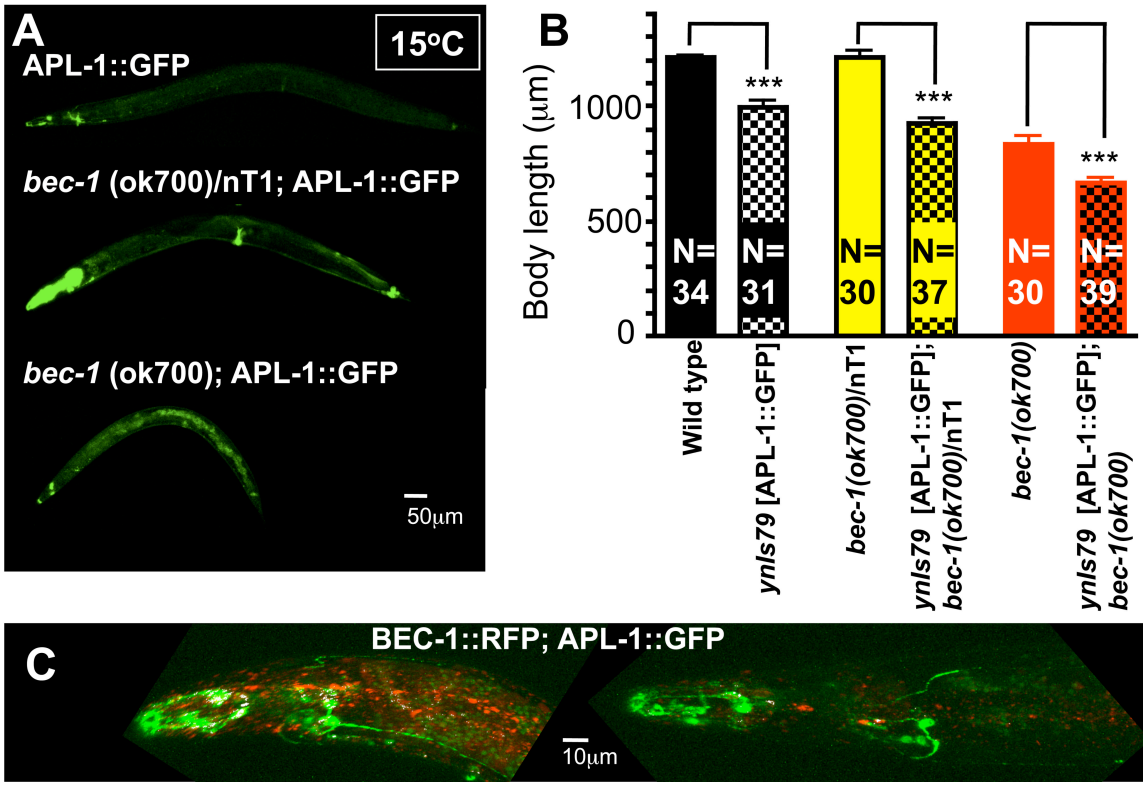

Figure 5. Impairment of autophagy enhances APL-1::GFP fluorescence and APL-1 induced short body-length

A. APL-1::GFP fluorescence is increased in heterozygous or homozygous *bec-1(ok700)* mutant backgrounds at 15°C. **B**. APL-1 overexpression 1-day old adult animals (*ynIs79*, checker cross-hatched bar) are shorter in body size than wild type (black bar) at 15°C.

The APL-1 induced shortness is enhanced in a homozygous *bec-1(ok700)* mutant background (checker cross-hatched red bar) at 15ºC. **C**. Head regions of two animals are shown. BEC-1::RFP does not co-localize with APL-1::GFP (areas of co-localization are highlighted in white). N indicates the number of animals scored.

A.4. Overexpression of APL-1 does not affect heat nor oxidative stress resistance

Downstream targets of DAF-16/FOXO include heat shock proteins, which protect against heat and catalases, which protect against hydrogen peroxide (Murphy *et al*. 2003). Hence, activation of DAF-16 makes animals resistant against heat and oxidative stress and lack of DAF-16 causes susceptibility (Kenyon 2005). Since APL-1 requires *daf-16*/FOXO activity to slow developmental progression and aging, we determined whether APL-1 would show any altered thermotolerance or oxidative stress resistance. All of the tested APL-1 lines showed similar heat and oxidative susceptibility as wild-type animals (Figures 6A and 6B).

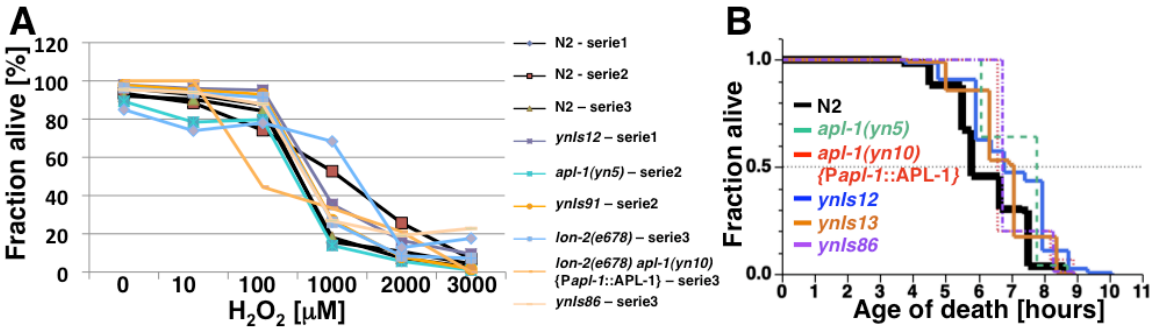

Figure 6. Animals with P*snb-1*::APL-1 expression are not hyper-resistant to oxidative- and thermal stress. A. Animals exposed to different concentrations of hydrogen peroxide for 2.5 hours. Shown are 3 independent trials. No statistical significance was found between wild type and APL-1 overexpression lines. B. 1 day adult animals exposed to a heat stress of 35ºC. Wild type [N2 (m=6.3±0.1, N=195)],

ynIs86 [P*apl-1*::APL-1] (m=7.1±0.1, N=98), *apl-1(yn10)*{P*apl-1*::APL-1} (m=6.9±0.1, N=30), *apl-1(yn5)* (m=7.2±0.1, N=100), *ynIs12* [P*snb-1*::APL-1] (m=7.0±0.1, N=204), and *ynIs13* [P*snb-1*::APL-1] (m=6.8±0.1, N=197). m= mean survival in hours. No statistical significance between wild type and APL-1 overexpression lines. *Is*, (), integrated transgene, *Ex*, {}, non-integrated transgene.

A.5. APL-1 overexpression induced phenotypes independent of *daf-16*/FOXO activity

Overexpression of APL-1 induces several phenotypes that are dependent on *daf-16*, such as short body size and low egg-laying rate. Hence, we tested a number of APL-1 induced phenotypes, such as egg retention, sluggishness, and serotonin-induced egg-laying, in a *daf-16* null background: all those phenotypes are mediated independent of *daf-16*/FOXO activity (Figure 7).

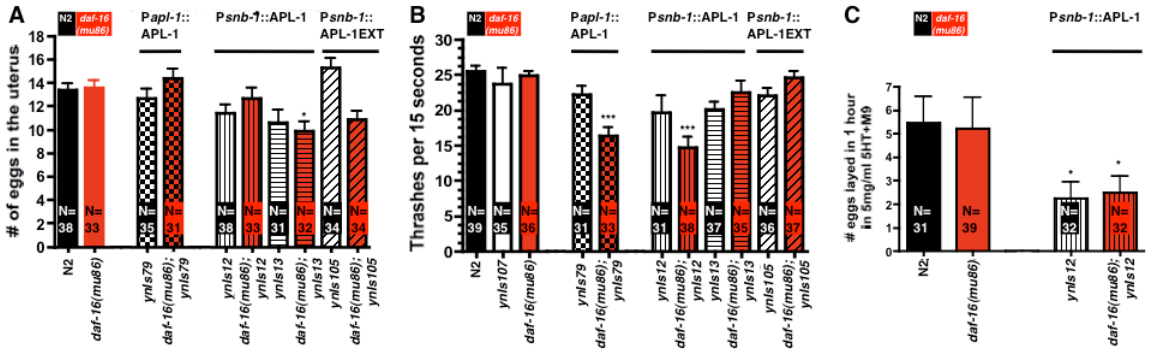

Figure 7. Several APL-1 overexpression phenotypes are independent of DAF-16 activity. A. Egg retention of day 2 adult animals. B. Swimming rates as assayed by number of thrashes per 15 seconds in M9 physiological buffer. Day 1 adult animals were used; each animal was scored three times and the mean calculated for that animal. C. Egg-laying induced by the presence of 5 mg/ml serotonin. T-test with Mann Whitney post-test *=P<0.05, **=P<0.001,*** P<0.0001. *Is*, (), integrated transgene.

A.6. APL-1 does not affect dauer formation

The alternative dauer stage can be induced by either starvation or higher temperature (Riddle & Albert 1997; Ailion & Thomas 2000). For instance, placing L1 animals at 27ºC induces dauer in 10% of wild-type animals (Ailion & Thomas 2000). APL-1 overexpression neither enhanced nor suppressed the 27ºC dauer formation either in a wild type or *daf-7, daf-12, daf-16* mutant or DAF-16 overexpression background (Table 2). Furthermore, dauer animals are resistant against 1% SDS (Cassada & Russell 1975). To determine whether APL-1 overexpression animals form proper dauers, we flooded starved plates with 1% SDS and scored for thrashing animals 15 minutes later. All APL-1 overexpression animals were SDS resistant, suggesting that they form proper dauers.

Table 2. APL-1 overexpression levels at 20°C, Dauer and Egg-laying			
Strain (Genotype)	No. Starvation dauers observed in 3 trials (1%SDS)	% dauer formation at 27°C (N= animals counted)	No. eggs in uterus of 2 days adults mean ± SE (N)
Controls			
N2 (wild type)	463	10 (910)	14 ± 0.5 (63)
lon-2(e678) apl-1(yn10)/ dpy-8(e130)	320	5 (497)	
ynIs107 [P*apl-1*::APL-1(mut)::GFP]	165		
Endogenous Overexpression of full-length APL-1			
ynIs86 [P*apl-1*::APL-1]	890	8 (589)	
ynIs79 [P*apl-1*::APL-1::GFP]	187	5 (538)	13 ± 0.8 (35)
lon-2(e678) apl-1(yn10) {P*apl-1*::APL-1}	129	8 (60)	
Endogenous Overexpression of the Extracellular Domain of APL-1 (APL-1EXT)			
apl-1(yn5)	415	9 (563)	
ynIs71 [P*apl-1*::APL-1EXT]	262	8 (289)	
Pan-neural expression of APL-1 driven by* rab-3 *promoter			
ynIs104 [P*rab-3*::APL-1]	351		13 ± 0.7 (43)
ynIs91 [P*rab-3*::APL-1]	210	3 (332)	
Overexpression of APL-1 driven by* snb-1 *promoter			
ynIs12 [P*snb-1*::APL-1]	501	3 (1046)	11 ± 1.0 (30)
ynIs13 [P*snb-1*::APL-1]	605	3 (793)	11 ± 0.9 (31)
Overexpression of APL-1 in a* daf-16(mu38) *null background			
daf-16(mu86)	0	0 (156)	14 ± 0.6 (45)
daf-16(mu86); ynIs86	0	0 (71)	
daf-16(mu86); ynIs79	0	0 (74)	14 ± 0.8 (31)
daf-16(mu86); apl-1(yn5)	0	0 (86)	
daf-16(mu86); ynIs104	0	0 (76)	13 ± 1.0 (32)
daf-16(mu86); ynIs12	0	0 (68)	11 ± 0.7 (34)
daf-16(mu86); ynIs13	0	0 (53)	10 ± 0.9 (33)
Overexpression of APL-1 and DAF-16			
zIs356 [DAF-16::GFP]*	17	36 (468)	
zIs356; *ynIs79*	4	28 (431)	
zIs356; *apl-1(yn5)*	9	17 (440)	
zIs356; *ynIs104*	13	13 (213)	
zIs356; *ynIs12*	15	29 (459)	
Overexpression of APL-1 in a* daf-7(e1372) *mutant background			
daf-7(e1372)		100 (78)	34 ± 2.0 (32)
daf-7(e1372); ynIs79		100 (123)	
daf-7(e1372); ynIs12			18 ± 1.2 (34)
daf-7(e1372); ynIs104			31 ± 1.4 (32)
Overexpression of APL-1 in a* daf-12(m20) *mutant background			
daf-12(m20)	7	0 (328)	14 ± 1.3 (32)
daf-12(m20); *ynIs12*	6	0 (253)	
daf-12(m20); *ynIs104*			12 ± 0.7 (32)

* *zIs356* [DAF-16::GFP] form incomplete dauer-like animals, where the buccal cavity is not fully closed and SDS can penetrate (Henderson & Johnson 2001)

A.7. APL-1 overexpression does not cause neurodegeneration of VC neurons

Because overexpression of APL-1 slows egg-laying rate, we determined whether neurons that are involved in the egg-laying system are altered. Eight neurons regulate egg-laying: 2 HSN neurons and six VC motor neurons (White *et al*. 1986). APL-1::GFP is expressed

in the ventral cord and in vulval muscles (Hornsten *et al*. 2007), but not in VC neurons (*ynIs79*). To visualize the six VC neurons we used transgenic animals that express GFP in all six VC neurons (*vsIs13*; (Bany *et al*. 2003)). We crossed the transgenic animals that express GFP in all six VC neurons (*vsIs13*) with different APL-1 overexpression lines. We did not see any neurodegeneration of the VC neurons in the transgenic APL-1 overexpression lines (Table 3).

Table 3. VC neurons are unaffected by APL-1 overexpression

Strain	All 6 VC neurons visible at L4 stage	All 6 VC neurons visible at day 3 of adulthood
vsIs13 [GFP in VC neurons]	122/122	78/78
vsIs13; ynIs79 [P*apl-1*::APL-1::GFP] at 20°C	109/109	30/30
vsIs13; ynIs79 [P*apl-1*::APL-1::GFP] shifted as L2 to 27°C	19/19	35/35
vsIs13; apl-1(yn5)	142/142	25/25
vsIs13 ynIs104 [P*rab-3*::APL-1::GFP]*	158/158	77/81**
vsIs13; ynIs91 [P*rab-3*::APL-1::GFP]	255/255	69/69

* P*rab-3*::APL-1::GFP is not visible in VC neurons.

**4 had very faint GFP expression in VC4 and VC5 cells; because of strong intestinal autofluorescence, it was difficult to see GFP expression. However, VC4 and VC5 cells were still visible with DIC Nomarski optics.

A.8. APL-1 does not enhance G_αs induced cell death or excitotoxicity

The lethality of *apl-1(yn10)* is not rescued by blocking apoptosis nor necrosis in *C. elegans* (Hornsten *et al*. 2007). Animals that overexpress APL-1 do not show any enhancement of dead apoptotic or necrotic cells as determined by DIC Nomarski optics. We further examined whether overexpression of APL-1 could enhance neurodegeneration in a sensitized G_αs or excitotoxicity background. Animals overexpressing GTP-binding protein G_αs driven by the *glr-1* (glutamate receptor) promoter (*nuIs5*; (Berger *et al*. 1998)) show neurodegeneration of only a few those *glr-1* receptor expressing neurons during development (Berger *et al*. 1998; Mano & Driscoll 2009). As adults, these G_αs overexpressing animals (*nuIs5*) showed strong impairment in

chemotaxis towards benzaldehyde (Figure 8A). Some of the dying *glr-1* receptor expressing neurons are interneurons that process sensory information (Mano & Driscoll 2009). The chemotaxis impairment of the G_{α}s animals was unaltered by introducing a transgene with pan-neuronal APL-1 expression (*nuIs5; ynIs104*), suggesting that pan-neuronal APL-1 expression cannot substitute for the missing interneurons. As a control, we used a triple mutant *glr-1; glr-2; nmr-1*, which encode orthologues of the NMDA or AMPA channels and are implicated in learning and cell death in mammals. The G_{α}s-induced neurodegeneration is enhanced by excitotoxicity caused by loss of the glutamate transporter *glt-3* (Mano & Driscoll 2009). However, neither endogenous nor neuronal overexpression of APL-1 (*ynIs79* and *ynIs104*) enhanced neurodegeneration in a G_{α}s overexpression or *glt-3* null background.

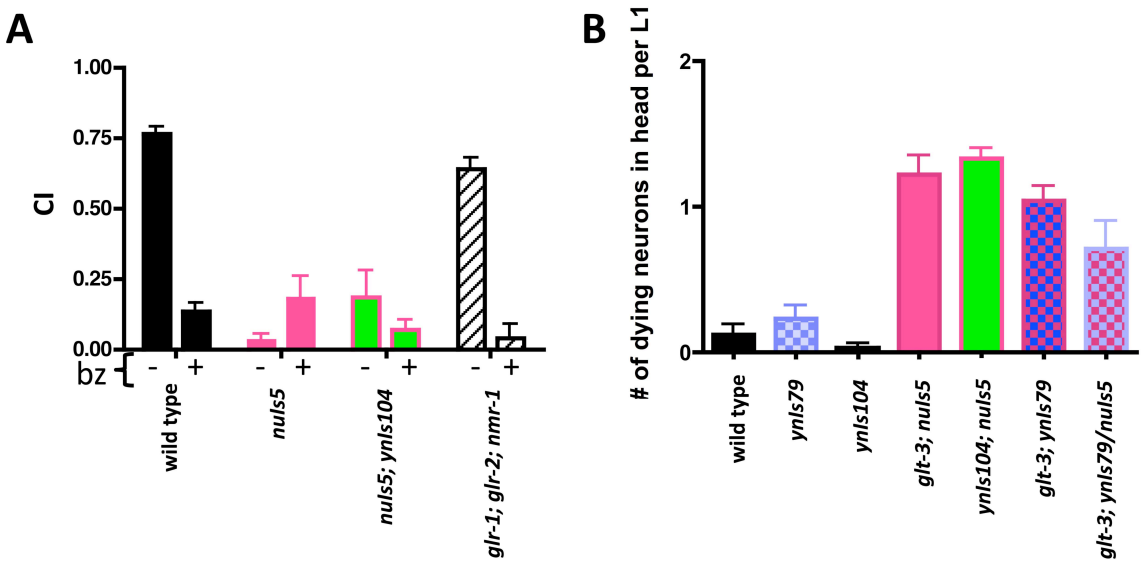

Figure 8. APL-1 over expression does not affect excitotoxicity nor G_{α}s induced neurodegeneration

A. Chemotaxis and avoidance response to benzaldehyde (Trials > 4). **B**. L1 animals were scored for neurodegenerative characteristics, such as swollen cells in the head region, particularly in the area of the nerve ring (N>35).

A.9. Suppression of the *apl-1(yn10)* null lethality.

Because tissue-specific expression of APL-1 in neurons was able to rescue the *apl-1(yn10)* null lethality, we screened for bypass suppressors of the *apl-1(yn10)* null lethality using predicted interactors of *apl-1*. Secreted sAPL-1α could act as a long range signaling mediator or sAPL-1α could stay bound to the neuronal surface and interact there with an unknown effector to initiate or modulate molting. The candidates for APL-1 interaction were predicted from a computer based integration of gene expression, phenotype, interactome, and functional annotation data from yeast, fly, and worms

(Zhong & Sternberg 2006). We selected six top candidates among the predicted APL-1 interactors** and crossed them with *apl-1*(*yn10)* mutants carrying an extrachromosomal rescue construct [APL-1] with a marker to test whether the predicted APL-1 interactors were able to rescue the *apl-1(yn10)* null lethality phenotype (**Predicted by http://tenaya.caltech.edu:8000/predict/; (Zhong & Sternberg 2006). F2 double mutant progeny were screened for animals that did not carry the rescue construct [APL-1]. The presence of the *yn10* deletion and *apl-1* rescue construct were confirmed by PCR. None of our selected candidates was able to suppress the *apl-1* lethality phenotype (Table 4).

Table 4. Predicted APL-1 interactors

Strain	Genotype / allele	Predicted homologue	Phenotype
VC1228	*klp-11 (tm324)*; IV	Kinesin like protein	
FF41	*unc-116 (e2310)*; III	Kinesin-1	Unc, Dpy (dumpy), coil
CB402	*unc-55 (e402)*; I	Hormone receptor	Unc (uncoordinated)
MT1444	*egl-2 (n683)*; V	Voltage-gated potassium channel	Egg-laying defect, bag of worms
NJ683	*exc-7 (rh252)*; II	RNA-binding protein ELAV	Excretory canal abnormal
CX51	*dyn-1 (ky51)*; X	Dynamin, Vesicular sorting protein VPS1	Egg-laying defect; Unc at 25°C

A.10. RNAi screen for suppressors of a*pl-1(yn10)* null lethality

To identify genes that can bypass the need for *apl-1*, we started an RNAi based screen for suppressors of the *apl-1(yn10)* null lethality. Possible ways to bypass the *apl-1* lethality are either by gain-of-function (gof) mutation of sAPL-1 downstream targets (e.g., receptor) or by loss-of-function (lof) mutations of negative regulators of the APL-1 pathway. So far, several screens for suppressors of the *apl-1* null lethality have been unfruitful. RNA interference or RNAi only knocks down protein levels. Lethal mutations, such as *apl-1* itself, are viable by RNAi, as seen by the groups of F. Slack and

P. Bazzicalupo (Zambrano *et al*. 2002). By performing an RNAi screen, at least the negative regulators of APL-1 can be identified. Most of the nearly 20,000 genes comprising the *C. elegans* genome are stored in a plasmid RNAi library, where each individual gene is represented by a dsRNA clone. Since APL-1 is abundantly expressed in neurons and neurons are generally immune to RNAi, we generated animals with enhanced RNAi sensitivity by using heterozygous *apl-1*(*yn10)* animals together with the *rrf-3* mutation (*rrf-3(pk1426)*II*; lon-2 (e678) apl-1 (yn10) / dpy-8(e130)* X). Mutations in *rrf-3* have been shown to sensitize neurons to feeding-induced RNAi (*rrf-3(pk1426)* II (Simmer *et al*. 2002)). To knock down candidate target genes, we used *E. coli* bacteria from the Ahringer genomic "feeding" RNAi library that expressed double-stranded RNA for genes of interest upon induction with IPTG. The F2 generation of heterozygous *apl-1*(*yn10)* animals grown on the dsRNA expressing bacteria were scored for Lon phenotype. Thus far, I screened 1260 clones with no success (576 clones on chromosome I, 372 clones on chromosome II and 312 clones on chromosome X).

A.11. Materials and Methods

A.11.1. Strains

Caenorhabtitis elegans strains were grown and maintained on MYOB plates (Church *et al*. 1995) containing OP50 Escherichia coli bacteria at 20ºC using methods as described (Brenner 1974), unless noted. All mutations used are described in Wormbase (www.wormbase.org) and include: LGI: *daf-16(mu86)*; LGII: *nmr-1(ak4), rrf-3(pk1426)*; LGIII: *daf-2(e1370), daf-7(e1372), glr-1(ky176), glr-2(ak10)*; LGIV: *glt-3(bz34), bec-1(ok691)*/nT1[*qIs51* (P*myo-2*::GFP)] (IV;V), *bec-1(ok700)*/ nT1[*qIs51*

(P*myo-2*::GFP)] (IV;V), and LGX: *daf-12(m20)*, *lon-2(e678), apl-1(yn5* and *yn10)*, and *dpy-8(e130)*. Construction of the APL-1 transgenes and the resulting transgenic lines are described (Hornsten *et al*. 2007). Integrated transgenic lines used were: *ynIs110* (BEC-1::mRFP; pRF4 *rol-6(su1006gf))*; LGI: *ynIs109* (P*snb-1*::APL-1(cDNA)::GFP); LGIII: *ynIs12* (P*snb-1*::APL-1(cDNA), *lin-15B*(+)); LGIV: *vsIs13* (*lin-11*::*pes-10*::GFP, *lin-15*(+))(Bany *et al*. 2003), *ynIs104* (P*rab-3*::APL-1(cDNA)::GFP, P*myo-2*::GFP); LGV: *ynIs13* (P*snb-1*::APL-1(cDNA), *lin-15B*(+)), *ynIs79* (P*apl-1*::APL-1::GFP), *nuIs5* [P*glr-1*::GFP; P*glr-1*::Gas(Q227L); *lin-15*(+)] (Berger *et al*. 1998); and LGX: *ynIs86* (P*apl-1*::APL-1, *sur-5*::GFP), *ynIs91* (P*rab-3*::APL-1, pRF4 *rol-6(su1006gf)*), *ynIs108* (P*apl-1*::APL-1(Δheparin ΔE2 domain)::GFP; Psur-5::GFP), and *ynIs107* (P*apl-1*::APL-1(*yn32* E71K/D342C/S362C)::GFP, P*myo-2*::GFP) (Hoopes *et al*. 2010).

A.11.2. Body length measurements

L4 animals of each strain were picked and allowed to develop for one day at 15ºC. Animals were mounted onto 2% agar pads containing a drop of 10 mM NaN_3 and pictures of the animals were taken at 100x magnification on a confocal microscope (Zeiss LSM 510 Confocal Laser Scanning System). The lengths of the worms were determined by drawing a line along the midline of the animals from the tip of the mouth to the tail. For statistical analysis one-way ANOVAs with Tukey post-test (95% confidence intervals) was performed to assess similarity between groups using Prism 4.0a software (GraphPad Software).

A.11.3. Measuring GFP intensity

Animals were mounted onto 2% agar pads containing a drop of 10 mM sodium azide. Pictures of the GFP fluorescent animals were taken at 100x magnification on a confocal microscope (Zeiss LSM 510 Confocal Laser Scanning System) using the always the same settings (GFP: excitation wavelength 488 nm, Laser intensity 5%, Filter BP505-530; Pinhole 1000μm). The intensity of the GFP fluorescence for each worm was derived by the sum of the frequency of grey values (0-255) above threshold 50 determined by Image J. For statistical analysis one-way ANOVAs with Tukey post-test (95% confidence intervals) was performed to assess similarity between groups using Prism 4.0a software (GraphPad Software).

A.11.4. Z-stacks and co-localization assays

Animals were mounted onto 2% agar pads containing a drop of 10 mM sodium azide. Images and z-stacks of the animals were taken at 400x magnification on a confocal microscope (Zeiss LSM 510 Confocal Laser Scanning System; slice thickness 0.49 μm; for GFP: excitation wavelength 488 nm, Laser intensity 5%, Filter BP505-530; pinhole 80 μm; for mRFP: excitation wavelength 543 nm, laser intensity 66%, filter LP560; pinhole 78 μm). The co-localization of the GFP and mRFP fluorescence for z-stacks of each worm was determined by Image J's "Colocalisation analysis (test and highlighter)".

A.11.5. Western blot analysis

Preparations of animal lysates and western blots were performed as described (Hornsten *et al*. 2007). Animals were grown in bulk at either 15ºC, 20ºC, or 25ºC. For 27ºC,

animals were first grown at 20ºC to reach a minimal density and then shifted for two days at 27ºC because APL-1 overexpression animals either die at L1 or, if past the L1 stage, become sterile at 27ºC. Total protein levels per animal extract were normalized according to actin levels. For each blot probed with an anti-APL-1 antiserum against the extracellular domain of APL-1 (Hornsten *et al*. 2007), another blot loaded with same amount of sample was run in parallel and was probed with an actin monoclonal antibody (JLA20 at 1:2000; Developmental Studies Hybridoma Bank; secondary antibody anti-mouse-goat-HRP at 1:1000). Relative protein levels were determined by relative intensity to wild type (N2) using NIH Image J Gel analyzer.

A.11.6. Oxidative stress assays

Synchronized day 1 adults were mounted from the plates and washed 3 times with distilled water. Animals were placed into 12 well plates (Costar) containing different concentrations of hydrogen peroxide (0, 10, 100, 1000, 2000, and 3000 μM) and incubated for 2.5 hours at room temperature (22-24ºC). Animals that thrashed were scored as alive; dead animals were usually stretched out in a line and without characteristic curves.

A.11.7. Thermal stress assays

About 100 L4 animals per strain were picked. One day later, in groups of 10, these animals were placed onto new plates and shifted to 35ºC. Every hour animals were scored: animals that moved or responded to prodding were scored as alive. Each trial included wild type as a control. Survival curves and P-values were determined by a

Kaplan-Meier survival plot and by the non-parametric Log-Rank test (Mantel-Cox text) to assess the similarity between groups using a JMP 7.0.2 statistics program (JMP®, Version 7, SAS).

A.11.8. Egg-retention assays

L4 animals were picked and maintained at 20ºC. After 48 hours, single animals were placed into 96 well plates (Costar) containing 0.1 ml M9 physiological buffer and 20% bleach (Clorox). After several minutes the animal was dissolved and the eggs, which are more resistant to Clorox, were counted. For statistical analysis T-tests (nonparametric, two-tailed, 95% confidence intervals) with Mann-Whitney post-test were performed to assess similarity between groups using Prism 4.0a software (GraphPad).

A.11.9. Thrashing and serotonin induced egg-laying assays

L4 animals were picked and maintained at 20ºC. After 24 hours, single animals were placed into 96 well plates (Costar) containing 0.1 ml M9 physiological buffer. The number of body flexations per 15 seconds was scored 3 times for each animal. Serotonin (Sigma) was added to a final concentration of 13 mM to induce egg-laying (modified from Trent *et al*. 1983). After 1 hour, the number of eggs laid was scored. For statistical analysis T-tests (nonparametric, two-tailed, 95% confidence intervals) with Mann-Whitney post-test were performed to assess similarity between groups using Prism 4.0a software (GraphPad).

A.11.10. Dauer formation at 27ºC assays

Animals were grown and maintained at 20ºC. 10 gravid adults were placed onto a new agar plate with food and allowed to lay eggs for 1-2 hours. The P_o animal was killed. As F1 eggs hatched, plates were transferred into a 27ºC incubator. Larval stages were scored 44 hours later.

A.11.11. SDS dauer assays

Plates on which animals have been starved at least for two weeks were flooded with 1% SDS and thrashing animals were counted after 15 minutes of incubation.

A.11.12. Neurodegeneration assays

A piece of agar of a freshly full-grown plate of worms was placed on a cover slip with the worm-side of the agar directly on the cover slip. Hence, free-moving animals without any anesthetics were observed by Nomarski Differential Interference Contrast optics with an inverted microscope (Zeiss Axiovert 100TV). L1 animals were scored for neurodegenerative characteristics (e.g., swollen cells in the head region, particularly in the nerve ring as described (Mano & Driscoll 2009)).

A.11.13. RNA interference assays

RNAi by feeding: day -1, a single RNAi clone (bacteria HT115) was picked from the Ahringer library (Kamath et al. 2001) (Geneservice), which is maintained at -80ºC on Luria broth medium (LB) agar plates with 25 μg/ml carbenicillin and 12.5 μg/ml tetracycline), and incubated in 1 ml LB containing 100 μg/ml ampicillin (at 37°C, 280

rpm) overnight; day 0, the 1 ml bacterial culture was transferred into 10 ml LB containing 100 μg/ml ampicillin and incubated for another 4-6 hours at 37°C at 280 rpm. 450 μl of the bacteria culture was spread onto MYOB plates containing 400 mM of βD-isothiogalactopyranoside (IPTG) and 50 μg/ml ampicillin and these RNAi plates were placed in 37°C overnight; day 1, six *rrf-3(pk1426); lon-2(e678) apl-1(yn10)* / *dpy-8(e130)* L4 animals (P_o) were placed on bacteria lawn that express double-stranded RNA (dsRNA); day 6, about six *rrf-3(pk1426); lon-2(e678) apl-1(yn10)* / *dpy-8(e130)* F1 L4 animals were transferred onto new plates containing the same dsRNA expressing bacteria; day 8, F2 animals were scored for long animals (*rrf-3(pk1426); lon-2(e678) apl-1(yn10)*).

A.12. Acknowledgments

We wish to thank Alicia Melendez's group for kindly providing their *bec-1(ok691)*/nT1, *bec-1(ok700)*/nT1, *bec-1(ok691) izEx*[BEC-1mRFP], Itzhak Mano's group for kindly providing *glt-3; nuIs5* and *nmr-1; glr-1; glr-2* strains, Danny (Xiaomeng) Xu for help with the western blots, Adanna Alexander, Pei Zhao and James Chon for help with the RNAi screen, Daniel Fimiarz for help with the confocal pictures, lab members for helpful discussions, and Sarah Tichelli for help with the length measurements.

A.13. References

Ailion M , Thomas JH (2000). Dauer formation induced by high temperatures in *Caenorhabditis elegans*. *Genetics*. **156**, 1047-1067.

Bany IA, Dong MQ , Koelle MR (2003). Genetic and cellular basis for acetylcholine inhibition of *Caenorhabditis elegans* egg-laying behavior. *J Neurosci*. **23**, 8060-8069.

Berger AJ, Hart AC , Kaplan JM (1998). G alphas-induced neurodegeneration in *Caenorhabditis elegans*. *J Neurosci*. **18**, 2871-2880.

Brenner S (1974). The Genetics of *Caenorhabditis elegans*. *Genetics*. **77**, 71-94.

Cassada RC , Russell RL (1975). The dauerlarva, a post-embryonic developmental variant of the nematode *Caenorhabditis elegans*. *Developmental biology*. **46**, 326-342.

Church DL, Guan KL , Lambie EJ (1995). Three genes of the MAP kinase cascade, *mek-2*, *mpk-1/sur-1* and *let-60 ras*, are required for meiotic cell cycle progression in *Caenorhabditis elegans*. *Development*. **121**, 2525-2535.

GuhaThakurta D, Palomar L, Stormo GD, Tedesco P, Johnson TE, Walker DW, Lithgow G, Kim S , Link CD (2002). Identification of a novel cis-regulatory element involved in the heat shock response in Caenorhabditis elegans using microarray gene expression and computational methods. *Genome Res*. **12**, 701-712.

Henderson ST , Johnson TE (2001). *daf-16* integrates developmental and environmental inputs to mediate aging in the nematode *Caenorhabditis elegans*. *Curr Biol*. **11**, 1975-1980.

Hoopes JT, Liu X, Xu X, Demeler B, Folta-Stogniew E, Li C , Ha Y (2010). Structural characterization of the E2 domain of APL-1, a *Caenorhabditis elegans* homolog of human amyloid precursor protein, and its heparin binding site. *The Journal of biological chemistry*. **285**, 2165-2173.

Hornsten A, Lieberthal J, Fadia S, Malins R, Ha L, Xu X, Daigle I, Markowitz M, O'Connor G, Plasterk R , Li C (2007). APL-1, a *Caenorhabditis elegans* protein related to the human beta-amyloid precursor protein, is essential for viability. *Proc Natl Acad Sci USA*. **104**, 1971-1976.

Kamath RS, Martinez-Campos M, Zipperlen P, Fraser AG , Ahringer J (2001). Effectiveness of specific RNA-mediated interference through ingested double-stranded RNA in *Caenorhabditis elegans*. *Genome Biol*. **2**, RESEARCH0002.

Kenyon C (2005). The plasticity of aging: insights from long-lived mutants. *Cell*. **120**, 449-460.

Lund J, Tedesco P, Duke K, Wang J, Kim SK , Johnson TE (2002). Transcriptional profile of aging in C. elegans. *Curr Biol*. **12**, 1566-1573.

Mano I , Driscoll M (2009). *Caenorhabditis elegans* glutamate transporter deletion induces AMPA-receptor/adenylyl cyclase 9-dependent excitotoxicity. *Journal of neurochemistry*. **108**, 1373-1384.

Melendez A , Neufeld TP (2008). The cell biology of autophagy in metazoans: a developing story. *Development*. **135**, 2347-2360.

Meléndez A, Tallóczy Z, Seaman M, Eskelinen EL, Hall DH , Levine B (2003). Autophagy genes are essential for dauer development and life-span extension in *C. elegans*. *Science*. **301**, 1387-1391.

Murphy CT, McCarroll SA, Bargmann CI, Fraser A, Kamath RS, Ahringer J, Li H , Kenyon C (2003). Genes that act downstream of DAF-16 to influence the lifespan of *Caenorhabditis elegans*. *Nature*. **424**, 277-283.

Riddle DL , Albert PS (1997). Genetic and Environmental Regulation of Dauer Larva Development. In *C. elegans II*. (DL Riddle, T Blumenthal, BJ Meyer , JR Priess, eds). New York: Cold Spring Harbor Laboratory Press, pp. 739–768.

Simmer F, Tijsterman M, Parrish S, Koushika SP, Nonet ML, Fire A, Ahringer J , Plasterk RH (2002). Loss of the putative RNA-directed RNA polymerase RRF-3 makes *C. elegans* hypersensitive to RNAi. *Curr Biol*. **12**, 1317-1319.

Takacs-Vellai K, Vellai T, Puoti A, Passannante M, Wicky C, Streit A, Kovacs AL , Müller F (2005). Inactivation of the autophagy gene *bec-1* triggers apoptotic cell death in *C. elegans*. *Curr Biol*. **15**, 1513-1517.

Trent C, Tsuing N , Horvitz HR (1983). Egg-laying defective mutants of the nematode *Caenorhabditis elegans*. *Genetics*. **104**, 619-647.

Zambrano N, Bimonte M, Arbucci S, Gianni D, Russo T , Bazzicalupo P (2002). feh-1 and apl-1, the *Caenorhabditis elegans* orthologues of mammalian Fe65 and beta-amyloid precursor protein genes, are involved in the same pathway that controls nematode pharyngeal pumping. *J Cell Sci*. **115**, 1411-1422.

Zhong W , Sternberg PW (2006). Genome-wide prediction of *C. elegans* genetic interactions. *Science*. **311**, 1481-1484.

BIOGRAPHICAL SKETCH

COLLIN Y. EWALD

EDUCATION/TRAINING

2005	B.Sc., Molecular Biology, University of Basel, Switzerland
2007	M.Sc., Molecular Biology, University of Basel, Switzerland
2008	M.Phil., Biology, City University of New York
2006-present	PhD candidate, Neuroscience, City University of New York. Laboratory of Dr. Chris Li

PROFESSIONAL EXPERIENCE

2005-2006	Master's research, Friedrich Miescher Institute (FMI) for Biomedical Research, University of Basel and part of the Novartis Research Foundation. Laboratories of Dr. Joy Alcedo and Dr. Nancy Hynes
2006-2007	Teaching Assistant, Department of Biology, City College of New York
2006-present	Research Assistant, Department of Biology, City College of New York

AWARD AND HONORS

2007	Competitive CUNY Research Grant for Doctoral Students
2007	"2007 NYAS Future Entrepreneur" recognized by the New York Academy of Sciences
2008	CCNY GSC 2008 Graduate Student Award for best progress and productivity in the Neuroscience research program of the City University of New York
2008	Sue Rosenberg Zalk Travel & Research Fund for the traveling and presenting at European *C. elegans* Meeting 2008 in Spain.
2009	Doctoral Student Council travel award for the Northeast Regional Meeting of the Society of Developmental Biology 2009
2009	Sue Rosenberg Zalk Travel & Research Fund for the traveling and presenting at International *C. elegans* meeting
2010	Competitive CUNY Research Grant for Doctoral Students

PUBLICATIONS

2010	Collin Y. Ewald and Chris Li: **Understanding the molecular basis of Alzheimer's disease using a *Caenorhabditis elegans* model system.** Review article. Brain Structure and Function, 214(2-3):263-83. Epub 2009 Dec 11. DOI: 10.1007/s00429-009-0235-3

ORAL PRESENTATIONS

2009	Collin Ewald and Chris Li: **GENETIC INTERACTIONS BETWEEN *apl-1*, A GENE ENCODING AN AMYLOID PRECURSOR-RELATED PROTEIN, AND *daf-16*, A REGULATOR OF LIFESPAN.** 17th International *C. elegans* meeting, UCLA, USA.

POSTER PRESENTATIONS

2005 Collin Ewald et al.: **Expression, Purification and NMR Spectroscopy of T-Cadherin Domain1.** Biozentrum Basel, Switzerland.

2006 Collin Ewald, Nancy Hynes, Joy Alcedo: **Characterization of the Worm Homolog of memo, a Gene that Acts Downstream of the Mammalian EGF Pathway.** European Worm Meeting, Hersonissos, Crete, Greece.

2007 Collin Ewald and Chris Li: **Does targeted overexpression of APL-1 in neurons extend lifespan?** International Worm Meeting, UCLA, USA.

2008 Collin Ewald and Chris Li: **The role of APL-1, an amyloid precursor-like protein in *C. elegans.*** European Worm Meeting, Seville, Spain

2008 Collin Ewald and Chris Li: **The role of APL-1, an amyloid precursor-like protein in *C. elegans.*** Ninth Annual Celebration of Science, Engineering and Mathematics. Graduate Center of the City University of New York, USA.

2008 Collin Ewald and Chris Li: **How worms can provide insights into Alzheimer's disease.** The Graduate Student Symposium at The City College of New York.

2008 Collin Ewald and Chris Li: **Lifespan Effects of APL-1, a *C. elegans* Protein Related to Human Amyloid Precursor Protein.** 2008 *C elegans* Neuronal Development, Synaptic Function, and Behavior Topic Meeting, University of Wisconsin-Madison, USA.

2009 Collin Ewald and Chris Li: **Overexpression of APL-1, a *C. elegans* amyloid precursor-related protein, causes an incompletely-penetrant larval lethality and slowed development.** Northeast Regional Meeting of the Society of Developmental Biology 2009, Woods Hole, MA, USA.

2010 Collin Ewald and Chris Li: **APL-1, an amyloid precursor-related protein, influences the activity of lifespan-determining transcription factor DAF-16/FOXO in *C. elegans*.** Genetics 2010: model organisms to human biology, Boston, MA, USA

2010 Vishal Shah, Ruby Cheng, Collin Ewald, Chris Li: **Neuronal Overexpression of APL-1, a Protein Related to Human Amyloid Precursor Protein, Disrupts Olfactory Adaptation.** *C. elegans* topic meeting 2010: Neuronal development, synaptic function & behavior, University of Wisconsin-Madison, USA.

2010 Collin Ewald and Chris Li: **The Extracellular Domain of APL-1, a Protein Related to Human Amyloid Precursor Protein, Signals through DAF-16/FOXO and DAF-12 to Influence Lifespan.** *C. elegans* topic meeting 2010: Aging, Metabolism, Pathogenesis, Stress, and Small RNAs, University of Wisconsin-Madison, USA.

2010 Collin Ewald *et al.*,: **Neuronal overexpression of APL-1, an amyloid precursor-related protein, impairs learning in *C. elegans.*** Graduate Center of the City University of New York, USA.

2010 Collin Ewald and Chris Li: **Increased dosage of the extracellular domain of APL-1, an APP-related protein, can increase lifespan and slow developmental progression via transcription factor DAF-16/FOXO and nuclear hormone receptor DAF-12.** Molecular Genetics of Aging 2010. Cold Spring Harbor Laboratory, NY, USA.